NATIONAL AERONAUTICS AND SPACE ADMINISTRATION

## Technical Report 32-1177

# Surveyor III Mission Report

## Part I. Mission Description and Performance

JET PROPULSION LABORATORY

CALIFORNIA INSTITUTE OF TECHNOLOGY

PASADENA, CALIFORNIA

September 1, 1967

NATIONAL AERONAUTICS AND SPACE ADMINISTRATION

*Technical Report 32-1177*

# *Surveyor III Mission Report*

## *Part I. Mission Description and Performance*

Approved for publication by:
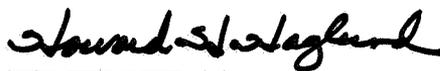
H. H. Haglund
Surveyor *Project Manager*

JET PROPULSION LABORATORY
CALIFORNIA INSTITUTE OF TECHNOLOGY
PASADENA, CALIFORNIA

September 1, 1967

*TECHNICAL REPORT 32-1177*

Copyright © 1967
Jet Propulsion Laboratory
California Institute of Technology

# Preface

This three-part document constitutes the *Surveyor III* Mission Report. It describes the third in a series of unmanned missions designed to soft-land on the moon and return data from the lunar surface.

Part I of this report consists of a technical description and an evaluation of engineering results of the systems utilized in the *Surveyor III* mission. Analysis of the data received from the *Surveyor III* mission is continuing, and it is expected that additional results will be obtained together with some improvement in accuracy. Part I was compiled using the contributions of many individuals in the major systems which support the Project. Some of the information for this report was obtained from other published documents; a list of these documents is contained in a bibliography.

Part II of this report presents the scientific data derived from the mission and the results of scientific analyses which have been conducted. Part III consists of selected pictures from *Surveyor III* and appropriate explanatory material.

# Contents

# Contents (contd)

## Tables

# Contents (contd)

## Tables (contd)

## Figures

# Contents (contd)

## Figures (contd)

# Contents (contd)

## Figures (contd)

# Contents (contd)

## Figures (contd)

# Abstract

*Surveyor III*, the third in a series of seven unmanned spacecraft designed to soft-land on the moon and return data, was launched from Cape Kennedy, Florida, on April 17, 1967. All established objectives for the mission were achieved. After a nominal lunar transit phase, a successful soft-landing, which included three separate touchdown events, was accomplished on April 20, 1967. The *Surveyor III* spacecraft was operated through the end of the lunar day (12 earth days) to provide a large quantity of new data from within a sizable crater on the lunar surface. Of special interest are the results, obtained via television pictures, of extensive operations conducted with a soil mechanics/surface sampler, an instrument which was included for the first time on this mission.
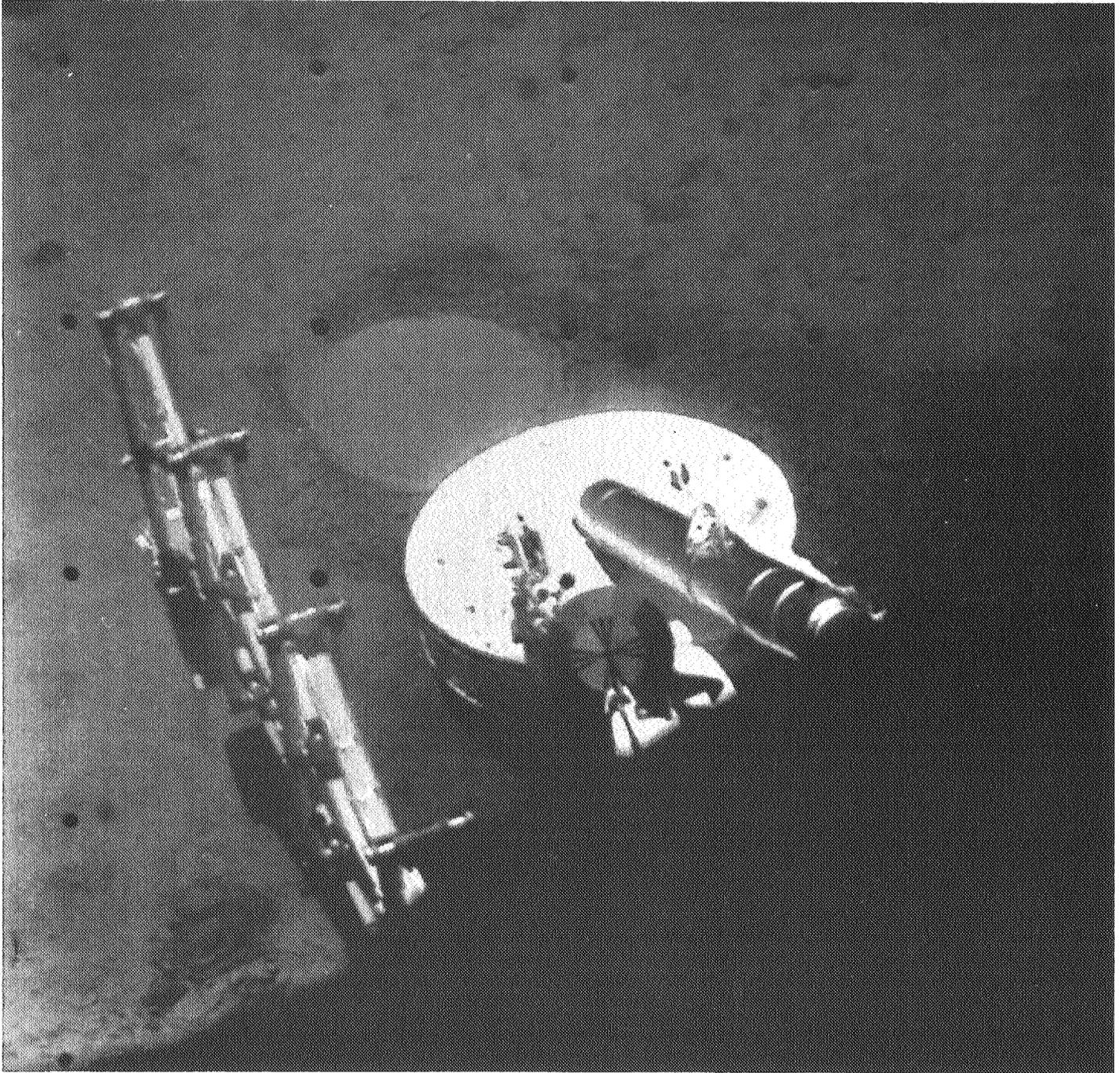
(Photograph received April 26, 1967, 11:42:46 GMT)

# I. Introduction and Summary

Surveyor III was launched from Cape Kennedy, Florida, at 07:05:01.059 GMT on April 17, 1967, and touched down on the moon at 00:04:17 GMT on April 20, 1967. A successful soft-landing was achieved, although the spacecraft lifted off twice after initial touchdown before finally coming safely to rest. The landing site is in the Ocean of Storms at 2.94 deg south latitude and 23.34 deg west longitude, about 625 km east of the site where Surveyor I successfully landed June 2, 1966. Spacecraft operations were conducted through the end of the lunar day, providing extensive engineering and scientific data which completely satisfied the mission objectives and largely confirmed the results obtained from Surveyor I.

Surveyor III landed on a sloping wall within a crater of about 200-m diameter, permitting, for the first time, observations of the interior of a sizable crater. For this mission, a unique soil mechanics/surface sampler instrument was added, and it, together with the television camera, provided valuable new data on the mechanical properties of the lunar surface material. The 12½-deg tilted attitude of the spacecraft permitted the camera also to take color photographs of a solar eclipse and of the crescent earth, which would not have been possible had the spacecraft landed on a level surface.

## A. Surveyor Project Objectives

The Surveyor Project has been designed to explore the moon with automated soft-landing spacecraft which are equipped to respond to earth commands and transmit back scientific and engineering data from the lunar surface. A total of seven flight missions are planned. Surveyor is one of two unmanned lunar exploration projects currently being conducted by the National Aeronautics and Space Administration. The other, Lunar Orbiter, is providing medium- and high-resolution photographs over broad areas to aid in site selection for the Surveyor and Apollo landing programs.

The overall objectives of the Surveyor Project are:

(1) To accomplish successful soft landings on the moon as demonstrated by operations of the spacecraft subsequent to landing.

(2) To provide basic data in support of Apollo.

(3) To perform operations on the lunar surface which will contribute new scientific knowledge about the moon and provide further information in support of Apollo.

The first two *Surveyor* spacecraft carried a survey television camera in addition to engineering instrumentation for obtaining in-flight and postlanding data. As an additional instrument, *Surveyor III* carried a soil mechanics/surface sampler (SM/SS) device to provide data based on picking, digging, and handling of lunar surface material.

*Surveyor I* was launched on May 30, 1966, and soft-landed near the western end of the *Apollo* zone of interest at 2.45 deg south latitude and 43.21 deg west longitude (based on *Lunar Orbiter III* data). Operations on the lunar surface were highly successful. In addition to a wide variety of other types of lunar surface data, over 11,000 television pictures were received in the course of operations during the first two lunar days. *Surveyor I* exhibited a remarkable capability to survive eight lunar day-and-night cycles involving temperature extremes of $+250$ and $-250°F$.

*Surveyor II* was launched on September 20, 1966, and achieved a nominal mission until execution of the mid-course velocity correction. One of the three vernier engines did not fire, which caused the spacecraft to tumble. Attempts to stabilize the spacecraft by repeatedly firing the verniers were unsuccessful. When nearly all the spacecraft battery energy had been consumed prior to lunar encounter, the mission was terminated shortly after firing of the main retro motor 45 hr after launch. A thorough investigation by a specially appointed Failure Review Board was unable to disclose the exact cause of failure. A number of recommendations were made to assure against a similar failure and to provide better diagnostic data on future missions.

The *Surveyor III* mission was highly successful in achieving Project Objectives for a new site. Important new data was obtained as a result of extensive postlanding operations with the SM/SS, television, and other spacecraft equipment. The lunar surface characteristics determined by *Surveyor III* confirm the findings of *Surveyor I* and indicate the suitability of an additional site for *Apollo*, which will utilize final descent and landing system technology similar to that of *Surveyor*.

## B. Project Description

The *Surveyor* Project is managed by the Jet Propulsion Laboratory for the NASA Office of Space Science and Applications. The Project is supported by four major administrative and functional elements or systems: Launch Vehicle System, Spacecraft System, Tracking and Data System (TDS), and Mission Operations System (MOS).

In addition to overall project management, JPL has been assigned the management responsibility for the Spacecraft, Tracking and Data Acquisition, and Mission Operations Systems. NASA/Lewis Research Center (LeRC) has been assigned responsibility for the *Atlas/Centaur* launch vehicle system.

## 1. Launch Vehicle System

*Atlas/Centaur* launch vehicle development began as an Advanced Research Projects Agency program for synchronous-orbit missions. In 1958, General Dynamics/Convair was given the contract to modify the *Atlas* first stage and develop the *Centaur* upper stage; Pratt & Whitney was given the contract to develop the high-impulse $LH_2/LO_2$ engines for the *Centaur* stage.

The Kennedy Space Center, Unmanned Launch Operations branch, working with LeRC, is assigned the *Centaur* launch operations responsibility. The *Centaur* vehicle utilizes Launch Complex 36, which consists of two launch pads (A and B) connected to a common blockhouse. The blockhouse has separate control consoles for each of the pads. Pad 36B was utilized for the *Surveyor III* mission.

The launch of *Atlas/Centaur* AC-12 on the *Surveyor III* mission was the third operational use of an *Atlas/Centaur* vehicle and the first operational flight to utilize the "parking orbit" mode of ascent. The first two operational flights (the successful launches of AC-10 and AC-7 on *Surveyors I* and *II*, respectively) utilized the "direct" ascent mode, wherein the *Centaur* second stage provided only one continuous burn to achieve injection into the desired lunar transfer trajectory. In the parking orbit or indirect ascent mode, the *Centaur* stage burns twice. The first burn injects the vehicle into a temporary parking orbit with a nominal altitude of 90 nm. After a coast period of up to 25 min, the *Centaur* reignites and provides the additional impulse necessary to achieve a lunar intercept trajectory. A total of eight R&D flight tests were conducted in the *Centaur* vehicle program. The last of these (AC-9) was conducted on October 29, 1966, and successfully demonstrated capability to launch via parking orbit.

The use of the parking orbit ascent mode permits the launching of *Surveyor* missions for all values of lunar declinations. This allows the design of launch periods which are compatible with favorable postlanding lunar lighting. For *Surveyor* direct ascent missions, lunar declination must be less than approximately $-14$ deg, which occurs for a period of only about 8 days per month.

## 2. Spacecraft System

*Surveyor* is a fully attitude-stabilized spacecraft designed to receive and execute a wide variety of earth commands, as well as perform certain automatic functions including the critical terminal descent and soft-landing sequences. Overall spacecraft dimensions and weight of 2200 to 2300 lb were established in accordance with the *Atlas/Centaur* vehicle capabilities. *Surveyor* has made significant new contributions to spacecraft technology through the development of new and advanced subsystems required for successful soft-landing on the lunar surface. New features which are employed to execute the complex terminal phase of flight include: a solid-propellant main retromotor with throttlable vernier engines (also used for midcourse velocity correction), extremely sensitive velocity- and altitude-sensing radars, and an automatic closed-loop guidance and control system. The demonstration of these devices on *Surveyor* missions is a direct benefit to the *Apollo* program, which will employ similar techniques. Design, fabrication, and test operations of the *Surveyor* spacecraft are performed by Hughes Aircraft Company under the technical direction of JPL.

## 3. Tracking and Data System

The TDS system provides the tracking and communications link between the spacecraft and the Mission Operations System. For *Surveyor* missions, the TDS system uses the facilities of (1) the Air Force Eastern Test Range for tracking and telemetry of the spacecraft and vehicle during the launch phase, (2) the Deep Space Network for precision tracking communications, data transmission and processing, and computing, and (3) the Manned Space Flight Network and the World-Wide Communications Network (NASCOM), both of which are operated by Goddard Space Flight Center.

The critical flight maneuvers and most picture-taking and SM/SS operations on *Surveyor* missions are commanded and recorded by the Deep Space Station at Goldstone, California (DSS 11), during its view periods. Other stations which provided prime support throughout the *Surveyor III* mission were DSS 42, near Canberra, Australia, and DSS 61 at Johannesburg, South Africa. Additional support, on a limited basis, was provided by DSS 51 (Johannesburg, South Africa) until one pass after touchdown, DSS 71 (Cape Kennedy) during prelaunch and launch phase, DSS 72 (Ascension Island) during launch phase and first postinjection pass, DSS 12 (Goldstone) as backup to DSS 11, and DSS 14 (with a 210-ft antenna at Goldstone) during terminal descent and landing.

## 4. Mission Operations System

The Mission Operations System essentially controls the spacecraft from launch through termination of the mission. In carrying out this function, the MOS constantly evaluates the spacecraft performance and prepares and issues appropriate commands. The MOS is supported in its activities by the TDS system as well as with special hardware provided exclusively for the *Surveyor* Project and referred to as mission-dependent equipment. Included in this caetgory are the Command and Data Handling Consoles installed in the DSS's, the Television Ground Data Handling System, and other special display equipment.

## C. Mission Objectives

All *Surveyor III* mission objectives were satisfied. These objectives, which were established before launch, were as follows:

(1) Primary flight objectives:
    (a) Perform a soft landing on the moon within the *Apollo* zone and east of the *Surveyor I* landing site.
    (b) Obtain postlanding television pictures of the lunar surface.

(2) Secondary flight objectives:
    (a) Obtain information on lunar surface bearing strength, radar reflectivity, and thermal properties.
    (b) Use the surface sampler to manipulate the lunar surface. Observe effects with the television camera.

For the *Surveyor III* mission, a five-day launch period from April 17 through April 21, 1967, was selected which optimized the postlanding lunar lighting conditions at the target site and satisfied the other mission constraints.

## D. Mission Summary

*Surveyor III* was launched on April 17, 1967, the first day of the selected launch period, from Pad 36B at Cape Kennedy with the *Atlas/Centaur* AC-12 vehicle. Because of a hold called near the end of the countdown to investigate an anomalous spacecraft telemetry signal, liftoff occurred 51 min after opening of the 70-min window, at 07:05:01.059 GMT. Very satisfactory launch phase performance was achieved. Following *Atlas* powered flight on a 100.8-deg azimuth, the *Centaur* first burn injected the spacecraft into a temporary parking orbit with an altitude close to the nominal 90 nm. After a 22-min coast

period, the *Centaur* was reignited and injected the spacecraft into a very accurate lunar transfer trajectory. The uncorrected lunar impact point was approximately 466 km from the prelaunch target point. The earth–moon trajectory and major events are depicted in Fig. I-1.

Following separation from the *Centaur*, the spacecraft properly executed the automatic antenna/solar panel positioning and sun acquisition sequences. These sequences established the desired attitude of the spacecraft roll axis and ensured an adequate supply of solar energy during the coast period.

Tracking and telemetry data received in one-way lock by stations of the AFETR, MSFN, and DSIF confirmed a normal mission during the near-earth portion of flight. As planned, DSS 42 was the first station to establish two-way lock and exercise control of the spacecraft by command. Thereafter, the DSIF stations provided nearly continuous two-way coverage of the flight, receiving and recording all desired spacecraft data and correctly transmitting all commands.

Spacecraft system performance during the transit coast phases was excellent. The SM/SS electronics temperature fell lower than expected but still was well above survival temperature. Additional gyro drift checks were conducted because the indicated gyro drift rates were near the specification limit of 1.0 deg/hr, but this condition had no adverse effect on the flight.

Spacecraft lock-on with the star Canopus was achieved according to plan about 9½ hr after launch. This provided 3-axes attitude reference which is required before the midcourse and terminal maneuvers can be executed.

Because of the small midcourse maneuver required and the accuracy of the premidcourse orbit determinations, it was possible to choose a new aiming point (2.92 deg south latitude, 23.25 deg west longitude) about 0.42 deg farther north than the original target to maximize the probability of soft-landing. Final selection of this site was based upon examination of *Lunar Orbiter III* high-resolution photographs. During the first "pass" over DSS 11, Goldstone, a roll–pitch maneuver sequence was conducted in preparation for midcourse velocity correction. Then, almost 22 hr after launch, at 05:00 GMT on April 18, 1967, a velocity correction of 4.19 m/sec was executed. Shortly after the velocity correction, the spacecraft was returned to the coast orientation with sun and Canopus lock by execution of the reverse pitch and roll maneuvers.

In preparation for terminal descent, a yaw–pitch–roll maneuver sequence was initiated 38 min before retro ignition to properly align the retrorocket nozzle. This sequence was selected to optimize telecommunication performance with Omniantenna B during the terminal maneuver and descent phases.

The spacecraft altitude marking radar provided a *mark* signal that initiated the automatic descent sequence. After
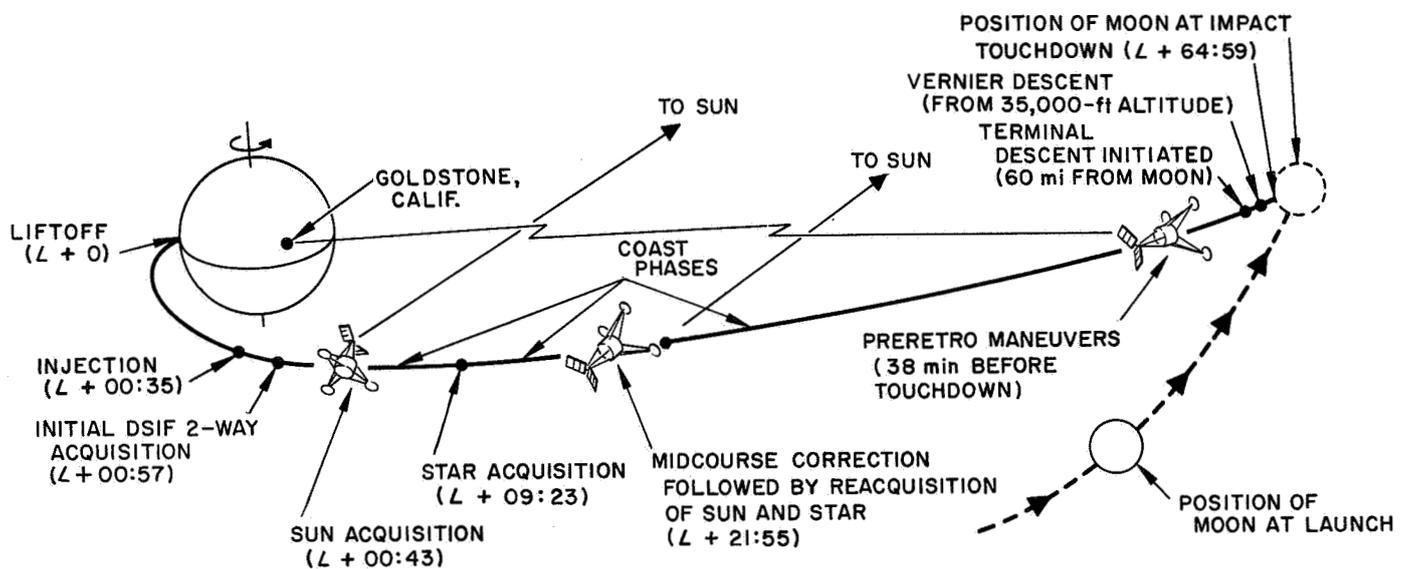


Fig. I-1. Earth-moon trajectory and major events

a delay of 5.1 sec, the three liquid-propellant vernier engines ignited, followed (after an additional 1.1-sec delay) by ignition of the solid-propellant main retro-motor at a lunar slant range of about 270,000 ft and velocity of about 8600 ft/sec. Main retro burnout occurred at a range of 36,000 ft after the spacecraft had been decelerated to a velocity of 492 ft/sec. After the solid motor case was ejected, the radar altimeter and doppler velocity sensor (RADVS) became operational and controlled the final descent by throttling the vernier engines.

The terminal descent phase was completed successfully, although the spacecraft lifted off twice after initial contact with the lunar surface, making three touchdowns before finally coming to rest. Initial touchdown occurred at 00:04:17 GMT on April 20, 1967, with a velocity of about 6 ft/sec. The vernier engines remained on through the first two touchdowns at a thrust level equal to about 90% of the spacecraft lunar weight, causing the spacecraft to rebound each time from the surface. The verniers were turned off by ground command about 1 sec before the third touchdown, and the spacecraft came to rest. A period of 24 sec elapsed between the first and second touchdowns, with an additional 12 sec before final touchdown. The landing occurred within a crater which is about 200 m in diameter and 15 m deep. The spacecraft finally came to rest on a slope about halfway between the eastern rim and center of the crater with the spacecraft Z-axis tilted about 12½ deg from lunar vertical. Interaction with the sloping surface caused the spacecraft to rebound in the downhill direction, although the flight control system acted during each liftoff to correct the spacecraft attitude to the pretouchdown state. The spacecraft traversed about 15 to 22 m during the first liftoff and 11 to 14 m during the second. A small translation of about ⅓ m took place in connection with the third touchdown event. The spacecraft lifted off again after the first two touchdowns because the RADVS lost lock at about 37 ft altitude, resulting in its failure to issue the *14-ft mark* signal, which is required to cut off the vernier engines before touchdown.

The *Surveyor III* landing site has been identified on *Lunar Orbiter III* high-resolution photographs (by correlation of features appearing on early *Surveyor III* television frames), permitting accurate determination of the site location in the Ocean of Storms at 2.94 deg south latitude and 23.34 deg west longitude. This is only 2.76 km from the final aim point and 3.1 km from the final postflight orbit determination. *Surveyor III* landed approximately 625 km (390 mi) east of the site where *Surveyor I* landed successfully on June 2, 1966.

Strain gage readings indicated that each of the *Surveyor III* touchdowns was more gentle than the landing of *Surveyor I*. Nevertheless, analysis of telemetry indicated some damage was sustained by *Surveyor III* subsystem electronics coincident with the second touchdown. Rather than resulting from mechanical landing forces, the damage may have resulted from arcing of high voltage in the presence of an ionized plasma which would have enveloped the spacecraft at touchdown with the vernier engines burning. The most serious effect on the spacecraft was the degradation of circuits in the analog-to-digital converters of the signal processing system, which caused the analog data to become erroneous at the time of second touchdown and resulted in considerable uncertainty in the status of the spacecraft immediately after touchdown. However, by making an intensive and methodical assessment of the spacecraft including the use of many nonstandard sequences, the general nature of the anomaly was determined within a relatively short period of time. It was found that all digital and television data were normal, and most analog data, if transmitted at the lowest rate of 17.2 bit/sec, were quite reliable and could be corrected with special calibration factors.

Early resolution of the telemetry anomaly made it possible to proceed with the planned postlanding operations, although special caution was exercised until confidence in the spacecraft was well established. Landing had occurred when the sun was just above the horizon, as viewed from the spacecraft, and operations were carried out throughout the lunar day until shortly after sunset.

The first television picture was obtained in 200-line mode about 1 hr after touchdown. A total of 54 200-line pictures were obtained before the spacecraft was reconfigured for transmission of 600-line pictures. The 600-line mode required positioning of the solar panel to receive maximum solar power and precise pointing of the planar array toward the earth to provide maximum signal strength. This operation was accomplished quickly under the adverse conditions of an unknown surface slope and incorrect spacecraft telemetry data.

Goldstone was able to receive 323 600-line pictures before the end of its first postlanding pass, when it was necessary to command the spacecraft to an engineering telemetry mode to enable transfer to DSS 42 at Canberra, Australia. A total of over 6300 pictures were received, with the camera being operated on each successive Goldstone pass of the lunar day, except near lunar noon on April 25, when operations were suspended to avoid exceeding thermal limits. The television frames included

(1) a large number of wide- and narrow-angle pictures providing panoramas of the lunar surface out to the horizon, which is the rim of the crater in all directions, (2) pictures taken in coordination with operation of the SM/SS, (3) pictures of Venus to aid in spacecraft attitude determination, (4) images obtained with different lens filters which can be reconstructed on earth in true color, (5) images obtained with different focus settings to provide a means of determining the approximate distance of objects from the camera, (6) pictures of the earth during a total eclipse of the sun and when approximately one-quarter illuminated, and (7) pictures of the visible parts of the spacecraft. Many television pictures were repeated during the lunar day to obtain views under different lighting conditions, and a series of spacecraft and crater shadow progression frames was obtained at the end of the lunar day, including some frames obtained by overseas DSIF stations.

Throughout the mission, the *Surveyor III* pictures received via Goldstone were monitored in real-time on conventional TV monitors using a JPL scan conversion system. The pictures received on the first Goldstone pass were also relayed to commercial TV networks for real-time transmission to the public.

Some of the *Surveyor III* television pictures contained more glare than did those of *Surveyor I*. This was partly due to the unfavorable landed roll orientation to which *Surveyor III* was restricted because of a RADVS beam cross-coupling characteristic, and partly to contamination or pitting of the upper portion of the camera mirror, which probably occurred as a result of landing with the vernier engines on. The camera also experienced some problems in stepping which restricted the television surveys and limited the total number of pictures which were taken.

Operations with the SM/SS were begun with a functional checkout during the second postlanding Goldstone pass. Extensive use was made of the SM/SS on most of the remaining Goldstone passes. Results of the SM/SS operations were obtained in the form of television pic-

tures taken at selected intervals between SM/SS "stepping" commands. The SM/SS performed very well and accomplished the following experiments: eight bearing tests in which the scoop was pushed into the surface with the door closed; 14 impact tests in which the scoop was dropped from different heights; the digging of four trenches with depths up to 7 in.; and the handling and dumping of various surface materials, including the clamping of a small rock.

*Surveyor III* experienced a total eclipse of the sun by the earth on April 24. The spacecraft recorded this event with television pictures of the earth's disc completely occulting the sun while the earth's atmosphere refracted light from the sun, which is visible in the frames. Advantage was also taken of this event to obtain temperature data from which the thermal response of the spacecraft and lunar surface can be derived. Additional thermal data were taken periodically during the lunar day and after sunset until the spacecraft transmitter was turned off.

Spacecraft engineering data were received frequently throughout the lunar day to enable repeated assessment of the spacecraft condition. In addition, two-way doppler tracking data were obtained whenever possible, and several special engineering tests were conducted with *Surveyor III*, many of which were for the purpose of determining the performance and other characteristics of the spacecraft/DSIF telecommunications link.

The condition of *Surveyor III* was considered to be excellent as the lunar day came to a close, and the spacecraft was secured for the night in a configuration which was believed most favorable for its reawakening the second lunar day. A command was sent turning off all spacecraft power (except to the receiver-decoders, which cannot be turned off) at 00:04 GMT on May 4, 14 days after touchdown.

From May 23 to June 2, on the second lunar day, commands were sent repeatedly to revive *Surveyor III*, but all attempts were unsuccessful.

# II. Space Vehicle Preparations and Launch Operations

The *Surveyor III* spacecraft was assembled and sub-jected to flight acceptance testing at the Hughes Aircraft Corporation facility, El Segundo, California. After com-pletion of these tests it was shipped by air to the Air Force Eastern Test Range (AFETR), Cape Kennedy, arriving on December 12, 1966. The *Atlas/Centaur* launch vehicle stages were shipped to AFETR after undergoing testing in the Combined System Test Stand (CSTS) at San Diego. Spacecraft problems with the flight control, propulsion and signal processing subsystems resulted in a decision to return the spacecraft to El Segundo for partial repeat of the flight acceptance testing. The space-craft was shipped from AFETR by truck on December 26, 1966. Reverification testing at El Segundo consisted of a modified solar–thermal–vacuum test sequence at low sun intensity, Z-axis vibration and vernier engine vibration. Upon completion of these tests, the spacecraft was again air-shipped to AFETR, arriving on February 13, 1967. Prelaunch assembly, checkout, and systems tests were accomplished successfully and the space vehicle was launched on April 17, 1967, at 07:05:01.059 GMT, 51 min after opening of the first scheduled launch window.

## A. Spacecraft Assembly and Testing

Tests and operations on each spacecraft are conducted by a test team and data analysis team which work with the spacecraft throughout the period from the beginning of testing until launch. The test equipment used to con-trol and monitor the spacecraft system performance at all test facilities includes (1) a system test equipment assembly (STEA) containing equipment for testing each of the spacecraft subsystems, (2) a command and data handling console (CDC) similar to the units located at each of the DSIF stations (see Section VI) for receiving telemetry and TV data and sending commands, and (3) a computer data system (CDS) for automatic monitoring of the spacecraft system. Automatic monitoring capability is necessary because of the large number of telemetered data points and high sampling frequency of most of the *Surveyor* telemetry modes. The CDS provides the fol-lowing features to aid the data analysis personnel in evaluating the spacecraft performance:

(1) Digital magnetic tape recording of all input data.

(2) Suppression of nonchanging data. Only data points which reflect a change are printed on display devices.

(3) Alarm limit capability. Critical telemetry functions are monitored for out-of-tolerance indications which would be damaging to the spacecraft. An audible alarm sounds if these limits are exceeded.

(4) Request message. In the event that telemetry data is desired for evaluation, a print of requested data is provided.

The *Surveyor III* spacecraft (SC-3) began system testing on April 20, 1966, and passed through the following test phases:

## 1. Spacecraft Ambient Testing

The ambient testing phase consists of initial system checkout (ISCO) and mission sequence tests. In the initial systems checkout, each subsystem is tested for compatibility and calibration with other subsystems and a systems readiness test is performed for initial system operational verification. The primary objectives of the mission sequence tests are to obtain system performance characteristics under ambient conditions and in the electromagnetic environment expected on the launch pad and in flight prior to separation from the *Centaur*.

During the ISCO test phase, one month of down time was required for STEA upgrade, which delayed completion of the test until July 20, 1966. After the initial system checkout, three mission sequences were completed. The last of these was a plugs-out run approaching flight configuration with simulated electromagnetic environment.

## 2. Solar–Thermal–Vacuum (STV) Testing

The STV test sequences are conducted to verify proper spacecraft performance in simulated missions at various solar intensities and a vacuum environment. In these tests, as well as the vibration test phase which follows, the propellant tanks are loaded with "referee" fluids to simulate flight weight and thermal characteristics.

Testing was begun with the *Surveyor III* spacecraft in the solar–vacuum chamber in mid-August, 1966. The first sequence (Phase A), conducted at 87% of nominal sun intensity, was successful and was followed immediately by a second sequence (Phase B) at 112% sun intensity. During Phase B, the chamber pressure increased and the spacecraft automatically shut down. Checkout of the spacecraft revealed a loss of referee fluid and iron oxide contamination of the fuel system. The fuel tanks and lines were changed and the spacecraft prepared for the third STV sequence (Phase C), which began on October 6, 1966. In this sequence problems were encountered with the Transmitter B RF transfer switch, auxiliary engineering signal processor (AESP), and oxidizer tank temperature. Verification of the fixes to these problems was accomplished by conducting a modified Phase C sequence with shortened mission time. During this test, problems were encountered with Transmitter A, the strain gage amplifiers, and an AESP failure. These problems were corrected and the Phase C sequence was repeated

for the full mission time. This test was successful, and the spacecraft was removed from the vacuum chamber and preparations for alignment and vibration testing were initiated.

## 3. System Vibration Testing

Vibration tests are conducted in the three orthogonal axes of the spacecraft to verify proper operations after exposure to a simulated launch-phase vibration environment. For these tests the spacecraft is placed in the launch configuration, with legs and omniantennas in the folded position. In addition, a vernier engine vibration (VEV) test is conducted, with vibration input at the vernier engine mounting points to simulate the environment during the midcourse maneuver and terminal descent phases of flight.

The *Surveyor III* vibration test phase began on October 28, 1966. The *Surveyor II* Failure Review Board changes to the spacecraft were incorporated during test preparations. The spacecraft progressed through the three axes of vibration with no major problems. The vibration testing was completed on November 26, 1966, and the spacecraft proceeded with postvibration alignment and vernier engine vibration. The VEV phase was completed on December 6, 1966, and the spacecraft shipped to AFETR by aircraft on December 11, 1966. The Combined System Test (CST) phase was eliminated from the SC-3 operations because of schedule limitations.

## B. Launch Vehicle Combined Systems Testing

Following successful completion of factory acceptance testing of each stage, the *Atlas* was installed in the CSTS at San Diego, California, on September 16, 1966, followed by the *Centaur* on October 4, 1966. Test sequences in the CSTS culminated in the vehicle Combined Acceptance Test on November 1. Minor hardware modifications and replacements were completed, and the NASA data review on November 8 and 9 determined the vehicle to be acceptable and ready for shipment to AFETR. The *Atlas* was shipped overland on November 9, followed by the nose fairing and interstage adapter on November 11. The *Centaur* was air-shipped on the Guppy aircraft on November 14, 1966.

## C. Initial Spacecraft Operations at AFETR

The spacecraft arrived at AFETR on December 12, 1966, and proceeded through receiving inspection. After completion of inspection and assembly, the performance verification tests (PVT) were started. An AESP failure

was found during PVT 1 and was attributed to an improperly grounded soldering iron. Checkout also showed possible damage to a strain gage amplifier. PVT 1 and the system readiness test (SRT) were completed, and the soil mechanics/surface sampler (SM/SS) hardware was installed and tested. As PVT 3 was started, a short in the ground equipment resulted in failure of the flight control sensor group (FCSG) and possible overstressing of other units. During this period, when Oxidizer Tank 2 was removed for rework of the temperature transducer stand-off, the bladders on the other two tanks were accidently collapsed. Leak checks were performed to verify bladder integrity. The combination of problems and unit replacements was reviewed and the decision was made to return the spacecraft to El Segundo for revalidation by environmental testing. The spacecraft was returned to El Segundo by truck and arrived on January 3, 1967.

## D. Spacecraft Retest at El Segundo

The retest program for the *Surveyor III* spacecraft consisted of a modified plugs-out full-length STV test with 87% sun intensity followed by Z-axis vibration and vernier engine vibration.

Analysis of truck vibration data, recorded during the return to El Segundo, indicated that the spacecraft had been subject to excessive loads. A complete review of the spacecraft mechanical and performance parameters revealed the television camera drive system to be the only damaged equipment. The camera was replaced and the spacecraft proceeded to STV testing. During this sequence of testing, the SM/SS hardware was also verified in the expected environmental conditions. No major problems were encountered during the environmental testing. A special propellant system flow test was performed after vibration to verify the total system flow capability. Vernier engine vibration (Fig. II-1) was completed on February 4, 1967 and the spacecraft was again shipped to AFETR by air and arrived on February 13, 1967.

## E. Final Launch Operations at AFETR

The major operations performed at AFETR after arrival of the launch vehicle and second arrival of the spacecraft are listed in Table II-1.

### 1. Initial Preparations

The *Atlas* and *Centaur* stages of AC-12 were erected on November 22 and 23, respectively. All required testing, preliminary to the Joint Flight Acceptance Composite Test

(J-FACT) was culminated with a successful Guidance/Autopilot (GAP) integrated test on December 16, 1966. When the spacecraft was returned to El Segundo on January 3, 1967, AC-12 was placed in a standby status. Vehicle monitoring activities and necessary flight and support equipment compatibility tests were conducted to maintain a proper condition of readiness until return of the spacecraft on February 13. A GAP test, the last major flight system test before spacecraft mating, was successfully rerun on March 2, 1967.

The spacecraft was re-assembled and PVT 1, PVT 3, and SRT A were performed. As a result of the *Surveyor II* failure review, a special vernier engine thrust chamber assembly (TCA) functional test was performed to verify TCA compatibility with the spacecraft.

PVT 4 and the TV calibration tests were performed. During these tests several problems were encountered which resulted in rework or replacement of spacecraft units. The roll actuator mounting studs came loose and the subsequent unit area checks showed an increase in the cogging voltage. Retro accelerometer variations were encountered and the unit was replaced. Telemetry variations were noted with the radar altimeter and doppler velocity sensor (RADVS) turned on, and a zener diode was added to isolate the interference. Parallel operations to prepare the main retro revealed a separation in the case liner, and the spare unit was processed for flight.

On February 27, 1967, the spacecraft was transported to the Explosive Safe Facility (ESF) where it was prepared for J-FACT launch pad operations. The spacecraft was encapsulated (Fig. II-2) on March 3, then transported to the pad and mated to the *Centaur* on March 4, 1967.

### 2. Joint Flight Acceptance Composite Test

After the spacecraft was mated with *Centaur*, an SRT and practice countdown were performed to verify proper operations of the spacecraft and all support equipment. On March 5 and 6, a compatibility test between the spacecraft and DSS 71 at Cape Kennedy was successfully accomplished.

J-FACT was performed on March 7, with the spacecraft operating in the actual prelaunch environment. This test included a simulation of launch events through spacecraft separation and *Centaur* retromaneuver. During the J-FACT, the shock absorber strain gage on Leg 2 of the spacecraft showed a frequency shift which could not be duplicated until the final launch pad operations, when
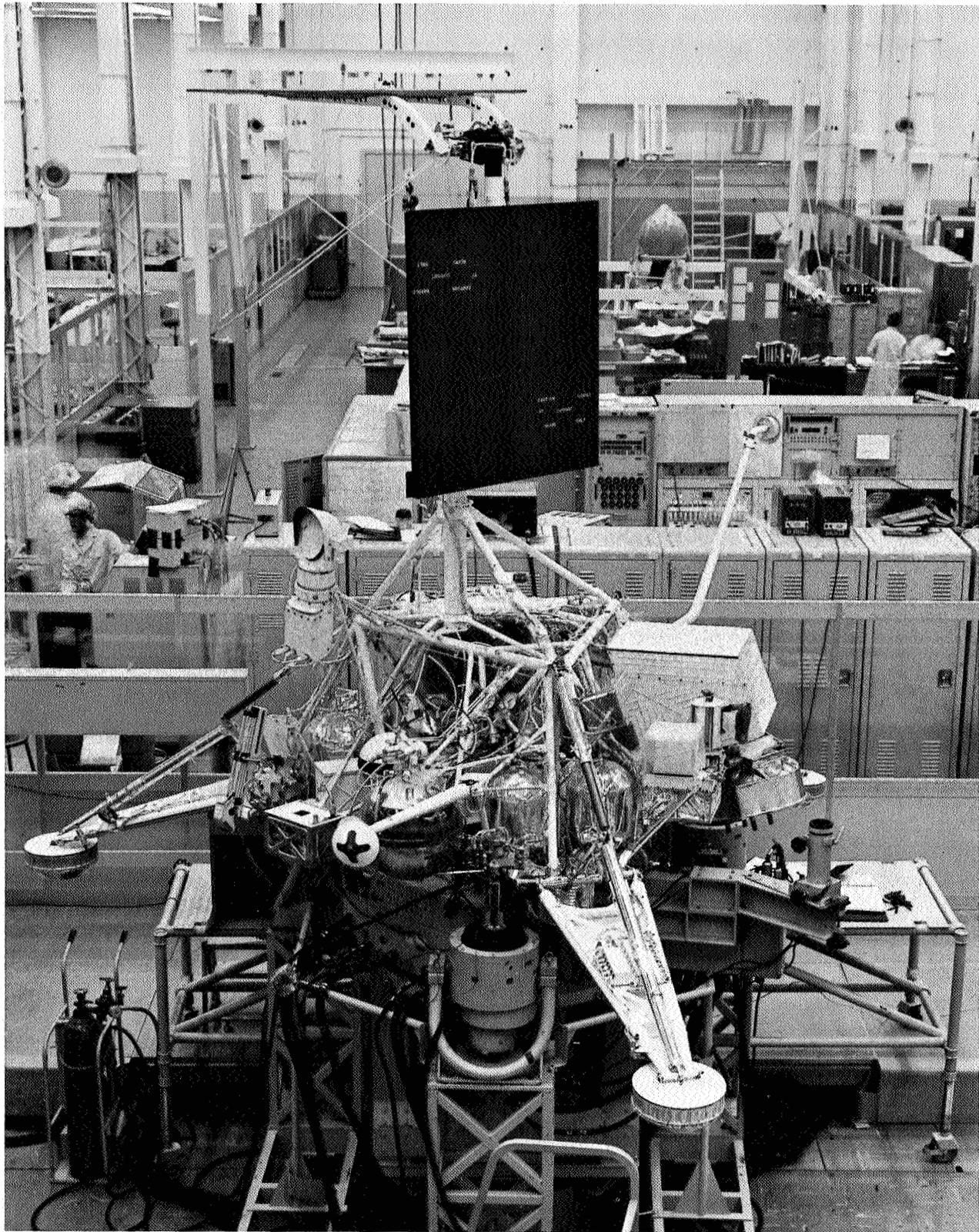
Fig. II-1. *Surveyor III* vernier engine vibration retest
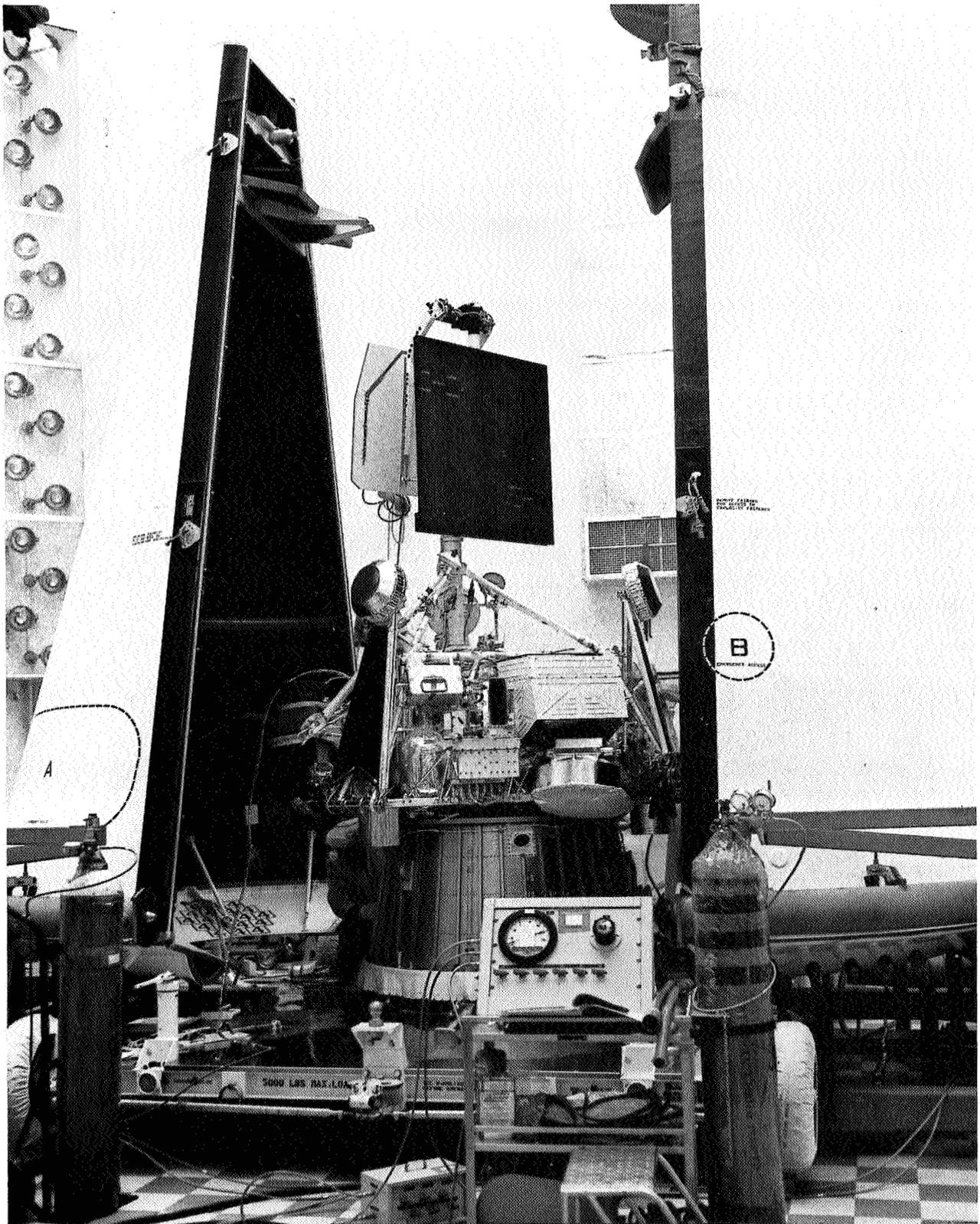
Fig. II-2. *Surveyor III* spacecraft prepared for encapsulation

## Table II-1. Major operations at Cape Kennedy

| Operation | Location | Date completed |
|---|---|---|
| AC-12ᵃ erection | Launch Complex 36B | November 23, 1966 |
| SC-3ᵇ inspection, reassembly, initial testing | Building AO | February 19, 1967 |
| SC-3 vernier engine spacecraft functional test | Building AO | February 22 |
| SC-3 TV system test and calibration | Building AO | February 26 |
| SC-3 preparations for Joint Flight Acceptance Composite Test (J-FACT) | Explosive Safe Facility (ESF) | March 3 |
| SC-3 mate to Centaur | Launch Complex 36B | March 4 |
| DSS 71/SC-3 compatability test | Launch Complex 36B | March 6 |
| AC-12/SC-3 J-FACT | Launch Complex 36B | March 7 |
| SC-3 demate | Launch Complex 36B | March 7 |
| SC-3 decapsulation, depressurization, removal of J-FACT items and initial alignment | Explosive Safe Facility | March 12 |
| SC-3 power profile test | Building AO | March 14 |
| SC-3 PVT 5 mission sequence | Building AO | March 19 |
| AC-12 propellant tanking test (first) | Launch Complex 36B | March 21 |
| SC-3 vernier system pressure leak test | Explosive Safe Facility | March 24 |
| AC-12 propellant tanking test (second) | Launch Complex 36B | March 24 |
| SC-3 propellant loading | Explosive Safe Facility | March 28 |
| AC-12 Flight Acceptance Composite Test (without SC-3) | Launch Complex 36B | March 31 |
| SC-3 final weight, balance, and alignment | Explosive Safe Facility | April 5 |
| AC-12 Composite Readiness Test (CRT) | Launch Complex 36B | April 10 |
| SC-3 encapsulation and Systems Readiness Test (SRT) | Explosive Safe Facility | April 11 |
| SC-3 final mate to Centaur | Launch Complex 36B | April 12 |
| AC-12 Atlas retanking | Launch Complex 36B | April 16 |
| Launch | Launch Complex 36B | April 17 |

ᵃAtlas/Centaur vehicle designation.
ᵇSurveyor III spacecraft designation.

it was attributed to *Centaur* telemetry interference. The accelerometer near spacecraft Attach Point 2 also showed erratic operation and was subsequently disconnected to avoid a shorting failure mode in the amplifier.

Spacecraft/*Centaur* separation is simulated in the J-FACT by manually disconnecting the field joint electrical connector. During the securing operations after J-FACT, the spacecraft main power bus was momentarily shorted to ground while remating this connector, resulting in a shutdown of the spacecraft transmitters. To avoid possible damage to the spacecraft, it was decided not to turn the spacecraft on again while mated to the *Centaur* and to reschedule the spacecraft RF system calibration test (which had been scheduled to be conducted immediately after J-FACT) after final mate to the vehicle. Accordingly, the spacecraft was demated on the same day and returned to the ESF, where it was decapsulated and depressurized. A complete visual and electrical checkout revealed no apparent damage and it was decided to proceed with final flight preparation.

The spacecraft temperature was maintained constant during the encapsulated period of J-FACT operations except during the J-FACT test itself to permit accurate pressure decay measurements of the vernier propulsion system and attitude control system.

### 3. Final Flight Preparations

During spacecraft depressurization after J-FACT, a calibration was performed on the helium and nitrogen pressure transducers. The dummy retro motor, altitude marking radar (AMR), and battery were removed and initial alignment was completed at the ESF (Fig. II-3).

On March 13, the spacecraft was transported back to the spacecraft checkout facility in Building AO. In accordance with the *Surveyor II* Failure Review Board recommendations, a power profile test was performed to provide calibrated power telemetry values. PVT 5 was performed as the final spacecraft systems test, after which the spacecraft was prepared for propellant loading.
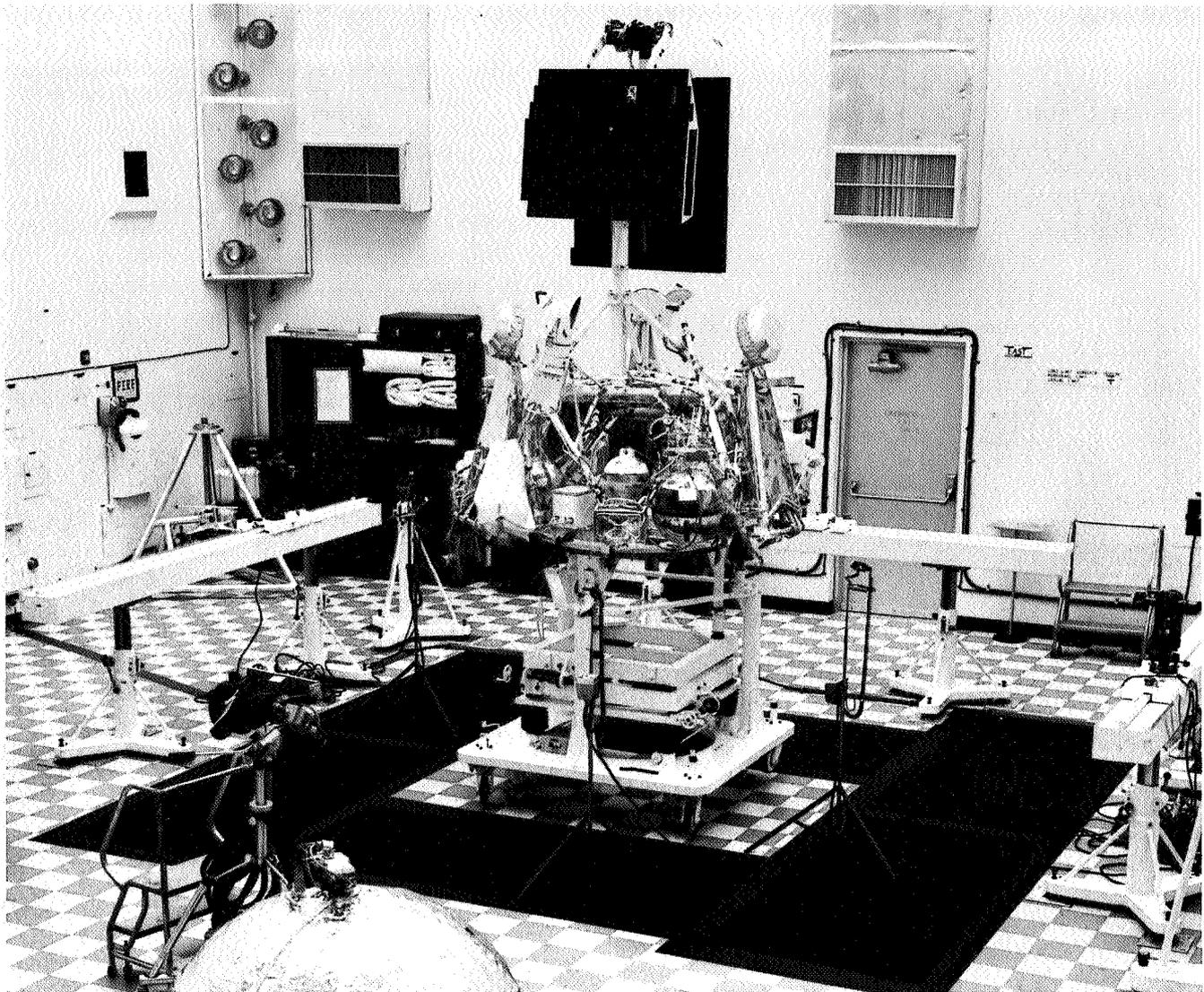
Fig. II-3. *Surveyor III* spacecraft undergoing alignment checks in ESF

On March 22, the spacecraft was returned to the ESF for final flight preparations. A leak test was performed with solvent at low and high pressures to validate the vernier propulsion system and calibrate the pressure transducer. A leak developed in Oxidizer Tank 1, and the tank was replaced. No apparent damage to the thermal control surfaces of the spacecraft resulted from the leak. The high-pressure test was repeated to verify system integrity, and propellant loading was completed on March 28. The spacecraft was then processed for pyrotechnic and retro installation and final alignment and weighing. PVT 6 test steps were phased with the final preparations. The squib connector verifications showed a broken wire in one connector, and the connector was replaced. This and other wire breakages encountered

during the ETR operations resulted in a decision to check all of this type of connector and pot the connectors with a soft compound for added support.

Tests that had been conducted on the spacecraft during the final assembly period at El Segundo indicated that a modification was required to the pin puller assemblies. The pin pullers were removed, modified, and reinstalled on the spacecraft.

Continuous toxic gas monitoring was performed subsequent to spacecraft liquid propellant loading. Small vapor leaks were noted at the bases of Oxidizer Tanks 1 and 3. Liquid was not detectable and the leak rate appeared constant. The oxidizer tank pressure was raised

to the maximum "man rating" limit to provide a better seal, and the leak rate dropped to nearly zero.

On April 6, the spacecraft was mated to the forward adapter and the helium and nitrogen tanks were brought to flight pressures. The spacecraft was then encapsulated and an SRT was performed on April 11. Final mate to *Centaur* occurred on April 12.

Following J-FACT, two *Atlas/Centaur* Propellant Tanking Tests were performed on March 21 and March 24 without the spacecraft. During a Propellant Tanking Test the vehicle is completely tanked with propellants and pressurized. The second tanking test was conducted because of several problems encountered during the first test. An *Atlas/Centaur* FACT was successfully completed as scheduled on March 31, and a CRT was run on April 10, 1967. When recycling during a hold in the CRT countdown, the *Atlas* inverter frequency shifted out of tolerance. A spare inverter was installed, and the CRT was accomplished successfully on the same day.

Final spacecraft and launch vehicle checks began immediately after spacecraft mating to the *Centaur*. Another spacecraft SRT was performed on April 12. On April 13, the spacecraft RF system was calibrated with the service tower in the launch position (removed), and the retro motor safe and arm check and a simulated countdown were performed. It was planned to run the simulated countdown with the service tower in the launch position, but high surface winds required moving the tower back around the launch vehicle.

On April 15, a decision was made to replace the *Atlas* sustainer actuator because of a generic shorting problem, which was first encountered with the feedback transducer on another unit during flight acceptance testing. Occurring so close to launch, this was a difficult component change requiring several major operations including detanking of the *Atlas* and the retesting of many vehicle systems. All required activities were accomplished without affecting the launch schedule, and the *Atlas* was retanked on April 16.

## 4. Countdown and Launch

The final spacecraft SRT was started at 17:44 GMT on April 16 at a countdown time of *T*-680 min and was completed at *T*-290 min. The vernier engine roll actuator position reading was observed to be erratic during the SRT. Therefore, a special flight control test was con-

ducted with SC-3, and it was noted that, although the actuator should be in a pinned position for launch, the position transducer of the roll actuator indicated motion during flight control gyro loop testing. In order to resolve this anomaly, SC-2 data were reviewed and verification tests were conducted on SC-5 in El Segundo.

While the spacecraft anomaly was being investigated, the countdown proceeded normally down to the scheduled 10 min hold at *T*-5 min. It was necessary, however, to extend the *T*-5 min hold because the spacecraft anomaly had not been resolved. Finally, results of the SC-5 test and the SC-2 data review verified that the behavior of the roll actuator position signal was characteristic of the system, and SC-3 was ready for launch. The countdown was resumed at 07:00 GMT, after a total delay of 51 min. Liftoff (Fig. II-4) occurred at 07:05:01.059 GMT, April 17, 1967, on a flight azimuth of 100.809 deg. It is a notable achievement that the launch vehicle developed no problems during the countdown and was able to proceed smoothly to liftoff after holding an extra 51 min with all cryogenics aboard.

A countdown time summary is shown in Table II-2. The countdown included a total of 70 min of planned, built-in holds—one of 60-min duration at *T*-90 min, and a second of 10-min duration at *T*-5 min. The launch window for April 17 extended from 06:14 to 07:24 GMT, providing a duration of 71 min, 51 min of which was consumed by the unscheduled hold at *T*-5 min.

**Table II-2. Surveyor III countdown time summary**

| Event | Countdown time, min | GMT |
|---|---|---|
| | | (April 16) |
| Started spacecraft SRT | T-680 | 17:44 |
| Completed spacecraft SRT | T-290 | 00:14 |
| Started 60-min built-in hold (BIH) | T-90 | 03:34 |
| Spacecraft joined launch vehicle countdown | T-90 | 04:19 |
| End BIH; resumed countdown | T-90 | 04:34 |
| | | (April 17) |
| Started 15-min BIH | T-5 | 05:59 |
| BIH extended | T-5 | 06:09 |
| Window opening | | 06:14 |
| Resumed countdown | T-5 | 07:00 |
| Liftoff (L + D) | T-0 | 07:05:01.059 |
| Window closing | L + 20 | 07:25 |
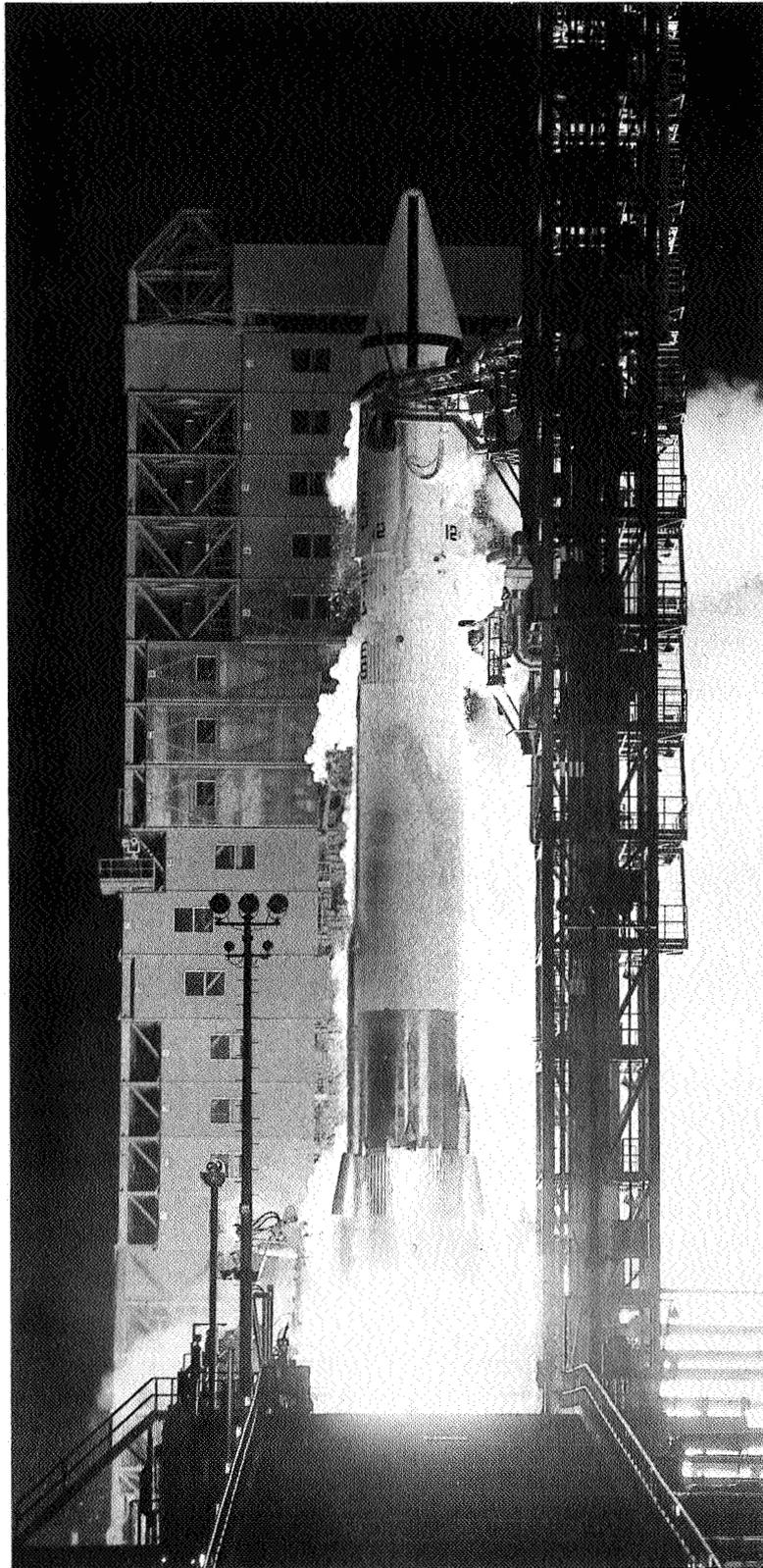
Fig. II-4. *Atlas/Centaur AC-12 launching Surveyor III*

All vehicle systems performed satisfactorily throughout the launch, and the spacecraft was accurately injected into a lunar transfer trajectory. The *Centaur* burn periods were longer than expected but had no detrimental effect on the mission. Damage to Launch Complex 36B was extremely light. The powered flight sequence of events and launch vehicle performance are described in Section III.

The atmospheric conditions during the launch operation were favorable, with unusually good visibility. (Photographic coverage of the launch was obtained until the vehicle passed over the horizon.) Surface winds were 4 knots from 210 deg. Surface temperature was 67°F, with relative humidity of 92% and a dewpoint of 64.4°F. Sea level atmospheric pressure was 1015.9 millibars. Scattered cloud cover of 0.2 stratus existed at 4500 ft. Maximum measured winds aloft were reported to be 43 knots from 316±20 deg at 46,000 ft. The maximum expected wind shear parameter was 10 ft/sec per thousand feet of altitude occurring between 39,300 and 41,800 ft from 315±20 deg.

## F. Launch Phase Real-Time Mission Analysis

The launch windows which were finally established for the April 1967 launch period are shown in Fig. II-5. Launching on days prior to April 17 was not acceptable because touchdown at the desired lunar landing site would have occurred in darkness (prior to sunrise). On April 17, the launch window was constrained to open at approximately 95 deg in order not to exceed the *Centaur* parking orbit coast time limit of 25 min. On the remaining days, window opening was constrained to avoid excessive gaps in telemetry coverage during parking orbit coast. Continuous spacecraft data during parking orbit was desired via spacecraft S-band or *Centaur* VHF link, although this requirement was relaxed somewhat on April 17 to increase the window length on that day. April 17 was considered the most favorable launch day because lunar landing could be achieved early in the lunar day at low sun angles, which was greatly desired primarily to enhance photographic results. As shown in Fig. II-5, the windows for April 20 and 21 closed at the 115-deg Range Safety azimuth constraint. However, this was dependent upon initial two-way acquisition by DSS 72, the plan for which had not been confirmed. The windows for these days would have been substantially reduced without the command capability of DSS 72 to switch the spacecraft transmitter from high to low power before high power would have been on in excess of 60 min.
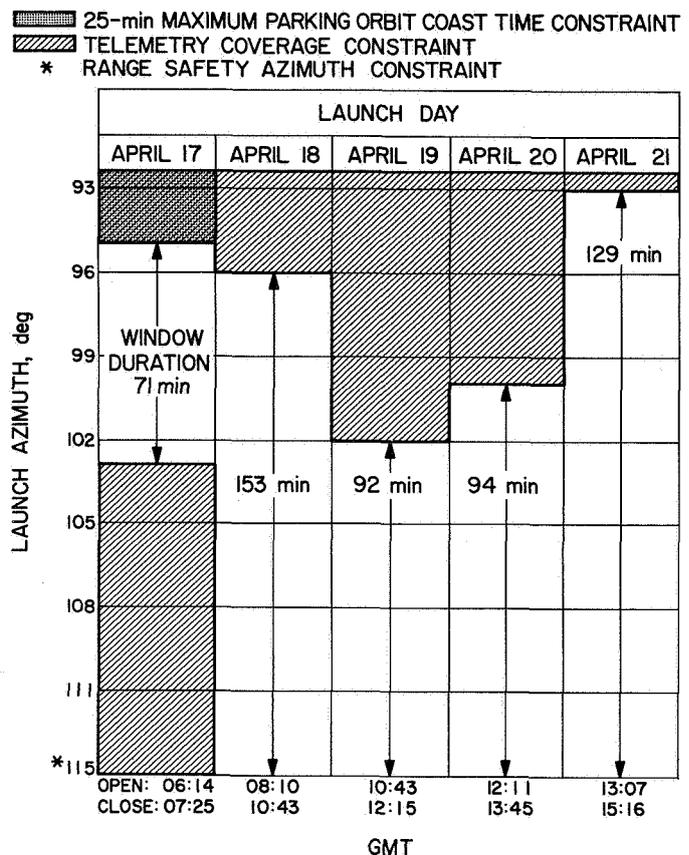


Fig. II-5. Final *Surveyor III* launch window design for April 1967

The telemetry coverage constraint causing the window to close at the 103-deg azimuth on April 17 was due to a problem which arose only a week before launch. The AFETR range instrumentation ship *Twin Falls*, which was to have played a key roll in providing tracking and telemetry coverage for higher azimuth launches during the *Centaur* second prestart and burn period, was unable to reach its station owing to serious illness aboard ship.

Pretoria station was able to provide required post-MECO 2 tracking coverage to 108 deg, but telemetry coverage of the second burn including the 40-sec prestart sequence only to 98 deg. To help fill the telemetry coverage gap, two AFETR telemetry aircraft were dispatched to stage from downrange. However, the aircraft could only extend the telemetry coverage capability to 103 deg azimuth. Nevertheless, this capability proved to be of critical importance since the launch did take place on an azimuth (100.809 deg) which was dependent upon the aircraft coverage. (Also refer to Section V-A for discussions of AFETR coverage.)

## 1. Countdown to Launch

During countdown operations, those factors acting to constrain the launch window or period were continually evaluated by the Launch Phase Mission Analyst. The Mission Director was advised of these evaluations for consideration in the launch or hold decision.

The Tracking and Data System (TDS) reported a few minor problems during the countdown. However, none of these problems constituted a hold condition and, by launch, they had all cleared up. The launch vehicle proceeded through the count without any problems, but the spacecraft developed the roll actuator telemetery signal anomaly described earlier, which delayed the launch until 51 min after window opening.

## 2. Launch to DSIF Acquisition

During the launch, the occurrence of space vehicle *mark* events was reported in near-real-time, followed later with reports of the times at which they occurred. The *mark* event times are presented in Appendix A, Table A-1. The only notable deviations in *mark* event times from nominal times were the durations of the first and second *Centaur* burn periods. All concern over the long first burn duration was removed when the first parking orbit computation of the real-time computer system (RTCS) at Cape Kennedy indicated nominal parking orbit insertion conditions. This first parking orbit deter-

mination, based on Antigua radar data, was computed about 5 min after first main engine cutoff (MECO 1). The normality of the flight from launch to parking orbit insertion was further confirmed by the following information sources: (1) the running commentary on the "quick-look" analysis of real-time launch vehicle telemetry data, which lasted until about 3 min after MECO 1, (2) the reports of uprange tracking station view periods, and (3) Range Safety analysis reports.

For the remainder of the near-earth flight phase, evaluation of the mission status was dependent upon RTCS trajectory calculations, and reports of spacecraft performance, *mark* events, and tracking station view periods. The only exception to expected station acquisitions was the failure of the *Twin Falls* to acquire the *Centaur* C-band beacon, although it did acquire the vehicle telemetry signals. The first lunar transfer orbit was computed by the RTCS 19 min after MECO 2, based on Pretoria station radar data. Although the fit of this orbit was considered "fair" because the data contained many off-track points, it did indicate that the spacecraft was on a lunar intercept trajectory well within the midcourse correction capability. Later RTCS and SFOF computations using DSS 42 data further confirmed a satisfactory transfer orbit. (Also refer to Section VII for discussion of transfer orbit determinations.) A *Centaur* stage orbit determination was also computed by the RTCS, which indicated that a satisfactory *Centaur* retromaneuver had been achieved.

# III. Launch Vehicle System

The *Surveyor III* spacecraft was successfully injected into its lunar transit trajectory by a General Dynamics *Atlas/Centaur* launch vehicle (AC-12). The vehicle was launched April 17, 1967, at 07:05:01.059 GMT on a "parking orbit" ascent trajectory from Launch Complex 36B of the AFETR at Cape Kennedy, Florida. This was the first *Atlas/Centaur* operational flight to utilize the indirect ascent mode wherein the *Centaur* second stage coasts for as long as 25 min in a parking orbit before reigniting and thrusting a second time to achieve the desired injection conditions. The first two operational flights of the *Atlas/Centaur* vehicle (AC-10 and AC-7) on the *Surveyor I* and *II* missions utilized the direct-ascent mode, which requires only one "burn" of the second stage to achieve injection. Several design modifications were incorporated in the *Centaur* stage for parking orbit missions in order to achieve propellant control under the low gravity environment during the coast period and to ensure successful second ignition. Operational capability for two-burn missions had been demonstrated with the final *Atlas/Centaur* development flight of AC-9 on October 29, 1966.

The *Atlas/Centaur* vehicle with the *Surveyor* spacecraft encapsulated in the nose fairing is 113 ft long and weighs 303,000 lb at liftoff (2-in. rise). The basic diameter of the vehicle is a constant 10 ft from the aft end to the base of the conical section of the nose fairing. The configuration of the completely assembled vehicle is illustrated in Fig. III-1. Both the *Atlas* first stage and *Centaur* second stage utilize thin-wall, pressurized, main propellant tank sections of monocoque construction to provide primary structural integrity and support for all vehicle systems. The first and second stages are joined by an interstage adapter section of conventional sheet and stringer design. The clamshell nose fairing is constructed of laminated fiberglass over a fiberglass honeycomb core and attaches to the forward end of the *Centaur* cylindrical tank section.

## A. Atlas Stage

The first stage of the *Atlas/Centaur* vehicle is a modified version of the *Atlas D* used on many previous NASA and Air Force missions such as *Ranger, Mariner,* and OGO. The *Atlas* utilizes the Rocketdyne MA-5 propulsion system, which burns RP-1 kerosene and liquid oxygen in each of its five engines to provide a total liftoff thrust of approximately 387,000 lb. The individual sea-level thrust ratings of the engines are: two booster engines at 165,000 lb each; one sustainer engine at

NOSE FAIRING

SURVEYOR
SPACECRAFT

FORWARD EQUIPMENT
COMPARTMENT

LIQUID HYDROGEN
TANK

INSULATION
PANEL (4)

CENTAUR
STAGE

LIQUID OXYGEN
TANK

CENTAUR MAIN
ENGINE (2)

INTERSTAGE
ADAPTER

LIQUID OXYGEN
TANK

ANTISLOSH BAFFLE
ASSEMBLY

LIQUID OXYGEN
DUCT

ATLAS
STAGE

FUEL TANK

EQUIPMENT POD (2)

ANTIVORTEX
BAFFLE

ATLAS RETROROCKET (8)

VERNIER THRUST
CHAMBER (2)

BOOSTER THRUST
CHAMBER (2)

SUSTAINER THRUST
CHAMBER

**Fig. III-1.** *Atlas/Centaur/Surveyor* **space vehicle configuration**

57,000 lb; and two vernier engines at 670 lb each. The *Atlas* can be considered a 1½-stage vehicle because the "booster section," weighing 6000 lb and consisting of the two booster engines together with the booster turbo-pumps and other equipment located in the aft section, is jettisoned after about 2.4 min of flight. The sustainer and vernier engines continue to burn until propellant depletion. A mercury manometer propellant utilization system is used to control mixture ratio for the purpose of minimizing propellant residuals at *Atlas* burnout. A change was incorporated in the AC-12 *Atlas* propulsion system providing for use of orifice restrictors and rerouting of helium control lines to avoid possible damage during booster staging and reduce resulting helium leakage which apparently caused early *Atlas* sustainer cutoff on the AC-9 flight.

Flight control of the first stage is accomplished by the *Atlas* autopilot, which contains displacement gyros for attitude reference, rate gyros for response damping, and a programmer to control flight sequencing until *Atlas/Centaur* separation. After booster jettison, the *Atlas* autopilot also is fed steering commands from the all-inertial guidance set located in the *Centaur* stage. Vehicle attitude and steering control are achieved by the coordinated gimballing of the five thrust chambers in response to autopilot signals.

The *Atlas* contains a single VHF telemetry system which transmits data until *Atlas* sustainer separation. The system operates on a frequency of 229.9 MHz over two antennas mounted on opposite sides of the vehicle at the forward ends of the equipment pods. On the AC-12 flight, 97 *Atlas* measurements were telemetered. Redundant range-safety command receivers and a single destructor unit are employed on the *Atlas* to provide the Range Safety Officer with means of terminating the flight by initiating engine cutoff and destroying the vehicle. The system is inactive after normal *Atlas/Centaur* staging occurs.

## B. Centaur Stage

The *Centaur* second stage is the first vehicle to utilize liquid hydrogen/liquid oxygen, high-specific-impulse propellants. The cryogenic propellants require special insulation to be used for the forward, aft, and intermediate bulkheads as well as the cylindrical walls of the tanks. The cylindrical tank section is thermally insulated by four jettisonable insulation panels having built-in fairings to accommodate antennas, conduits, and other tank protrusions. Most of the *Centaur* electronic equipment packages are mounted on the forward tank bulkhead in a compartment which is air-conditioned prior to liftoff.

The *Centaur* is powered by two Pratt & Whitney constant-thrust engines rated at 15,000 lb thrust each in vacuum. Each engine can be gimballed to provide control in pitch, yaw, and roll. Propellant is fed from each of the tanks to the engines by boost pumps driven by hydrogen peroxide turbines. In addition, each engine contains integral "boot-strap" turbopumps driven by hydrogen propellant, which is also used for regenerative cooling of the thrust chambers. A propellant utilization system is used on the *Centaur* stage to achieve minimum residual of one propellant at depletion of the other. The system controls the mixture ratio valves as a continuous function of propellant in the tanks by means of capacitive-type tank probes and an error ratio detector. The nominal oxygen/hydrogen mixture ratio is 5:1 by weight.

The AC-12 *Centaur* stage utilized RL10A-3-3 main engines which were improved over those used on previous operational flights. The engine turbopumps were redesigned to operate at lower NPSH, and the specific impulse was increased from 433 to 444 sec by improving the propellant injector design and increasing the nozzle expansion ratio. Nozzle expansion ratio was increased by reducing the throat area, increasing the nozzle exit area, and increasing the chamber pressure from 300 to 400 psi to maintain the 15,000-lb thrust level. Special design features are incorporated in the hydrogen tank design for parking orbit missions to ensure propellant control during the coast phase. These include (1) an antiswirl/antislosh baffle located at the hydrogen level at the end of first burn, (2) diffusers for energy dissipation at the tank inlets of propellant return and helium pressurization lines, and (3) special ducting to provide balanced thrust venting of the hydrogen tank.

The second stage utilizes a Minneapolis-Honeywell all-inertial guidance system containing an on-board computer which provides a pitch and yaw corrective program for wind shear relief during *Atlas* booster phase and vehicle steering commands after jettison of the *Atlas* booster section. The *Centaur* guidance signals are fed to the *Atlas* autopilot until *Atlas* sustainer engine cutoff and to the *Centaur* autopilot after *Centaur* main engine ignition. During flight, platform gyro drifts are compensated for analytically by the guidance system computer rather than by applying corrective gyro torquing signals. The *Centaur* autopilot system provides the primary control functions required for vehicle stabilization during powered flight, execution of guidance system steering commands, and attitude orientation during parking orbit coast and following the powered phase of flight. In addition, the autopilot system employs an electromechanical

timer to control the sequence of programmed events during the *Centaur* phase of flight, including a series of commands required to be sent to the spacecraft prior to spacecraft separation. A dual-timer configuration was used on AC-12 to provide for the additional programmer events required on a parking orbit mission.

The *Centaur* reaction control system provides thrust to control the vehicle during parking orbit coast and after powered flight. For small corrections in yaw, pitch, and roll attitude control, the system utilizes six individually controlled, fixed-axes, constant-thrust, hydrogen peroxide reaction engines. These engines are mounted in clusters of three, 180 deg apart, near the periphery of the main propellant tanks just aft of the interstage adapter separation plane. Each cluster contains one 6-lb-thrust engine for pitch control and two 3.5-lb-thrust engines for yaw and roll control. In addition, four 50-lb-thrust and four 3-lb-thrust hydrogen peroxide engines are installed on the aft bulkhead, with thrust axes parallel with the vehicle axis. (The 3-lb-thrust engines are not installed for direct-ascent missions.) These engines are used to provide axial acceleration for propellant control during parking orbit coast, to achieve initial separation of the *Centaur* from the spacecraft prior to retromaneuver blowdown, and for executing larger attitude corrections if necessary.

The *Centaur* stage utilizes a VHF telemetry system with a single antenna transmitting through the nose fairing cylindrical section on a frequency of 225.7 MHz. The telemetry system provides data from transducers located throughout the second stage and spacecraft interface area as well as a spacecraft composite signal from the spacecraft central signal processor. On the AC-12 flight, 169 measurements were transmitted by the *Centaur* telemetry system.

Redundant range safety command receivers are employed on the *Centaur,* together with shaped-charge destruct units for the second stage and spacecraft. This provides the Range Safety Officer with means to terminate the flight by initiating *Centaur* main engine cutoff and destroying the vehicle and spacecraft retrorocket. The system can be safed by ground command, which is normally transmitted by the Range Safety Officer when the vehicle has reached orbital energy.

A waiver has been obtained for *Surveyor* missions to permit elimination of the inadvertent separation system, which was designed to provide for the automatic destruction of the *Centaur* and spacecraft in the event of premature spacecraft separation.

A C-band tracking system is contained on the *Centaur* which includes a light-weight transponder, circulator, power divider, and two antennas located under the insulation panels. The C-band radar transponder provides real-time position and velocity data for the range safety instantaneous impact predictor as well as data for early orbit determination and postflight guidance and trajectory analysis.

## C. Launch Vehicle/Spacecraft Interface

The general arrangement of the *Surveyor/Centaur* interface is illustrated in Fig. III-2. The spacecraft is completely encapsulated within a nose fairing/adapter system in the final assembly bay of the Explosive Safe Facility at AFETR prior to being moved to the launch pad. This encapsulation provides protection for the space-craft from the environment before launch as well as from aerodynamic loads and heating during ascent. An ablative type coating (Thermolag) is applied over the nose fairing and *Centaur* insulation panels to provide added thermal protection.

The spacecraft is first attached to the forward section of a two-piece, conical adapter system of aluminum sheet and stringer design by means of three latch mechanisms, each containing a dual-squib pin puller. The following equipment is located on the forward adapter: three separation spring assemblies each containing a linear potentiometer for monitoring separation; a 52-pin electrical connector with a pyrotechnic separation mechanism; three pedestals for the spacecraft-mounted separation sensing and arming devices; a shaped-charge destruct
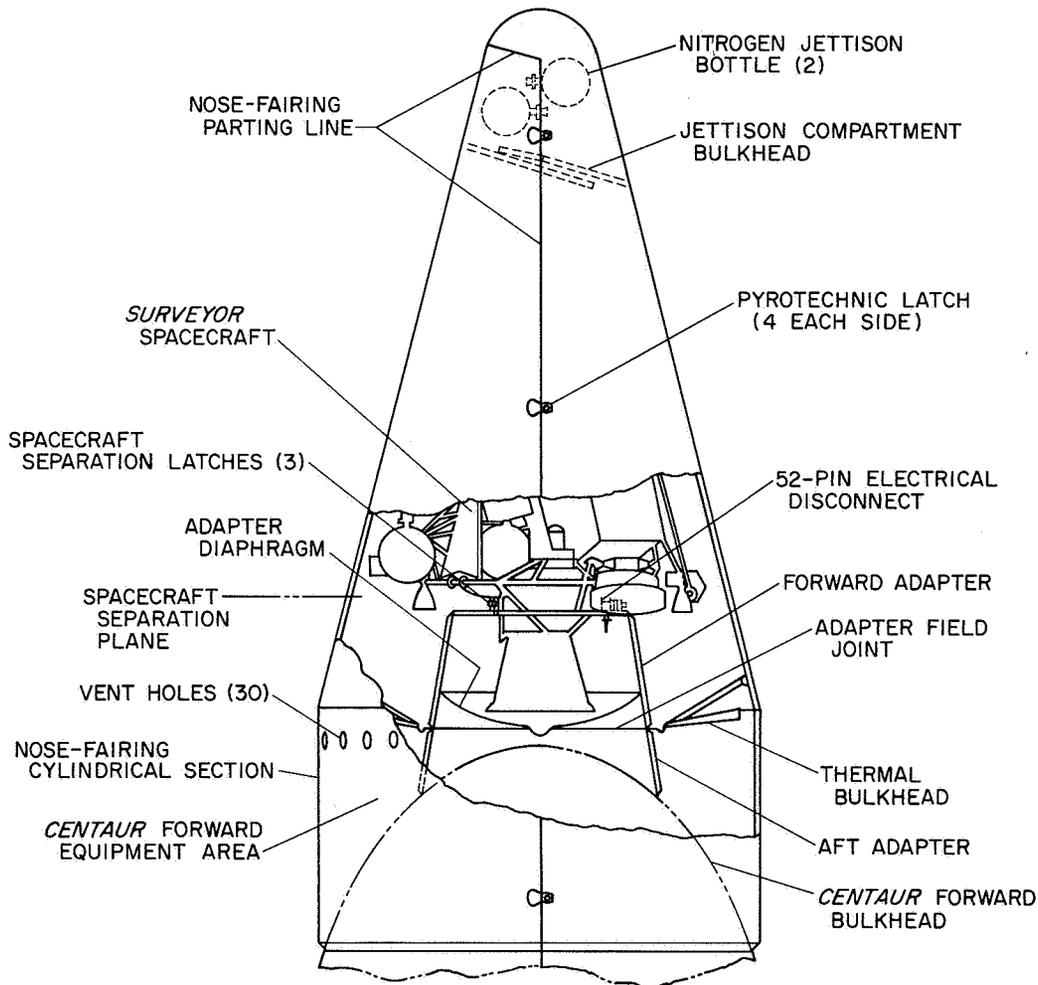


**Fig. III-2.** *Surveyor/Centaur* interface configuration

assembly directed toward the spacecraft retromotor; an accelerometer for monitoring lateral vibration at the separation plane (four additional accelerometers are located on the spacecraft side of the separation plane as shown in Fig. IV-8); and a diaphragm to provide a thermal seal and to prevent contamination from passing to the spacecraft compartment from the *Centaur* forward equipment compartment.

The low-drag nose fairing is an RF-transparent, clamshell configuration consisting of four sections fabricated of laminated fiberglass cloth faces and honeycomb fiberglass core material. Two half-cone forward sections are brought together over the spacecraft mounted on the forward adapter. An annular thermal bulkhead between the adapter and base of the conical section completes encapsulation of the spacecraft.

The encapsulated assembly is mated to the *Centaur* with the forward adapter section attaching to the aft adapter section at a flange field joint requiring 72 bolts. The conical portion of the nose fairing is bolted to the cylindrical portion of the fairing, the two halves of which are attached to the forward end of the *Centaur* tank around the equipment compartment prior to mating of the spacecraft. Doors in the cylindrical sections provide access to the adapter field joint. The electrical leads from the forward adapter are carried through three field connectors and routed across the aft adapter to the *Centaur* umbilical connectors and to the *Centaur* programmer and telemetry units.

Special distribution ducts are built into the nose fairing and forward adapter to provide air conditioning of the spacecraft cavity after encapsulation and until liftoff. Seals are provided at the joints to prevent shroud leakage except out through vent holes in the cylindrical section. Prior to launch, the shroud cavity is monitored for possible spacecraft propellant leakage by means of a toxic gas detector tube which disconnects at liftoff. This was the first mission on which tubes were also inserted into each of the vernier engine combustion chambers to permit nitrogen purging for humidity control and leak detection until manual removal before the service tower was rolled away.

The entire nose fairing is designed to be ejected by separation of two clamshell pieces, each consisting of a conical and cylindrical section. Four pyrotechnic pin-puller latches are used on each side of the nose fairing to carry the tension loads between the fairing halves. A bolted connection with a flexible linear-shaped charge for separation transmits loads between the nose fairing and *Centaur* tank. A nitrogen bottle is mounted in each half of the nose fairing near the forward end to supply gas for cold gas jets to force the panels apart. Hinge fittings are located at the base of each fairing half to control ejection, which occurs under vehicle acceleration of approximately 1 g during the *Atlas* sustainer phase of flight.

## D. Vehicle Flight Sequence of Events

All vehicle flight events occurred satisfactorily. The only significant deviations from nominal sequence times were the longer-than-expected durations of *Centaur* burn periods due to low thrust of the main engines, but this caused no adverse effects on the mission. Predicted and actual times for the vehicle flight sequence of events are included in Table A-1 of Appendix A. Fig. III-3 illustrates the major nominal events. Following is a brief description of the vehicle flight sequence of events, with all times referenced to liftoff (2-in. rise) unless otherwise noted. (Refer to Section II-E for a description of the countdown.)

### 1. Atlas Booster Phase of Flight

Hypergolic ignition of all five *Atlas* engines was initiated 2 sec before liftoff. Vehicle liftoff occurred 51 min after opening of the launch window on the first day of the launch period at 07:05:01.059 GMT, April 17, 1967. The launcher mechanism is designed to begin a controlled release of the vehicle when all engines have reached nearly full thrust. At 2 sec after liftoff, the vehicle began a 13-sec programmed roll from the fixed launcher azimuth setting of 115 deg to the desired launch azimuth of 100.81 deg. The programmed pitchover of the vehicle began 15 sec after liftoff and lasted until booster engine cutoff (BECO).

The vehicle reached Mach 1 at 58 sec and maximum aerodynamic loading occurred at 74 sec. During the booster phase of flight the booster engines were gimballed for pitch, yaw, and roll control, and the vernier engines were active in roll control only while the sustainer engine was centered.

At 142.3 sec, BECO was initiated by a signal from the *Centaur* guidance system when vehicle acceleration equalled 5.74 g (expected value: 5.7±0.08 g). At 3.1 sec after BECO, with the booster and sustainer engines centered, the booster section was jettisoned by release of pneumatically operated latches.

**Fig. III-3. Launch phase nominal events**

## 2. *Atlas* Sustainer Phase of Flight

At BECO + 8 sec, the *Centaur* guidance system was enabled to provide steering commands for the *Atlas* sustainer phase of flight. During this phase the sustainer engine was gimballed for pitch and yaw control, while the verniers were active in roll. The *Centaur* insulation panels were jettisoned by firing shaped charges at 176.1 sec at an altitude of approximately 48.6 nm, where the aerodynamic heating rate was rapidly decreasing. At 202.5 sec, squibs were fired to unlatch the clamshell nose fairing, which was jettisoned 0.5 sec later by means of nitrogen gas thruster jets activated by pyrotechnic valves.

Other programmed events which occurred during the sustainer phase of flight were: the unlocking of the *Centaur* hydrogen tank vent valve to permit venting as required to relieve hydrogen boiloff pressure; starting of the *Centaur* boost pumps 45 sec prior to *Centaur* first main engine start (MES 1); and locking of the *Centaur* oxidizer tank vent valve followed by "burp" pressurization of the tank.

Sustainer and vernier engine cutoff (SECO and VECO) occurred at 237.7 sec as a result of oxidizer depletion, which was the predicted cutoff mode. Shutdown began with an exponential thrust decay phase of about 1-sec duration due to low oxidizer inlet pressure to the turbopump and resulting loss in turbopump performance. Then, final fast shutdown by the propellant valve closure was initiated by actuation of a switch when fuel manifold pressure dropped to 650±50 psi. Also, at the SECO event, the *Centaur* hydrogen tank vent valve was locked and burp pressurization of the tank was begun.

Separation of the *Atlas* from the *Centaur* occurred 1.9 sec after SECO by firing of shaped charges at the forward end of the interstage adapter. This was followed by ignition of eight retrorockets located at the aft end of the *Atlas* tank section to back the *Atlas*, together with the interstage adapter, away from the *Centaur*.

## 3. *Centaur* First Burn Phase of Flight

The *Centaur* prestart sequence for providing chilldown of the propulsion system was initiated 8 sec before first ignition of the *Centaur* main engines (MES 1). MES 1 was commanded 11.5 sec after SECO at 249.2 sec. *Centaur* guidance was reenabled 4 sec after MES 1 to provide steering commands during the *Centaur* first burn. Main engine cutoff (MECO 1) was commanded by guidance at 589.7 sec, when sufficient impulse had been

delivered for injection into the desired parking orbit. *Centaur* first-burn duration was 340.5 sec, or 13.9 sec longer than predicted due to lower than expected thrust from each of the main engines. MECO 1 occurred within 3 sec of the programmed MECO 1 backup command.

## 4. *Centaur* Coast Phase of Flight

Coincident with MECO 1, two of the 50-lb-thrust hydrogen peroxide engines were turned on and provided a low level of axial acceleration to overcome transient disturbances to the propellants caused by main engine shutdown. After 76 sec, the 50-lb engines were turned off and two of the 3-lb axial engines were turned on to retain the propellants at the proper location in the tanks. During the parking orbit coast period the hydrogen peroxide engines also were enabled for attitude control.

The required parking orbit coast time varies with actual liftoff time. For this flight, the coast period (MECO 1 to MES 2) lasted for 1327.6 sec (22.1 min). The *Centaur* stage can support coast periods of from 116 sec to 25 min in duration.

First hydrogen tank venting during the coast period occurred 516 sec after MECO 1. Hydrogen venting continued thereafter until vent valve closure at the start of pressurization for second burn.

At 40 sec before the end of the coast period, the 3-lb engines were turned off and two of the 50-lb engines turned on again until MES 2 to ensure propellant control during the events preceding ignition, which included "burp" pressurization of the propellant tanks, starting of the boost pumps 28.2 sec before MES 2, and initiation of the prestart (chilldown) sequence 16.8 sec before MES 2.

## 5. *Centaur* Second Burn Phase of Flight Through Spacecraft Separation

Second main engine start occurred at 1917.3 sec, followed 4 sec later by *guidance enable* for second burn steering control. After a burn time of 111.3 sec, when sufficient velocity had been attained, the *Centaur* engines were shut down by guidance command at 2028.6 sec. *Centaur* second burn duration was also longer than expected (by 2.9 sec) owing to low thrust level. At main engine cutoff, the hydrogen peroxide engines were enabled again for attitude stabilization.

During the 64.7-sec period between MECO 2 and spacecraft separation, the following signals were transmitted to the spacecraft from the *Centaur* programmer:

*extend spacecraft landing gear; unlock spacecraft omni-antennas;* and *turn on spacecraft transmitter high power.* An arming signal also was provided by the *Centaur* during this period to enable the spacecraft to act on the preseparation commands.

The *Centaur* commanded separation of the spacecraft electrical disconnect 5.5 sec before spacecraft separation, which was initiated at 2093.3 sec. The *Centaur* attitude-control engines were disabled for 5 sec during spacecraft separation in order to minimize vehicle turning moments.

### 6. Centaur Retromaneuver Phase of Flight

At 5 sec after spacecraft separation, the *Centaur* began a turnaround maneuver using the attitude-control engines to point the aft end of the stage in the direction of the flight path. About 40 sec after beginning the turn, which required approximately 100 sec to complete, two of the 50-lb-thrust hydrogen peroxide engines were fired for a period of 20 sec while the *Centaur* continued the turn. This provided initial lateral separation of the *Centaur* from the spacecraft. About 240 sec after separation, the propellant blowdown phase of the *Centaur* retromaneuver was initiated by opening the hydrogen and oxygen pre-start (chilldown) valves. Oxygen was vented through the engine nozzles while hydrogen discharged directly from the chilldown valves. The oxygen tank pressure remained essentially constant, indicating that liquid oxygen remained in the tank throughout the blowdown. At 60 sec from start of blowdown, liquid hydrogen depletion was indicated, after which time only gaseous hydrogen is believed to have been present in the tank. Propellant blowdown was terminated after 250 sec by closing the prestart valves.

Coincident with termination of propellant blowdown, a hydrogen peroxide depletion experiment was initiated by firing two of the 50-lb engines. Hydrogen peroxide depletion was indicated 38 sec after the start of the experiment. A similar experiment conducted on the final *Atlas/Centaur* development flight (AC-9) resulted in depletion 40 sec after engine turn on. After 100 sec, the hydrogen peroxide experiment was concluded by energizing the *Centaur* power change-over switch at 2683.5 sec, which turned off all power except telemetry and the C-band beacon.

## E. Performance

The *Atlas/Centaur* AC-12 vehicle performance was very satisfactory, providing injection into the desired parking orbit followed by successful restart and accurate injection of the *Surveyor III* spacecraft into the prescribed lunar transfer trajectory.

### 1. Guidance and Flight Control

The guidance system performed well throughout the flight. A satisfactory parking orbit was achieved, having an apogee of 92 nm, a perigee of 86 nm, and a period of 87.7 min. The spacecraft was injected on a lunar transfer trajectory which would have resulted in an uncorrected impact only 466 km from the prelaunch target point. Reconstruction of guidance system performance indicates about half the injection error was due to guidance system software errors. Off-nominal *Centaur* shutdown impulse contributed approximately half the remaining error, the balance of which was due to hardware and coast phase thrust errors. (Refer to Section VII for a presentation of vehicle guidance accuracy results in terms of equivalent midcourse velocity correction.)

All guidance system discrete commands, including BECO, SECO backup, MECO 1, and MECO 2, were generated as planned. Vehicle attitude errors remained small during the closed-loop steering phases of flight except for the initial errors which existed and were quickly nulled each time guidance was enabled.

Autopilot performance was satisfactory throughout the flight with proper initiation of programmed events and control of vehicle stability. Vehicle disturbances during the *Atlas* phase of flight were at or below the expected levels and were quickly damped following *Atlas* auto-pilot activation at 42-in. motion. Vehicle stability was also satisfactorily maintained during the *Centaur* phase of flight. Disturbing torques were somewhat larger than expected at times during the coast and retro periods. However, the maximum rates imparted to the vehicle by hydrogen venting were small. During the *Centaur* phase of flight, the vehicle is rate-stabilized in roll rather than roll-position-stabilized. Analysis indicates 18 deg of clockwise roll had occurred at MECO 1+76 sec, and 230±15 deg of clockwise roll had occurred at MECO 2, relative to the local vertical.

The *Centaur* reaction control system performed properly, maintaining desired vehicle attitude during the coast phases and providing the necessary low level axial thrust for propellant control and initial lateral separation from the spacecraft. The vehicle rate gyros indicated a brief (0.04 sec) and unexplained loss of thrust from the attitude control engines 1 sec after start of *Centaur* retro turn-around. The hydrogen peroxide depletion test indicated

approximately 26 lb of usable propellant existed at the end of retro blowdown; a similar result was obtained on the AC-9 flight.

## 2. Propulsion and Propellant Utilization

The *Atlas* propulsion system performed very close to nominal. Normal sustainer cutoff characteristics were exhibited following oxidizer depletion, which had been predicted. Performance of the *Atlas* propellant utilization (PU) system resulted in nearly minimum "burnable" residuals. However, unburnable fuel and oxidizer residuals remaining in the *Atlas* were greater than had been predicted in preflight trajectory simulations based on the current sustainer engine shutdown model. The predicted *Atlas* residuals (propellant above pump) are compared in Table III-1 with preliminary actual values computed from flight data.

Table III-1. *Atlas* propellant residuals, lb

| | Actual | Predicted |
|---|---|---|
| Oxidizer | 523 | 56 |
| Fuel | 538 | 197 |

The *Centaur* propulsion system also provided satisfactory performance, although the *Centaur* main engines burned considerably longer than expected in each powered flight phase to provide the required impulse. The first burn duration of 340.5 sec was 13.9 sec longer than expected; the second burn duration of 111.3 sec was 2.9 sec longer than expected. Each of the five *Atlas/Centaur* flights preceding this mission has experienced a *Centaur* first burn which has been longer than predicted by an average of 4.6 sec. Reconstruction of the AC-12 trajectory indicates the extended burn time, in excess of the average bias of 4.6 sec experienced on previous flights, was apparently the result of approximately 400 lb low thrust from each engine. Low thrust was probably due to low chamber pressure regulation, which is performed independently on each engine by separate thrust controllers which use orifice-controlled reference pressures.

Prior to first MES, the *Centaur* oxidizer boost pump speed data exhibited unexpected trends involving a temporary dip in speed. Somewhat similar speed changes have been recorded during previous flights, but the cause of these variations is not known. Shortly after second MES, both the oxidizer and fuel boost pump turbine inlet pressures experienced a rise followed by a decay, which is indicative of gas flow through the hydrogen peroxide catalyst beds. This occurrence was accompanied

by boost pump speed decreases of about 1200 rpm, but there were no apparent adverse effects on main engine performance.

The *Centaur* PU system performed very well during both burn periods. The predicted and computed actual *Centaur* usable residuals after MECO 1 and MECO 2 are compared in Table III-2.

Table III-2. *Centaur* usable propellant residuals, lb

| | Actual | Predicted |
|---|---|---|
| MECO 1 | | |
| Oxidizer | 6733 ±160 | 6699 |
| Fuel | 1447 ±44 | 1393 |
| MECO 2 | | |
| Oxidizer | 367 | 317 |
| Fuel | 112 | 83 |

Based on an average mixture ratio of 5.23:1, the usable residuals would have provided 6.5 sec additional burn time before theoretical oxidizer depletion, with an ultimate fuel residual of approximately 41.7 lb. Comparing this to the predicted value of 20 lb residual hydrogen indicates a *Centaur* PU system error of only 21.7 lb excess hydrogen.

## 3. Pneumatic, Hydraulic, and Electrical Power Systems

Operation of the *Atlas* pneumatic system including the programmed tank pressurization and pneumatic control functions was properly accomplished throughout the flight. Both *Centaur* propellant tanks were maintained at satisfactory levels during all phases of flight, with normal occurrence of the "burp" pressurization sequences and hydrogen tank venting. The *Centaur* engines control regulator outlet pressure indicated abnormal increases to the relief valve setting three times during the flight (at BECO, insulation panel jettison, and start of *Centaur* turnaround) followed by sudden decays to the normal operating level. This anomaly had no apparent effect on the system. (The anomaly also occurred on AC-9, for which flight it was attributed to excessive regulator leakage.)

Performance of the vehicle hydraulic and electrical power systems was satisfactory throughout the flight. Minor transient anomalies were noted in the *Atlas* electrical power circuits which apparently resulted from the *Atlas/Centaur* separation event.

## 4. Telemetry, Tracking, and Range Safety Command

The *Atlas* and *Centaur* instrumentation and telemetry systems functioned well, with only a few minor measurement anomalies. Generally good data were obtained over all vehicle flight phases, including the critical second prestart sequence for which the data were received by two downrange aircraft.

The *Centaur* C-band radar apparently operated normally, although, as on some previous flights, it is believed that *Centaur* roll may have contributed to weak signal strength and some loss of data by downrange receivers. An evaluation of the system can only be made on the basis of received tracking data and station operator logs because the airborne system is not instrumented. (See also Section V.)

The *Atlas* and *Centaur* range safety command systems performed satisfactorily. About 7 sec after parking orbit injection (MECO 1), a range safety command to disable the destruct systems was sent from Antigua and properly executed.

## 5. Vehicle Loads and Environment

Vehicle loads and thermal environment were within expected ranges throughout the flight. Maximum axial accelerations were 5.74 g at BECO during the booster phase and 1.81 g about 3 sec before SECO during the sustainer phase. Longitudinal oscillations during launch reached a maximum (0.59 g peak-to-peak at 7 Hz) at 0.6 sec and damped out by 20 sec.

Four of the five accelerometers installed in the vicinity of the *Centaur/Surveyor* interface were operable during the flight. (One was disconnected prior to flight due to an amplifier failure.) These indicated expected steady-state vibration levels during the flight which agreed closely with previously measured data. Shocks of 600–700 Hz were observed in response to shaped-charge firings at insulation panel jettison and *Atlas/Centaur* separation but, as expected, the magnitude exceeded the 20-g peak-to-peak range of the telemetry channel. (See Section IV-A for a discussion of spacecraft launch phase vibration environment.)

The *Surveyor* compartment thermal and pressure environments were normal throughout flight. The ambient temperature within the compartment was 85°F at launch and gradually decreased to 74°F by 83 sec as a result of expansion during ascent. The ambient pressure decayed characteristically to essentially zero prior to nose fairing jettison.

## 6. Separation and Retro Maneuver Systems

All vehicle separation systems functioned normally. Booster section jettison occurred as planned, with resulting vehicle rates comparable to previous flights.

Satisfactory insulation panel jettison was confirmed by normal transient effects on vehicle rates, axial acceleration, vibration, etc. The times of 35-deg rotation of the four insulation panels during jettison are provided by a breakwire at one hinge arm of each panel. A somewhat wider dispersion in panel rotation rates was computed from the breakwire data for AC-12 as compared to previous flights for which this instrumentation was provided.

Normal separation of the nose fairing was verified by indications of 3-deg rotation from disconnect wires which are incorporated in the pullaway electrical connectors of each fairing half.

*Atlas/Centaur* separation occurred as planned. Displacement data obtained with respect to time are in close agreement with expected values and indicate successful *Atlas* retro rocket operation.

At spacecraft separation, first motion of all three springs occurred simultaneously within the accuracy of the extensometer (linear potentiometer) data. Spring extension to the full 1-in. position was normal and nearly identical, producing a spacecraft separation rate of approximately 1 ft/sec. The spacecraft angular rates resulting from the separation event have been computed and are presented in Table III-3 based upon the vector sum of the *Centaur* residual rates prior to separation plus the tipoff rates as determined from the extensometer traces. The resulting net spacecraft angular rate of 0.56 deg/sec is well within the specified maximum acceptable rate of 3.0 deg/sec.

**Table III-3. Spacecraft angular separation rates,[a] deg/sec**

| | Centaur residual rate (prior to separation) | Spacecraft/ Centaur relative rate | Net spacecraft rate (after separation) |
|---|---|---|---|
| Pitch | + 0.22 | + 0.08 | + 0.30 |
| Yaw | − 0.19 | + 0.66 | + 0.47 |
| Roll | − 0.03 | − | − 0.03 |
| Vector sum | 0.29 | | 0.56 |

[a] Both vehicle and spacecraft rates are based upon spacecraft coordinate system reference.

(Refer to Section IV-F for discussion of angular separation rates as determined from spacecraft gyro data.)

All phases of the *Centaur* retromaneuver were executed as planned. Five hours after spacecraft separation, the *Centaur/Surveyor* separation distance was computed to be over 3000 km, which is far in excess of the required minimum distance of 336 km at that time. The *Centaur* closest approach to the moon was computed to be 34,100 km and occurred at 09:21 GMT on April 20, 1967.

# IV. Surveyor Spacecraft

The basic objectives of the *Surveyor III* spacecraft system were: (1) accomplish a soft landing on the moon at a new site within the *Apollo* zone of interest (the final aim point was 2.92 deg south latitude, 23.25 deg west longitude); (2) demonstrate spacecraft capability to soft-land on the moon with an unbraked, off-vertical approach angle not less than 18 deg nor greater than 45 deg; (3) obtain postlanding television pictures; (4) obtain data on the mechanical properties of the lunar surface using the soil mechanics/surface sampler (SM/SS); and (5) obtain data on radar reflectivity, thermal characteristics, touchdown dynamics, and other measurements of the lunar surface through the use of various spacecraft equipment.

*Surveyor III* met all of its objectives. Liftoff occurred at 07:05:01.059 GMT on April 17, 1967. A small midcourse correction of 4.19 m/sec was properly executed during the first Goldstone pass, and a successful soft landing was accomplished early in the lunar day at 00:04:17 GMT on April 20, 1967. Because the vernier engines did not shut off automatically before contact with the lunar surface, the spacecraft lifted off after initial touchdown and again after second touchdown. The vernier engines were commanded off from earth just before third touchdown, and the spacecraft finally came to rest.

Landing occurred at 2.94 deg south latitude and 23.34 deg west longitude inside a 200-m crater on a sloping surface, which resulted in a 12½-deg tilt of the spacecraft.

Extensive use was made of the SM/SS, and over 6300 television pictures, in addition to other spacecraft data, were received from the lunar surface until after sunset. A telemetry anomaly occurred during the landing which impaired early lunar operations. However, corrective calibration permitted use of nearly all data received at the lowest bit rate (17.2 bit/sec).

## A. Spacecraft System

In the *Surveyor* spacecraft design, the primary objective was to maximize the probability of successful spacecraft operation within the basic limitations imposed by launch vehicle capabilities, the extent of knowledge of transit and lunar environments, and the current technological state of the art. In keeping with this primary objective, design policies were established which (1) minimized spacecraft complexity by placing responsibility for mission control and decision-making on earth-based equipment wherever possible, (2) provided the

capability of transmitting a large number of different data channels from the spacecraft, (3) included provisions for accommodating a large number of individual commands from the earth, and (4) made all subsystems as autonomous as practicable.

Figure IV-1 illustrates the *Surveyor* spacecraft in the cruise mode and identifies many of the major components. A simplified functional block diagram of the spacecraft system is shown in Figure IV-2. The spacecraft design is discussed briefly in this section and in greater detail
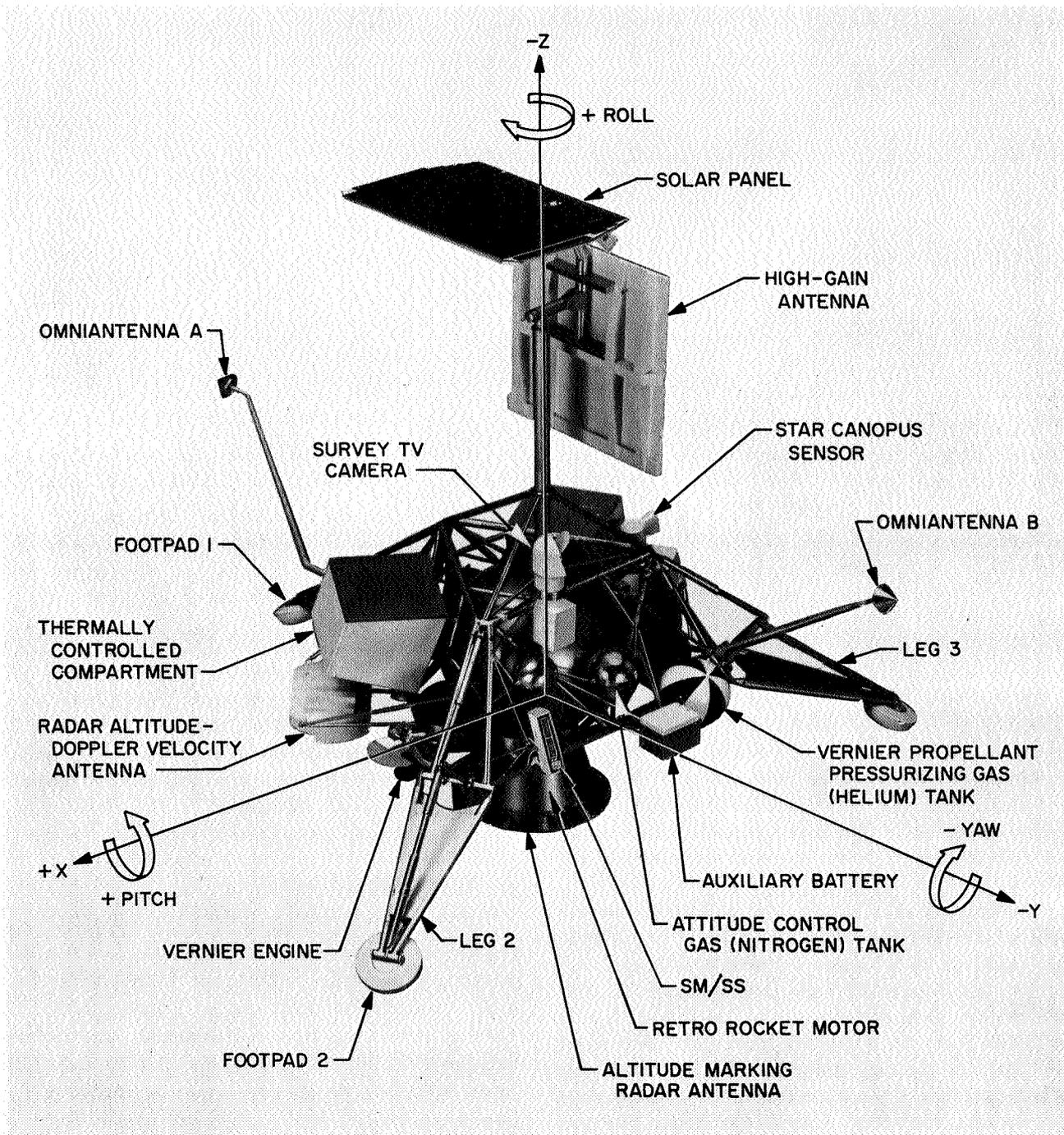


**Fig. IV-1.** *Surveyor III* spacecraft in cruise mode
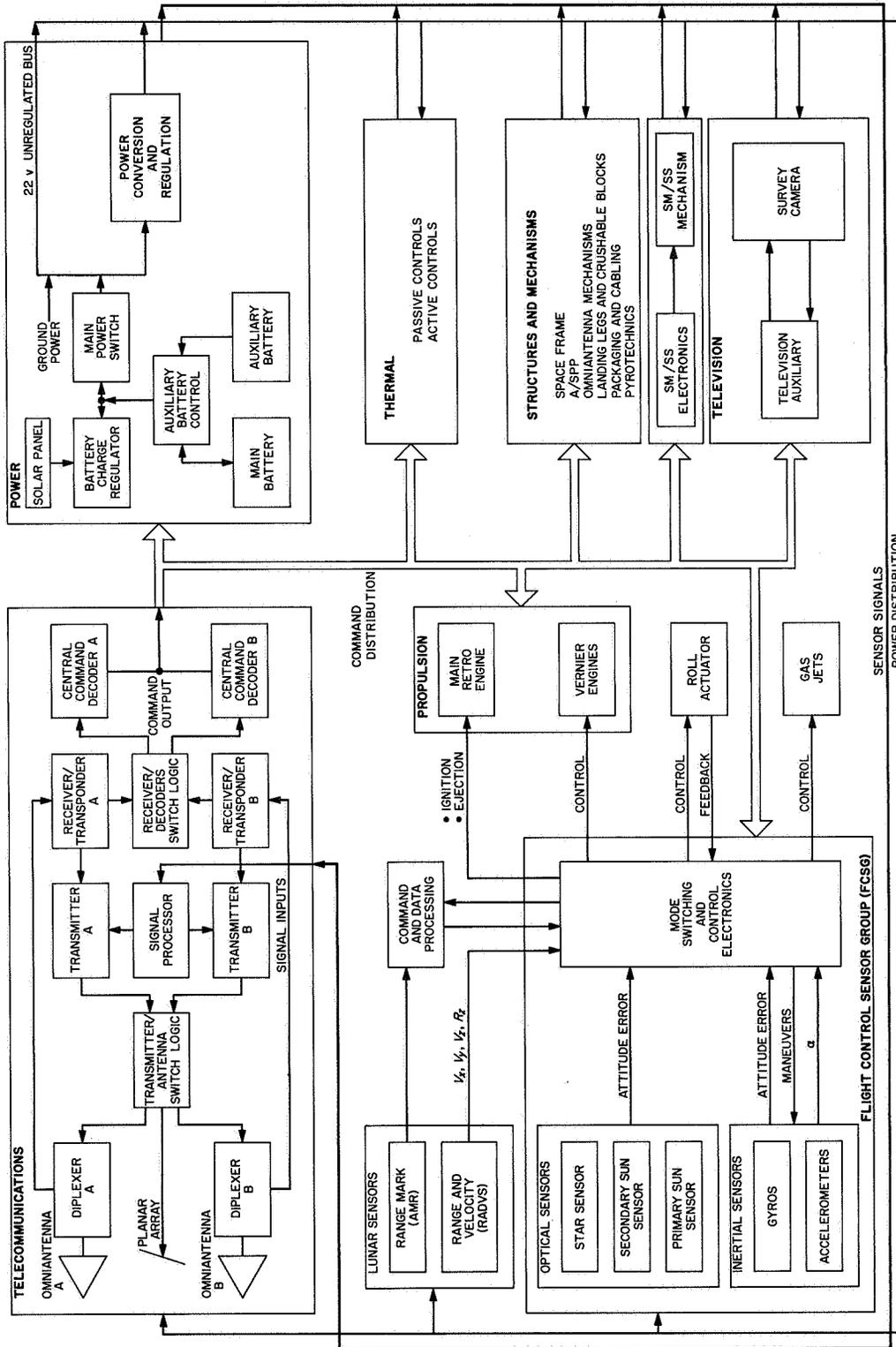
**Fig. IV-2. Simplified spacecraft functional block diagram**

in the subsystem sections which follow. A detailed configuration drawing of the spacecraft is contained in Appendix B. The configuration of the *Surveyor* spacecraft is dictated by the selection of a tripod landing gear with three foldable landing legs for the soft landing.

## 1. Spacecraft Coordinate System

The spacecraft coordinate system is an orthogonal, right-hand Cartesian system. Figure IV-3 shows the spacecraft motion about its coordinate axes relative to the celestial references. The cone angle of the earth is the angle between the sun vector and the earth vector as seen from the spacecraft. The clock angle of the earth is measured in a plane perpendicular to the sun vector from the projection of the star Canopus vector to the projection of the earth vector in the plane. The spacecraft coordinate system may be related to the cone and the clock angle coordinate system, provided sun and Canopus lock-on has been achieved. In this case the spacecraft minus Z-axis is directed toward the sun, and the minus X-axis is coincident with the projection of the Canopus vector in the plane perpendicular to the direction of the sun. The spacecraft +Z-axis is in the direction of the retro motor thrust vector, and Leg 1 lies in the X-Y plane.



$0° \leq CONE \leq 180°$
$0° \leq CLOCK < 360°$
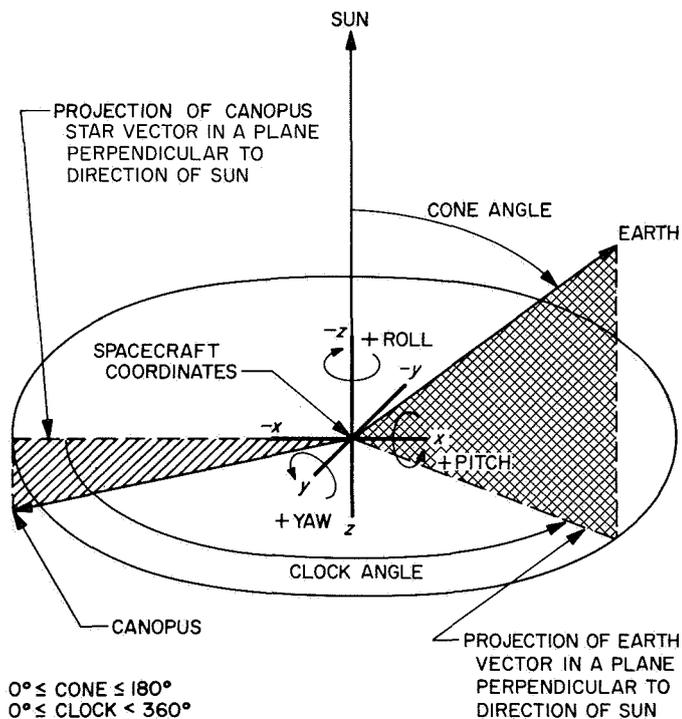
**Fig. IV-3. Spacecraft coordinates relative to celestial references**

## 2. Spacecraft Mass Properties

The *Surveyor III* spacecraft weighed 2281.3 lb at separation and 657 lb at final touchdown. Center of gravity of the vehicle is kept low to obtain stability over a wide range of landing conditions. Center-of-gravity limits after *Surveyor/Centaur* separation for midcourse and retro maneuvers are constrained by the attitude correction capabilities of the flight control and vernier engine subsystems during retrorocket burning. Limits of travel of the vertical center of gravity in the touchdown configuration are designed to landing site assumptions and approach angle requirements so that the spacecraft will not topple when landing.

## 3. Structures and Mechanisms

The structures and mechanisms subsystem provides basic structural support (including touchdown stabilization), mechanical actuation, thermal protection, and electronic packaging and cabling. A tubular aluminum spaceframe is utilized for basic structural support. Three landing leg assemblies and crushable blocks for lunar landing are attached to the spaceframe. Other mechanisms provided are the high-gain antenna and solar panel positioner (A/SPP), two omniantenna mechanisms, a separation sensing and arming device, the secondary sun sensor, and pyrotechnic devices. Two compartments incorporating special insulation and thermal switches are provided for thermal protection of critical spacecraft components.

## 4. Thermal Control

Thermal control of equipment over the extreme temperature range of the lunar surface (+260 to −260°F) is accomplished by a combination of passive, semipassive, and active methods including the use of heaters controlled by ground command. The design represents the latest state of the art in the application of thermal design principles to lightweight spacecraft. The spacecraft thermal design includes "passive" controls such as super-insulation and special surface finishes, "active" heater systems, and "semiactive" thermal switches.

## 5. Electrical Power

The electrical power subsystem is designed to generate, store, convert, and distribute electrical energy. A single solar panel is utilized which is capable of generating continuous unregulated power at 90 to 55 W, depending upon environmental temperature and incidence

angle of solar radiation. Peak unregulated power capability is limited to 1000 W by the two spacecraft batteries (main and auxiliary). The initial energy storage of the subsystem is 4400 W-hr. Only one battery, the main battery, can be recharged, to an energy storage of 3520 W-hr. The batteries determine the unregulated power voltage and are designed to sustain a voltage between 17.5 and 27.5 V, with a nominal value of 22 V. The unregulated power is distributed to the loads via an unregulated bus.

Regulated power is provided by a boost regulator at 29 V, controlled to 1% for the flight control and "nonessential" loads and to 2% for the "essential" loads. The maximum regulated power capability of the boost regulator is 270 W.

## 6. Propulsion

The propulsion subsystem supplies thrust force during the midcourse correction and terminal descent phases of the mission. The propulsion subsystem, consisting of a bipropellant vernier engine system and a solid-propellant main retrorocket motor, is controlled by the flight control system through preprogrammed maneuvers, commands from earth, and maneuvers initiated by flight control sensor signals.

The three thrust chambers of the vernier engine subsystem supply the thrust forces for midcourse maneuver velocity vector correction, attitude control during main retrorocket burning, and velocity vector and attitude control during terminal descent. The thrust of each vernier engine can be throttled over a range of 30 to 104 lb.

The main retro motor is utilized to remove the major portion of the spacecraft approach velocity during terminal descent. It is a spherical solid-propellant motor with partially-submerged nozzle to minimize overall length. The motor provides a thrust of 8,000 to 10,000 lb for a duration of about 41 sec.

## 7. Flight Control

The purpose of the flight control subsystem is to control spacecraft flight parameters throughout the transit portion of the mission. Flight control uses three forms of reference to perform its function. These are celestial sensors, inertial sensors, and radar sensors. The outputs of each of these sensors are utilized by analog electronics to create thrust commands for operation of attitude gas jets and the spacecraft vernier and main retro propulsion systems. Flight control requires ground commands for

initiation of various sequences and performance of "manual" operations. Flight control programming initiates and controls other sequences.

The celestial sensors allow the spacecraft to be locked to a specific orientation defined by the vectors to the sun and the star Canopus and the angle between them. Initial search and acquisition of the sun is accomplished by the secondary sun sensor. The primary sun sensor then maintains the orientation with the sun line.

Of the inertial sensors, integrating gyros are used to maintain spacecraft orientation inertially when the celestial references are not available. Accelerometers measure the thrust levels of the spacecraft propulsion systems during midcourse correction and terminal descent phases.

The attitude gas jets are cold gas (nitrogen) reaction devices for control of the orientation of spacecraft attitude in all three axes during coast phases of the flight. They are installed in opposing pairs near the ends of the three landing legs. The three vernier engines provide thrust, which can be varied over a wide range, for midcourse correction of the spacecraft velocity vector and controlled descent to the lunar surface. A roll actuator tilts the thrust axis of Vernier Engine 1 away from the spacecraft roll axis for attitude and roll control during thrust phases of flight when the attitude gas jets are not effective.

## 8. Radar

Two radar systems are employed by the *Surveyor* spacecraft. An altitude marking radar (AMR) provides a mark signal to initiate the main retro sequence. In addition, a radar altimeter and doppler velocity sensor (RADVS) functions in the flight control subsystem to provide three-axis velocity, range, and altitude mark signals for flight control during the main retro and vernier phases of terminal descent. The RADVS consists of a doppler velocity sensor, which computes velocity along each of the spacecraft X, Y, and Z axes, and a radar altimeter, which computes slant range from 50,000 ft to 14 ft and generates *1000-ft mark* and *14-ft mark* signals.

## 9. Telecommunications

The spacecraft telecommunications subsystem provides for (1) receiving and processing commands from earth, (2) angle tracking and one- or two-way doppler data for orbit determination, and (3) processing and transmitting spacecraft telemetry data.

Continuous command capability is assured by two identical receivers which remain on throughout the life of the spacecraft and operate in conjunction with two omniantennas and two command decoders through switching logics.

Operation of a receiver in conjunction with a transmitter through a transponder interconnection provides a phase-coherent system for doppler tracking of the spacecraft during transit and after touchdown. Two identical transponder interconnections (Receiver/Transponder A and Receiver/Transponder B) are provided for redundancy. Transmitter B with Receiver/Transponder B is the transponder system normally operated during transit.

Data signals from transducers located throughout the spacecraft are received and prepared for telemetry transmission by signal processing equipment which performs commutation, analog-to-digital conversion, and pulse-code and amplitude-to-frequency modulation functions. Most of the data signals are divided into six groups ("commutator modes") for commutation by two commutators located within the telecommunications signal processor. (An additional commutator is located within the television auxiliary for processing television frame identification data.) The content of each commutator mode has been selected to provide essential data during particular phases of the mission (Table IV-1 and Appendix C). Other signals, such as strain gage data which is required

**Table IV-1. *Surveyor III* spacecraft telemetry mode summary**

| | Data mode | Method of transmission | Data rate | Number of signals | | Signals emphasized | Primary use |
|---|---|---|---|---|---|---|---|
| | | | | Analog | Digital | | |
| Engineering commutator | 1 | PCM/FM/PM | All | 41 | 40 | Flight control, propulsion | Canopus acquisition midcourse maneuver |
| Engineering commutator | 2 | PCM/FM/PM | All | 78 | 59 | Flight control, propulsion, approach TV, AMR, RADVS | Transit interrogations, backup for main retro phase |
| Engineering commutator | 3 | PCM/FM/PM | All | 17 | 39 | Inertial guidance, approach TV, AMR, RADVS, vernier engines | Backup for vernier descent phase |
| Engineering commutator | 4 | PCM/FM/PM | All | 72 | 30 | Temperatures, power status, telecommunications | Transit interrogations, lunar operations |
| Engineering commutator | 5 | PCM/FM/PM | All | 108 | 50 | Flight control, power status, temperature | Midcourse and terminal attitude maneuvers, launch and primary cruise data, lunar interrogations |
| Engineering commutator | 6 | PCM/FM/PM | All | 47 | 74 | Flight control, power status, AMR, RADVS, vernier engine conditions | Terminal descent thrust phase |
| Television commutator | 7 | PCM/FM | Only 4400 bit/sec | 17 | | TV survey camera | TV camera interrogation, TV camera operation |
| Shock absorber strain gages | | FM/PM | Continuous | 3 | | Strain gages | Touchdown force on spacecraft legs |
| Gyro speed | | FM/PM | 50 Hz | 3 | | Inertial guidance unit | Verify gyro sync |
| Accelerometers | | (a) Contour VHF (b) FM/FM | Continuous | (a) 4 (b) 4 | | Launch phase accelerometers | (a) Launch phase vibration (b) Not used |

continuously over brief intervals, are applied directly to subcarrier oscillators.

Summing amplifiers are used to combine the output of any one commutator mode with continuous data. The composite signal from the signal processor, or television data from the television auxiliary, is sent over one of the two spacecraft transmitters. The commutators can be operated at five different rates (4400, 1100, 550, 137.5, and 17.2 bit/sec) and the transmitters at two different power levels (10 W or 0.1 W). In addition, switching permits each of the transmitters to be operated with any one of the three spacecraft antennas (two omniantennas and a planar array) at either the high or low power level. Selection of data mode(s), data rate, transmitter power, and transmitter-antenna combination is made by ground command. A data rate is selected for each mission phase which will provide sufficient signal strength at the DSIF station to maintain the telemetry error rate within satisfactory limits. The high-gain antenna (planar array) is utilized for efficient transmission of video data.

## 10. Television

The *Surveyor III* television subsystem consists of a survey camera and a television auxiliary for final decoding of commands and processing of video and frame identification data for transmission by either of the spacecraft transmitters. The survey camera is designed for postlanding operation to provide photographs of the lunar surface panorama, portions of the spacecraft, and the lunar sky. Photographs may be obtained in either of two modes: a 200-line mode for relatively slow transmission over an omniantenna or a 600-line mode for more efficient transmission over the planar array.

## 11. Soil Mechanics/Surface Sampler (SM/SS)

The SM/SS consists of extendable tongs and a scoop with associated electronics. The instrument is designed for postlanding operation and is capable of digging, picking, and scratching the lunar surface. The tongs can be extended 64 in. and can be moved 54 deg in vertical motion and 112 deg in azimuth motion. The results of SM/SS operations are obtained primarily through TV pictures. The only telemetry data obtained on the instrument itself are current measurements of the four drive motors from which approximate force information may be derived.

## 12. Instrumentation

Transducers are located throughout the spacecraft system to provide signals that are relayed to the DSIF stations by the telecommunication subsystem. These signals are used primarily to assess the condition and performance of the spacecraft. Some of the measurements also provide data useful in deriving knowledge of certain characteristics of the lunar surface.

In most cases the individual subsystems provide the transducers and basic signal conditioning required for data related to their equipment. All the instrumentation signals provided for the *Surveyor III* spacecraft are summarized by category and responsible subsystem in Table IV-2.

All of the temperature transducers are resistance-type units except for two microdiode bridge amplifier assemblies used in the television subsystem.

The voltage (signals) and position (electronic switches) measurements consist largely of signals from the command and control circuits.

A strain gage is mounted on each of the vernier engine brackets to measure thrust and on each of the three landing leg shock absorbers to monitor touchdown dynamics.

The flight control accelerometer is mounted on the retro motor case to verify motor ignition and provide gross retro performance data. Of the remaining eight accelerometers, four are designed to provide data on the vibration environment during launch phase and four are designed to provide data on the dynamic response of spacecraft elements to flight events which occur after spacecraft separation. Only data from the retro motor accelerometer and launch phase accelerometers has been telemetered on *Surveyor* missions to date.

Additional discussion of instrumentation is included with the individual subsystem descriptions.

## 13. Terminal Maneuver and Descent Phase Design

The system design for automatic terminal descent, which has been developed and used for the first time in the *Surveyor* program, is described here to illustrate the critical functions required to be performed by several of the subsystems.

Table IV-2. *Surveyor III* instrumentation

| Sensor type | Subsystem location | | | | | | | | | |
| --- | --- | --- | --- | --- | --- | --- | --- | --- | --- | --- |
| | Structures, mechanisms, and thermal control | Electrical power | Propulsion | Flight control | Radar | Telecommunications | | SM/SS | Television | Total |
| | | | | | | Signal processing | Radio and command decoding | | | |
| Temperature (thermisters) | 33 | 5 | 16 | 9 | 7 | | 2 | 1 | 2 | 75 |
| Temperature (bridges) | | | | | | | | | 2 | 2 |
| Pressure | | 1 | 2 | 1 | | | | | | 4 |
| Position (potentiometers) | 7 | | | | | | | | 6 | 13 |
| Position (mechanical switches) | 10 | 1 | | 1 | | | | | | 12 |
| Position (electrical switches) | 1 | 2 | | 33 | 15 | 3 | 8 | 2 | 4 | 68 |
| Current | | 12 | | | | | | 1 | | 13 |
| Voltage (power) | | 6 | | | | | | | | 6 |
| Voltage (signals) | | | | 14 | 7 | | 6 | | | 27 |
| Strain gages | 3 | | 3 | | | | | | | 6 |
| Accelerometers | 8 | | | 1 | | | | | | 9 |
| Inertial sensors (gyro speed) | | | | 3 | | | | | | 3 |
| RF power | | | | | | | 2 | | | 2 |
| Optical | | | | 9 | | | | | | 9 |
| Calibration | | | | 1 | | 10 | | | 1 | 12 |
| Totals | 62 | 27 | 21 | 72 | 29 | 13 | 18 | 4 | 15 | 261 |

*a. Terminal descent sequence.* The terminal phase begins with the preretro attitude maneuvers (Fig. IV-4). These maneuvers are commanded from earth to reposition the attitude of the spacecraft from the coast phase sun-star reference such that the expected direction of the retro thrust vector will be aligned with respect to the spacecraft velocity vector. Following completion of the attitude maneuvers, the AMR is activated. It has been preset to generate a *mark* signal when the slant range to the lunar surface is 60 miles nominal. A backup *mark* signal, delayed a short interval after the AMR *mark* should occur, is transmitted to the spacecraft to initiate the automatic sequence in the event the AMR *mark* is not generated. A delay between the *altitude mark* and main retro motor ignition has been preset in the flight control programmer by ground command. Vernier engine ignition is automatically initiated 1.1 sec prior to main retro ignition.

During the main retro phase, spacecraft attitude is maintained in the inertial direction established at the end of the preretro maneuvers by differential throttle control of the vernier engines while maintaining the total vernier thrust at the midthrust level. The main retro burns at essentially constant thrust for about 40 sec, after which the thrust starts to decay. This tailoff is detected by an inertial switch which increases vernier thrust to the high level and initiates a programmed time delay of about 12 sec, after which the main retro motor case is ejected. The main retro phase removes more than 95% of the spacecraft velocity and puts the spacecraft position, velocity, and attitude relative to the lunar surface within the capability of the final, vernier phase.

The vernier phase generally begins at altitudes between 10,000 and 50,000 ft and velocities in the range of 100 to 700 ft/sec. This wide range of vernier-phase initial conditions exists because of statistical variations in parameters which affect main retro burnout. About 2 sec after separation of the main retro case, vernier thrust is reduced and controlled to produce a constant spacecraft deceleration of 0.9 lunar g, as sensed by an axially oriented accelerometer. The spacecraft attitude is held in the preretro position until the doppler velocity sensor locks onto the lunar surface (Fig. IV-5). The thrust axis is then aligned and maintained to the spacecraft velocity

CRUISE ATTITUDE

NOTE: ALTITUDES, VELOCITIES, AND TIMES ARE NOMINAL

PRERETRO MANEUVER 30 TO 40 min BEFORE TOUCHDOWN ALIGNS MAIN RETRO WITH FLIGHT PATH

MAIN RETRO START BY ALTITUDE-MARKING RADAR WHICH EJECTS FROM NOZZLE; SPACECRAFT STABILIZED BY VERNIER ENGINES AT 60-mi SLANT RANGE, 6100 mph

MAIN RETRO BURNOUT AND EJECTION; VERNIER PROPULSION SYSTEM TAKEOVER AT 25,000 ft, 240 mph

VERNIER ENGINES SHUTOFF AT 14 ft, 3-1/2 mph

TOUCHDOWN AT 10 mph

Fig. IV-4. Terminal descent nominal events
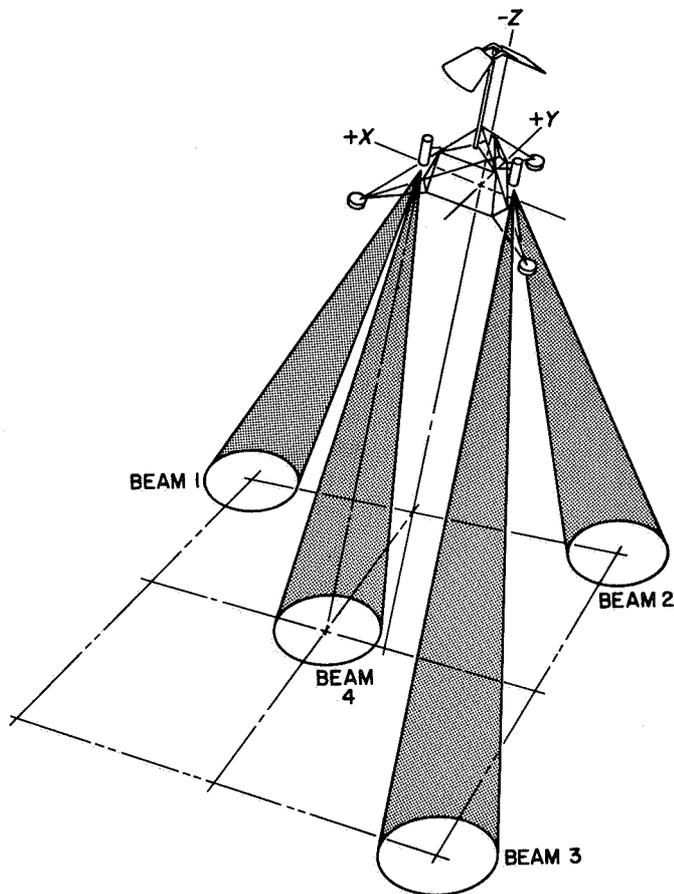
Fig. IV-5. RADVS beam orientation



Fig. IV-6. Range—velocity diagram

vector throughout the remainder of the descent until the terminal sequence is initiated (when the attitude is again held inertially fixed). With the thrust axis maintained in alignment with the velocity vector, the spacecraft makes a "gravity turn," wherein gravity tends to force the flight path towards the vertical as the spacecraft decelerates.

The vehicle descends at 0.9 lunar $g$ until the radars sense that the "descent contour" has been reached (Fig. IV-6). This contour corresponds, in the vertical case, to descent at a constant deceleration. The vernier thrust is commanded such that the vehicle follows the descent contour until shortly before touchdown, when the terminal sequence is initiated. Nominally, the terminal sequence consists of a constant-velocity descent from 40 to 14 ft at 5 ft/sec, followed by a free fall from 14 ft, resulting in touchdown at approximately 13 ft/sec.

*b. Terminal descent design constraints.* Constraints on the allowable main retro motor burnout conditions are of major importance in *Surveyor* terminal descent design.

RADVS operational limitations contribute to constraints on the main retro burnout conditions. Linear operation of the doppler velocity sensor is expected for slant ranges below 50,000 ft and for velocities below 700 ft/sec. The altimeter limit is between 30,000 and 40,000 ft, depending on velocity. These constraints are illustrated in the range-velocity plane of Fig. IV-6.

The allowable main retro burnout region is further restricted by the maximum thrust capability of the vernier engine system. To accurately control the final descent, the minimum thrust must be less than the least possible landed weight (lunar gravity) of the vehicle. The result is a minimum thrust of 90 lb. This in turn constrains the maximum vernier thrust to 312 lb because of the limited range of throttle control which is possible.

Descent at the maximum thrust to touchdown defines a curve in the range-velocity plane below which main retro burnout cannot be allowed to occur. Actually, since the vernier engines are also used for attitude stabilization by differential thrust control, it is necessary to allow some margin from the maximum thrust level. Furthermore, since it is more convenient to sense deceleration than thrust, the vernier phase of terminal descent is performed at nearly constant deceleration rather than at constant thrust. Therefore, maximum thrust will be utilized only at the start of the vernier phase.

The maximum vernier phase deceleration defines a parabola in the altitude-velocity plane. For vertical descents at least, this curve defines the minimum altitude at which main retro burnout is permitted to occur with a resulting soft landing. This parabola is indicated in Fig. IV-6. (For ease of spacecraft mechanization, the parabola is approximated by a descent contour consisting of straight-line segments.)

Main retro burnout must occur sufficiently above the descent contour to allow time to align the thrust axis with the velocity vector before the trajectory intersects the contour. Thus, a "nominal burnout locus" (also shown in Fig. IV-6) is established which allows for altitude dispersions plus an alignment time which depends on the maximum angle between the flight path and roll axis at burnout.

The allowable burnout region having been defined, the size of the main retro motor and ignition altitude are determined such that burnout will occur within that region.

In order to establish the maximum propellant requirements for the vernier system, it is necessary to consider dispersions in main retro burnout conditions as well as midcourse maneuver fuel expenditures. The principal sources of main retro burnout velocity dispersion are the imperfect alignment of the vehicle prior to main retro ignition and the variability of the total impulse. In the case of a vertical descent, these variations cause dispersions of the type shown in Fig. IV-6, where the ellipse defines a region within which burnout will occur with probability 0.99. The design chosen provides enough fuel so that, given a maximum midcourse correction, the probability of not running out is at least 0.99.

The spacecraft landing gear is designed to withstand a horizontal component of the landing velocity. The horizontal component of the landing velocity is nominally zero. However, dispersions arise primarily because of the following two factors:

(1) Measurement error in the doppler system resulting in a velocity error normal to the thrust axis.

(2) Nonvertical attitude due to: (a) termination of the "gravity turn" at a finite velocity, and (b) attitude control system noise sources.

Since the attitude at the beginning of the constant-velocity descent is inertially held until vernier engine cutoff, these errors give rise to a significant lateral velocity at touchdown.

## 14. Design Changes

Table IV-3 presents a summary of notable differences in design between the Surveyors II and III.

## 15. Spacecraft Reliability

The prelaunch reliability estimate for the Surveyor III spacecraft was 0.74 at 50% confidence level for the flight through landing phases of the mission, assuming successful injection. The reliability estimates for the Surveyor III spacecraft vs systems test experience are shown in Fig. IV-7. Table IV-4 lists the prelaunch reliability estimates for each subsystem. For comparative purposes, Surveyor I and II estimates are also shown. The primary source of data for these reliability estimates is the time and cycle information experienced by spacecraft units during systems tests. Data from Surveyor I and II test and flight experience was included where there were no significant design differences between the units. In general, a failure is considered relevant if it could occur during a mission.
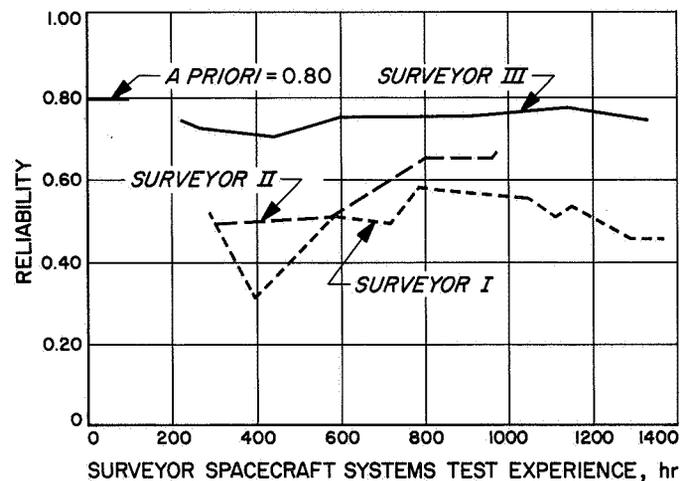


Fig. IV-7. Surveyor spacecraft reliability estimates

## Table IV-3. Notable differences between Surveyors II and III: changes incorporated on Surveyor III

| Item | Description |
|------|-------------|
| SM/SS instrument | The approach camera was replaced with the SM/SS instrument |
| Two special viewing mirrors | These mirrors were added to enable the TV survey camera to view as much as possible in area of crushable blocks and vernier engines |
| Landing gear kickout springs | Kickout springs were added to overcome static friction during initial deployment of legs |
| Electrical bonding of shocks | A grounding path of low impedance was provided from the squibs to the space-frame to prevent premature squib firing which would cause landing gear shock absorber lock |
| Retro motor impulse | The impulse of the main retro motor was increased by increasing the amount of propellant |
| A/SPP pin pullers | A vent hole was added to ensure complete travel of the pin puller upon squib firing |
| Canopus sensor sun filter change | The Canopus sensor sun filter was changed to reduce the effective gain of the sensor to 1.05 to 1.10 $\times$ Canopus because the gain on Surveyors I and II had been greater than predicted |
| Canopus sensor O-ring lubricant | The silicone grease was removed to increase star window temperature and reduce or eliminate internal fogging |
| Retro motor harness | The squib firing harness and attaching hardware were modified to comply with AFETR safety requirements |
| RF cables | The connectors were potted to prevent loosening during vibration |
| RADVS signal data converter | Antenna sidelobe skewing of 2.0 deg instead of 0.2 deg necessitated cross-coupled sidelobe logic modification |
| Landing gear | Modified shock absorbers and improved landing gear locking squibs were installed |
| Compartment B wiring harness | Zener diode limiters were added to $V_x$ and $V_y$ outputs to prevent possible erroneous readings in other telemetry channels |
| TV camera hood extension | An extension was added to the camera hood to prevent direct sunlight from entering mirror hood at sun angles from zenith to 45 deg |
| Thermal switch opening temperature | All the thermal switches were set to open at 40 $\pm$5°F |

## Table IV-4. Surveyor spacecraft subsystem reliability estimates

| Subsystem | Surveyor I | Surveyor II | Surveyor III |
|-----------|-----------|-------------|--------------|
| Telecommunication | 0.925 | 0.944 | 0.965 |
| Vehicle mechanisms | 0.816 | 0.868 | 0.907 |
| Propulsion | 0.991 | 0.991 | 0.968 |
| Electrical power | 0.869 | 0.958 | 0.935 |
| Flight controls | 0.952 | 0.889 | 0.971 |
| Systems interaction factor | 0.736 | 0.949 | 0.967 |
| Spacecraft | 0.456 | 0.658 | 0.745 |

Relevance of failures is based on a joint reliability/systems engineering decision.

Owing to the number of unit changes on the spacecraft, the reliability estimate is considered generic to *Surveyor III* rather than descriptive of the exact *Surveyor III* spacecraft configuration. At the 80% confidence level, *Surveyor III* reliability was 0.67. This value was based upon application of the binomial distribution.

### 16. Spacecraft System Performance

A summary of *Surveyor III* spacecraft system performance is presented below by mission phases. Also refer to Sections IV-B through IV-J for spacecraft subsystem performance; Section VI-C presents a chronology of mission operations.

*a. Countdown and launch phase performance.* The spacecraft condition was normal during the countdown except for an erratic indication from the vernier engine roll actuator position signal. This resulted in a 51-min extension of the L-5 min scheduled hold during which the anomaly was investigated by conducting a special test with SC-5*. Results of this test indicated that the telemetry signals were normal, and the countdown was allowed to proceed. Postlaunch analysis has revealed that the erratic signals resulted from apparent movement of the roll actuator (which is locked in the launch configuration) largely due to motion of the gear train at the point of position measurement pickoff. This was caused by structural compliance of the parts under torques commanded when the roll gyro was precessed from its null position.

Liftoff occurred at 07:05:01.059 GMT on April 17, 1967, with the spacecraft in the standard launch configuration

---

*Serial designation for the *Surveyor* spacecraft scheduled for the fifth *Surveyor* mission.

(transmitter low power on, launch phase accelerometer amplifiers on, legs and omniantennas folded, solar panel and planar array stowed and locked, etc). Performance during the launch phase was as expected.

During the boost phase of flight, the *Surveyor* spacecraft is subjected to a variable vibration environment consisting of acoustically induced random vibration and the transient response to discrete flight events. The *Surveyor III* space vehicle was instrumented with five accelerometers in order to obtain information on this vibration environment. The location and orientation of these accelerometers in the launch vehicle/spacecraft interface are shown in Fig. IV-8. Output of the Z-axis accelerometer, CY520, was telemetered continuously; outputs of the other four accelerometers were telemetered on a commutated channel. Accelerometer CY530 was de-

activated prior to launch due to anomalous behavior of its amplifier.

Typical *Surveyor III* accelerometer data is shown in Table IV-5 for those events which were recorded and is comparable, in general, to the *Surveyor I* and *II* flight data, which is also shown. The 95th percentile (approximately $1.64\sigma$) estimate of the acceleration spectral density (over the frequency bandwidth of 100-1500 Hz) at *Surveyor III* liftoff is 0.010 $g^2$/Hz.

Aerodynamic heating during the launch phase was equal to or less than that expected for the nominal trajectory. The Compartment A and B thermal switch radiators experienced a temperature rise of approximately 20°F during parking orbit coast, but the compartment internal temperatures were not affected.
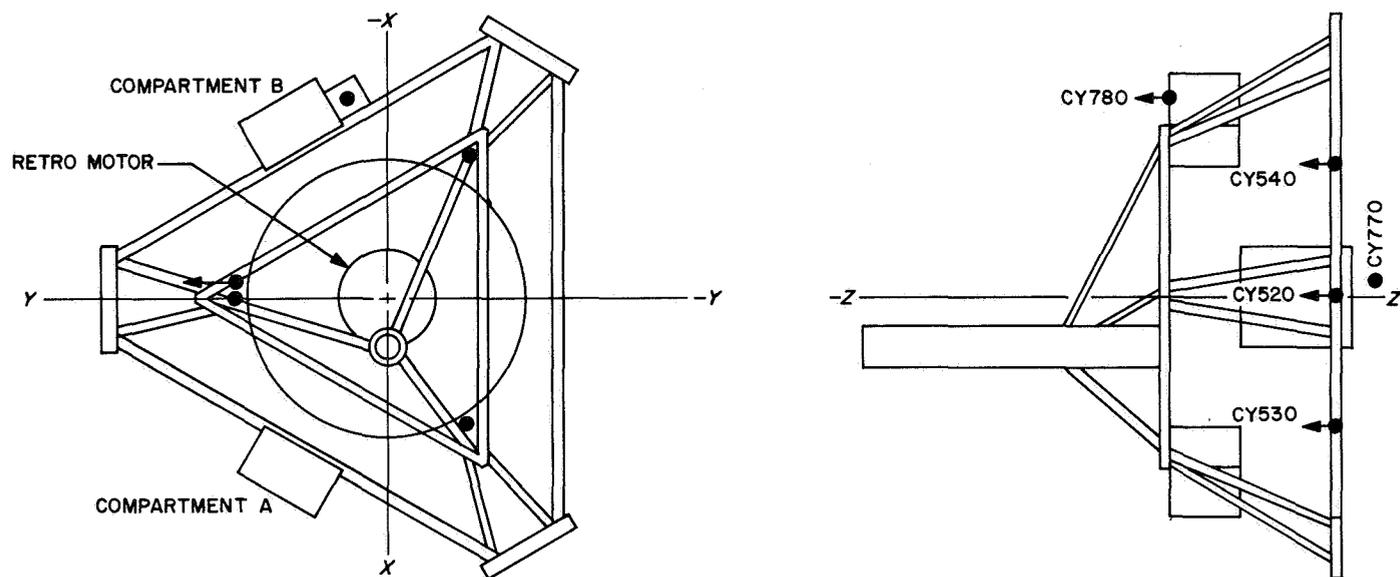
| TRANSDUCER | LOCATION | RANGE, $g$ | FREQUENCY RANGE, cps | REMARKS |
|---|---|---|---|---|
| CY520 | SPACECRAFT, NEAR ADAPTER ATTACH POINT I | ±10 | 2-2500 | CONTINUOUS |
| CY530 | SPACECRAFT, NEAR ADAPTER ATTACH POINT 2 | ±10 | 2-1260 | COMMUTATED |
| CY540 | SPACECRAFT, NEAR ADAPTER ATTACH POINT 3 | ±10 | 2-1260 | COMMUTATED |
| CY770 | ADAPTER, NEAR SPACECRAFT ATTACH POINT I | ±10 | 2-1260 | COMMUTATED |
| CY780 | SPACECRAFT, IN FCSG | ±10 | 2-1260 | COMMUTATED |

**Fig. IV-8. Launch-phase accelerometer location**

| | | Accelerometer | | | | | | | Accelerometer | | | | |
|---|---|---|---|---|---|---|---|---|---|---|---|---|---|
| | | CY520 | CY530 | CY540 | CY770 | CY780 | | | CY520 | CY530 | CY540 | CY770 | CY780 |
| Liftoff | I | 3 | 4 | 4 | 12 | 2 | Main engine | I | e | e | e | e | e |
| | II | a | a | 3 | a | 3 | start 2 | II | e | e | e | e | e |
| | III | 4.8 | a | 4.1 | 16.6 | 3.1 | | III | 2.0 | a | c | c | c |
| Maximum | I | b | b | b | b | b | Main engine | I | e | e | e | e | e |
| aerodynamic | II | b | b | b | b | b | cutoff 2 | II | e | e | e | e | e |
| loading | III | 2.4 | a | 2.2 | 5.7 | 1.64 | | III | 0.45 | a | c | c | c |
| Booster | I | 3 | c | c | c | c | Legs extend | I | 20 | c | 10 | c | c |
| engine | II | a | a | c | a | 3 | | II | a | a | c | a | c |
| cutoff | III | 3.3 | a | c | 3.73 | 1.3 | | III | 18 | a | c | 13 | c |
| Insulation | I | $>20^d$ | c | c | $20^d$ | c | Omniantennas | I | 20 | c | 12 | c | c |
| panel | II | a | a | c | a | c | deploy | II | a | a | c | a | c |
| jettison | III | $>20^d$ | a | c | c | c | | III | 16 | a | c | c | c |
| Shroud | I | 3 | c | c | c | c | | | | | | | |
| separation | II | a | a | c | a | 2.6 | | | | | | | |
| | III | 4.3 | a | c | c | c | | | | | | | |
| Sustainer | I | 1 | c | 1 | c | c | | | | | | | |
| engine | II | a | a | c | a | c | | | | | | | |
| cutoff | III | 1.2 | a | 1.3 | c | c | | | | | | | |
| Atlas/Centaur | I | $>20^d$ | $>20^d$ | c | c | c | | | | | | | |
| separation | II | a | a | c | a | c | | | | | | | |
| | III | $>20^d$ | a | c | c | c | | | | | | | |
| Main engine | I | 1 | 1 | c | c | c | | | | | | | |
| start 1 | II | a | a | c | a | c | | | | | | | |
| | III | 1.4 | a | c | c | c | | | | | | | |
| Main engine | I | 4.5 | c | c | 4.5 | c | | | | | | | |
| cutoff 1 | II | a | a | c | a | c | | | | | | | |
| | III | 3.3 | a | c | 3.3 | c | | | | | | | |

[a] These transducers were inoperative.
[b] Data not available.
[c] Commutated channel. This transducer was not being monitored at this event.
[d] Exceeded bandwidth of channel.
[e] Not applicable.

The spacecraft properly executed all preseparation events initiated by the *Centaur* programmer, which included turning on the transmitter high power, extending the landing legs, and extending the omniantennas. Spacecraft separation from the *Centaur* was also accomplished as desired. The automatic solar panel and A/SPP roll axis stepping sequence was initiated by spacecraft separation and occurred normally. The solar panel was unlocked and required about 359 sec to step through −56 deg to its transit position, where it was locked. Upon locking of the solar panel, the A/SPP was unlocked and rolled +60 deg in a period of about 252 sec to its desired transit position, where it was locked.

Spacecraft separation also enabled the cold gas attitude control system and initiated the automatic sun acquisition sequence after a timed delay of about 51 sec, which is designed to allow adequate time for the separation tipoff rates to be nulled. The angular rates had been reduced to 0.1 deg/sec within 20 sec. The sun acquisition sequence occurred properly and began with a 356-deg roll through −181 deg, which was terminated upon illumination of the acquisition sun sensor. Then followed a 77-sec yaw turn through +38 deg, which was terminated upon illumination of the primary sun sensor center cell.

*b. Coast phase performance.* After DSIF two-way acquisition had been established by DSS 42 about 57 min after liftoff, an initial assessment was made in the transmitter high-power mode. (A profile of the *Surveyor III* telemetry data bit rates and commutator modes during all flight phases is presented in Fig. IV-9.) Following this assessment, which indicated all systems to be normal, the spacecraft responded correctly to an initial sequence of commands to place the spacecraft in the cruise configuration. In the cruise configuration, the launch phase accelerometer power was off and the transmitter was operated on low-power at 1100 bit/sec with

Fig. IV-9. Surveyor III transit phase telemetry data rate/mode profile
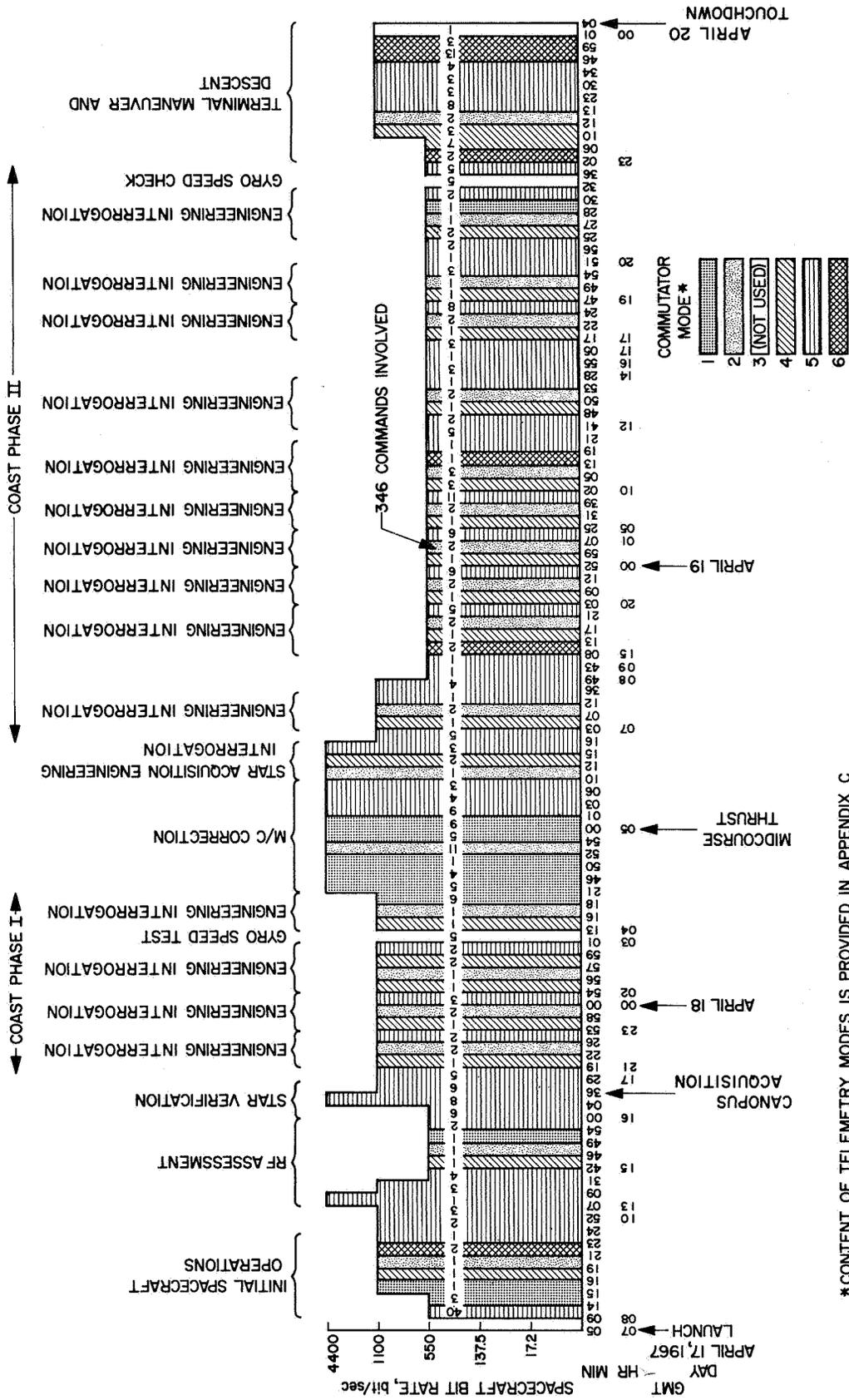
*CONTENT OF TELEMETRY MODES IS PROVIDED IN APPENDIX C

the coast phase commutator on. The commanding of flight control to cruise mode was delayed owing to a high-intensity signal from the Canopus sensor, which indicated the presence of the earth in the field of view. After 3½ hr from launch, the signal intensity had decreased, indicating that the earth had left the field of view, and the spacecraft was commanded to cruise mode, which insured that the flight control system would revert to inertial mode if sun lock was lost.

Automatic Canopus lock-on occurred successfully almost 9½ hr after launch, when acquisition was attempted after an initial roll to generate a star map. The total spacecraft roll was 565 deg. During the first 360 deg of roll, signals from two objects were noted which did not appear on the predicted star map. Since the objects did not appear again when the same roll positions were passed to achieve Canopus lock-on, it was concluded that the objects were particles which passed through the field of view during the first rotation. The Canopus sensor performance was close to preflight predictions. The effective gain of the sensor had been set to about 1.05 to 1.10 $\times$ Canopus for the *Surveyor III* mission by changing the sun filter transmission characteristics.

Telecommunications system performance was satisfactory throughout the flight, although techniques used by the DSIF for measuring sideband power indicated lower than nominal values. Special sequences commanded during the first DSS 51 postinjection pass verified that the spacecraft sideband power was at the correct level.

Deviations from the predicted received signal levels were noted on both the up-link and down-link. Gyro drift checks performed during this period accounted for omni-antenna gain variations that were not taken into consideration when the predictions were generated. A deviation in Receiver B received signal level over that expected due to gyro drifts further indicated, as did the Canopus and midcourse data, that a $-2$-db bias existed in the receiver performance or calibration data.

There were no significant disturbing torques acting on the vehicle during the coast phases. The three-axes gas jet pulsing rate was observed for 2 hr 45 min of optical limit cycle operation. The mean-time between gas jet pulses for this period was 85 sec, which essentially agreed with the predicted pulsing rate of 103 sec.

The number of gyro drift checks conducted during the coast phases was larger than normal because of indications that drift rates were exceeding the specification

value of 1.0 deg/hr. The final drift rates computed for use in planning the terminal descent were: $+1.1$ deg/hr roll; $+0.6$ deg/hr pitch; and $-0.8$ deg/hr yaw.

Performance of the spacecraft thermal control system was excellent during transit. The actual spacecraft temperatures were near the normal predictions as indicated by most sensors. Of the 75 temperature sensors on the spacecraft, 43 were within $\pm5°F$, 16 were within $\pm10°F$, 7 were within $\pm15°F$, and 8 were within $\pm20°F$ of their predicted values. The SM/SS electronics auxiliary was 15°F lower than the minimum predicted value, requiring greater than anticipated heater usage, but was still well above the minimum survival temperature of $-67°F$.

Battery energy consumption was close to predicted during transit. The average optimum charge regulator efficiency was approximately 80%, and the average boost regulator efficiency was approximately 77%. Energy remaining at touchdown was about 99 A-hr in the main battery and about 30 A-hr in the auxiliary battery.

*c. Midcourse correction performance.* After the premidcourse attitude maneuvers had been accomplished, vernier engine ignition was commanded on at approximately 22 hr after liftoff for a 4.277-sec period to provide a 4.19 m/sec velocity correction. Ignition was smooth, with small pitch and yaw attitude changes. The midcourse maneuver corrected the miss distance to within 2.76 km of the final aim point.

The peak gyro angles were less than 2 deg after vernier engine shutdown, which was well within the minimum gyro gimbal range of $\pm10$ deg. Inertial reference was therefore retained and reacquisition of the sun and Canopus was accomplished via the standard reverse maneuver sequence.

Postmidcourse analysis of engine thrust command data indicated there was a possible unbalance in thrust levels of the vernier engines. Since the spacecraft attitude remained stable during midcourse and touchdown, it appears that the indication was due to telemetry inaccuracies.

*d. Terminal maneuver and descent performance.* The spacecraft properly executed the commanded terminal maneuvers, which were initiated about 38 min prior to retro ignition.

The automatic descent sequence was initiated by the altitude marking radar *mark* signal. The predicted and actual event times and parameter values for the terminal

**Table IV-6. Predicted and actual times corresponding to terminal descent events (GMT April 20, 1967)**

| Event | Predicted | Actual (best estimate) |
|---|---|---|
| AMR mark | 00:01:11.5 | 00:01:11.6 |
| Main retro ignition | 00:01:17.6 | 00:01:17.7 |
| 3.5-g level | 00:01:59.0 | 00:01:59.4 |
| Retro case eject | 00:02:11.0 | 00:02:11.4 |
| Vernier phase start (RADVS control) | 00:02:13.2 | 00:02:13.4 |
| Descent segment intercept | 00:02:43.2 | 00:02:32.5 |
| 1000-ft mark | 00:03:55.2 | 00:03:51.8 |
| 10-ft/sec mark | 00:04:12.9 | 00:04:09.4 |
| 14-ft mark | 00:04:18.4 | Not issued |
| Touchdown (initial) | 00:04:20.1 | 00:04:16.9 |

**Table IV-7. Predicted and actual values of terminal descent parameters**

| Parameter | Predicted | Actual (best estimate) |
|---|---|---|
| Main retro phase initial conditions | | |
| Time, GMT, April 20, 1967 | 00:01:17.8 | 00:01:17.9 |
| Z-axis angle with lunar vertical, deg | 22.9 | 22.9 |
| Slant range, ft | 273,170 | 271,334 |
| Velocity, ft/sec | 8617 | 8617 |
| | | |
| Main retro burnout conditions | | |
| Slant range, ft | 34,734 | 36,158 |
| Longitudinal velocity, ft/sec | 461.4 | 462.4 |
| Lateral velocity, ft/sec | | 168.1 |
| Z-axis angle with lunar vertical, deg | | 23.8 |
| Flight path angle with lunar vertical, deg | 9.15 | 3.8 |
| | | |
| Misalignment during main retro phase | | |
| In plane, deg | 0 | 0.34 |
| Out of plane, deg | 0 | 0.02 |
| | | |
| 1000-ft mark conditions | | |
| Slant range, ft | 1010.4 | 998.9 |
| Velocity, ft/sec | 106.5 | 103.3 |
| Z-axis angle with lunar vertical, deg | 1.1 | 0.5 |
| | | |
| 10 ft/sec mark conditions | | |
| Slant range, ft | 43 | 46 |
| Velocity, ft/sec | 8.6 | 8.6 |
| Z-axis angle with lunar vertical, deg | 0 | 0 |
| | | |
| Vernier engine cutoff conditions | | |
| Slant range, ft | 13 | |
| Velocity, ft/sec | 5 | |
| Z-axis angle with lunar vertical, deg | 0 | |

descent are presented in Tables IV-6 and IV-7, respectively. Vernier engines ignition, retromotor ignition, RADVS turn on, retromotor burnout, and retro separation occurred normally. The moment disturbance produced by the retromotor firing was small. RADVS acquisition and lock-on in both velocity and range were accomplished prior to retro burnout. The altimeter apparently lost lock momentarily two times (the last time probably caused by retro case separation) but was back in lock in one sweep of the tracker.

The vernier phase was initiated 2 sec after retro separation. Realignment of the Z-axis to the existing velocity vector was accomplished in 3 to 4 sec, and the vernier engines, under control of the RADVS, kept the spacecraft on the desired descent contour. The 1000-ft and 10-ft/sec mark signals were generated as expected. However, approximately 2 to 3 sec after the 10-ft/sec mark, RADVS Beam 3 tracker lost lock, preventing the generation of the 14-ft mark. Analysis indicates that the system behaved as though there had occurred a false sidelobe rejection of the main beam. A momentary fade in signal of Beam 3 or increase in signal of Beam 2 (as might occur if the beams traverse a surface irregularity) will cause the rejection logic to work. Once rejection occurs at low velocity, it is virtually impossible to reacquire lock. Upon loss of lock, flight control is mechanized to hold the spacecraft attitude fixed in inertial mode and maintain a near-minimum vernier engine thrust level equivalent to 0.9 lunar g.

The loss of lock occurred at an altitude of about 37 ft and a velocity of 5 ft/sec. The spacecraft then accelerated at 0.1 lunar g for 6.5 sec and made first contact with the lunar surface at a velocity of about 6 ft/sec.

The normal and anomalous events which occurred during the *Surveyor III* terminal descent and landing are indicated in the chart of Fig. IV-10.

*e. Landing performance.* Initial touchdown occurred at 00:04:16.9 GMT on April 20 on a slope of about 10 deg with the verniers still on at a thrust level almost equal to the lunar weight. The spacecraft lifted off after initial touchdown and remained aloft for approximately 24 sec (see Fig. IV-11). Liftoff also occurred after second touchdown, the spacecraft remaining aloft for an additional 12 sec before third touchdown.

On each touchdown, Leg 2 impacted the surface first in the uphill direction followed by almost simultaneous impacts of Legs 1 and 3. In attempting to correct the
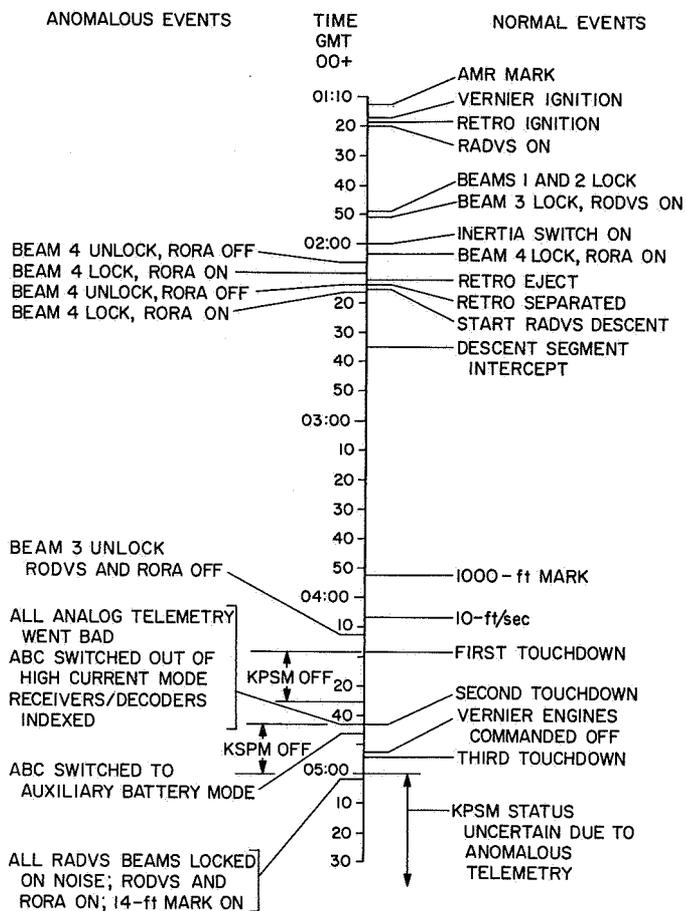
**Fig. IV-10.** *Surveyor III* terminal descent and landing events chart

spacecraft attitude to the pretouchdown state, the flight control system momentarily increased the thrust of the engines. This additional thrust and the spring forces in the landing legs caused the spacecraft to lift off in the downhill direction. The loads sensed by the touchdown strain gages indicated that forces in the shock absorbers were on the order of less than half that indicated on *Surveyor I*, as would be expected for landing with engines thrusting. When the spacecraft attitude had been corrected following the first and second touchdowns, the attitude was held stable and a nominal vernier thrust level of 0.9 lunar *g* was maintained while the spacecraft was aloft.

A ground command was sent 35 sec after initial touchdown which turned off the vernier engines approximately 1 sec before the third touchdown. After the spacecraft made contact the third time with the engines off, it only moved approximately a foot laterally before coming to rest. As shown in Fig. IV-11, the spacecraft traversed an estimated 15 to 22 m between the first and second touch-

downs and an additional 11 to 14 m before the third touchdown. The landing location, as located on *Lunar Orbiter III* photographs (see Section VII), is in the Ocean of Storms at 2.94 deg south latitude and 23.34 deg west longitude. The spacecraft finally came to rest at an angle of about 12½ deg with the vertical (Fig. IV-12), about halfway between the eastern rim and the center of a crater having a diameter of approximately 200 m. The footpad impressions made by the second touchdown event have been identified in the mosaic of *Surveyor III* television frames shown in Fig. IV-13. The erosion effect of Vernier Engine 3 is also believed to be visible in the frames. The impression left by Footpad 2 before moving laterally during the final touchdown event is seen in Fig. IV-14. The touchdown impressions made by *Surveyor III* appear comparable to those which were made by *Surveyor I* some 625 km to the west.

The final spacecraft landed roll orientation, as shown in Fig. IV-12, was approximately 6 deg counterclockwise from the predicted roll orientation. The roll orientation desired by Project Science was about 120 deg clockwise from the final orientation, but this could not be met because the spacecraft roll position was constrained to prevent cross-coupling of the RADVS beam side lobes. The spacecraft attitude shown in Fig. IV-12 is based upon determinations made from postlanding planar array and solar panel positioning experiments.

The landing sequence adversely affected some of the spacecraft subsystems. Concurrently with both the first and second touchdowns, the RADVS klystron power supply modulator (KPSM) switched off. The KPSM, which provides RADVS high voltage, came back on after 18 sec, as it should (Fig. IV-10). Status of the KPSM after second turn-off is uncertain owing to anomalous behavior of the RADVS current signal from which KPSM voltage level is determined. Turn-off of the KPSM would normally indicate that a drop of 6 V had occurred on the 22-Vdc input for a duration of 3 msec.

At the time of second touchdown all analog telemetry signals became erroneous. Also concurrent with this event, switching occurred from Receiver/Decoder B to A, and the battery control logic switched from the high-current mode to the main battery mode. Three seconds later, the control logic switched to the auxiliary battery mode, which was probably a normal occurrence considering the existing state of the battery charge.

The telemetry anomaly was found to be localized in the signal processing analog-to-digital converters (ADC),

15 TO 22 m · 11 TO 14 m

24 sec · 12 sec

FIRST
TOUCHDOWN

SECOND
TOUCHDOWN

THIRD
TOUCHDOWN
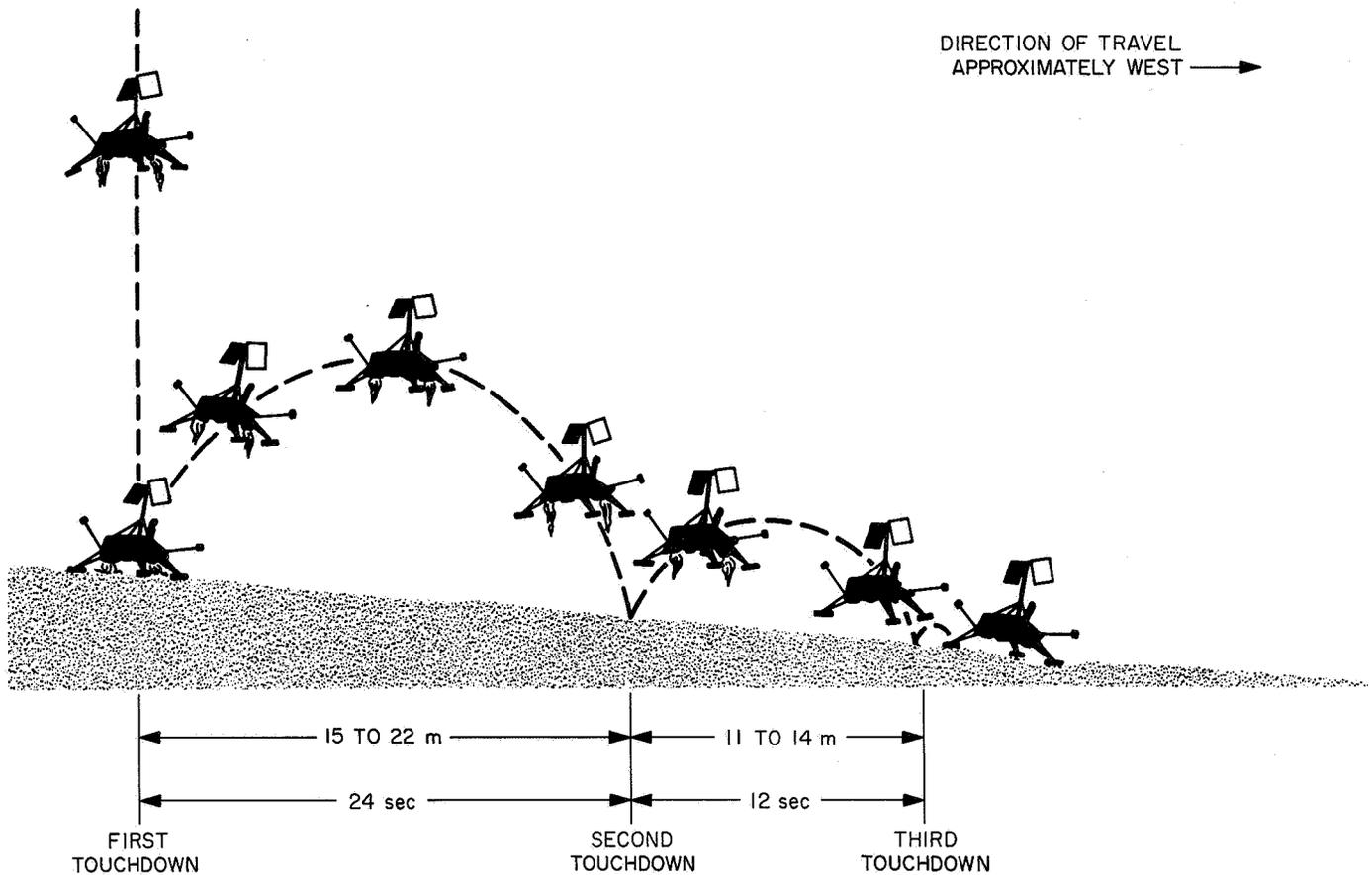
**Fig. IV-11.** *Surveyor III* **landing sequence**

since the digital and television data remained normal. Analysis has indicated that the direct cause of the data problem was the serious degradation of the transistor switches in the engineering signal processor (ESP) and the auxiliary engineering signal processor (AESP). A suspected basic cause of the signal processing failure is related to the anomaly in the KPSM. Analysis of the plasma dynamics, as the spacecraft touched down with engines operating, indicates that sufficient ionization may have entered the KPSM to cause arcing of the high voltage. This would provide an explanation of the repeated KPSM turnoff coincident with the first two touchdowns and, if insulation had been burned away, could have resulted in a high voltage being applied to the commutator transistor switches, which are connected to a measurement in the KPSM.

*f. Postlanding performance.* Initial indications after landing were that there was an acute power system problem. However, as the result of special sequences to investigate this problem and the general analog telemetry anomaly, it was found that the power system was normal,

and the problem was confined to the signal processing system. Further investigation led to the conclusion that most analog data obtained in the lowest rate mode (17.2 bit/sec) was fairly reliable and could be corrected with simple calibration factors. Analysis is continuing in an attempt to correct some of the data obtained at higher rates.

The initial uncertainty in spacecraft status caused some delay in conducting the early television, SM/SS, and other planned lunar surface experiments. Nevertheless, over 6300 television pictures were received before the spacecraft transmitter was turned off shortly after sunset. More television picture glare occurred on *Surveyor III* as compared to *Surveyor I*. This was especially true for pictures taken soon after touchdown, when the sun was near the horizon. *Surveyor III* was equipped with a modified sun shade to minimize glare but, because of the landed orientation on a sloping surface, many of the early pictures were taken with unfavorable sun angle, which increased the glare. It is apparent that considerable glare occurred on pictures taken at some sun angles due to contamination or pitting of the upper part of the camera

SECTION ALONG LINE $A-A'$
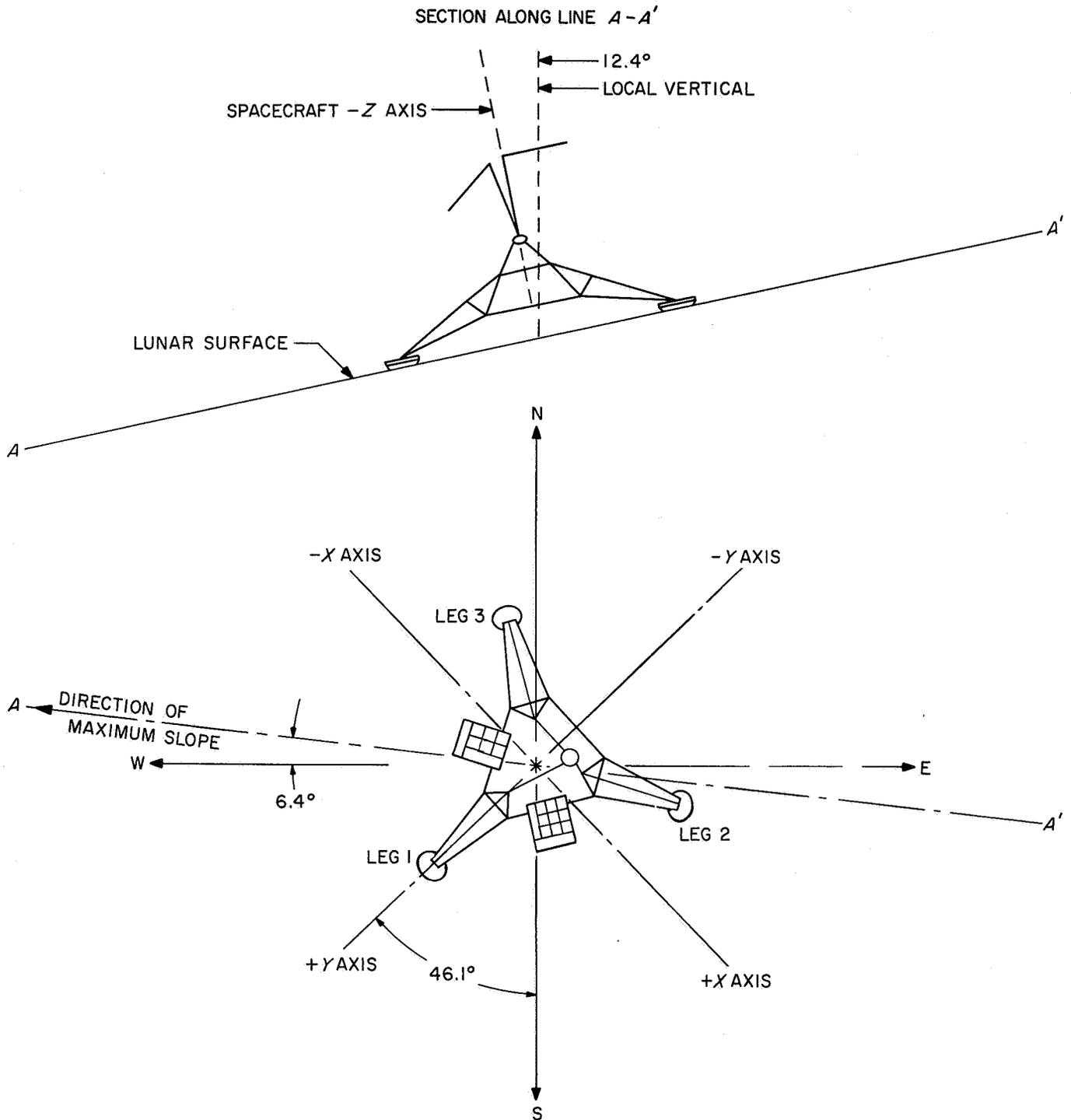


Fig. IV-12. *Surveyor III* landed attitude
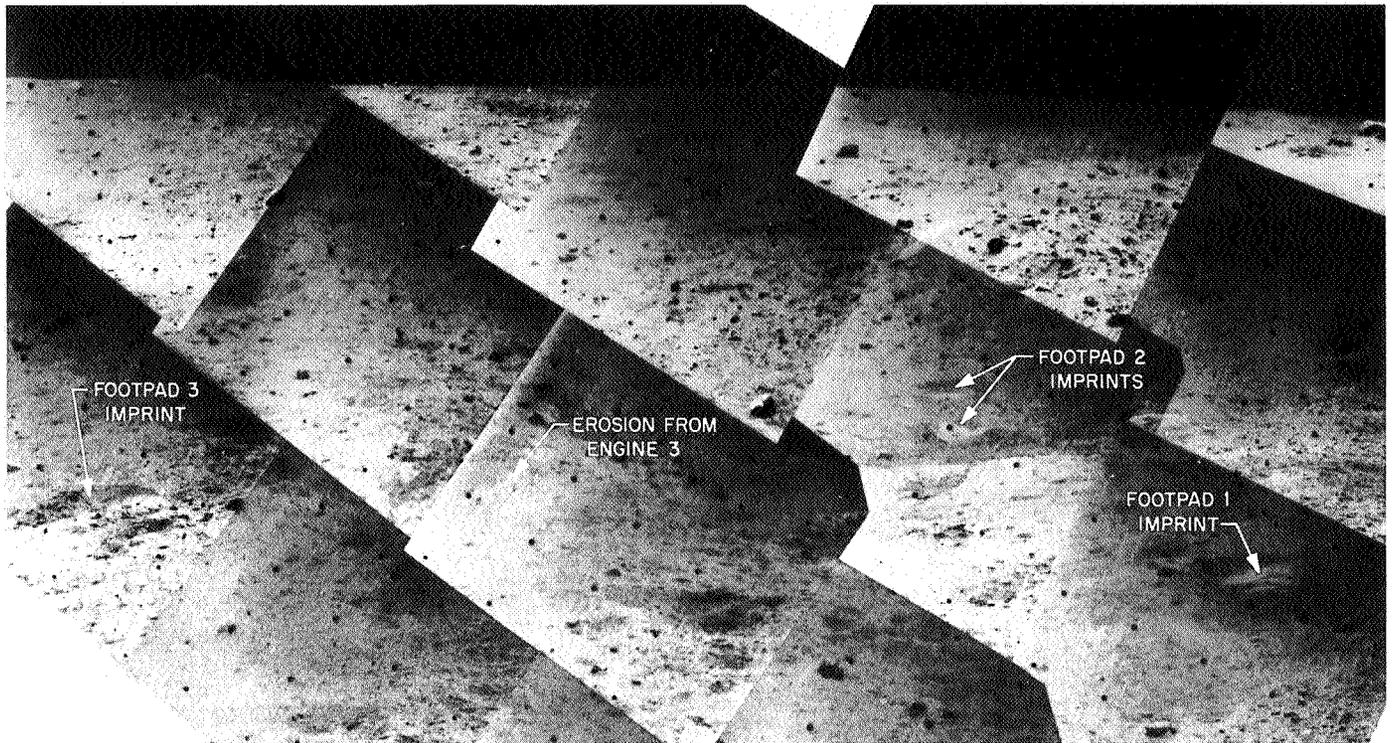
Fig. IV-13. *Surveyor III* second touchdown footpad imprints (April 26, 1967, 08:37:36 GMT)

mirror. This condition is believed to have occurred as a result of landing with the engines thrusting. The television camera also experienced some problems in stepping, which reduced the rate at which pictures were taken.

After being unlocked, the A/SPP responded normally to stepping commands, permitting acquisition of the earth by the planar array and sun by the solar panel. These are necessary events to permit transmission of 600-line pictures and obtain adequate power for continued lunar operations. The A/SPP continued to function properly throughout the lunar day when it was required to (1) reposition the solar panel as sun elevation changed, (2) change the panel shadow patterns for thermal control of critical components such as the camera, and (3) step the planar array for antenna pattern mapping and spacecraft attitude determination. The progressive shadow patterns of the spacecraft through the lunar day are shown in Fig. IV-15.

The SM/SS and its electronics auxiliary responded correctly to all commands during the periods of time it was on, which totaled 18 hr, 22 min. The many operations performed with the SM/SS included: 8 bearing tests in which the scoop was pushed into the surface with the door closed; 14 impact tests in which the scoop was

dropped from different heights with or without the door open; the digging of four trenches, two of which were dug with repeated passes; and the picking up of various surface material and the handling and dumping of it at desired locations such as the top of Footpad 2. SM/SS data was obtained by the coordinated operation of the television camera. Valid SM/SS motor current data could not be obtained because of the telemetry anomaly occurring at touchdown.

The *Surveyor III* spacecraft experienced a total eclipse of the sun while on the lunar surface. The spacecraft performed well throughout the eclipse and returned valuable thermal response data and television pictures of the earth during the eclipse event.

*Surveyor III* performance was considered excellent at the end of the lunar day, and the spacecraft was placed in a configuration which was considered optimum for survival on the second lunar day. Battery energy had been conserved so that nearly a full charge existed, and the solar panel was positioned so that it would provide power on the second day after the insulated compartments would have warmed sufficiently. After sunset, cooldown of the compartments to 0°F was rapid, indicating that some of the thermal switches had not opened in the
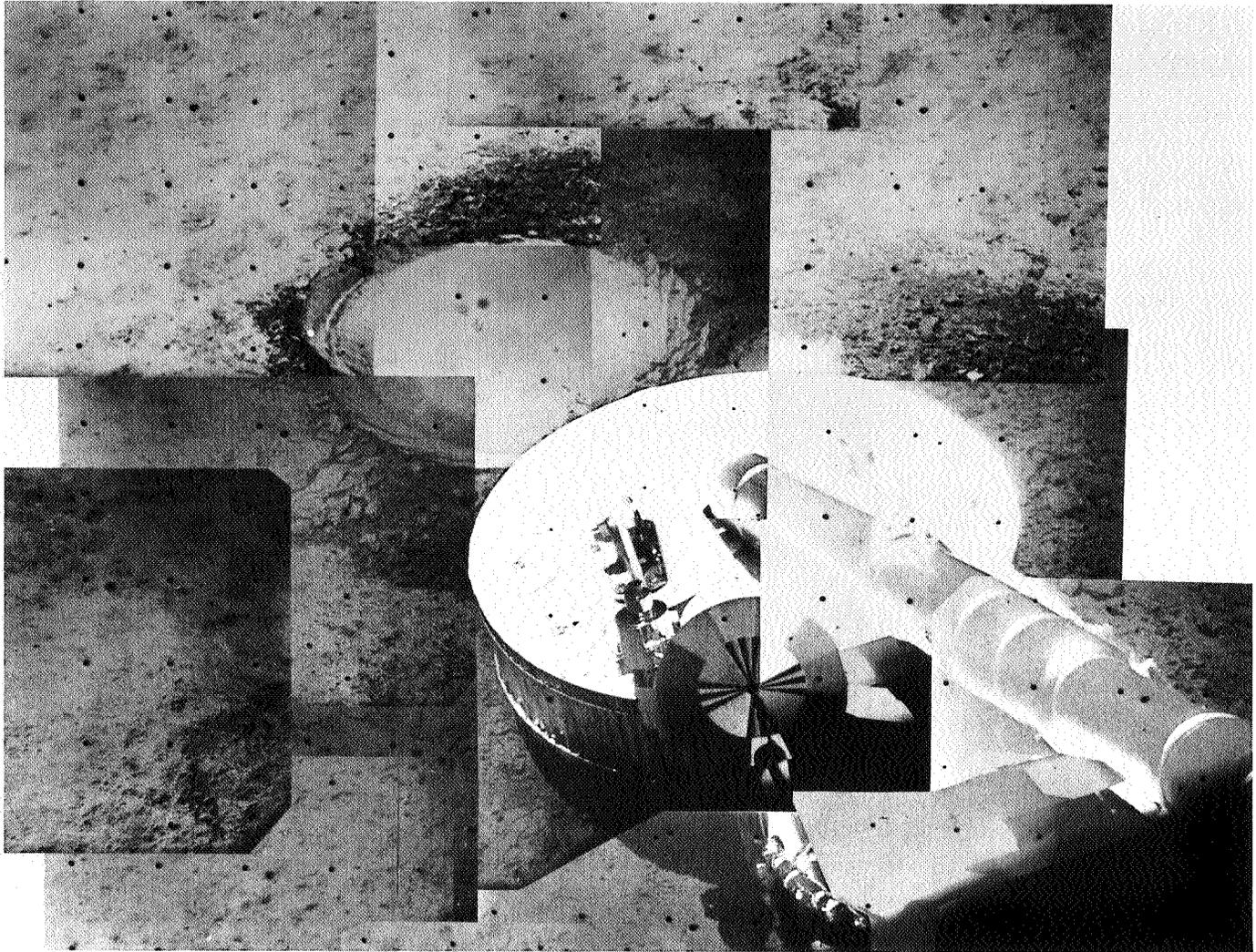
**Fig. IV-14. Footpad 2 impression from third touchdown event (April 26, 1967, 07:06:46 through 09:27:06 GMT)**

specified temperature range of 40±5°F. When the compartment reached 0°F, all spacecraft power was commanded off, leaving only the receivers on in the hope that the spacecraft would respond to commands the second lunar day. However, no response from *Surveyor III* was detected the second lunar day though repeated commands were sent between May 23 and June 2.

## B. Structures and Mechanisms

The vehicle and mechanisms subsystem provides support, alignment, thermal protection, electrical interconnection, mechanical actuation, and touchdown stabilization for the spacecraft and its components. The subsystem includes the basic spaceframe, landing gear mechanism, crushable blocks, omnidirectional antenna mechanisms,

antenna/solar panel positioner (A/SPP), pyrotechnic devices, electronic packaging and cabling, thermal compartments, thermal switches, separation sensing and arming device, and secondary sun sensor.

## 1. Spaceframe and Substructure

The spaceframe, constructed of thin-wall aluminum tubing, is the basic structure of the spacecraft. The landing legs and crushable blocks, the retrorocket engine, the *Centaur* interconnect structure, the vernier propulsion engines and tanks, and the A/SPP attach directly to the spaceframe. Substructures are used to provide attachment between the spaceframe and the following subsystems: the thermal compartments, TV, SM/SS, RADVS antennas, flight control sensor group, attitude control nitrogen tank, and the vernier system helium tank.

LEG 3
LOCAL LUNAR COORDINATES
COMPARTMENT B
SURVEY TV CAMERA
DOWNHILL DIRECTION (MAX SLOPE)
SM/SS
W
6.4°
SPACECRAFT COORDINATES
LEG 2
-X
+Y
LEG 1
46.1°
S
COMPARTMENT A
APRIL 20, 00:04:17 GMT
TOUCHDOWN CONFIGURATION

APRIL 23, ZERO HOUR

APRIL 21, ZERO HOUR

APRIL 24, ZERO HOUR

APRIL 22, ZERO HOUR
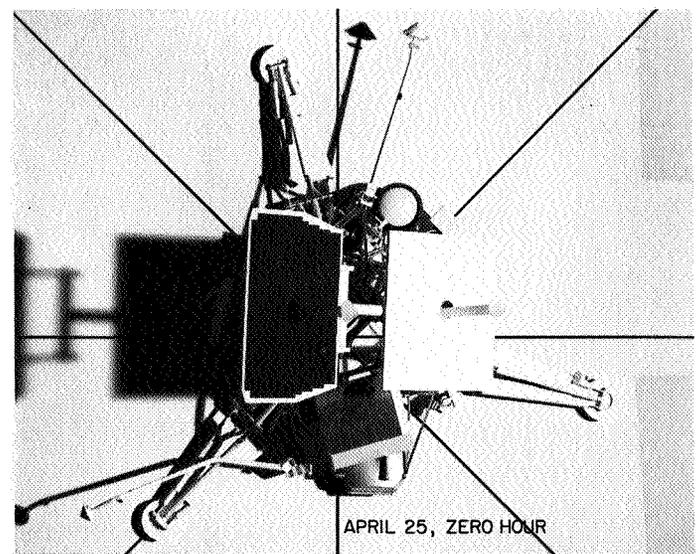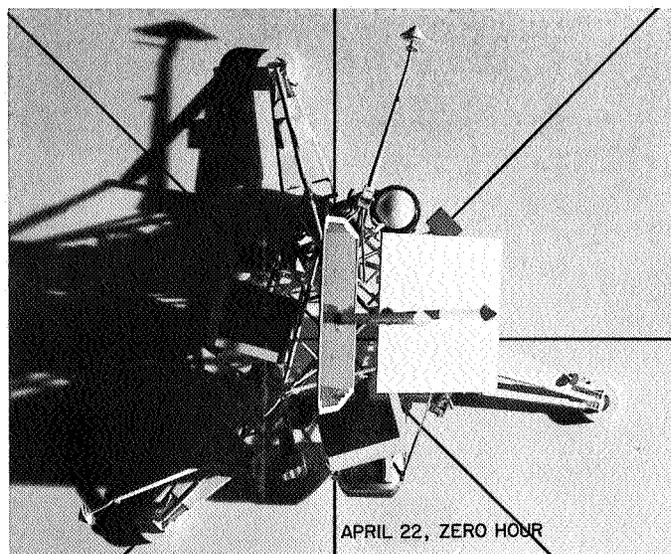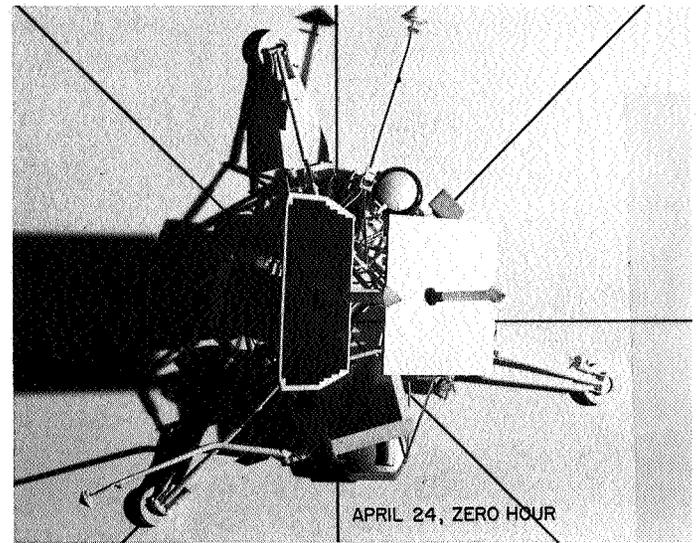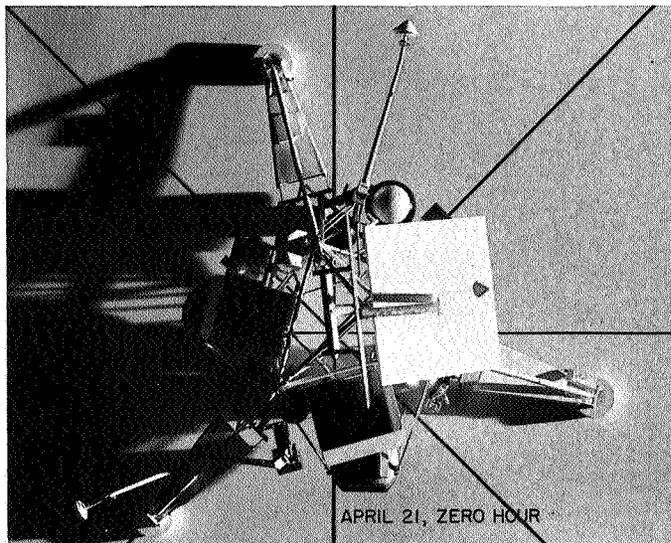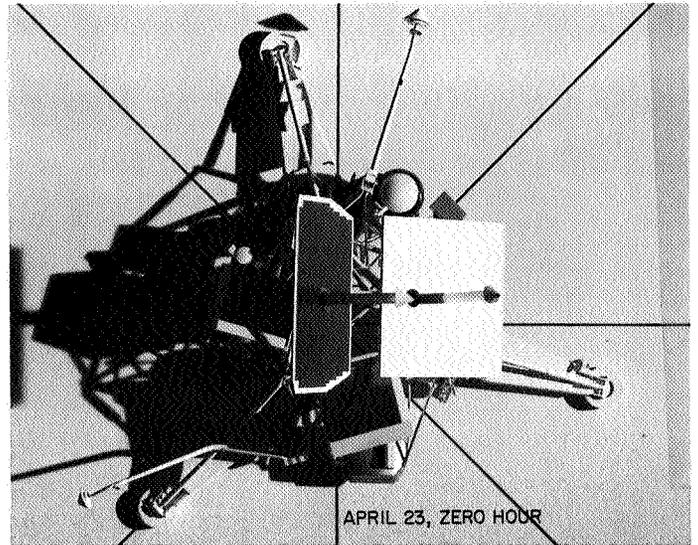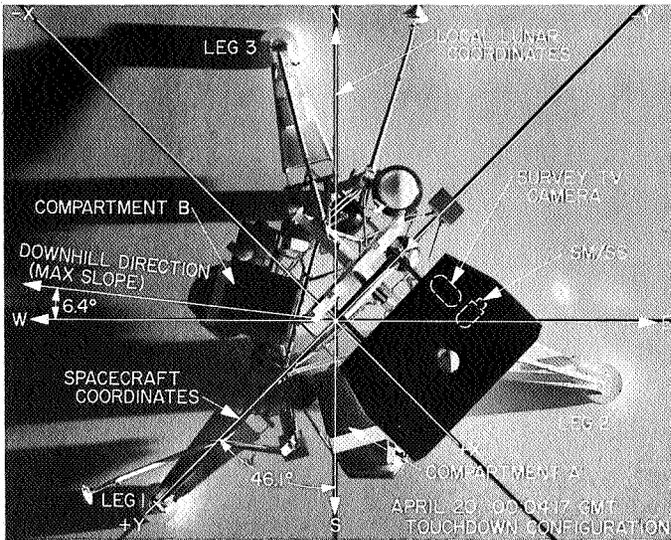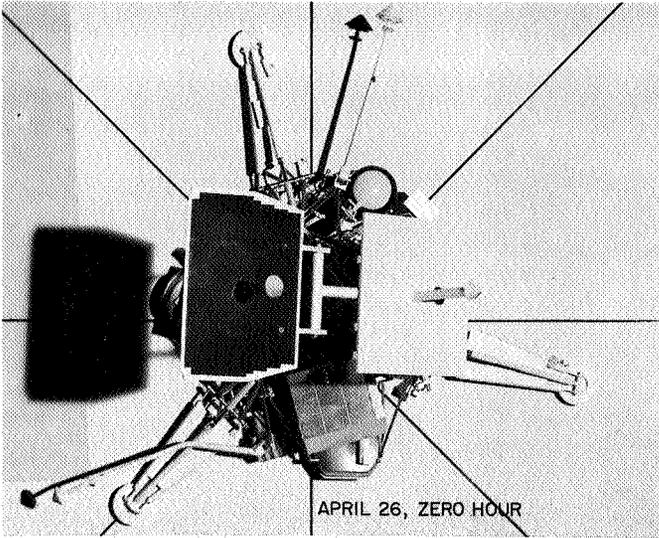
APRIL 25, ZERO HOUR
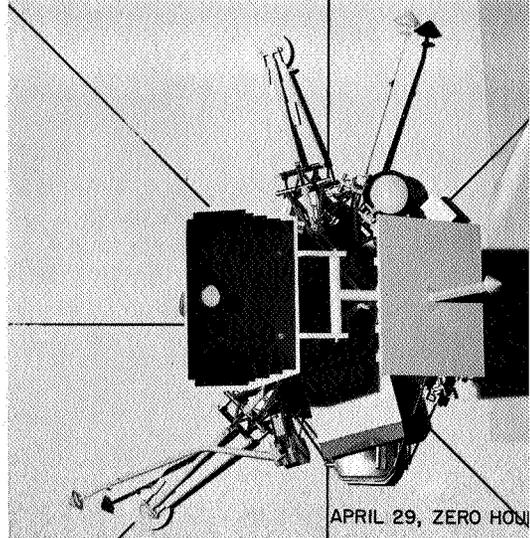
APRIL 26, ZERO HOUR

APRIL 29, ZERO HOUR
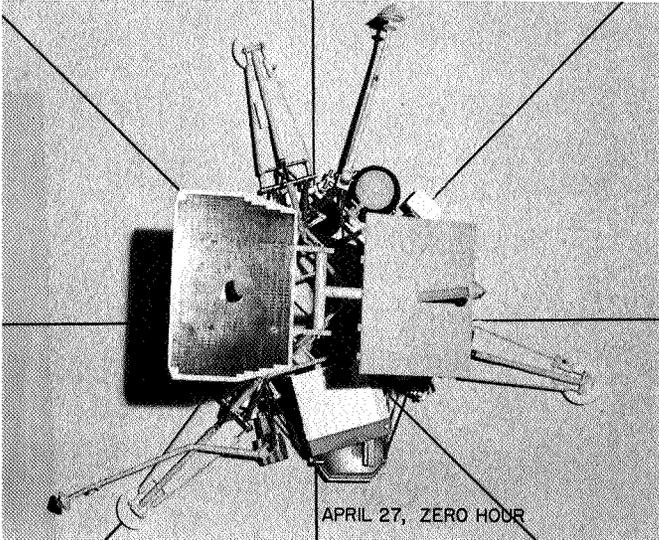
APRIL 27, ZERO HOUR
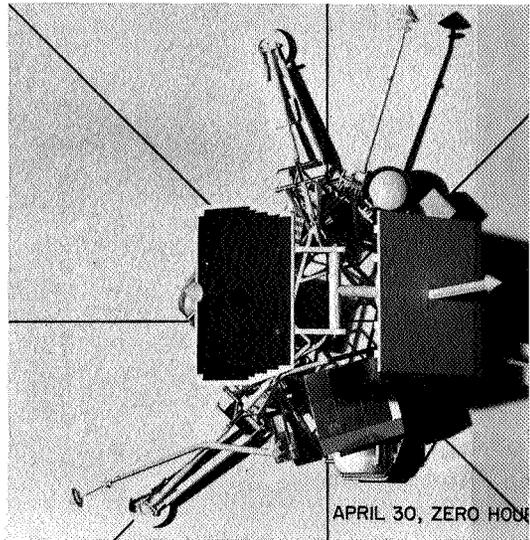
APRIL 30, ZERO HOUR
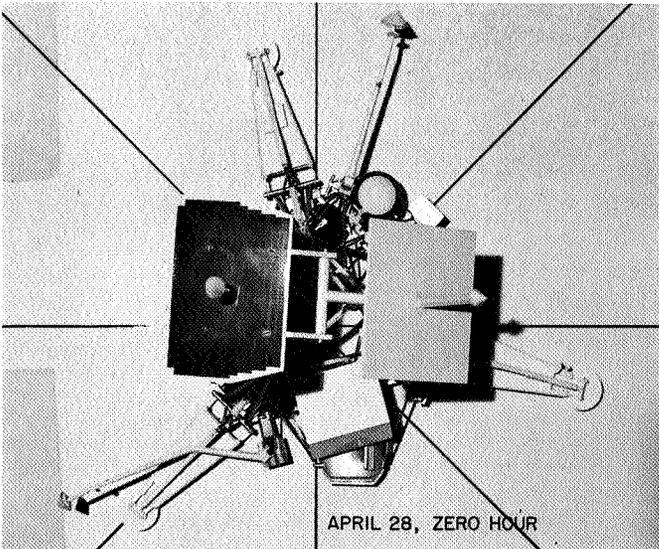
APRIL 28, ZERO HOUR
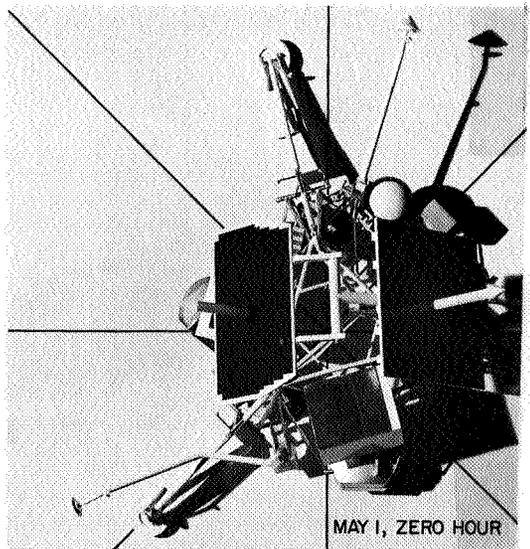
MAY 1, ZERO HOUR
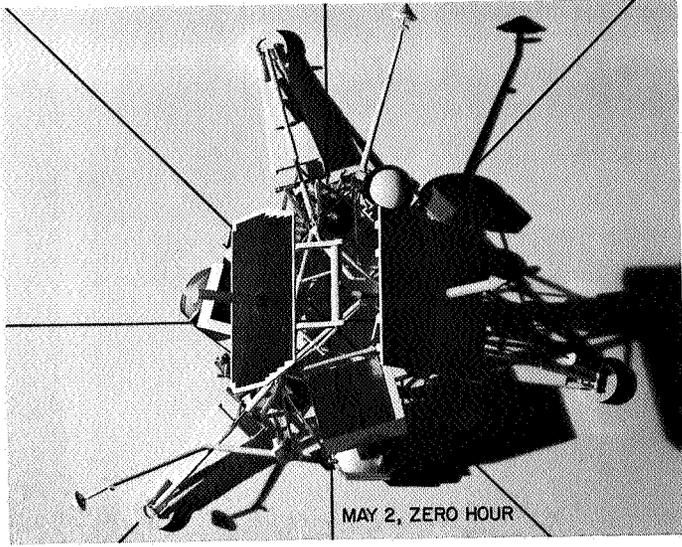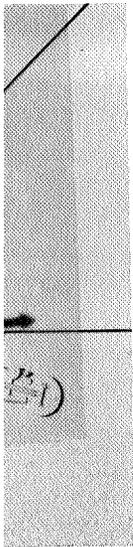
MAY 2, ZERO HOUR
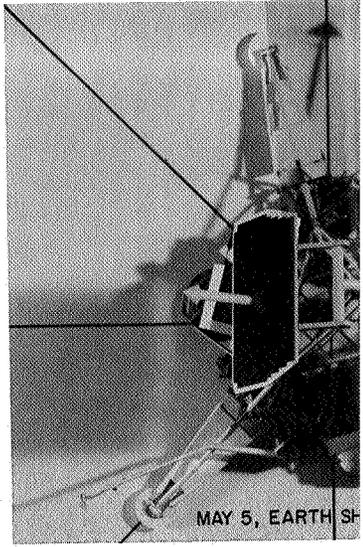

MAY 5, EARTH SH
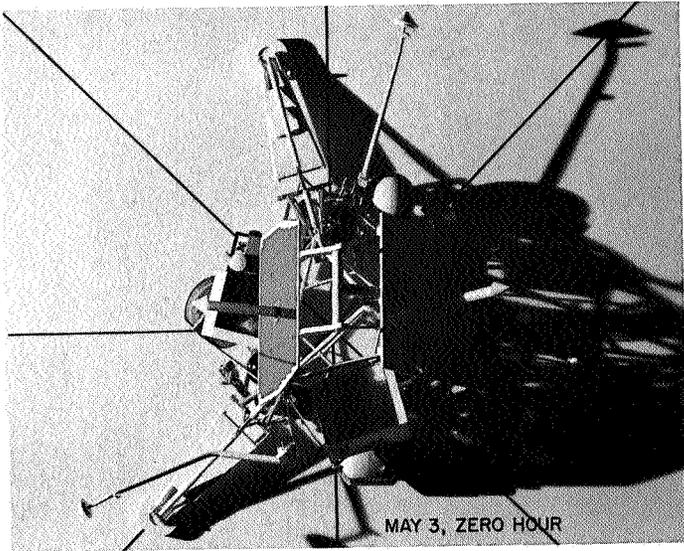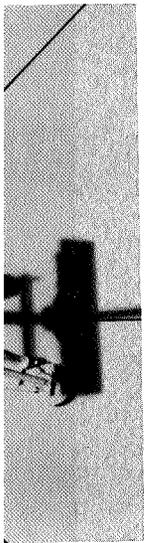

MAY 3, ZERO HOUR


MAY 4, ZERO HOUR

IE, ZERO HOUR



70°
60°
50°
40°
30°
20°
10°

W 0°      MAY 1     APRIL 29     APRIL 27     ○ LANDING SITE

10°
20°

MARE HUMORUM

30°
40°
50°
60°
70°

54-3
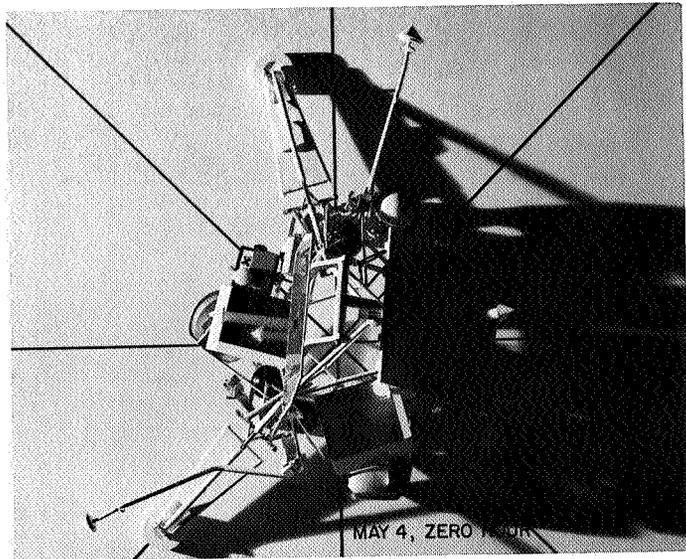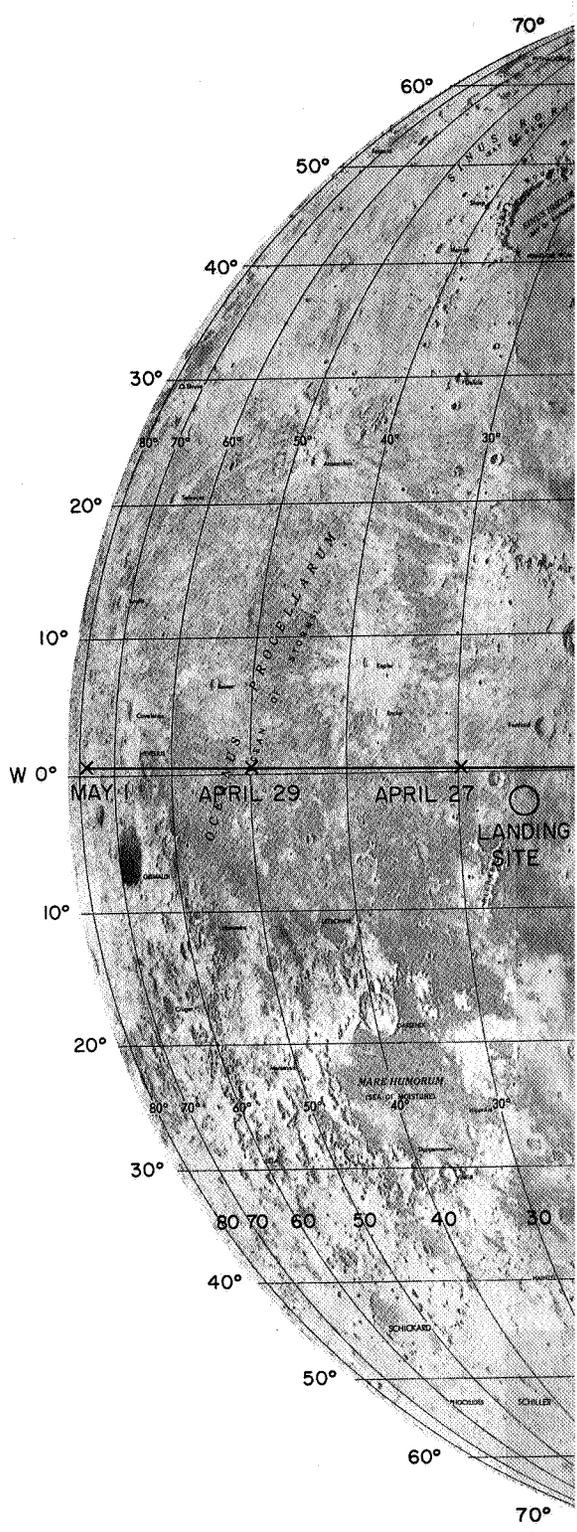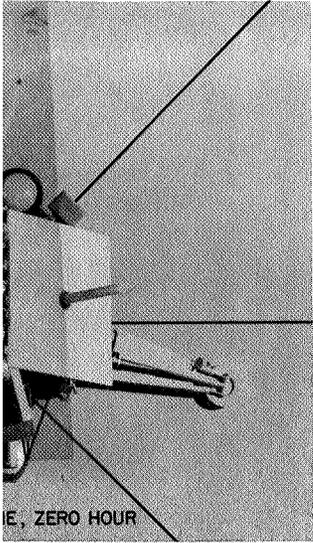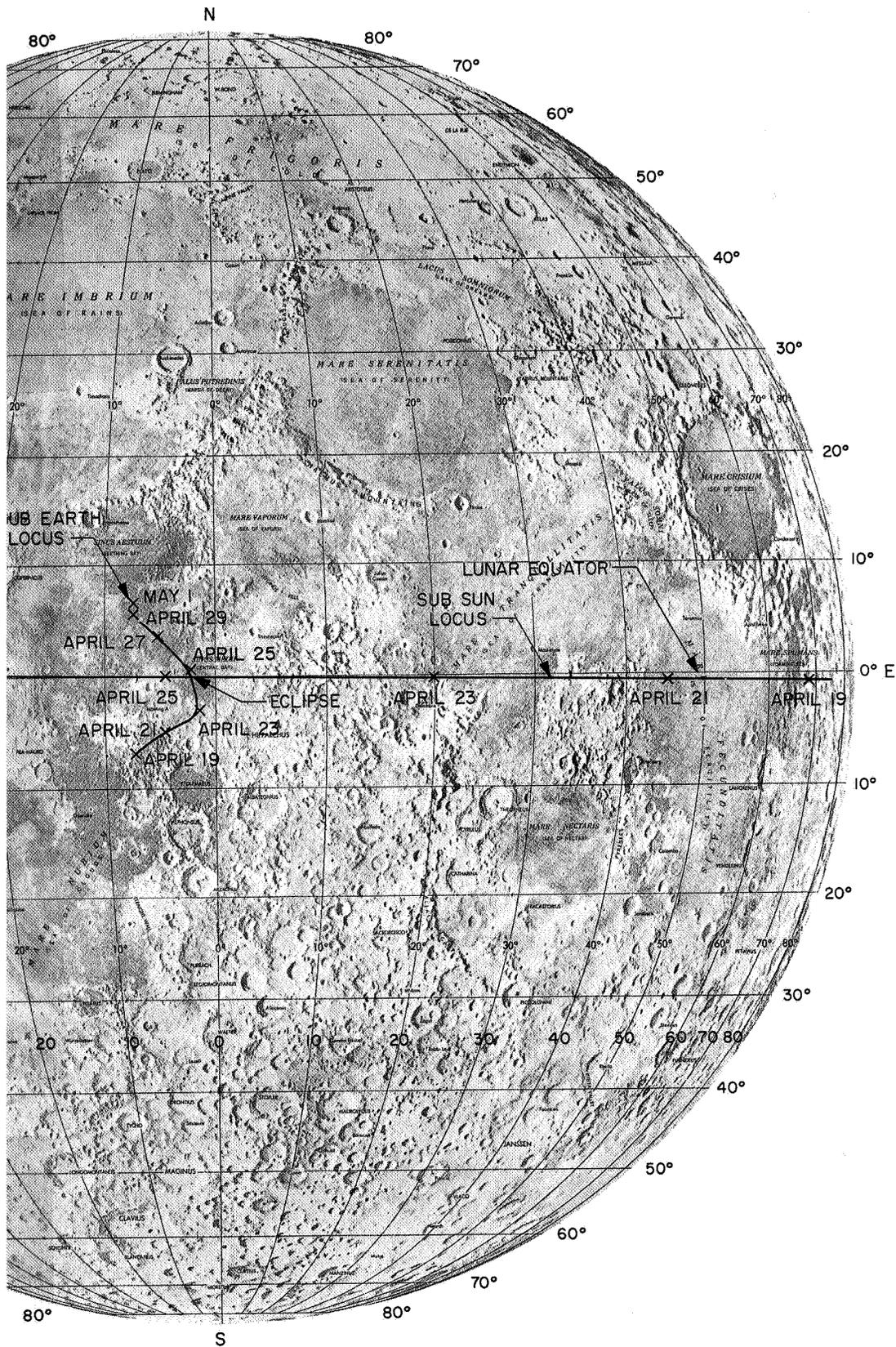
**Fig. IV-15.** *Surveyor III posttouchdown shadow patterns*

During the *Surveyor III* mission there was no indication of any failures or anomalies due to structural malfunctions.

## 2. Landing Gear

The landing gear consists of three landing leg assemblies and three crushable honeycomb blocks attached to the spaceframe (Fig. IV-16). The leg assemblies are made up of a tubular inverted tripod structure, an A-frame, a lock strut, and a honeycomb footpad.

During launch, the legs are folded for stowage under the shroud. Shortly before spacecraft separation, upon command from the *Centaur* programmer, the legs are released by squib-actuated pin pullers and are extended automatically by torsion springs located at the leg hinge axes. After extension, the leg positions are measured by three potentiometers which are also located near the hinge axes.

Upon landing, each leg pivots about its hinge axis. Landing loads are absorbed by compression of the upper member of the tripod, which is a combined shock absorber and spring assembly. The shock absorber columns are instrumented with strain gages. Axial loads measured by the strain gages are telemetered to provide continuous analog traces during the terminal descent and touchdown phase.

For a vertical landing on a hard, level surface at a velocity in excess of about 8.5 ft/sec, the crushable blocks will contact the surface. Energy will then be dissipated if the blocks penetrate the surface or by crushing of the blocks if the surface bearing strength exceeds 40 psi. Crushing of the honeycomb footpads is not expected for landing velocities below about 11.5 ft/sec or for surface bearing strength less than about 10 psi.

On the *Surveyor III* mission, the performance of the landing gear subsystem was as expected and very satisfactory in every respect. Landing gear deployment was normal. The landing gear also functioned properly during landing and as would be predicted for the abnormal conditions which existed. Fig. IV-17 shows the strain gage force histories of the three shock absorbers throughout the landing phase. Portions of the strain gage data are also shown on an expanded time scale for the three individual touchdown events. Each touchdown consisted of an impact first by Leg 2 in the uphill direction followed by almost simultaneous impacts of Legs 1 and 3 and, then, a second impact by Leg 2. The peak axial loads and corresponding times for these events are presented in Table IV-8.

A slight rebound of *Surveyor I* was experienced after touchdown and, hence, also was expected in the *Surveyor III* mission. This can occur due to spring action of the shock absorber columns. Owing to continued
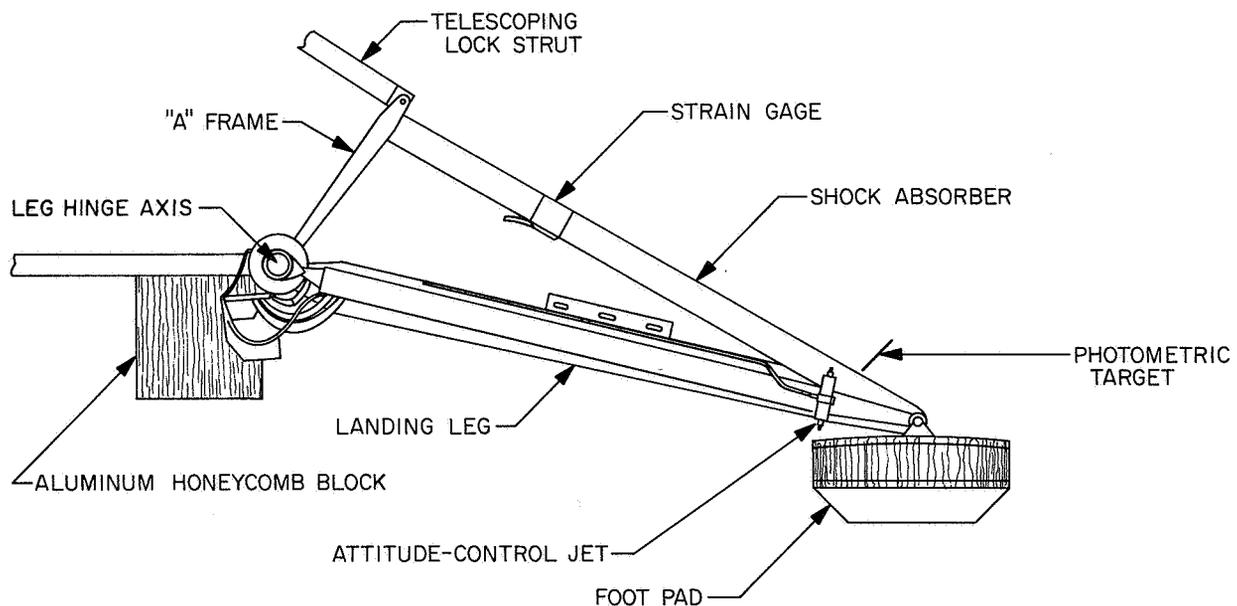


Fig. IV-16. Landing leg assembly
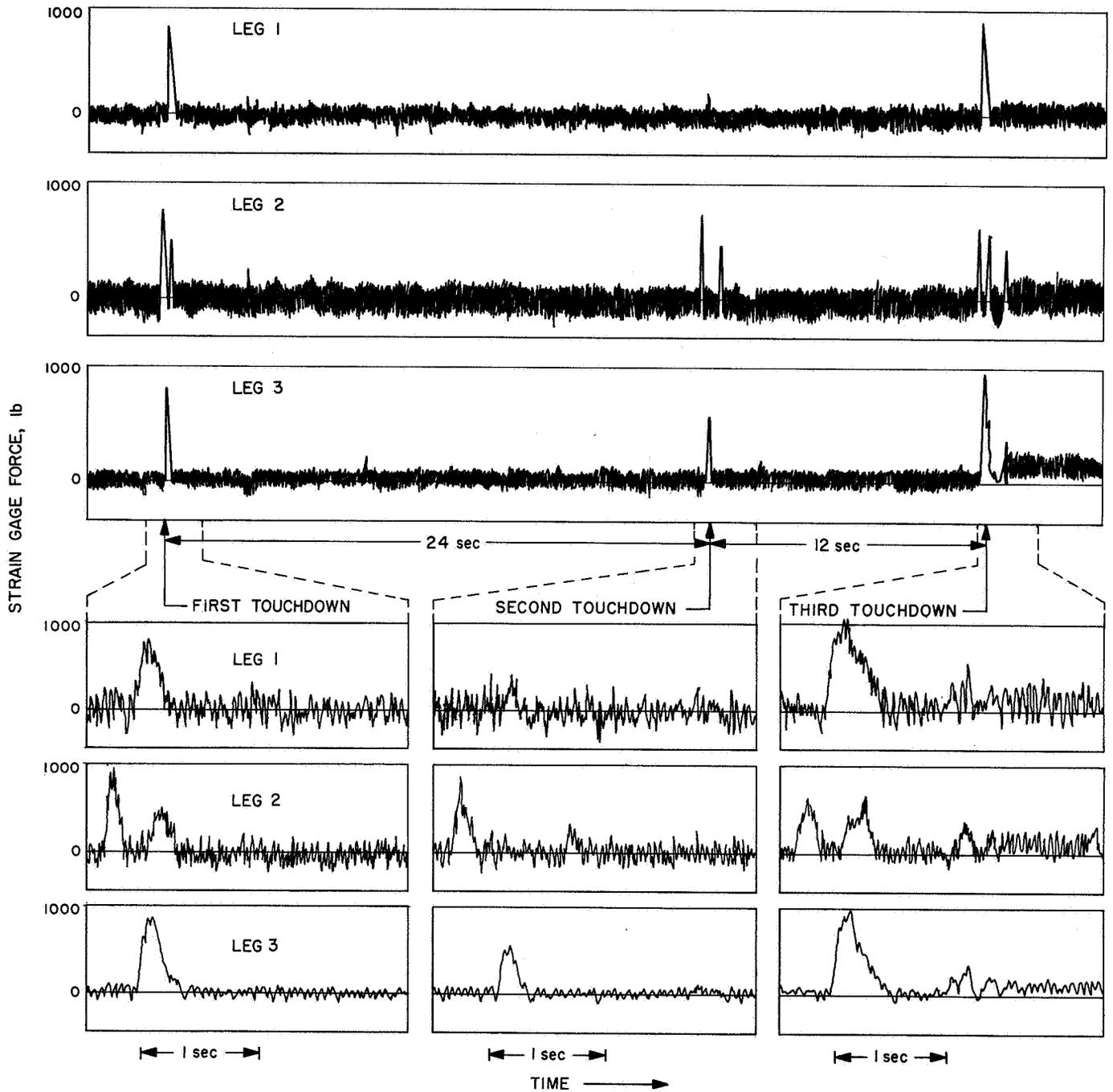
Fig. IV-17. Loads on spacecraft shock absorbers during landing sequence

**Table IV-8. Peak axial loads during landing sequence (time of beginning of force rise also shown, GMT)**

|  |  | First touchdown, lb | Second touchdown, lb | Third touchdown, lb |
|---|---|---|---|---|
| Leg 1 |  | 670 (04:18:36.0) | 320 (04:42:51.0) | 870 (04:54:66.0) |
| Leg 2 | First impact | 690 (04:18:07.5) | 630 (04:42:07.0) | 550 (04:54:42.0) |
|  | Second impact | 410 | 210 | 440 |
| Leg 3 |  | 830 (04:18:33.5) | 530 (04:42:44.5) | 930 (04:54:69.5) |

thrusting of the vernier engines (which effectively reduced the spacecraft weight by 90%) during landing on the *Surveyor III* mission, this rebound was considerably amplified when the surface was impacted by the spacecraft on the first two touchdowns. The engines were commanded off about 1 sec before the third contact, which resulted in a very slight rebound before the spacecraft settled down, as indicated by the steady offset in the strain gage traces which represents the static spacecraft load of about 120 lb.

The data reduction and determination of landing conditions was hampered by three factors: (1) a considerable amount of noise is present in the analog data; (2) analytical simulations of Touchdown Events 1 and 2 are complicated by the necessity to include the flight control and vernier propulsion system effects in the analysis; and (3) for Touchdown Event 3, which does not require the complex simulation, important data (RADVS range, velocity, gyro signals, etc.) are not available because of the analog-to-digital signal processing failure which occurred at the time of second touchdown.

Nevertheless, from the magnitude of the peak values from the strain gage data, it can be estimated that the vertical velocity was probably below 5 ft/sec for the first two touchdown events. Free-fall estimates based upon the time of vernier engine shutdown result in an upper bound of 6 ft/sec for the vertical landing velocity of the third touchdown. For the third touchdown, a horizontal velocity of approximately 3 ft/sec in a direction opposite to Leg 2 is estimated from photographs of the footpad made during the second and third touchdowns. Landing simulations indicated an angle between 8 and 14 deg existed between the surface and the spacecraft horizontal plane (X-Y plane) for all three touchdowns. An estimate of the effective friction coefficient

between the footpads and the lunar surface was also derived from simulations of the third touchdown. Best agreement between analytical and telemetered shock absorber histories was obtained for a friction coefficient between 1.0 and 1.2.

No indications of footpad crushing or crushable block contacts were obtained. However, as pointed out above, neither of these occurrences would be expected for landing velocities as low as those with which *Surveyor III* appears to have landed.

The legs were not locked after landing in order to permit reigniting of the vernier engines for a static firing or hopping experiment. No vernier firing was conducted. Although the legs were not locked, the spacecraft remained in a fixed position during the entire lunar day, indicating no leakage of the shock absorbers.

### 3. Omnidirectional Antennas

The omnidirectional antennas are mounted on the ends of folding booms hinged to the spaceframe. Pins retain the booms in the stowed position during launch. Squib-actuated pin pullers release the booms upon command from the *Centaur* shortly before spacecraft separation. A leaf-type kickout spring on each omniantenna boom initiates movement. Torsion springs continue the movement to the fully deployed positions, where the booms are automatically locked.

The omniantenna booms were extended by *Centaur* command, and both antennas were locked in the landing or transit position as indicated by the telemetry.

### 4. Antenna and Solar Panel Positioner (A/SPP)

The A/SPP supports and positions the high-gain planar array antenna and solar panel. The planar array antenna and solar panel have four axes of rotation: roll, polar, solar, and elevation (Fig. IV-18). Stepping motors rotate the axes in either direction in response to commands from earth or during automatic deployment following *Centaur*/spacecraft separation. This freedom of movement permits orienting the planar array antenna toward the earth and the solar panel toward the sun.

The solar axis is locked in a vertical position for stowage in the nose shroud. After launch, the solar panel is positioned parallel to the spacecraft X-axis. The A/SPP remains locked in this position until after touchdown, at which time the roll, solar, and elevation axes are released.

PLANAR ARRAY ANTENNA

SOLAR PANEL AXIS

SOLAR PANEL

POLAR AXIS

ELEVATION AXIS

ROLL AXIS
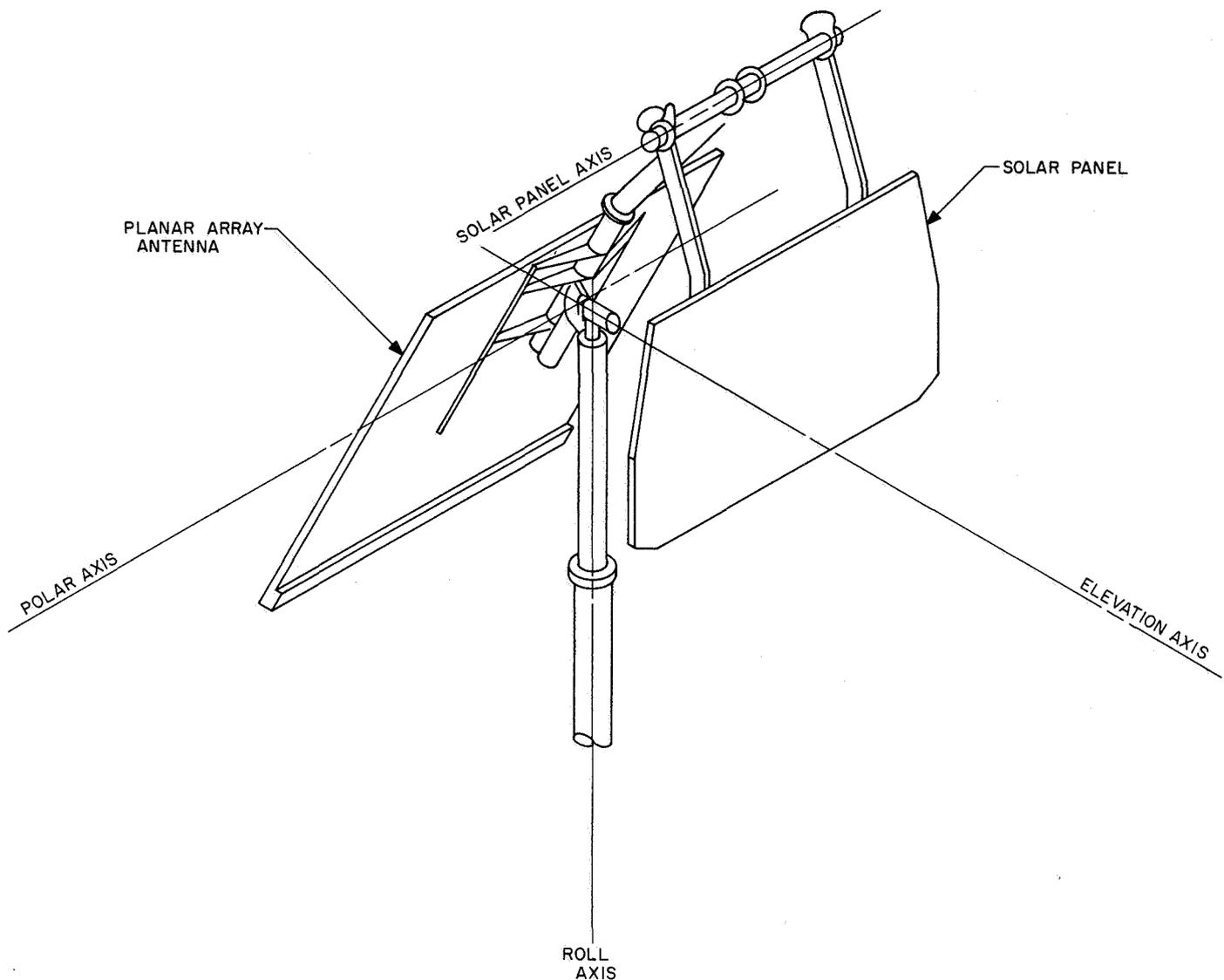
**Fig. IV-18. Antenna/solar panel configuration**

Potentiometers on each axis are read to indicate A/SPP orientation. Each command from earth gives ⅛ degree of rotation in the roll, solar, and elevation axes and ¹⁄₁₆ degree in the polar axis.

The A/SPP operated as expected during the mission. After the shroud was ejected, the roll and solar axes moved to their transit positions.

**5. Thermal Compartments**

Two thermal compartments (A and B) house thermally sensitive electronic items. Equipment in the compartments is mounted on thermal trays that distribute heat throughout the compartments. An insulating blanket, consisting of 75 sheets of 0.25-mil-thick aluminized mylar, is installed between the inner shell and the outer protective cover of the compartments. Each compartment employs thermal switches (9 on Compartment A and 6 on Compartment B) which are capable of varying the thermal conductance between the inner compartment and the external radiating surface. The thermal switches maintain thermal tray temperature below +125°F. Each compartment contains a thermal control and heater assembly to maintain the temperature of the thermal tray above a specified temperature (above 40°F for Compartment A and above 0°F for Compartment B). The thermal control and heater assembly is capable of automatic

operation, or may be turned on or off by earth command. Components located within the compartments are identified in Table IV-9.

**Table IV-9. Thermal compartment component installation**

| Compartment A | Compartment B |
|---|---|
| Receivers (2) | Central command decoder |
| Transmitters (2) | Boost regulator |
| Main battery | Central signal processor |
| Battery charge regulator | Signal processing auxiliary |
| Engineering mechanisms auxiliary | Engineering signal processor |
| Television auxiliary | Low data rate auxiliary |
| Thermal control and heater assembly | Thermal control and heater assembly |
| Auxiliary battery control | Auxiliary engineering signal processor |

## 6. Thermal Switch

The thermal switch is a thermal-mechanical device which varies the conductive path between an external radiation surface and the top of the compartment (Fig. IV-19). The switch is made up of two contact surfaces which are ground to within one wavelength of being optically flat. One surface is then coated with a conforming substance to form an intimate contact with the mating surface. The contact actuation is accomplished by four bimetallic elements located at the base of the switch. These elements are connected mechanically to the top of the compartment so that the compartment temperature controls the switch actuation. The switches are identical, and were adjusted to open at a temperature of 40 ±5°F on the *Surveyor III* mission.

The external radiator surface is such that it absorbs only 12% of the solar energy incident on it and radiates 74% of the heat energy conducted to its surface. When the switch is closed and the compartment is hot, the switch loses its heat energy to space. When the compartment gets cold, the switch contacts open about 0.020 in., thereby opening the heat-conductive path to the radiator and thus reducing the heat loss through the switch to almost zero. Three of the switches on each compartment are instrumented with temperature sensors attached to the radiators. The temperature sensors provide an indication of switch actuation for those switches which are monitored.

On the *Surveyor III* mission, the thermal switches were closed during flight and kept the electronics at or below the maximum allowable temperature at all times.

All the thermal switches also remained closed during the lunar day after landing except, during the eclipse of the sun, it was indicated that Switch 1 on Compartment B opened when the tray temperature reached 31°F.

The rate at which the compartments cooled after sunset indicated that most of the thermal switches were stuck in the closed position. At the time the compartments reached 0°F and the spacecraft was shut down, all the instrumented switches were stuck except Switch 1 on Compartment B, which opened at about 15°F. The other switches may have opened after shutdown.

It is believed that sticking of the thermal switches was due to volatile material which outgassed from the contact surface coating. Sufficient amounts of this material probably deposited on the surface to cause sticking. To overcome this problem on future missions, the coating material will be soaked at elevated temperature before assembly to drive out volatile constituents.

## 7. Pyrotechnic Devices

The pyrotechnic devices installed on *Surveyor III* are indicated in Table IV-10. All the squibs used in these devices are electrically initiated, hot-bridgewire, gas-generating devices. Qualification tests for flight squibs included demonstration of reliability at a firing current level of 4 or 4.5 A. "No Fire" tests were conducted at a 1-A or 1-W level for 5 min. Electrical power required to initiate pyrotechnic devices is furnished by the spacecraft main battery. Power distribution is through 19.0- and 9.5-A constant-current generators in the engineering mechanism auxiliary (EMA).

All pyrotechnic devices functioned normally upon command. Mechanical operation of locks, valves, switches, and plunger, actuated by squibs, was indicated on telemetry signals as part of the spacecraft engineering measurement data.

## 8. Electronic Packaging and Cabling

The electronic assemblies for *Surveyor III* provided mechanical support for electronic components in order to insure proper operation throughout the various environmental conditions to which they were exposed during the mission. The assemblies (or control items) were constructed utilizing sheet metal structure, sandwich-type

INNER CONTACT RING

BI-METAL CLAMP

BI-METAL ACTUATOR

INNER CONTACT PLUG

CONDUCTOR FOIL

RADIATING PLATE

OUTER CONTACT RING
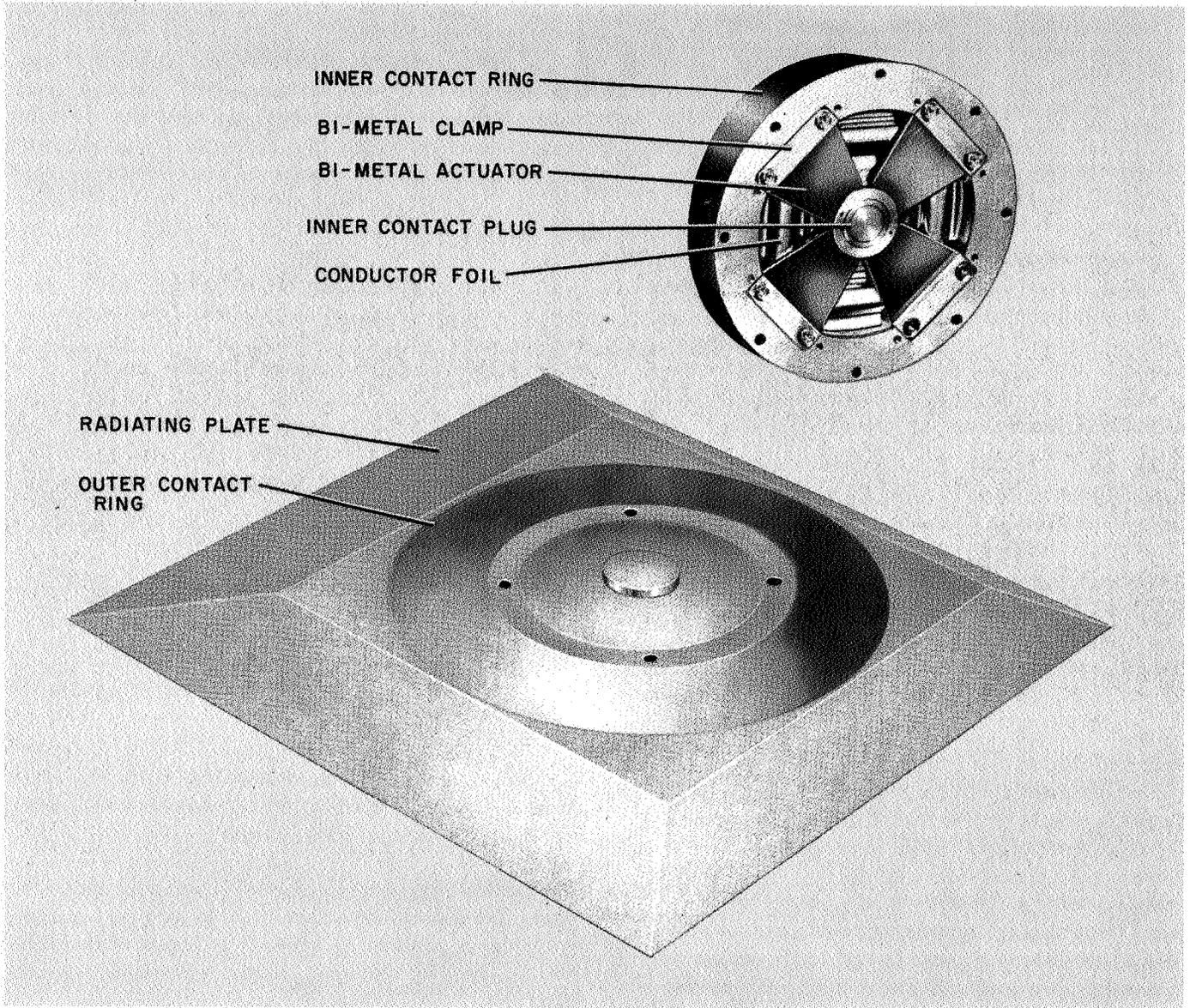
Fig. IV-19. Thermal switch

## Table IV-10. Pyrotechnic devices

| Type | Location and use | Quantity of devices | Quantity of squibs | Command source |
|---|---|---|---|---|
| Pin pullers | Lock and release Omniantennas A and B | 2 | 2 | Centaur programmer |
| Pin pullers | Lock and release landing legs | 3 | 3 | Centaur programmer |
| Pin pullers | Lock and release planar antenna and solar panel | 7 | 7 | Separation sensing and arming device and ground station |
| Pin puller | Lock and release Vernier Engine 1 | 1 | 1 | Ground station |
| Pin puller | SM/SS unlatch mechanism | 1 | 1 | Ground station |
| Separation nuts | Retro rocket attach and release | 3 | 6 | Flight control subsystem |
| Valve | Helium gas release and dump | 1 | 2 | Ground station |
| Pyro switches | EMA Board 4, RADVS power on and off | 4 | 4 | Ground station and flight control subsystem |
| Initiator squibs | Safe and arm assembly retrorocket initiators | 1 | 2 | Flight control subsystem |
| Locking plungers | Landing leg, shock absorber locks | 3 | 3 | Ground station |
| | | 26 | 31 | |

etched circuit board chassis with two-sided circuitry, plated through holes, and/or bifurcated terminals. Each control item, in general, consists of only a single functional subsystem and is located either in or out of the two thermally controlled compartments, depending on the temperature sensitivity of the particular subsystem. Electrical interconnection is accomplished primarily through the main spacecraft harness. The cabling system is constructed utilizing a light-weight, minimum-bulk, and abrasion-resistant wire which is an extruded teflon having a dip coating of modified polyimide.

## C. Thermal Control

The thermal control subsystem is designed to provide acceptable thermal environments for all components during all phases of spacecraft operation. Spacecraft items with close temperature tolerances were grouped together in thermally controlled compartments. Those items with wide temperature tolerances were thermally decoupled from the compartments. The thermal design fits the "basic bus" concept in that the design was conceived to require minimum thermal design changes for future missions. Monitoring of the performance of the spacecraft thermal design is done by 77 engineering temperature sensors which are distributed throughout the spacecraft as follows:

| Flight control | 9 |
|---|---|
| Mechanisms | 3 |
| Radar | 7 |
| Electrical power | 5 |
| Transmitters | 2 |
| Survey TV | 4 |
| Vehicle structure | 30 |
| Propulsion | 16 |
| SM/SS electronics | 1 |

The spacecraft thermal control subsystem is designed to function in the space environment, both in transit and on the lunar surface. Extremes in the environment as well as mission requirements on various pieces of the spacecraft have led to a variety of methods of thermal control. The spacecraft thermal control design is based upon the absorption, generation, conduction, and radiation of heat. Figure IV-20 shows those areas of the spacecraft serviced by different thermal designs.

The radiative properties of the external surfaces of major items are controlled by using paints, by polishing, and by using various other surface treatments. Reflecting mirrors are used to direct sunlight to certain components. In cases where the required radiative isolation cannot be achieved by surface finishes or treatments, the major item is covered with an insulating blanket composed of multiple-sheet aluminized mylar. This type of thermal control is called "passive" control.

**SUPER INSULATION LOCATIONS**

LEG 1

COMPARTMENT A

FUEL AND OXIDIZER TANKS (6)

COMPARTMENT B

RETROROCKET MOTOR

+X — — — -X

SM/SS ELECTRONICS

LEG 2

LEG 3

AUXILIARY BATTERY

-Y

**THERMAL SWITCH LOCATIONS (SEMI-ACTIVE CONTROL)**

+Y

LEG 1

COMPARTMENT A

COMPARTMENT B

+X — — — -X

LEG 2

LEG 3

-Y

**PASSIVE AREAS**

+Y

OMNIANTENNA A

LEG 1

POWER SUPPLY AND MODULATOR

VERNIER ENGINE 1

ALTIMETER/VELOCITY SENSING ANTENNA

VELOCITY-SENSING ANTENNA

FLIGHT CONTROL SENSORS

+X — — — -X

VERNIER ENGINE 2

SIGNAL DATA CONVERTER

SM/SS

TV CAMERA (SURVEY)

VERNIER ENGINE 3

LEG 2

LEG 3

NITROGEN TANK

HELIUM TANK

OMNIANTENNA B

AUXILIARY BATTERY

-Y

**ACTIVE HEATER LOCATIONS**

+Y

A/SPP ORIENTATION FOR TRANSIT

LEG 1

VERNIER ENGINE 1 LINES

COMPARTMENT A

COMPARTMENT B

SOLAR PANEL

ALTITUDE-MARKING RADAR

FUEL TANK 2

GYROS

+X — — — -X

VERNIER ENGINE 2 LINES

OXIDIZER TANK 3

OXIDIZER TANK 2

VERNIER ENGINE 3 LINES

LEG 2

LEG 3

TV CAMERA (SURVEY)

PLANAR ARRAY ANTENNA

SM/SS ELECTRONICS

-Y

**Fig. IV-20. Thermal design**

The major items whose survival or operating temperature requirements cannot be achieved by surface finishing or insulation alone use heaters that are located within the unit. These heaters can be operated by external command, thermostatic actuation, or both. The thermal control design of those units using auxiliary heaters also includes the use of surface finishing and insulating blankets to optimize heater effectiveness and to minimize the electrical energy required. Heaters are considered "active control."

Items of electronic equipment whose temperature requirements cannot be met by the above techniques are located in thermally controlled compartments (A and B). Each compartment is enclosed by a shell covering the bottom and four sides and contains a structural tray on which the electronic equipment is mounted. The top of each compartment is equipped with a number of temperature-actuated switches (9 in Compartment A and 6 in Compartment B). These switches, which are attached to the top of the tray, vary the thermal conductance between the tray and the outer radiator surfaces, thereby varying the heat-dissipation capability of the compartments. When the tray temperature increases, heat transfer across the switch increases. During the lunar night, the switch opens, decreasing the conductance between the tray and the radiators to a very low value in order to conserve heat. When dissipation of heat from the electronic equipment is not sufficient to maintain the required minimum tray temperature, a heater on the tray supplies the necessary heat. The switches are considered "semi-active."

Examples of units which are controlled by active, semi-active, or passive means are shown in Fig. IV-20.

During transit, the thermal performance of the spacecraft was as predicted, with the exception of the SM/SS electronics auxiliary. Vernier Oxidizer Lines 2 and 3 cycled normally with duty cycles comfortably low. Vernier Engine 2 showed larger variations in temperature during the gyro drift checks than previous missions, but the direction of spacecraft drift was in the opposite direction, thereby accounting for the larger temperature variations. The SM/SS electronics temperature was approximately 30°F cooler than expected but still well above its survival limit. This temperature was also influenced by the gyro drift checks, but the primary reason for the low SM/SS temperature is considered to be uncertainty in the location of the shadow of the solar panel. Appendix D contains plots of transit temperatures.

Once the spacecraft came to rest on the lunar surface, most analog telemetry data became erroneous, and initial attempts to determine the thermal status were hampered. There was great uncertainty in the temperature of the SM/SS instrument. Since there was no thermal sensor on the instrument, extremely conservative estimates of the instrument temperature were used to determine a safe operating time. As time went on and more confidence was obtained in the nature of the telemetry anomaly, the thermal status of the spacecraft became more certain. Most of the subsystems appeared to be reacting generally like *Surveyor I*, with some differences due to the different landed orientation.

When it was determined how to correct the analog telemetry data obtained at 17.2 bit/sec, it was noticed that the television temperature data processed by the television auxiliary indicated substantially higher temperatures than the data processed by the spacecraft telecommunications subsystem. Investigation revealed that erroneous calibration curves were used to reduce the telemetered thermal data processed by the TV auxiliary. When the correct curves were used, good agreement was obtained. The *Surveyor III* television temperatures compare favorably with those obtained on *Surveyor I*. During the lunar eclipse, the TV heaters held the TV at an acceptable level. The compartment internal temperatures remained at acceptable levels during the eclipse, while external temperatures moved through a wide range. Thermal data obtained during the eclipse was used in an attempt to resolve the anomalous analog telemetry, though without particular success. After sunset, spacecraft operations continued until the compartment temperatures reached 0°F without the use of the heaters. At that time, it appeared as if most of the thermal switches were stuck in the closed position. Owing to the desire to keep the battery at as high a charge as possible, the spacecraft was shut down after minimum postsunset operations.

Appendix D contains plots of spacecraft temperatures on the lunar surface.

## D. Electrical Power

The electrical power subsystem is designed to generate, store, convert, and distribute electrical energy. A block diagram of the subsystem is shown in Fig. IV-21. The subsystem derives its energy from the solar panel and the spacecraft battery system. The solar panel converts solar radiation energy into electrical energy. Solar panel power capability is affected by temperature and the incidence of solar radiation and varies from 90 to 55 W.
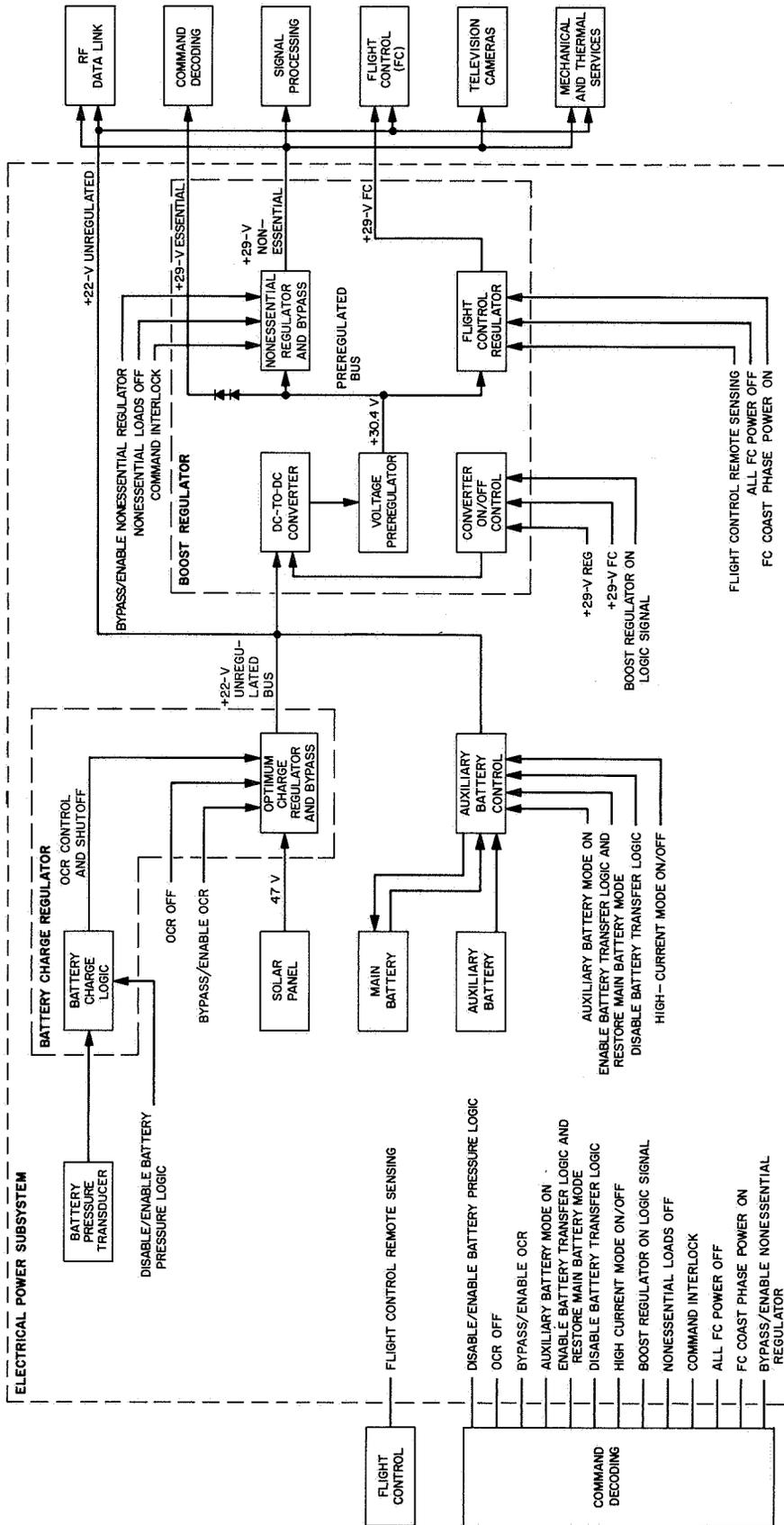
Fig. IV-21. Simplified electrical power functional block diagram

The spacecraft battery system consists of a main battery and an auxiliary battery. The main battery is a secondary or rechargeable battery; the auxiliary battery is a primary or nonrechargeable battery.

The batteries provide about 1690 W-hr during transit, the balance of the energy being supplied by the solar panel. The maximum storage capacity of the main battery is 180-A-hr; that of the auxiliary battery is 50 A-hr. The selection of battery operation mode is determined by the auxiliary battery control (ABC). There are three modes of battery operation: *main battery* mode, *auxiliary battery* mode, and *high-current* mode. In the *main battery* mode only the main battery is connected to the unregulated bus. This is the nominal configuration. In the *auxiliary battery* mode, the main battery is connected to the unregulated bus through a series diode while the auxiliary battery is directly connected. In the *high-current* mode, both the main and auxiliary batteries are connected to the unregulated bus without the series diode. The battery modes are changed by earth commands except that the ABC automatically switches to *auxiliary battery* mode from *main battery* mode in case of main battery failure. This automatic function can be disabled by earth command.

The four modes of solar panel operation are controlled by the battery charge regulator (BCR). In the *on* mode, the optimum charge regulator (OCR) tracks the volt-ampere characteristic curve of the solar panel and hunts about the maximum power point. In the OCR *off* mode, the solar panel output is switched off. This mode is intended to prevent overcharging of the main battery by the solar panel. In the OCR *bypass* mode, the solar panel is connected directly to the unregulated bus. This mode is used in case of OCR failure. In the *trickle charge* mode, the main battery charging current is controlled by its terminal voltage. All of the BCR modes, except the *trickle charge* mode, are controlled by earth commands.

The OCR *off* and *trickle charge* modes are automatically controlled by the battery charge logic (BCL) circuitry. When the main battery terminal voltage exceeds 27.5 V or its manifold pressure exceeds 65 psia, the BCR goes automatically to the *off* mode. The *trickle charge* mode is automatically enabled when the main battery terminal voltage reaches 27.23 V. The BCL can be disabled by earth command.

Current from the BCR and spacecraft batteries is distributed to the unregulated loads and the boost regulator (BR) via the unregulated bus. The voltage on the un-

regulated bus can vary between 17.5 and 27.5 V, with a nominal value of 22 V. The BR converts the unregulated bus voltage to 29.0 V ±1% and supplies the regulated loads. The preregulator supplies a regulated 30.4 V to the preregulated bus. The essential loads are fed by the preregulated bus through two diodes in series. The diodes drop the preregulated bus voltage of 30.4 V to the essential bus voltage of 29.0 V. The preregulated bus also feeds the flight control regulator and the nonessential regulator, which in turn feeds the flight control and nonessential busses, respectively. These regulators can be turned on and off by earth commands. The nonessential regulator has a bypass mode of operation which connects the preregulated bus directly to the nonessential bus. This mode is used if the nonessential regulator fails.

The power subsystem operated normally throughout the mission. The data presented in Table IV-11 verifies that telemetered parameters were in close agreement with the predicted values during transit. The average

**Table IV-11. Summary of power subsystem performance**

| Parameter | Time from liftoff | Predicted | Actual |
|---|---|---|---|
| Solar panel power, W | Throughout transit | 89 | 90 |
| Optimum charge regulator (OCR) power output, W | Throughout transit | 70 | 71 |
| Main battery stored energy, A-hr | 0 hr | 165 | 161.5 |
| | 22 | 139 | 137 |
| | 40 | 118 | 120.5 |
| | 50 | 111 | 114 |
| | 60 | 106 | 110 |
| | 65 | 102 | 99.2 |
| Auxiliary battery stored energy, A-hr | 0 | 45 | 45 |
| | 50 | 45 | 45 |
| | 60 | 39 | 39 |
| | 65 | 30 | 29.7 |
| Average OCR efficiency, % | Throughout transit | 78 | 80 |
| Average boost regulator efficiency, % | Throughout transit | 77 | 77 |
| Battery discharge current, A | High-power periods | 4.35 | 4.5 |
| | Low-power periods | 0.7 | 0.63 |
| Regulated current, A | High-power periods | 3.95 | 4.0 |
| | Low-power periods | 1.65 | 1.7 |
| OCR output current, A | High-power periods | 3.2 | 3.2 |
| | Low-power periods | 3.2 | 3.2 |
| Unregulated current, A | High-power periods | 1.3 | 0.8–1.2 |
| | Low-power periods | 1.3 | 0.8–1.2 |
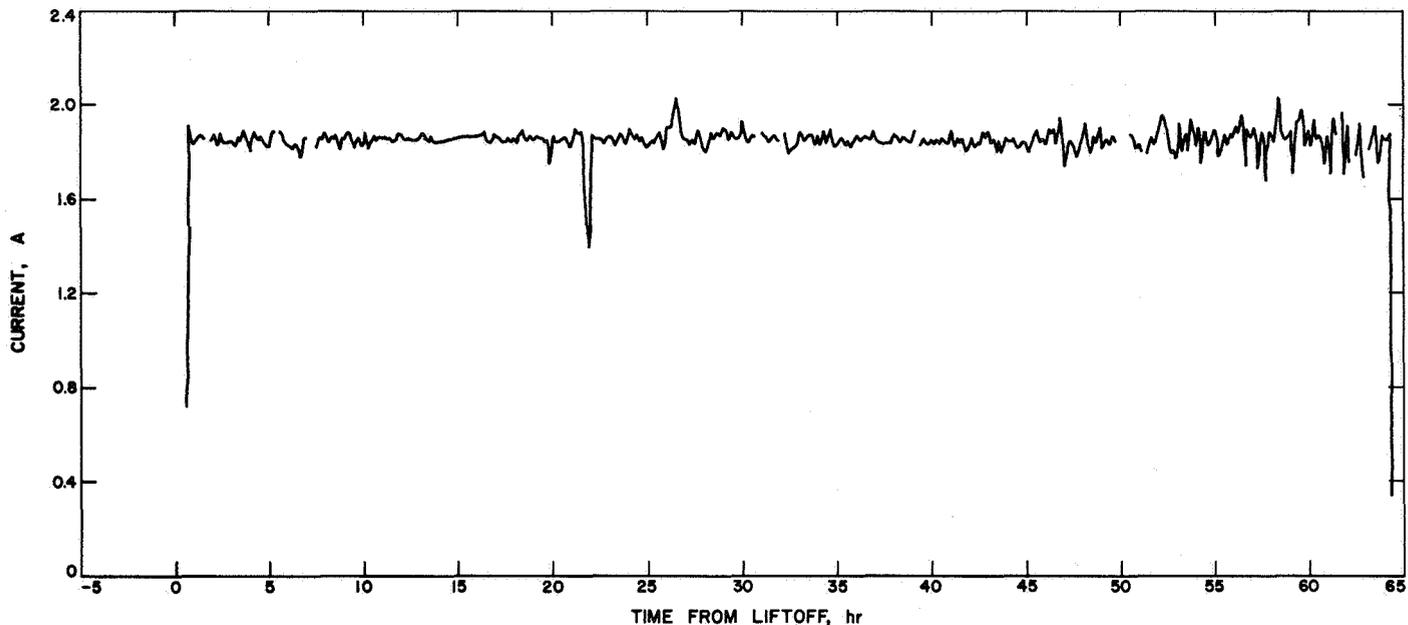
**Fig. IV-22. Solar panel output current during transit**
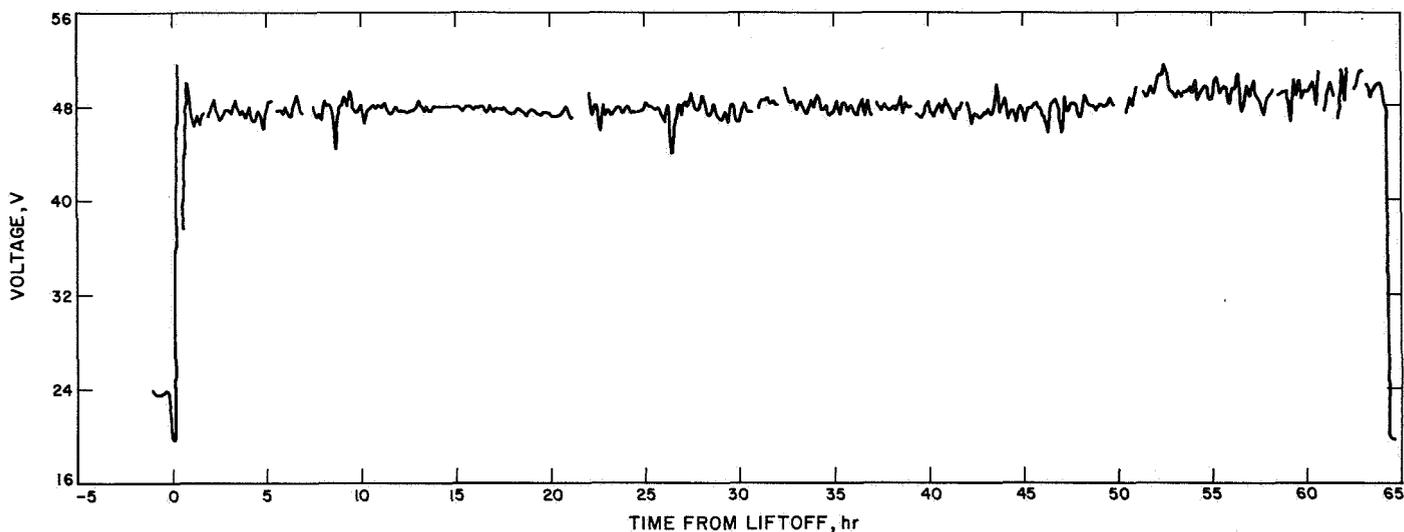


**Fig. IV-23. Solar panel output voltage during transit**

solar panel output current (Fig. IV-22) was 1.85 A at an average voltage (Fig. IV-23) of 47.4 V. Average OCR output current (Fig. IV-24) was 3.2 A, which agrees with test data. Overall OCR efficiency was about 80%.

The main and auxiliary battery energy levels at liftoff were 3608 and 1150 W-hr, respectively. In transit, the solar panel supplied an average of 83.5% of the total system electrical loads during low-power periods and 41.5% during high-power periods. The spacecraft batteries provided the balance of electrical power required.

Profiles of stored battery energy during transit are shown in Fig. IV-25. The profiles closely follow the power management program curve. Total battery discharge current is shown in Fig. IV-26.

The main battery pressure stabilized during transit to 13.4 psia at a steady-state battery temperature of 86.8°F, both measurements falling well within the normal safe operating limits. During the last part of the transit phase, the auxiliary battery temperature was raised by operating in *auxiliary battery* mode to insure adequate voltage
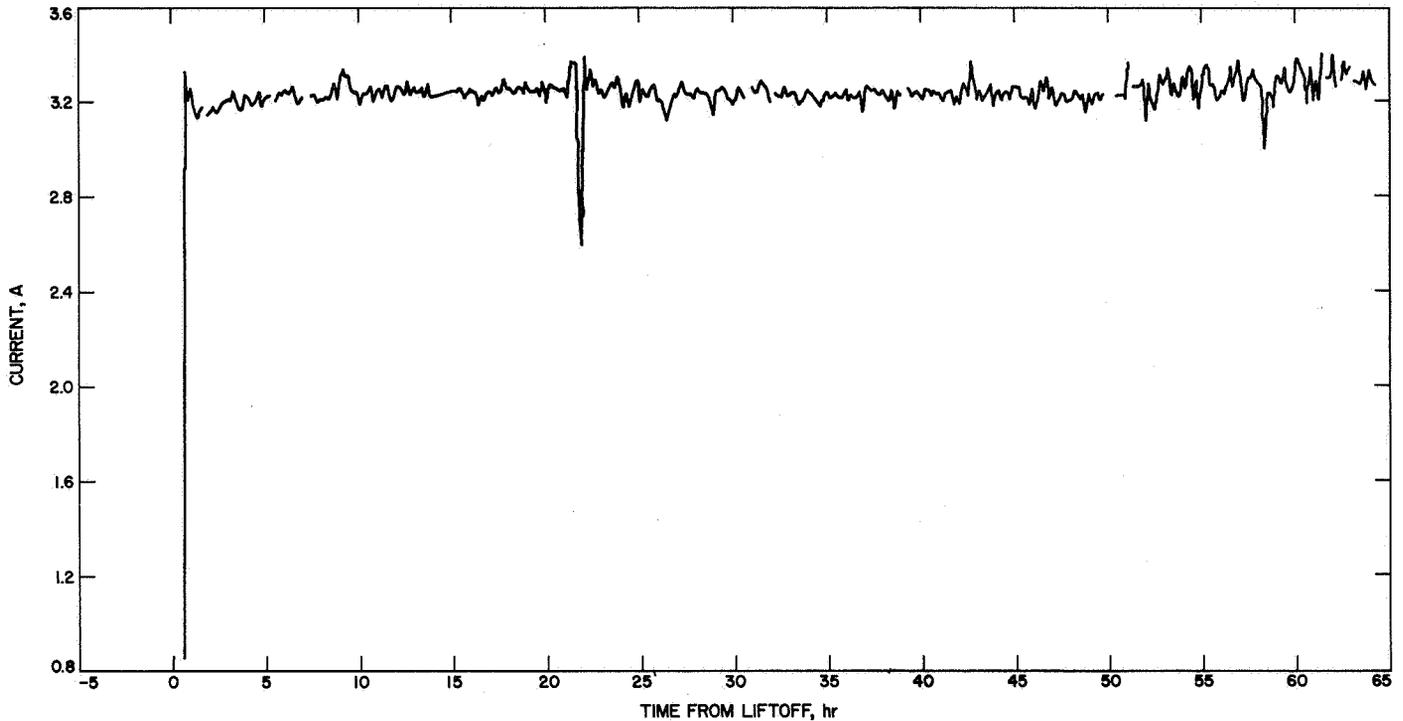
Fig. IV-24. Optimum charge regulator output current during transit
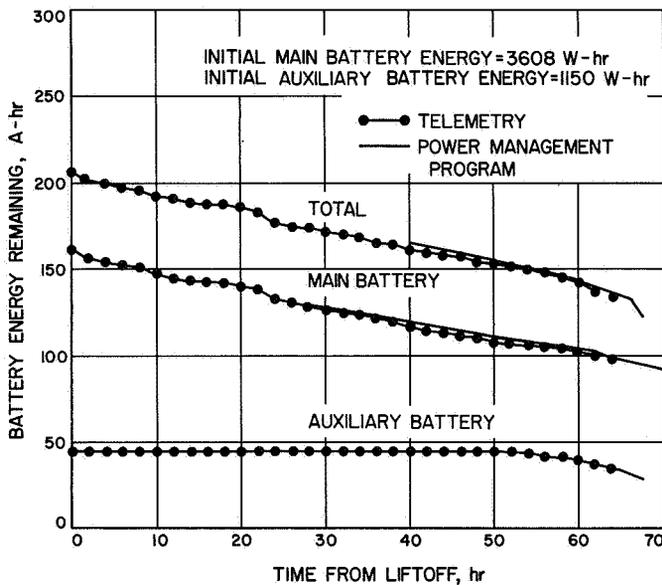


Fig. IV-25. Battery energy remaining during transit

(Fig. IV-27). This mode of operation also allowed the main battery to retain a greater amount of energy at touchdown. The main battery energy at touchdown was estimated to be 1980 W-hr.

The transit values of unregulated bus voltage and unregulated output current are presented in Figs. IV-28,

-29, respectively. Boost regulator differential current and total regulated output current during transit are presented in Figs. IV-30, -31, respectively.

The electrical power subsystem performed nominally during the first lunar day with the following exception. On April 24, the total regulated current and battery discharge current sensors indicated loads of several amperes. The spacecraft was turned off and brought up again but still displayed the power anomaly. The solar panel was positioned vertically for the solar eclipse and, shortly after this position was attained, the current readings slowly decreased to nominal. Analysis of the above data indicated that the auxiliary battery positive terminal had shorted to spacecraft ground. As the auxiliary battery was "off line" and the spacecraft was operating on the main battery, the shorting of the auxiliary battery had no effect on the mission. Eventual failure of the auxiliary battery after landing is expected, as it was designed as a limited life unit.

## E. Propulsion

The propulsion subsystem supplies thrust force during the midcourse correction and terminal descent phases of the mission. The propulsion subsystem consists of a vernier engine system and a solid-propulsion main retro-rocket motor. The propulsion subsystem is controlled by
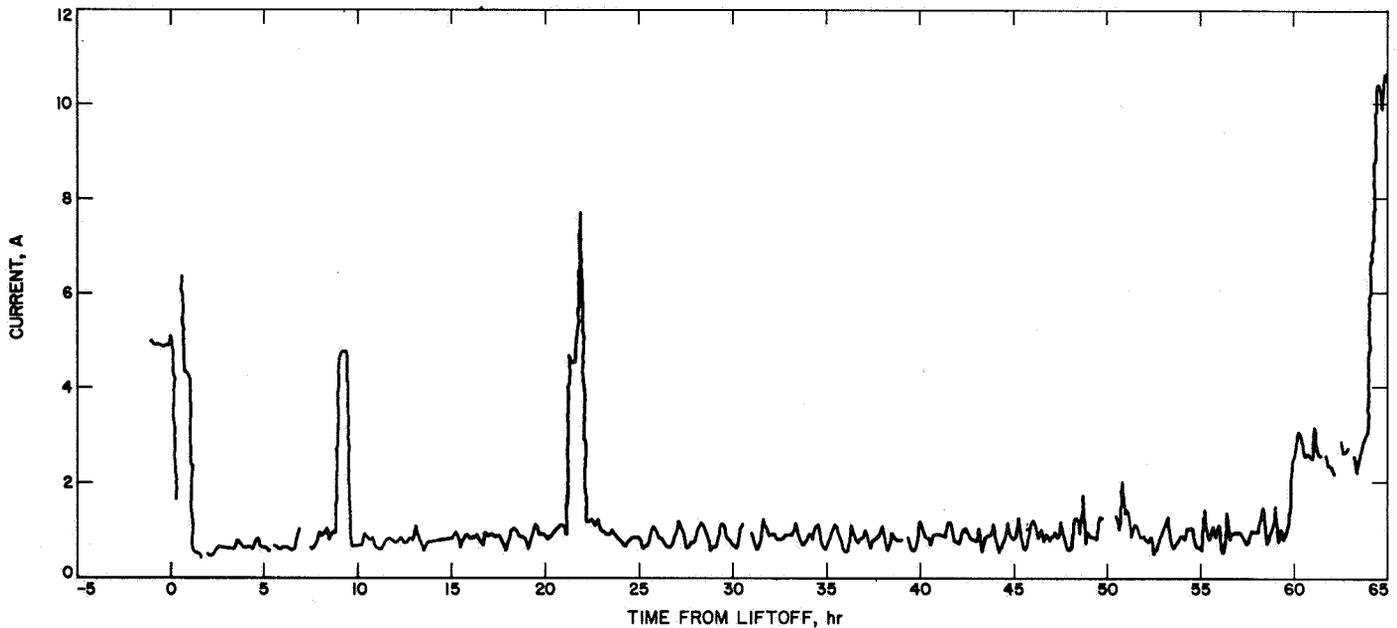
**Fig. IV-26. Total battery discharge current during transit**
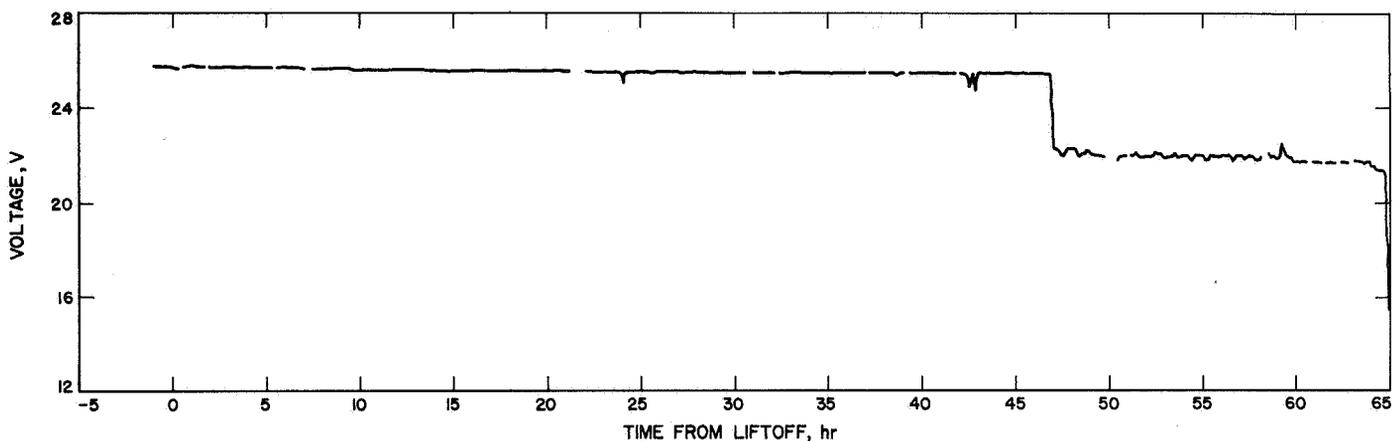


**Fig. IV-27. Auxiliary battery voltage during transit**

the flight control system through preprogrammed maneuvers, commands from earth, and maneuvers initiated by flight control sensor signals.

## 1. Vernier Propulsion

The vernier propulsion subsystem supplies the thrust forces for midcourse maneuver velocity vector correction, attitude control during main retrorocket motor burning, and velocity vector and attitude control during terminal descent. The vernier engine system consists of three thrust chamber assemblies and a propellant feed system. The feed system is composed of three fuel tanks,

three oxidizer tanks, a high-pressure helium tank, propellant lines, and valves for system arming, operation, and deactivation.

Fuel and oxidizer are contained in six tanks of equal volume, with one pair of tanks for each engine. Each tank contains a teflon expulsion bladder to permit complete and positive expulsion and to assure propellant control under zero-g conditions. The oxidizer is nitrogen tetroxide ($N_2O_4$) with 10% by weight nitric oxide (NO) to depress the freezing point. The fuel is monomethyl hydrazine monohydrate ($MMH \cdot H_2O$). Fuel and oxidizer ignite hypergolically when mixed in the thrust chamber.
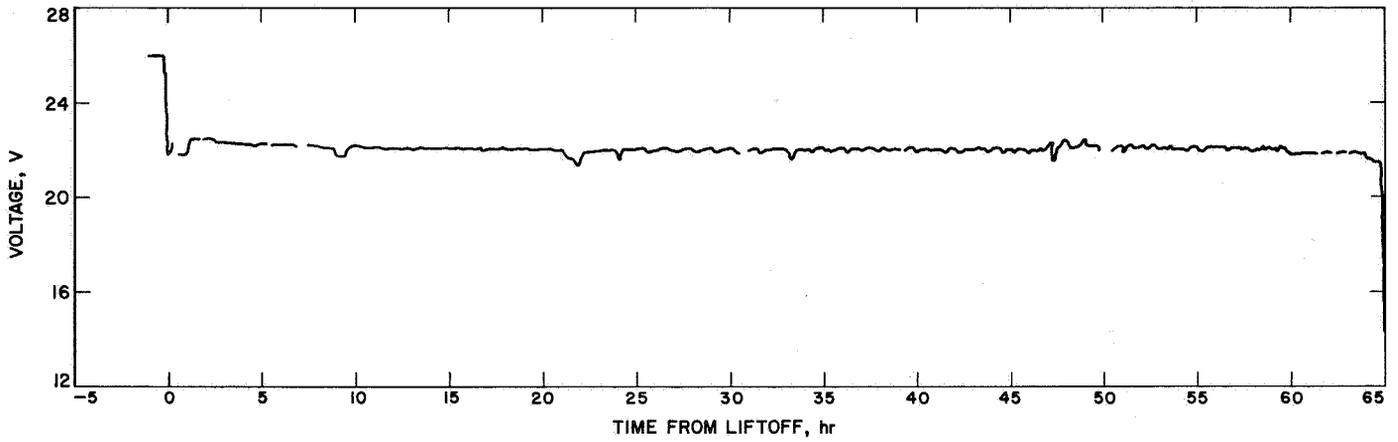
Fig. IV-28. Unregulated bus voltage during transit
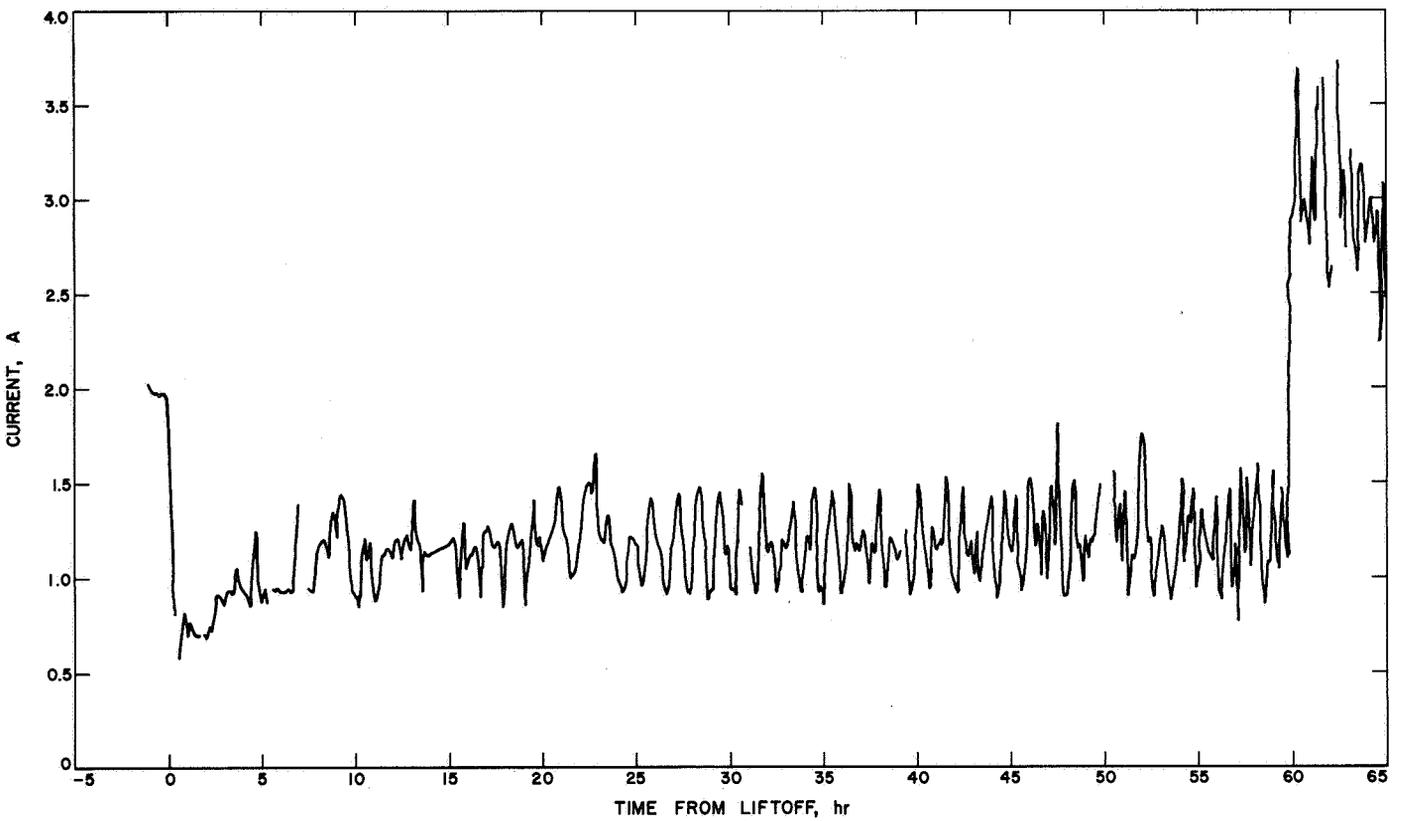


Fig. IV-29. Unregulated output current during transit
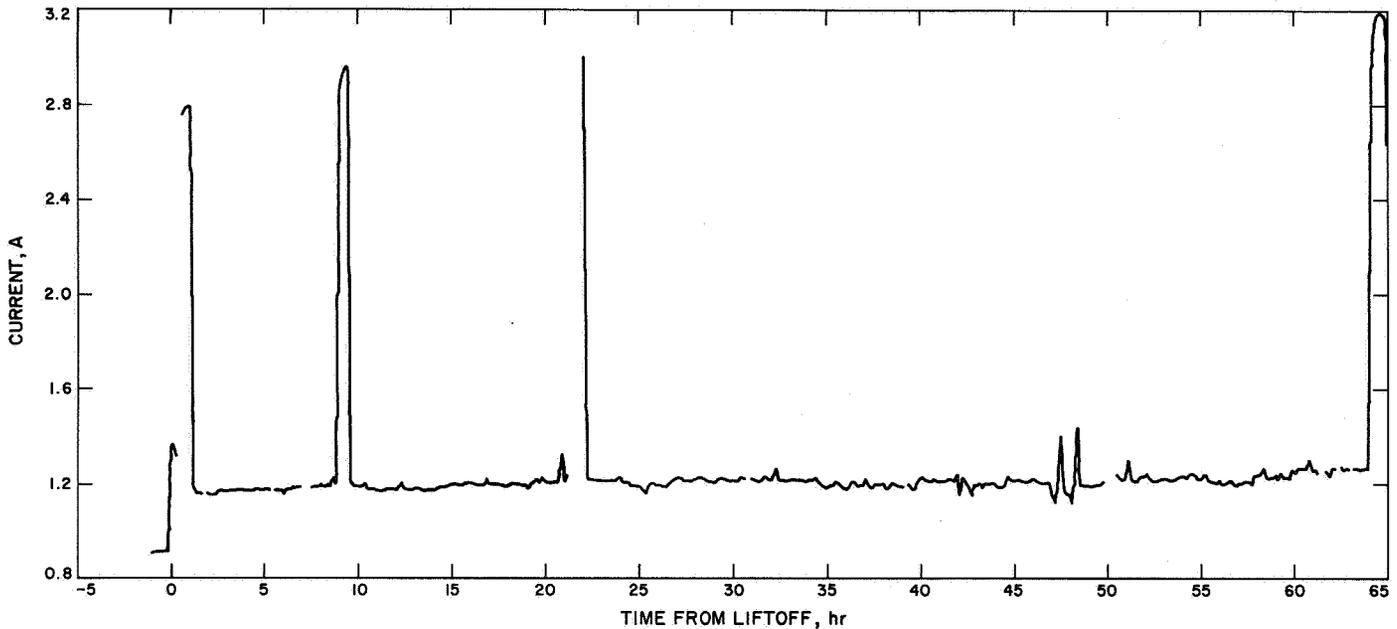
**Fig. IV-30. Boost regulator differential current during transit**
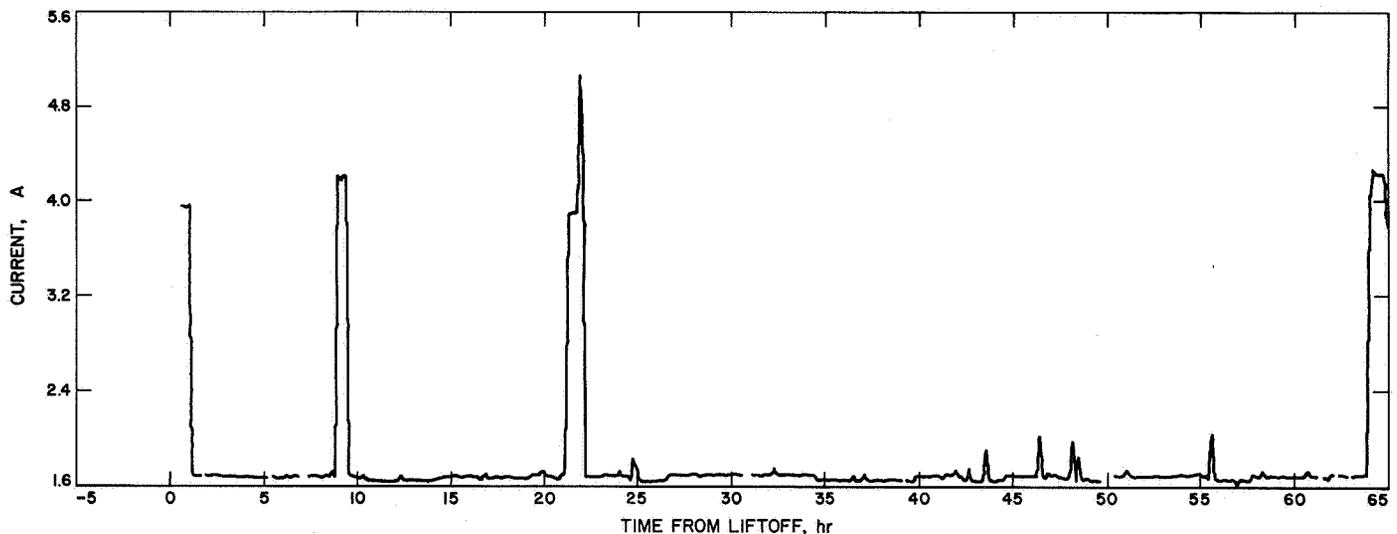


**Fig. IV-31. Total regulated output current during transit**

The total minimum usable propellant load is 178.3 lb. The arrangement of the tanks on the spaceframe is illustrated in Fig. IV-32. Propellant freezing or overheating is prevented by a combination of active and passive thermal controls, utilizing surface coatings, multilayered blankets, and electrical and solar heating. The propellant tanks are thermally isolated to insure that the spacecraft structure will not function as a heat source or heat sink.

Propellant tank pressurization is provided by the helium tank and valve assembly (Fig. IV-33). The high-pressure helium is released to the propellant tanks by activating a squib-actuated helium release valve. A single-stage regulator maintains the propellant tank pressure at 730 psi. Helium relief valves relieve excess pressure from the propellant tanks in the event of a helium pressure regulator malfunction.

HELIUM LINES

OXIDIZER TANK (3)

FUEL TANK (3)

VERNIER ENGINE 2
(FIXED)

HELIUM TANK

LEG 3

VERNIER ENGINE 3
(FIXED)

VERNIER ENGINE 1
(GIMBALLED)

LEG 1
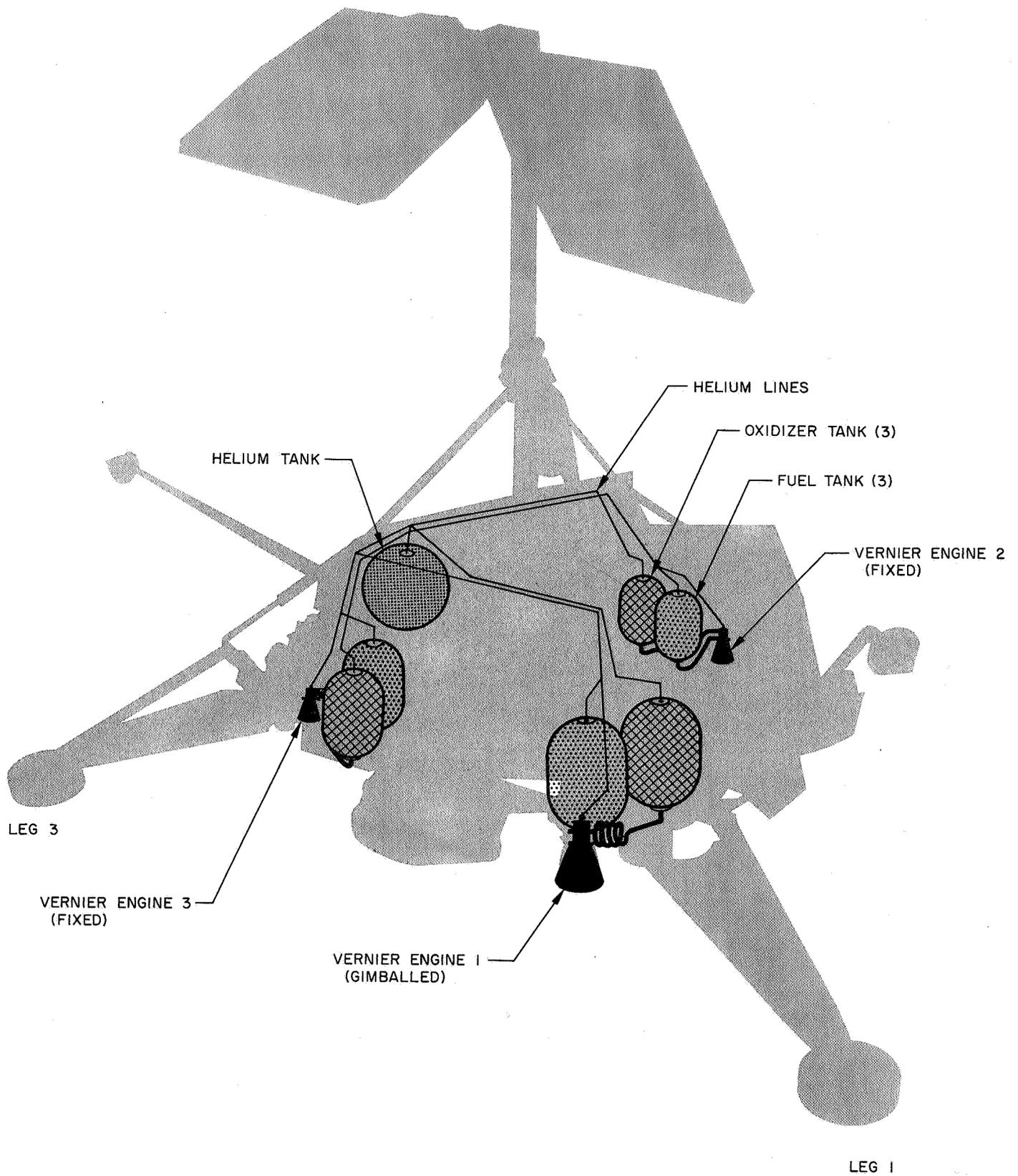
Fig. IV-32. Vernier propulsion system installation
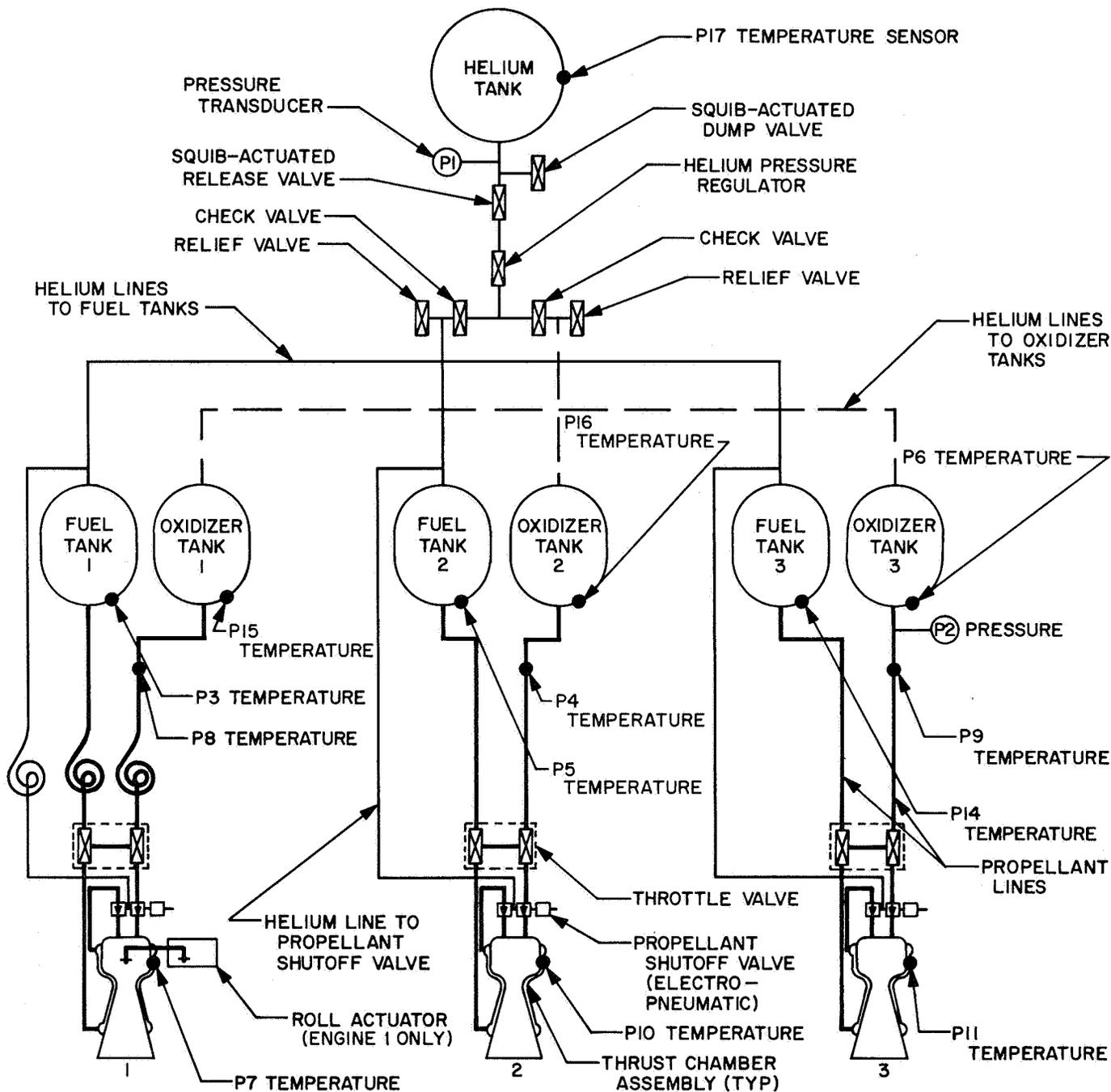
Fig. IV-33. Vernier propulsion system schematic showing locations of pressure and temperature sensors

The thrust chambers (Fig. IV-34) are located near the hinge points of the three landing legs on the bottom of the main spaceframe. The moment arm of each engine is about 38 in. Engine 1 can be rotated ±6 deg about an axis in the spacecraft $X$-$Y$ plane for spacecraft roll control. The Engine 1 roll actuator is unlocked by the same command that actuates the helium release valve.

Engines 2 and 3 are not movable. The thrust of each engine (which is monitored by strain gages installed on each engine mounting bracket) can be throttled over a range of 30 to 104 lb. The specific impulse varies with engine thrust.

Based on available data on the *Surveyor III* mission, the vernier propulsion subsystem remained well within its temperature operating limits during flight (Fig. IV-35). The subsystem adequately fulfilled all the requirements placed on it, providing the command velocity corrections and necessary attitude control.

When the helium release valve and roll actuator unlocking squibs were fired before midcourse thrusting, observations of the oxidizer pressure and the roll actuator position telemetry confirmed that pressurization and roll actuator release had occurred as expected. However, the difference in the readings of the helium supply tank pressure before and after pressurization resulted in a pressure
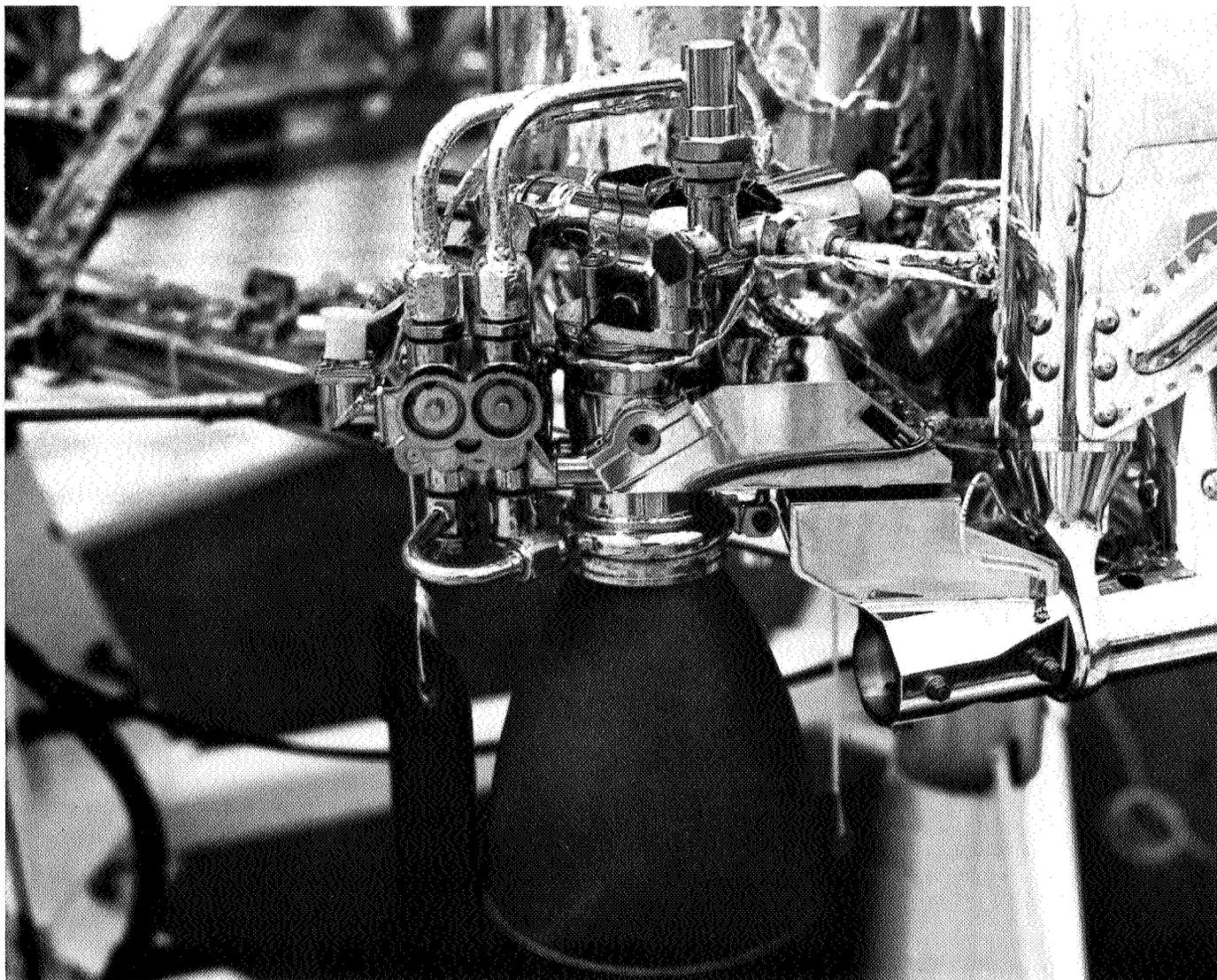


Fig. IV-34. Vernier engine thrust chamber assembly

SPECIFICATION LIMITS
RANGE OF FLIGHT DATA

UPPER RETRO
LOWER RETRO
FUEL TANK I
FUEL TANK 2
FUEL TANK 3
OXIDIZER TANK I
OXIDIZER TANK 2
OXIDIZER TANK 3
OXIDIZER LINE I
OXIDIZER LINE 2
OXIDIZER LINE 3
ENGINE I                                    165°F
ENGINE 2                                    165°F
ENGINE 3                                    165°F
HELIUM TANK

-10  0    20    40    60    80    100    120

TRANSIT TEMPERATURE RANGE, °F
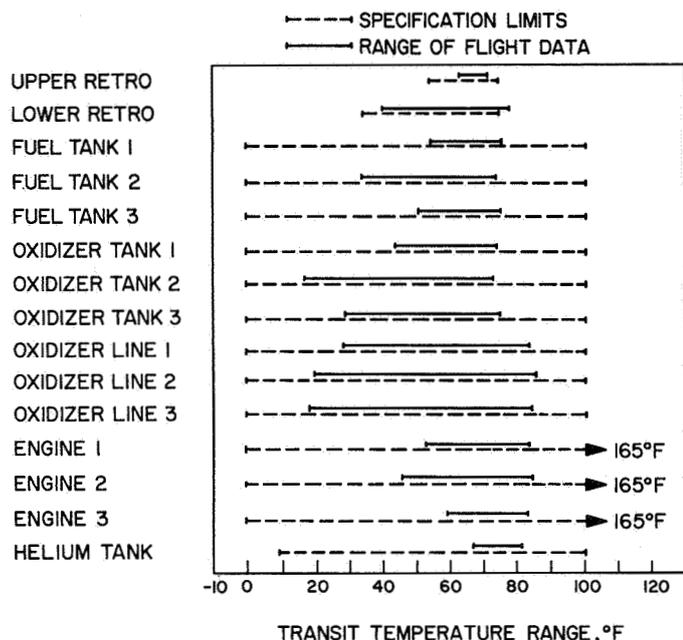
**Fig. IV-35. Range of temperature during transit**

drop somewhat less than twice the expected amount. In addition, examination of the telemetered readings of the helium pressure transducer near the time of squib actuation showed a data point approximately 110 psi higher than the prepressurization level. Consequently, a transducer zero shift is suspected.

Following pressurization of the vernier system, the midcourse velocity correction was initiated by ground command at 05:00:02 GMT on April 18, 1967. The desired thrust duration of 4.3 sec was established by previous ground command stored in the flight control. The difference between the actual firing duration and the command duration was less than the resolution level of the telemetry system. The shutdown impulse provided by the engines was between 0.0 and 0.9 lb-sec.

During midcourse correction, the thrust commands to the vernier engines from the flight control electronics were telemetered from the spacecraft. Examination of this data indicated that the three engines were not each commanded to the same thrust level. That is, Engine 1 was commanded to approximately 83 lb of thrust while Engines 2 and 3 operated at approximately 75 lb of thrust. Such a thrust imbalance would normally be the result of a spacecraft attitude error or a shift in the spacecraft center of mass. Telemetered values of the data channels which would indicate irregular spacecraft behavior or motion, such as gyro error signals or acceler-

ation error signal, failed to confirm the indications of the thrust command signals. Also, doppler and trajectory data obtained during and after the maneuver indicated that the midcourse maneuver had been performed as planned and showed no errors as indicated by the thrust commands.

During the retro case separation phase of terminal descent, where the engines were commanded to high thrust, the thrust command data had the same characteristics as during the midcourse correction maneuver. Review of the spacecraft data from the entire terminal descent, however, showed no indication of abnormal spacecraft operation. Consequently, it is felt that the difference in thrust commands is primarily due to inaccuracies in the calibration of the thrust command data channels which in no way affected the performance of the mission or endangered the terminal descent. The engine strain gages were not useful in this investigation because they lack adequate thrust level resolution.

Near the end of the terminal descent, one of the RADVS beams lost lock, causing the spacecraft to continue the descent in inertial mode and at low thrust. In this condition spacecraft altitude is not sensed; consequently, a 14-ft *mark* was not generated. It is this 14-ft *mark* which initiates vernier engines cutoff. Therefore, the vernier engines were still firing as the spacecraft touched down on the lunar surface. At touchdown, the flight control electronics attempted to maintain a constant spacecraft attitude, which, at low thrust, caused the engines to increase their total thrust level. This, coupled with the rebound of the spacecraft landing legs, caused the spacecraft to lift off the lunar surface. This action repeated itself at the second spacecraft touchdown. Just before the end of the second hop, the engines were commanded off by a ground command at 00:04:53 GMT.

At the final spacecraft touchdown, the shock absorber strain gages indicated a spacecraft landing attitude essentially identical to the two previous touchdowns, when the spacecraft was under inertial control. From this it can be inferred that there was little or no angular rate given the spacecraft at vernier engine cutoff and, therefore, any shutdown impulse variation between the engines must have been quite small.

Table IV-12 presents the propellant consumption data of the vernier propulsion system for the *Surveyor III* mission.

## Table IV-12. Vernier propellant consumption, lb

| | | |
|---|---|---|
| Vernier propellant loaded | | 184.04 |
| Expended during midcourse | 3.58 | |
| Expended during terminal descent to first touchdown | 146.31 | |
| Expended from first touchdown to engine cutoff | 10.8 | |
| Total expended | 160.69 | |
| Remaining | | 23.35 |
| Unusable | 2.2 | |
| Remaining usable | | 21.15 |

The temperature ranges experienced by the vernier system during the lunar day after landing are shown in Fig. IV-36.
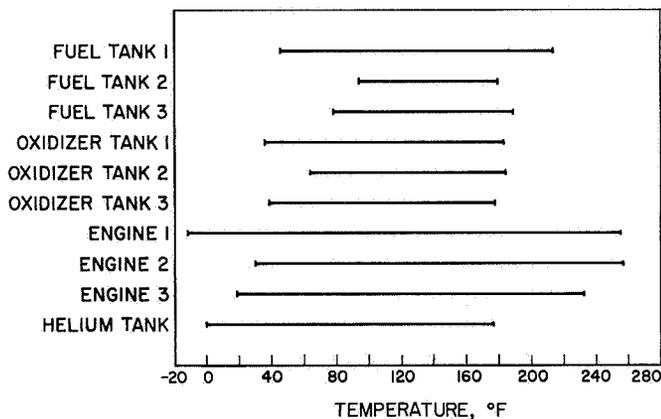


**Fig. IV-36. Vernier system temperature ranges during lunar day**

## 2. Main Retrorocket

The main retrorocket, which performs the major portion of the deceleration of the spacecraft during terminal descent, is a spherical, solid-propellant unit with a partially submerged nozzle to minimize overall length (Fig. IV-37). The motor utilizes a carboxyl/terminated polyhydrocarbon composite-type propellant and conventional grain geometry.

The motor case is attached at three points on the main spaceframe near the landing leg hinges, with explosive nut disconnects for postburnout ejection. Friction clips around the nozzle flange provide attachment points for the altitude marking radar (AMR). The *Surveyor III* retrorocket, including the thermal insulating blankets,

weighed approximately 1445 lb. This total included about 1300 lb of propellant. The thermal control design of the retrorocket motor is completely passive, depending on its own thermal capacity and insulating blanket (21 layers of aluminized mylar plus a cover of aluminized teflon). The prelaunch temperature of the unit is 70 ±5°F. At terminal maneuver, when the motor is ignited, the propellant will have cooled to a thermal gradient with a bulk average temperature of about 50 to 55°F.

The AMR normally triggers the terminal maneuver sequence. When the retro firing sequence is initiated, the retrorocket gas pressure ejects the AMR. The motor operates at a thrust level of 8,000 to 10,000 lb for approximately 41 sec at an average propellant temperature of 55°F.

Beginning at a launch bulk average temperature of approximately 70°F, the retro cooled at the predicted rate and arrived at an average temperature of 52°F at the time of ignition. At this temperature the burn time was predicted to be 41.09 sec. The postflight data analysis indicates a burn time of 41.37 sec or a difference of 0.7%. The maximum thrust developed was 9,550 lb against a prediction of 9,600 lb. The modulation of vernier engine thrust commands and the output of the gyros were small, which indicated a stable spacecraft during the retro phase. The data also showed that the actual total impulse of the main retro was less than 0.3% below the predicted value.

Approximately midway through the retro burn phase the spacecraft telemetry indicated a pitch or yaw moment of 236 in.-lb. Moments occurring throughout the retro burn phase were well within the total pitch- or yaw-compensating capability of approximately 2,000 in.-lb. The pitch or yaw capability of the spacecraft comes from the ability of the vernier propulsion system to differ the thrust levels of each of the 3 vernier engines such as to produce a righting moment. The above value of moment was found by ascertaining the vernier engine thrust difference which existed during the retro burn time.

Similarly, flight telemetry indicated a maximum roll moment of 70 in.-lb, which was within the spacecraft roll capability of approximately 100 in.-lb. The indicated value occurred during the burnout or pressure tail-off portion of retro burning, when the roll actuator was positioned at +1.54 deg off null. Retro motor separation from the spacecraft occurred normally.
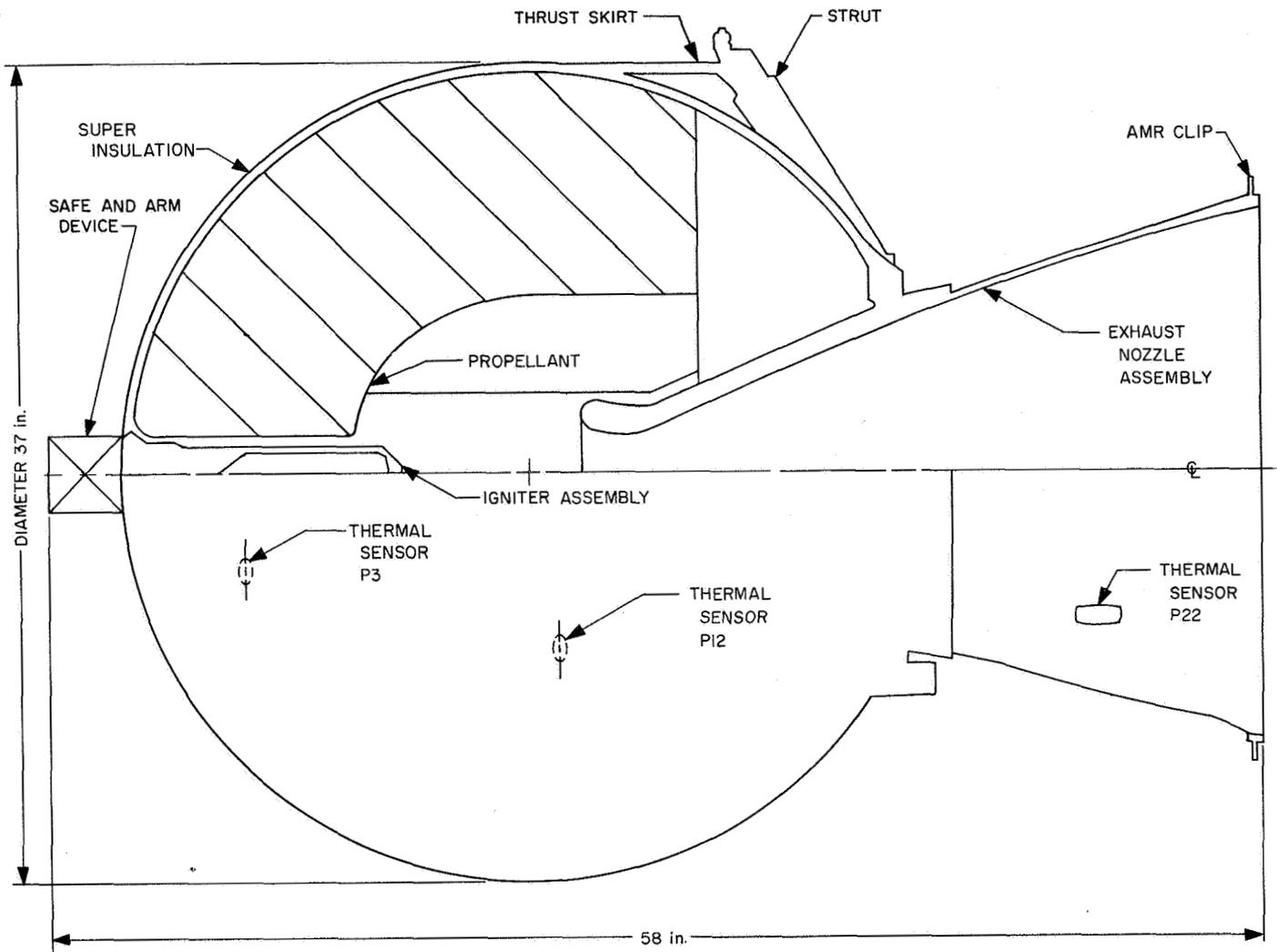
**Fig. IV-37. Main retrorocket motor**

## F. Flight Control

The flight control subsystem is designed to (1) acquire and maintain spacecraft orientation with respect to the sun and the star Canopus, (2) orient the spacecraft for a mid-mission trajectory error correction, (3) execute an incremental velocity change and maintain spacecraft stability during midcourse correction and terminal descent, (4) execute a lunar terminal orientation, and (5) in conjunction with a radar system (RADVS), a solid-propellant retro motor, and three liquid-propellant (vernier) engines, soft-land (at a nominal touchdown velocity of 13 ft/sec) the spacecraft on the lunar surface.

The flight control subsystem consists of the appropriate electronic equipment associated with a Canopus star sensor (roll), primary sun sensors (pitch and yaw) for spacecraft attitude in pitch, yaw, and roll during cruise, an acquisition sensor for initial sun acquisition, three gyros (pitch, yaw, and roll) for rate stabilization and inertial control, and a $\pm 0.75$-$g$ precision accelerometer for midcourse velocity control and acceleration control during the terminal descent.

The control electronics process the reference sensor outputs, earth-based commands, and the flight control programmer and decoder outputs to generate the necessary control signals for use by the vehicle control elements. A simplified flight control functional diagram appears in Fig. IV-38. The vehicle control elements consist of the attitude-control gas-jet activation valves, the vernier engine thrust level control valves and gimbal actuator, and the main retro motor ignitor and separation pyrotechnics.
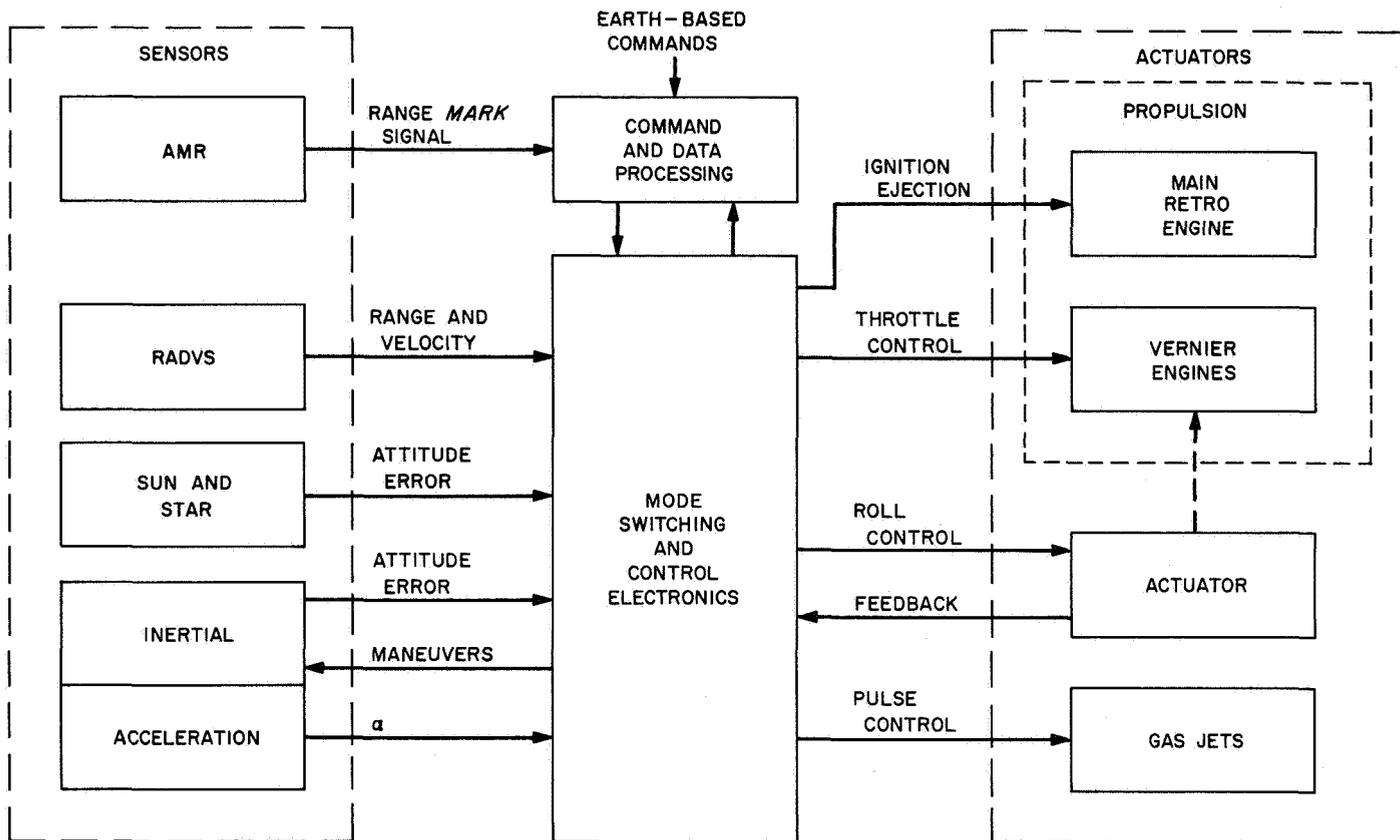
**Fig. IV-38. Simplified flight control functional diagram**

The gas-jet attitude control system is a cold gas system using nitrogen as a propellant. This system consists of a gas supply system and three pairs of solenoid-valve-operated gas jets interconnected with tubing (see Fig. IV-39). The nitrogen supply tank is initially charged to a nominal pressure of 4600 psia. Pressure to the gas jets is controlled to 40 ±2 psia by a regulator.

Spacecraft attitude, acceleration, and velocity are controlled as required by various "control loops" throughout the coast and thrust phases of flight, as shown in Table IV-13. Stabilization of the spacecraft tipoff rates after *Centaur* separation is achieved through the use of rate feedback gyro control (rate mode). After rate capture, an inertial mode is achieved by switching to position feedback gyro control.

Because of the long duration of the transit phase and the small unavoidable drift error of the gyros, a celestial reference is used to continuously update the inertially controlled attitude of the spacecraft.

The celestial references (Fig. IV-3), the sun and the star Canopus, are acquired and maintained after the spacecraft separates from the *Centaur* stage and after automatic deployment of the solar panel. The sun is first acquired by the acquisition sun sensor during a spacecraft roll maneuver which is automatically initiated at completion of solar panel deployment. The 10-deg wide by 196-deg fan-shaped field of view of the acquisition sun sensor includes the Z-axis and is centered about the X-axis. The roll command is terminated after initial sun acquisition, and a yaw command is initiated which allows the narrow-view primary sun sensor to acquire and lock on the sun. Automatic Canopus acquisition and lock-on are normally achieved after initiation of a roll command from earth. This occurs because the Canopus sensor angle is preset with respect to the primary sun sensor prior to launch for each mission. Star mapping for Canopus verification is achieved by commanding the spacecraft to roll while maintaining sun lock. A secondary sun sensor, mounted on the solar panel, provides a backup for manual acquisition of the sun if the automatic sequence fails.

The transit phase is performed with the spacecraft in the celestial-referenced mode except for the initial rate-stabilization, midcourse, and terminal descent maneuvers.

## Table IV-13. Flight control modes

| Control loop | Flight phase | Modes | Remarks |
|---|---|---|---|
| **Attitude control loop** | | | |
| Pitch and yaw | Coast | Rate<br>Inertial<br>Celestial | Gas jet matrix signals |
| | Thrust | Inertial<br>Lunar radar | Vernier engine matrix signals |
| Roll | Coast | Rate<br>Inertial<br>Celestial | Leg 1 gas jet signals |
| | Thrust | Inertial | Vernier Engine 1 gimbal command |
| **Acceleration control loop** | | | |
| Thrust axis | Thrust (midcourse)<br>Thrust (terminal descent) | Inertial (with accelerometer)<br>Inertial (with accelerometer) | Nominal 3.22 ft/sec$^2$<br>Minimum 4.77 ft/sec$^2$<br>Maximum 12.56 ft/sec$^2$ |
| **Velocity control loop** | | | |
| Thrust axis | Thrust | Lunar radar | Command segment signals to 43-ft altitude<br>Constant 5-ft/sec velocity signals to 14-ft altitude |
| Lateral axis | Thrust | Lunar radar | Lateral/angular conversion signals |
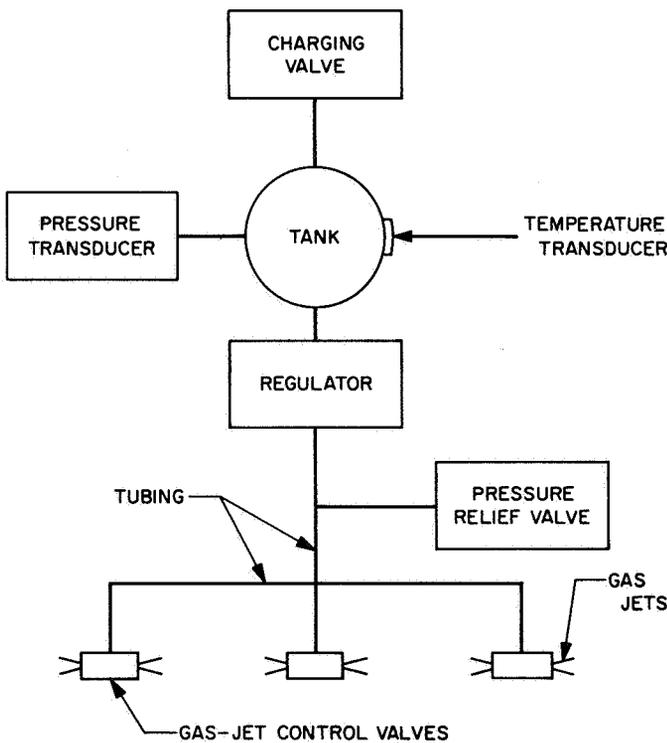


**Fig. IV-39. Gas-jet attitude control system**

The midcourse and main retro orientation maneuvers are achieved in the inertial mode. Acceleration control is used for controlling the magnitude of the midcourse velocity increment. During the interval from retro case separation to initiation of radar velocity control, acceleration control is used to control the descent along the spacecraft thrust axis, and velocity control is used for pitch and yaw control to align the spacecraft thrust axis with the velocity vector.

The lunar reference is first established by a signal from an AMR subsystem when the spacecraft is nominally 60 miles slant range from the lunar surface. (Refer to Section IV-G for discussion of radar control during the standard terminal descent phase.)

### 1. Launch Phase

During the System Readiness Test conducted just before the spacecraft countdown, a questionable indication was observed on the vernier roll actuator. The roll actuator position signal monitored by telemetry channel FC-43 indicated random variations on the order of 13 binary coded digital (BCD) units (0.14 deg). Since the roll actuator was pinned when the fluctuations on FC-43 were

observed, there was concern over the condition of the pinning mechanism.

A special test was devised to check the integrity of the actuator pinning. This test consisted of torquing the roll gyro to see if the actuator would respond. The roll actuator position signal showed a movement of about 2.5 deg. Since it was not clear whether the 2.5-deg movement of the roll actuator was an actual mechanical movement or an electrical signal from the roll gyro affecting FC-43, it was decided to conduct the same test on SC-5* while holding the launch countdown of SC-3*. The test on SC-5 yielded results very similar to those on SC-3. On the basis of this similarity it was assumed that the roll actuator on SC-3 was displaying a normal signature (although previously undetected because of the 10-bit suppression limit on the data printer). Hence, the countdown was resumed after a hold of about 51 min.

Postflight investigations revealed that the observed behavior of the roll actuator on SC-3 was normal. The 2.5-deg fluctuation on FC-43 was found to be caused by the following factors: (1) 0.96 deg actual output arm motion, (2) 1.13 deg compliance across output shaft, and (3) 0.4 deg due to electrical mixing of roll error signal and FC-43.

The gyro temperatures just prior to launch were: roll, 172.7°F; pitch, 168.1°F; and yaw, 167.4°F. The roll and yaw gyro temperature controllers were cycling at the time of launch, and the pitch gyro controller started cycling about 9 min after launch.

The nitrogen tank of the gas-jet attitude control system was loaded with 4.5 lb of nitrogen at 4832 psi and a tank temperature of 84.8°F.

Separation of the *Surveyor* from *Centaur* was normal. Just prior to separation, the combined *Surveyor/Centaur* vehicle had the following rates, as computed from spacecraft gyro data:

| | |
|---|---|
| Pitch | +0.06 deg/sec |
| Yaw | −0.25 |
| Roll | +0.1 |

Just after separation the *Surveyor* rates were as follows:

| | |
|---|---|
| Pitch | +0.0 deg/sec |
| Yaw | −0.265 |
| Roll | +0.0 |

---

*Spacecraft serial designation.

From these figures it becomes evident that extremely minute rates (not more than 0.1 deg/sec per axis) were imparted to the spacecraft via the separation springs. Since the gyro telemetry is sampled once every 2.4 sec, small differences between *Centaur* and *Surveyor* rates can be attributed to the low sampling rates on the *Surveyor* gyros. (Also see Section III-E for launch vehicle separation rate data.)

## 2. Sun Acquisition

A very nominal sun acquisition sequence was automatically executed. The acquisition sun sensor was illuminated after a negative roll of 181 deg. This was followed by a positive yaw turn of 38 deg, which established the attitude required to illuminate the primary sun sensor and generate the *sun-lock* signal. The sun acquisition and lock-on sequence took about 7 min.

## 3. Star Acquisition

A *sun and roll* command was sent about 9 hr after liftoff to initiate the Canopus search sequence. Analysis of star intensity signals permitted the positive identification of Canopus, Jupiter, Procyon, Adhara and Altair, plus the moon and earth. Since *lock-on* signals were received when Jupiter and the earth were in the field of view, it was decided to send the *sun and star* command after Jupiter had passed the field of view for the second time. At 522 deg of roll the *sun and star* command was sent, allowing Canopus error signals to control the roll position of the spacecraft when the Canopus *lock* signal was generated at 560 deg.

This was the first time that Canopus acquisition was obtained automatically. On the *Surveyor I* and *II* missions, the Canopus intensity signal was larger than the automatic lock threshold, thus preventing automatic star acquisition.

Since the effective gains of the Canopus trackers on *Surveyors I* and *II* were larger than predicted, it was decided to reduce the effective gain of the *Surveyor III* Canopus sensor to 1.05 to 1.10 × Canopus by changing the transmission characteristics of the sun filter. By admitting more sunlight into the sun channel, the effective gain is lowered, resulting in decreased star intensity signals.

Referring to the tabulation of *Surveyor III* star intensity responses presented in Table IV-14, it is noted that Procyon indicated 24% brighter than predicted, Adhara indicated 26% brighter, Canopus 16% brighter, and Altair 28% brighter. Since Jupiter is twice the intensity

**Table IV-14. Star angles and intensities:
indicated and predicted**

| Roll angle, deg | Source | Angle from Canopus, deg | | Intensity | |
|---|---|---|---|---|---|
| | | Indicated | Predicted | Indicated, V | Predicted, V |
| 0 | (Start of roll) | | −205 | | |
| 121 | Moon | −84 | −84 | 0.996 | — |
| 128 | Jupiter | −77 | −77 | 4.453 | 5.00 |
| 144 | Procyon | −60 | −60 | 1.259 | 1.00 |
| 179 | Adhara | −26 | −25 | 0.864 | 0.68 |
| 205 | Canopus | 0 | 0 | 3.793 | 3.31 |
| 317 | Earth | +112 | +112 | 3.569 | — |
| 338 | Altair | +133 | +133 | 1.093 | 0.85 |
| 479 | Moon | +274 | +276 | 0.961 | — |
| 486 | Jupiter | +283 | +283 | 4.448 | 5.00 |
| 504 | Procyon | +299 | +300 | 1.230 | 1.00 |
| 540 | Adhara | +335 | +335 | 0.859 | 0.68 |
| 565 | Canopus | 0 | 0 | 4.170 | 3.55 |

of Canopus and the star intensity signal saturates at approximately 1.6 × Canopus, it was predicted that the nominal star intensity saturation voltage of 5.00 V would be attained. However, it appears that the actual saturation voltage of the *Surveyor III* Canopus sensor is lower than nominal (about 4.45 V). Since Jupiter yields a saturated signal (also about 4.45 V), it is meaningless to attempt a comparison of in-flight vs predicted saturated values to determine effective gain.

Since the ratio of in-flight to predicted intensities ranges from 1.16 to 1.28, it appears that some combination of higher-than-predicted Canopus tracker gain and higher-than-predicted intensity of the stellar bodies could account for the discrepancy.

### 4. Gyro Drift and Limit Cycle Dead Bands—Cruise Mode

A total of eight 3-axes gyro drift checks were made during the mission. Two of them were made prior to the midcourse velocity correction. Four roll-axis-only drift checks were also made. Two techniques were used to measure the drift rates. The first was based on average slopes of the optical error signals. In the second technique, iterated calculations were used. The terminal attitude maneuvers included compensation for the following gyro drift rates (in deg/hr): roll, +1.1; pitch, +0.6; yaw, −0.8.

Based on the analysis used in the gyro drift checks, the peak-to-peak single-axis optical deadbands were determined to be (in deg): roll, 0.48; pitch, 0.38; yaw, 0.48.

### 5. Premidcourse Maneuvers

The maneuver combination executed to orient the spacecraft in the desired direction for the midcourse velocity correction consisted of +56.7 deg roll followed by 39.1 deg pitch.

### 6. Midcourse Velocity Correction

The spacecraft was programmed for a midcourse thrust duration of 4.28 sec. This was intended to provide a velocity change of 4.19 m/sec. Ignition was smooth and the entire correction was performed in a very nominal fashion. The peak gyro angles during ignition were less than 1 deg. After vernier engine shutdown, the gas jet system was easily able to stabilize the spacecraft with none of the gyro error signals exceeding 2 deg. Since the minimum gyro gimbal range of ±10 deg was not exceeded, inertial reference was maintained and reacquisition of the sun and Canopus was accomplished via the standard reverse maneuver sequence.

Telemetry indicated that the engine thrust commands to the three engines were not uniform. However, this did not affect the midcourse thrusting since, in actuality, all engines thrusted nominally. This was concluded from the fact that attitude stability was maintained, and tracking data verified that the expected velocity correction was attained.

Analysis of the flight control thrust command telemetry circuits shows that, in the worst case, telemetry errors would not account for more than ±0.66 lb. Since this is almost an order of magnitude below the thrust command discrepancies, no complete explanation is yet available. However, investigations are still continuing.

### 7. Terminal Maneuvers and Descent

The first terminal maneuver (yaw) was initiated approximately 38 min before retro ignition. The maneuver magnitudes (in deg) were: yaw, −157.9; pitch, −76.7; roll, −63.9. The effect of gyro drift on pointing error during terminal descent was expected to be negligible because the attitude maneuver magnitudes were compensated for measured values of gyro drift.

The *reset nominal thrust bias* command was sent about 23 min before main retro ignition to provide a total nominal vernier engine thrust of 201 lb during retro motor

burn. A vernier engine ignition delay of 5.075 sec follow-ing AMR *mark* was also sent by command and entered into the magnitude register. The AMR *enable* command was sent about 1½ min before the terminal descent se-quence was automatically initiated by the AMR *mark* signal.

The terminal sequence was flawlessly executed up to the time when the RADVS should have provided the 14-ft *mark* signal. The 14-ft *mark* was not generated, and the vernier engines were not shut down prior to lunar touch-down because the *reliable operate* signal was lost at about 35 ft above the lunar surface. Continued thrusting of the verniers resulted in the spacecraft making three touch-downs before coming to rest. All three contacts with the lunar surface were soft, causing less impact acceleration than would occur in a normal landing.

Changes in spacecraft attitude were small at vernier engine ignition and main retro ignition and remained small through retro case separation. The attitude error angles which existed are shown in Table IV-15.

**Table IV-15. Attitude errors during terminal descent**

| Time | Pitch gyro error, deg | Yaw gyro error, deg | Roll gyro error, deg | Roll actuator position, deg |
|---|---|---|---|---|
| Before vernier ignition | +0.14 | −0.03 | 0 | +0.49 |
| Retro ignition (max angle) | −0.22 | +0.157 | −0.35 | +0.97 |
| Retro thrusting (steady state) | −0.08 | 0 | +0.165 | +0.21 |
| Retro burnout (max angle) | −0.08 | 0 | −0.87 | +1.54 |

The slant range vs Z-component of velocity during the terminal descent is shown in Figs. IV-40 and IV-41. The actual curve appears above the predicted curve because of a bias in the slant range telemetry signal.

The peak spacecraft attitude changes resulting from the first touchdown were (in deg): pitch gyro, +6.42; yaw gyro, +7.53; roll gyro, −0.55; roll actuator, −1.87. The gyro error signals were quickly damped out, and spacecraft attitude was stable to the final touchdown.

The vernier engines were finally shut down by com-manding *thrust phase power off* approximately 1 sec before the third touchdown. Analog data were erroneous
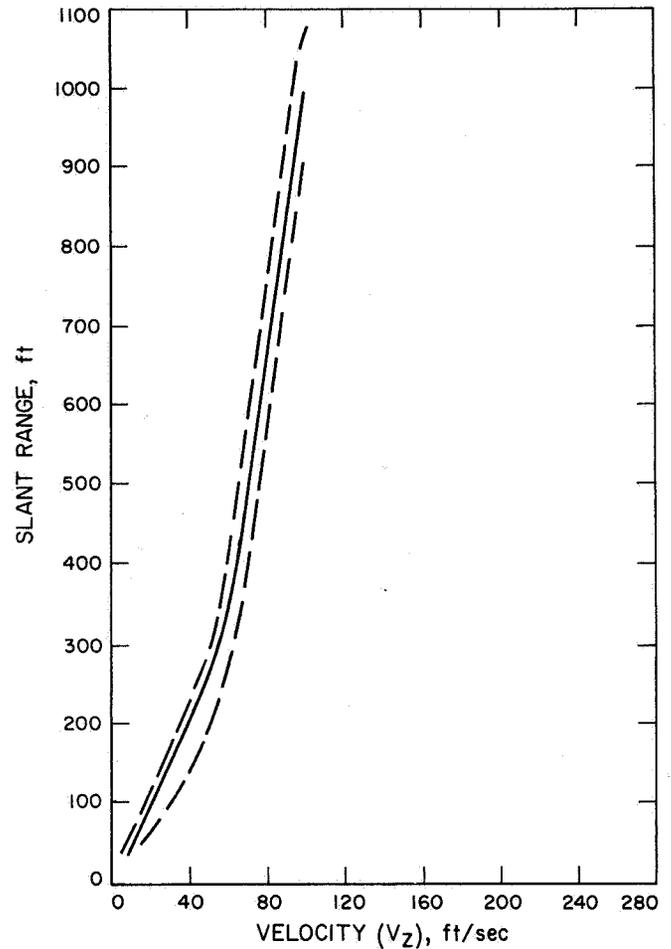


**Fig. IV-40. Descent profile, below 1000 ft**

after the second touchdown, and digital signals were used to verify that flight control 29-V coast phase power turned off.

**8. Nitrogen Gas Consumption**

The estimated nitrogen gas consumption for the *Surveyor III* mission is shown in Table IV-16. It was calculated that 4.50 lb of nitrogen was loaded prior to launch. Since the final prelaunch estimate of nitrogen weight using telemetered data indicated that 4.63 lb was on board, all subsequent estimates were corrected by subtracting 0.13 lb.

It can be seen that the actual and expected values compare favorably until after midcourse. It was estimated that the *Surveyor III* mission used about 0.94 lb of nitro-gen up to the time of retro ignition. This compares with 0.68 lb for the *Surveyor I* mission. The difference, 0.26 lb, is relatively unimportant to the mission but can be ex-plained by considering the number and types of maneuvers
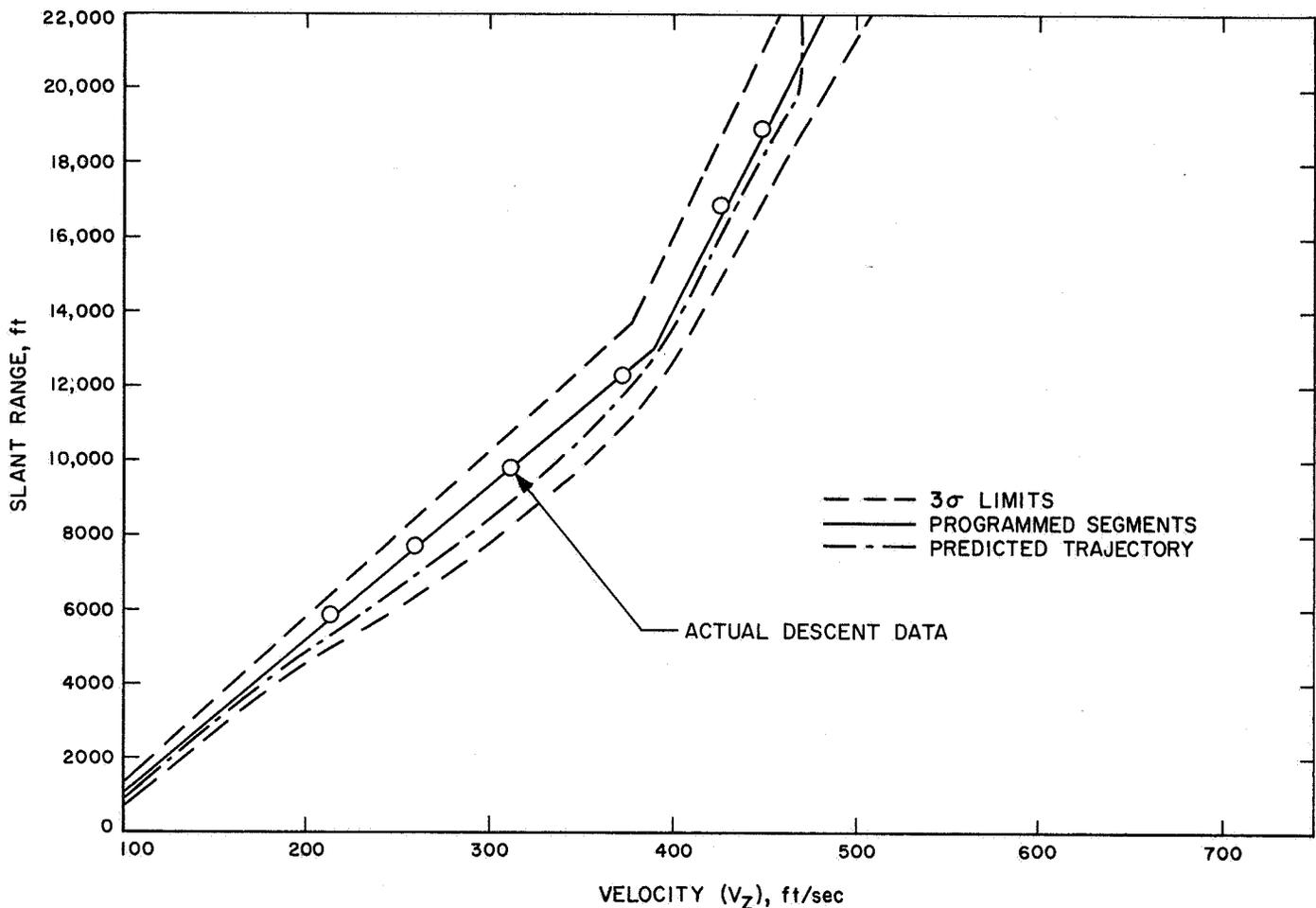
Fig. IV-41. Descent profile, above 1000 ft

and gyro drift checks accomplished by *Surveyor III* compared to *Surveyor I*. It is estimated that 0.09 lb more gas was required to perform the midcourse and terminal maneuvers on *Surveyor III*. Also, *Surveyor III* did six more gyro drift checks than *Surveyor I*, and it is estimated that this would account for the remaining 0.17 lb of nitrogen.

## G. Radar

Two radar devices, the altitude marking radar (AMR) and the radar altimeter and doppler velocity sensor (RADVS), are employed on the *Surveyor* spacecraft for use during the terminal descent phase.

### 1. Altitude Marking Radar

The AMR (Fig. IV-42) is a pulse-type fixed-range measuring radar which provides a *mark* signal at a slant range from the lunar surface that can be preset between

52 and 70 miles. The *mark* signal is used by the flight control subsystem to initiate the automatic operations for spacecraft terminal descent.

The AMR operates at a frequency of 9.3 GHz. The range is obtained by use of dual-channel video (early and late gate signals). The early and late gates are adjacent at the preset range (60 miles for *Surveyor III*) so that, as the spacecraft approaches, the lunar surface video return becomes equally distributed between two gates. When the main lobe return is of equal magnitude in both gates and of such an amplitude to overcome a preset bias, the *mark* signal is generated.

The AMR mounts in the retro rocket nozzle and is retained by friction clasps around the nozzle flange with spring washers between the AMR and the flange. When the retro rocket is ignited, the gas generated by the ignitor develops sufficient pressure to eject the AMR from

## Table IV-16. Nitrogen gas consumption

| Time, GMT | Telemetry data | | Nitrogen remaining, lb | |
| --- | --- | --- | --- | --- |
| | Pressure, psi | Temperature, °F | Actual | Expected |
| April 17, 1967 07:31 (Prelaunch) | 4815 | 83 | 4.5 (4.63)[a] | 4.5 |
| 08:27 (After sun acquisition) | 4689 | 85.7 | 4.39 (4.52) | 4.4 |
| April 18 05:48 (After midcourse) | 3598 | 37.2 | 4.0 (4.13) | 4.1 |
| April 19 13:44 | 3495 | 50.4 | 3.77 (3.9) | — |
| 23:23 | | | 3.7 | — |
| 23:47 (After terminal maneuvers) | | | 3.56[b] | — |

[a] Quantities in parentheses are before 0.13-lb correction.

[b] Based on estimated consumption for maneuvers as follows: yaw, 0.034 lb; pitch, 0.068 lb.

the nozzle. The AMR draws power from 22 Vdc through a breakaway plug that also carries input commands, the output *mark* signal, and telemetry information.

On the *Surveyor III* mission, the AMR functioned normally in all respects. The 60-mile *mark* was initiated at the proper time and, with a time delay of 6.175 sec commanded into the magnitude register, retro ignition was initiated at the proper altitude.

AMR power output as measured by magnetron input current was essentially nominal and steady at 2 W average from AMR *enable* through AMR ejection.

As indicated in Fig. IV-43, AMR AGC was normal, with signal power to the feed increasing steadily and smoothly until radar *mark*, and thence ejection. The received pulse was approximately 15.4 $\mu$sec in width, and the received power at mark was −76 dbm. AMR performance was within 2 db of the predicted performance, which is also shown in the figure. The predicted curve is based upon the Muhleman reflectivity model for a total
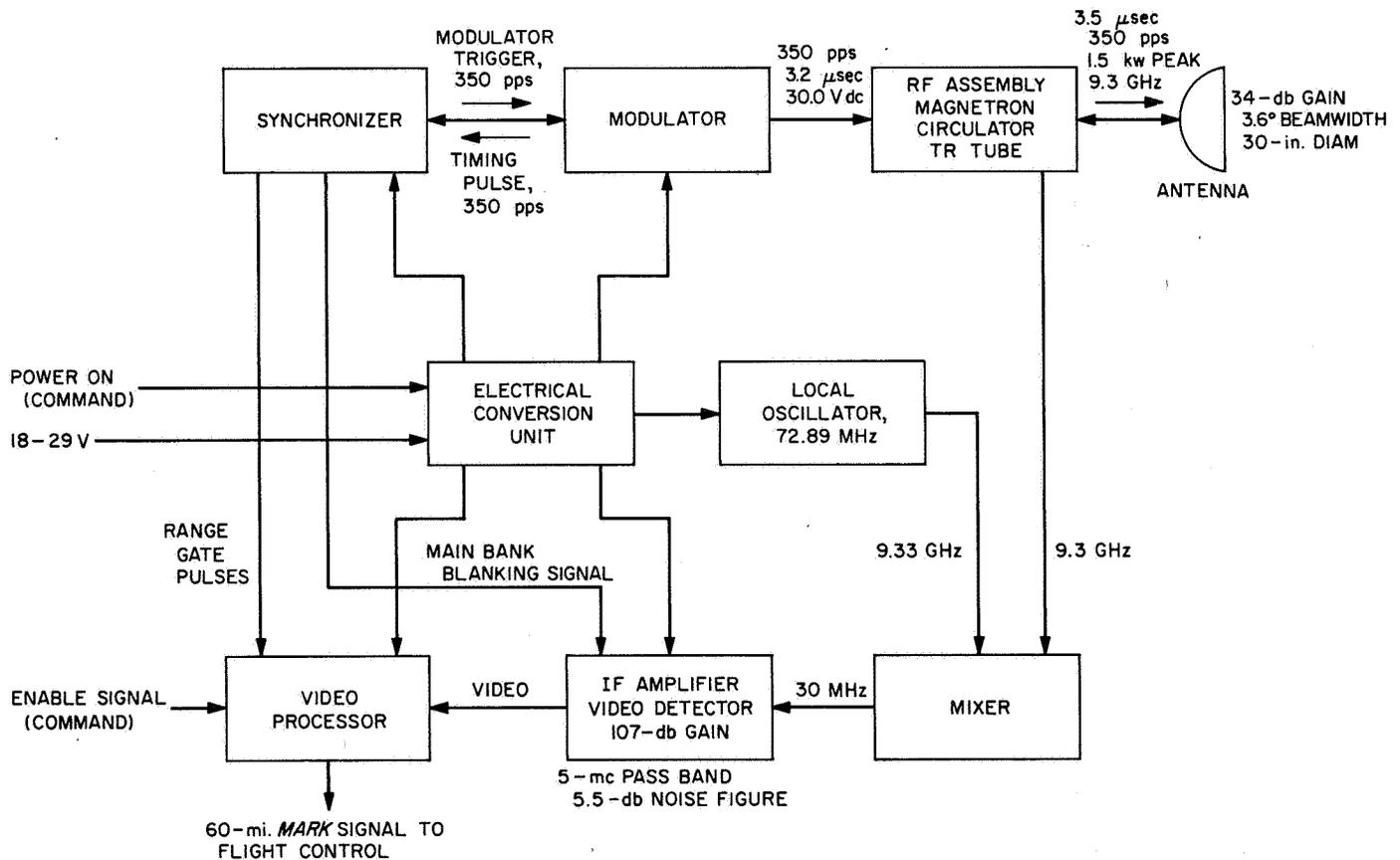


Fig. IV-42. Altitude marking radar functional diagram
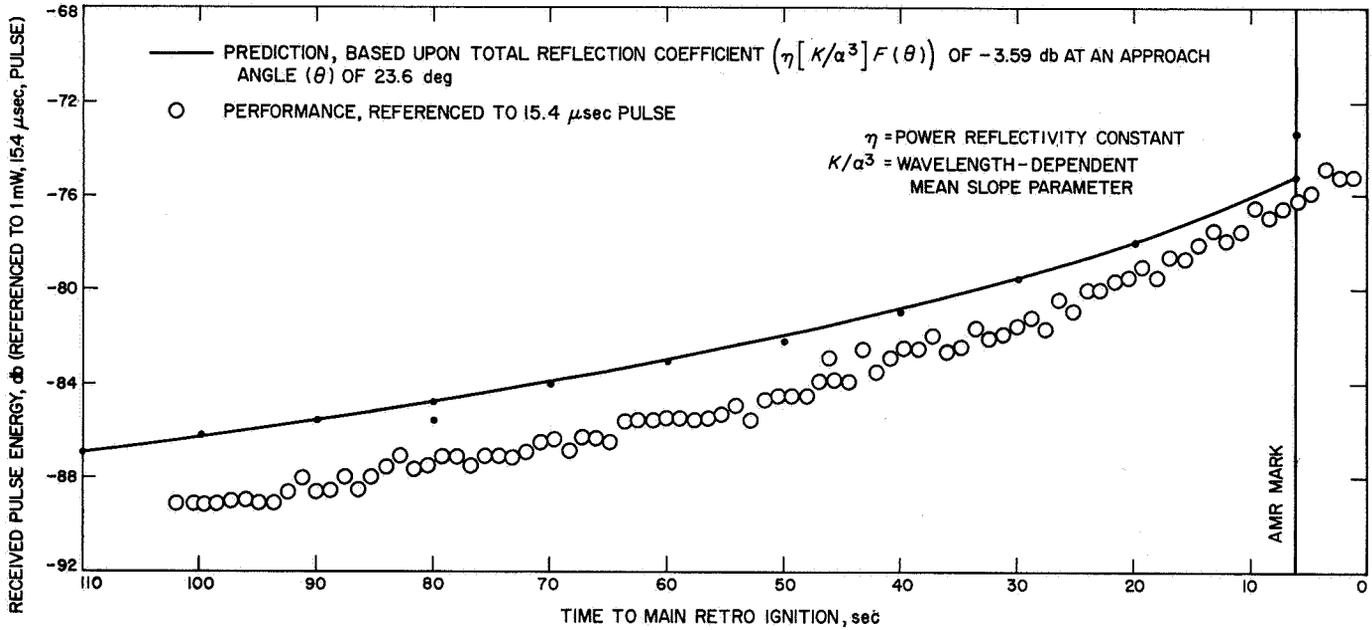
Fig. IV-43. Altitude marking radar AGC

reflection coefficient $[\eta(k/\alpha^3)F(\theta)]$ of 3.59 db at an approach angle $(\theta)$ of 23.6 deg. The agreement between the curves is considered very good since the predicted curve has not been corrected for actual AGC response and was based upon an average spacecraft velocity.

AMR temperatures were as expected and compared favorably with those of the *Surveyor I* mission. AMR temperatures are not telemetered during terminal descent, so the last temperatures are those just prior to AMR enable. A comparison of the last temperatures telemetered on *Surveyors I* and *III* is presented below:

|  | Surveyor I, °F | Surveyor III, °F |
| --- | --- | --- |
| Antenna, edge | −187 | −200 |
| Antenna, inside rear | −12 | 0 |
| AMR electronics | +16 | +17.5 |

## 2. Radar Altimeter and Doppler Velocity Sensor

The RADVS (Fig. IV-44) functions in the flight control subsystem to provide three-axis velocity, range, and altitude *mark* signals for flight control during the main retro and vernier phases of terminal descent. The RADVS consists of a doppler velocity sensor (DVS), which computes velocity along the spacecraft X, Y, and Z axes, and a radar altimeter (RA), which computes slant range from 40,000 to 14 ft and generates 1000-ft and 14-ft *mark* signals. The RADVS comprises five assemblies: (1) kly-

stron power supply/modulator (KPSM), which contains the RA and DVS klystrons, klystron power supplies, and altimeter modulator, (2) altimeter/velocity sensor antenna, which contains Beams 1 and 4 transmitting and receiving antennas and preamplifiers, (3) velocity sensing antenna, which contains Beams 2 and 3 transmitting antennas and preamplifiers, (4) RADVS signal data converter, which consists of the electronics to convert doppler shift signals into dc analog signals, and (5) interconnecting waveguide. The RADVS is turned on at about 50 miles above the lunar surface and is turned off at about 13 ft.

*a. Doppler velocity sensor.* The doppler velocity sensor (DVS) operates on the principle that a reflected signal has a doppler frequency shift proportional to the approaching velocity. The reflected signal frequency is higher than the transmitted frequency for the closing condition. Three beams directed toward the lunar surface enable velocities in an orthogonal coordinate system to be determined.

The KPSM provides an unmodulated DVS klystron output at a frequency of 13.3 kmc. This output is fed equally to the DVS 1, DVS 2, and DVS 3 antennas. The RADVS velocity sensor antenna unit and the altimeter velocity sensor antenna unit provide both transmitting and receiving antennas for all three beams. The reflected signals are mixed with a small portion of the transmitted frequency at two points ¾ wavelength apart for phase

VELOCITY SENSOR ANTENNA — SIGNAL DATA CONVERTER
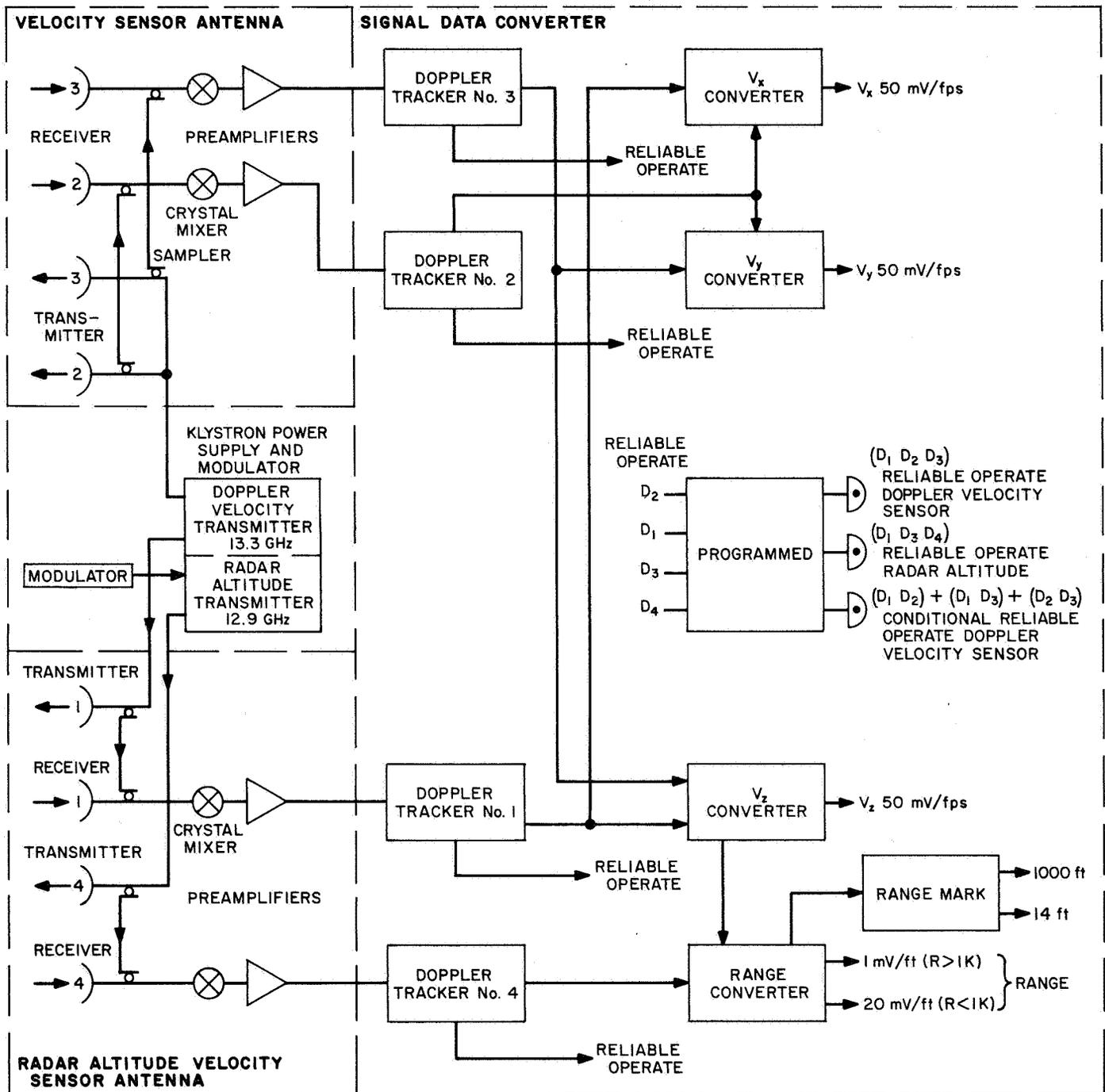
**Fig. IV-44. Simplified RADVS functional block diagram**

determination, detected, and amplified by variable-gain amplifiers providing 40, 65, or 90 db of amplification, depending on received signal strength. The preamp output signals consist of two doppler frequencies, shifted by ¾ transmitted wavelength, and preamp gain-state signals for each beam. The signals are routed to the trackers in the RADVS signal data converter.

The D1 through D3 trackers in the signal data converter are similar in their operation. Each provides an output which is 600 kHz plus the doppler frequency for approaching doppler shifts. If no doppler signal is present, the tracker will operate in search mode, scanning frequencies between 82 kHz and 800 Hz before retro burnout, or between 22 kHz and 800 Hz after retro burnout. When a doppler shift is obtained, the tracker will operate as described above and initiate a lock-on signal. The tracker also determines amplitude of the reflected signal and routes this information to the signal processing electronics for telemetry.

The velocity converter combines tracker output signals $D_1$ through $D_3$ to obtain dc analog signals corresponding

to the spacecraft $X$, $Y$, and $Z$ velocities; $D_1 + D_3$ is also sent to the altimeter converter to compute range.

Reliability and reference circuits produce a *reliable operate* signal if $D_1$ through $D_3$ lock-on signals are present or if these signals are present 3 sec after retro burnout. The *reliable operate* DVS signal is routed to the flight control electronics and to the signal processing electronics telemetry.

**b. Radar altimeter.** Slant range is determined by measuring the reflection time delay between the transmitted and received signals. The transmitted signal is frequency-modulated at a changing rate so that return signals can be identified.

The RF signal is radiated, and the reflected signal is received by the altimeter/velocity sensor antenna. The received signal is mixed with two samples of transmitted energy ¾ wavelength apart, detected, and amplified by 40, 60, or 80 db in the altimeter preamp, depending on signal strength. The signals produced are difference frequencies resulting from the time lag between transmitted
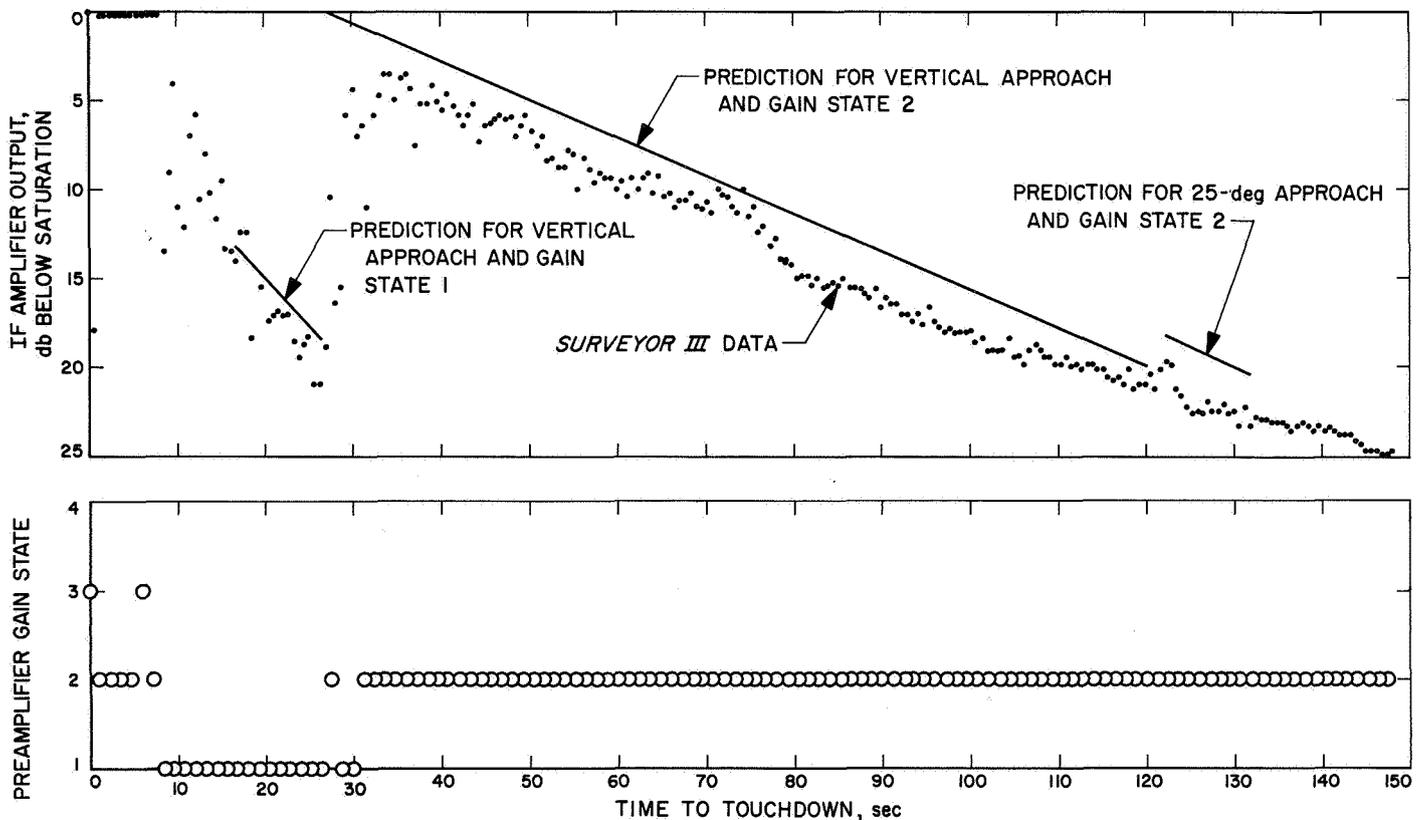


Fig. IV-45. Reflectivity of RADVS Velocity Beam 1 during descent

and received signals of a known shift rate, coupled with an additional doppler frequency shift because of the spacecraft velocity.

The altimeter tracker in the signal data converter accepts doppler shift signals and gain-state signals from the altimeter/velocity sensor antenna and converts these into a signal which is 600 kHz plus the range frequency plus the doppler frequency. This signal is routed to the altimeter converter for range dc analog signal generation.

The range mark, reliability, and reference circuits produce the 1000-ft *mark* signal and the 14-ft *mark* signal from the *range* signal generated by the altimeter converter where the doppler velocity $V_z$ is subtracted giving the true range.

The *range mark* and *reliable* signals are routed to flight control electronics. The signals are used to rescale the *range* signal, for vernier engine shutoff and to indicate whether or not the *range* signal is reliable. The *reliable operate* signal is also routed to signal processing for transmission to DSIF.

*c. RADVS performance.* On the *Surveyor III* mission, the RADVS performed as planned down to about 37-ft altitude. Reflectivity of the RADVS beams (IF amplifier output in decibels below saturation) is shown in Figs. IV-45 through IV-48 along with preamplifier gain state. Predicted reflectivity is also shown in the figures for an initial 25-deg approach angle with 67-deg roll angle and for a vertical attitude which was only gradually approached after steering occurred at about 124 sec before touchdown. The predictions appear to be only about 2 to 3 db higher than the actual data for the three velocity beams. This compares quite favorably with the AMR data (described above), which was also about 2 db lower than predicted. The data of *Surveyor III* correlates with the data of *Surveyor I* even better than with the predicted values. Considerable care must be exercised in interpretation of points near gain switching because sampling of gain state is done less often than sampling of reflectivity and because telemetry time constants are long enough so that data is unreliable near a gain switch.

The velocity beam trackers (Beams 1, 2, and 3) locked onto the reflected signal at about 50,000 ft slant range.
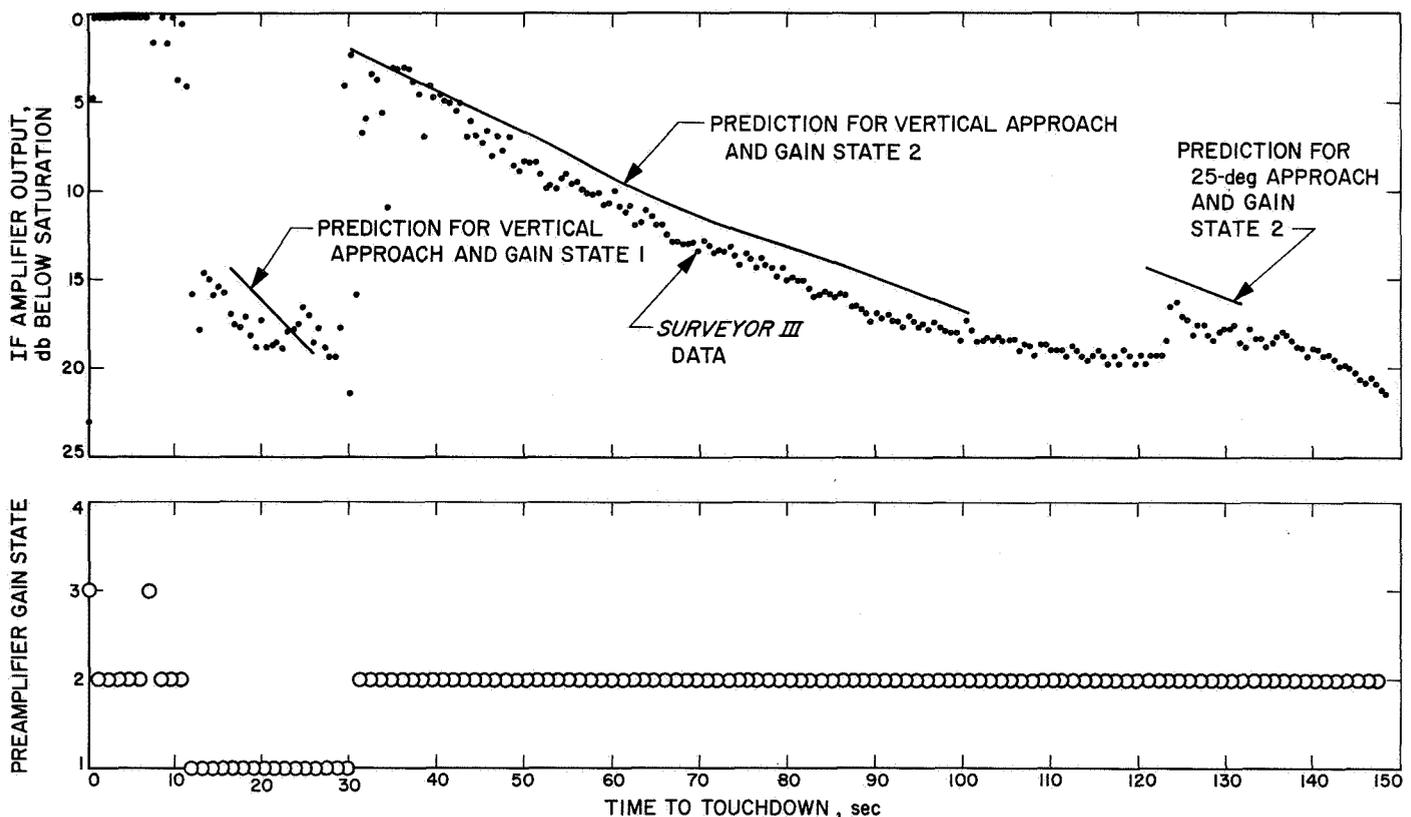


Fig. IV-46. Reflectivity of RADVS Velocity Beam 2 during descent
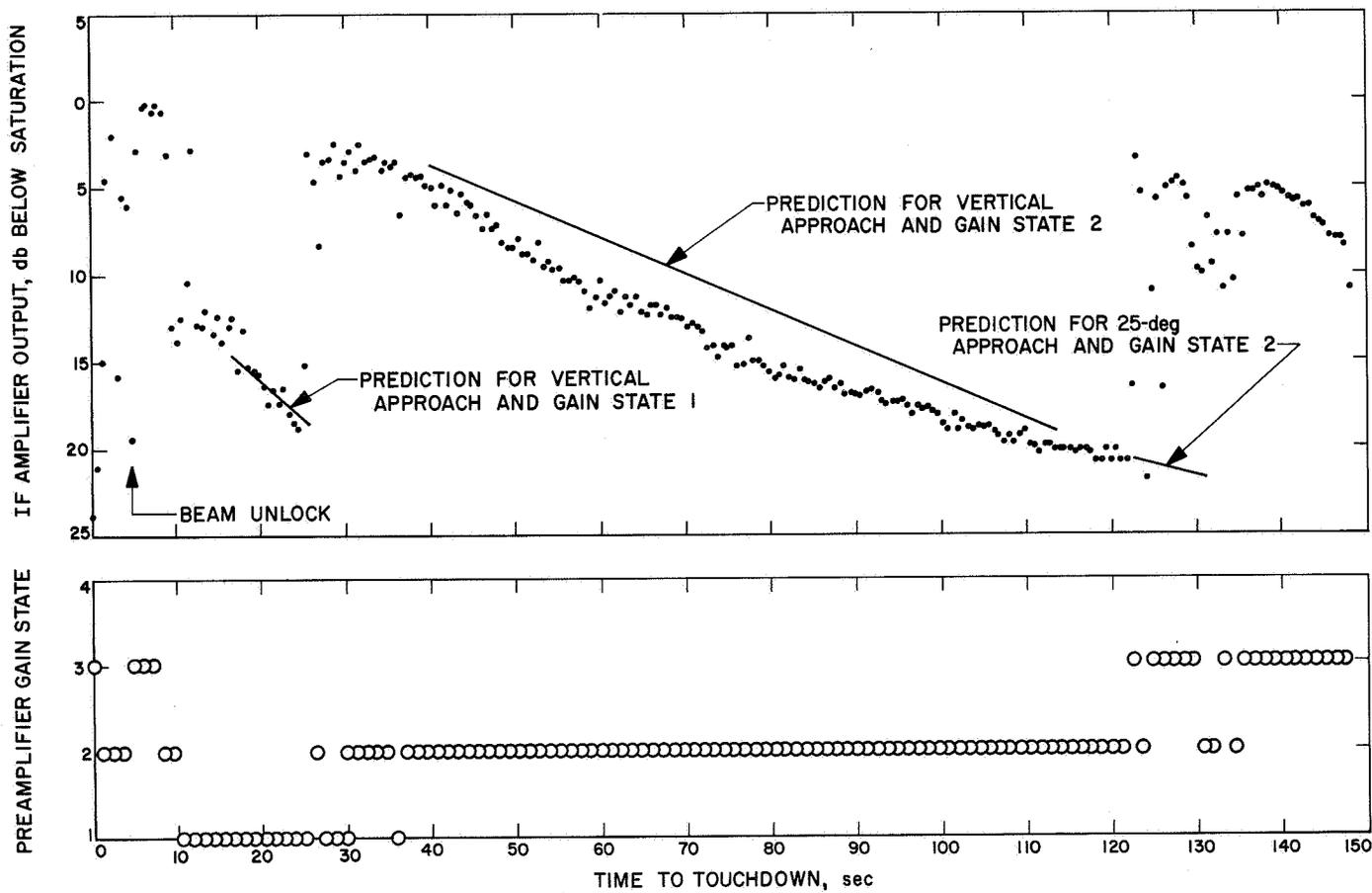
Fig. IV-47. Reflectivity of RADVS Velocity Beam 3 during descent
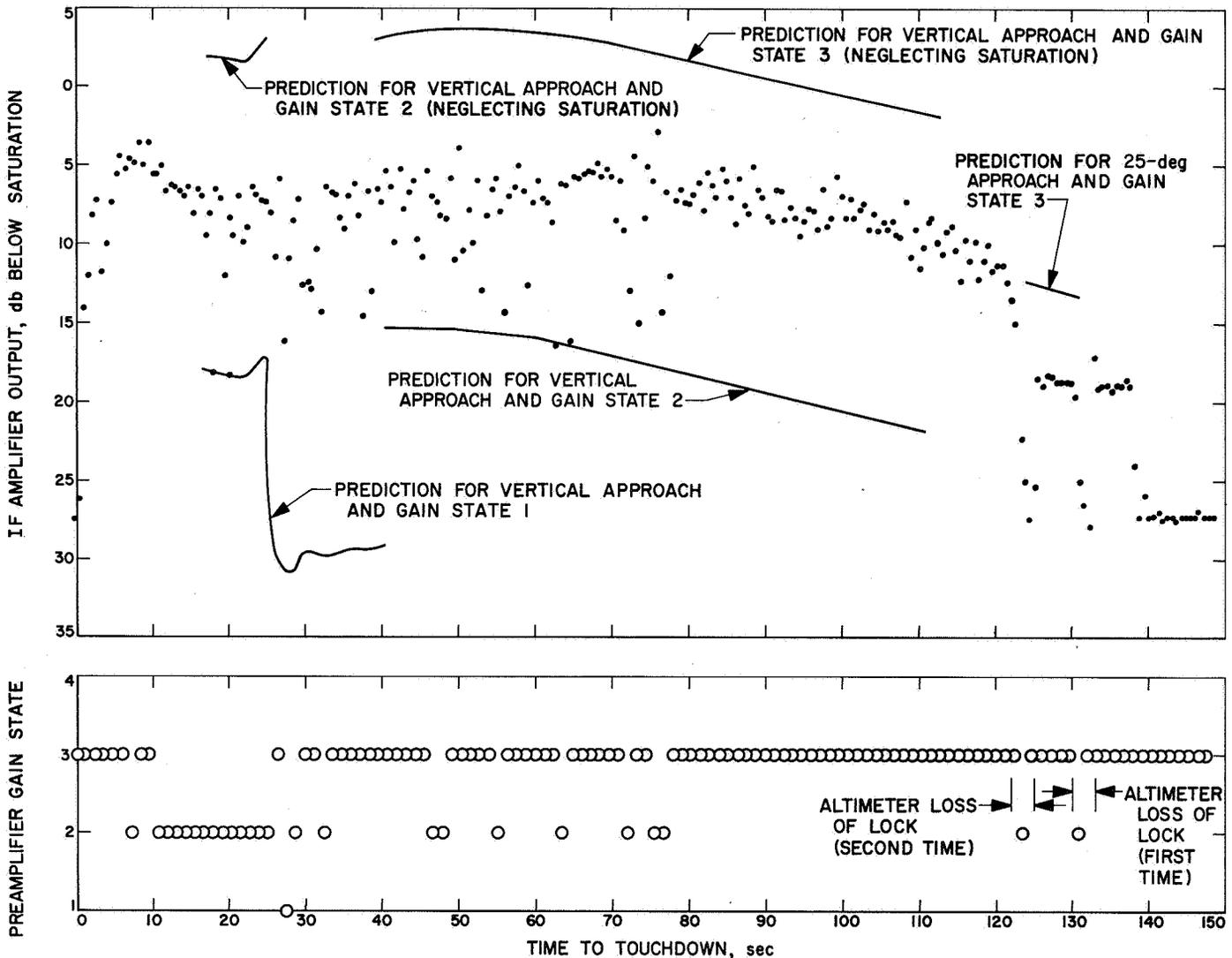
Fig. IV-48. Reflectivity of RADVS Velocity Beam 4 during descent

The altimeter tracker locked on at a slant range of 39,500 ft. Altimeter lock was lost 4.8 sec later during retro tail-off, which may have caused the break lock. The signal was reacquired in one sweep but was lost again 5 sec later. The second unlock occurred just after retro ejection, and probably was caused by the retro case passing through the beam. On the *Surveyor I* mission,

Beam 3 was broken at about the same time after retro ejection. Both break locks occurred when the return signal level was high (Fig. IV-48), indicating a close target. The altimeter will not lock onto a receding target.

Figures IV-49 through IV-51 are plots of the velocity components along each of the three spacecraft axes
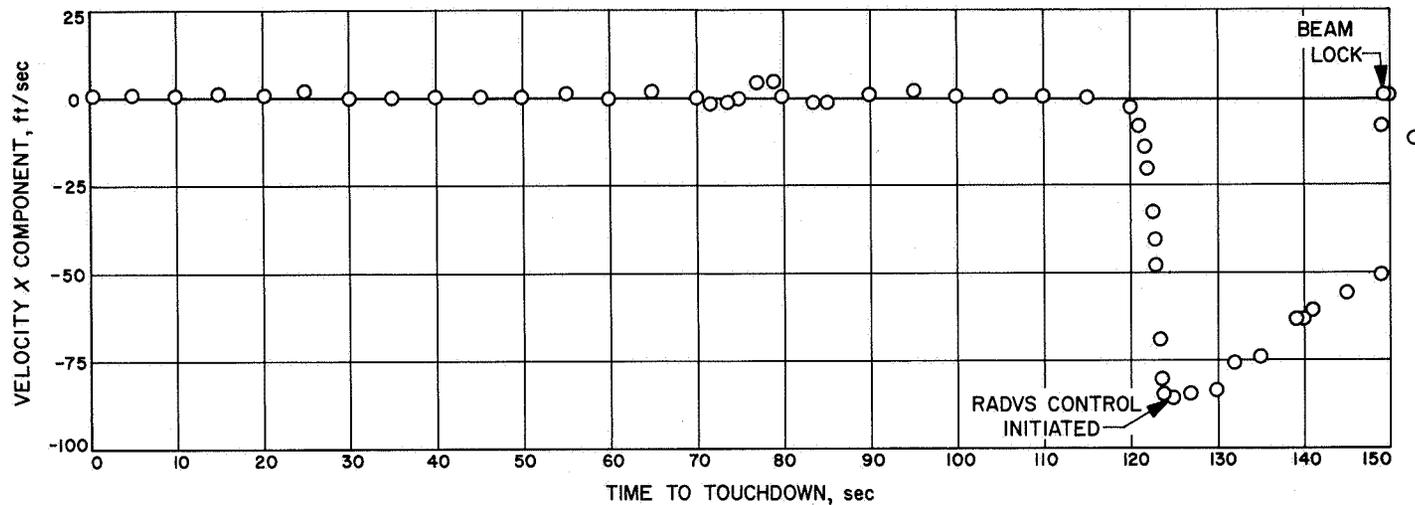


Fig. IV-49. X-component of velocity during descent
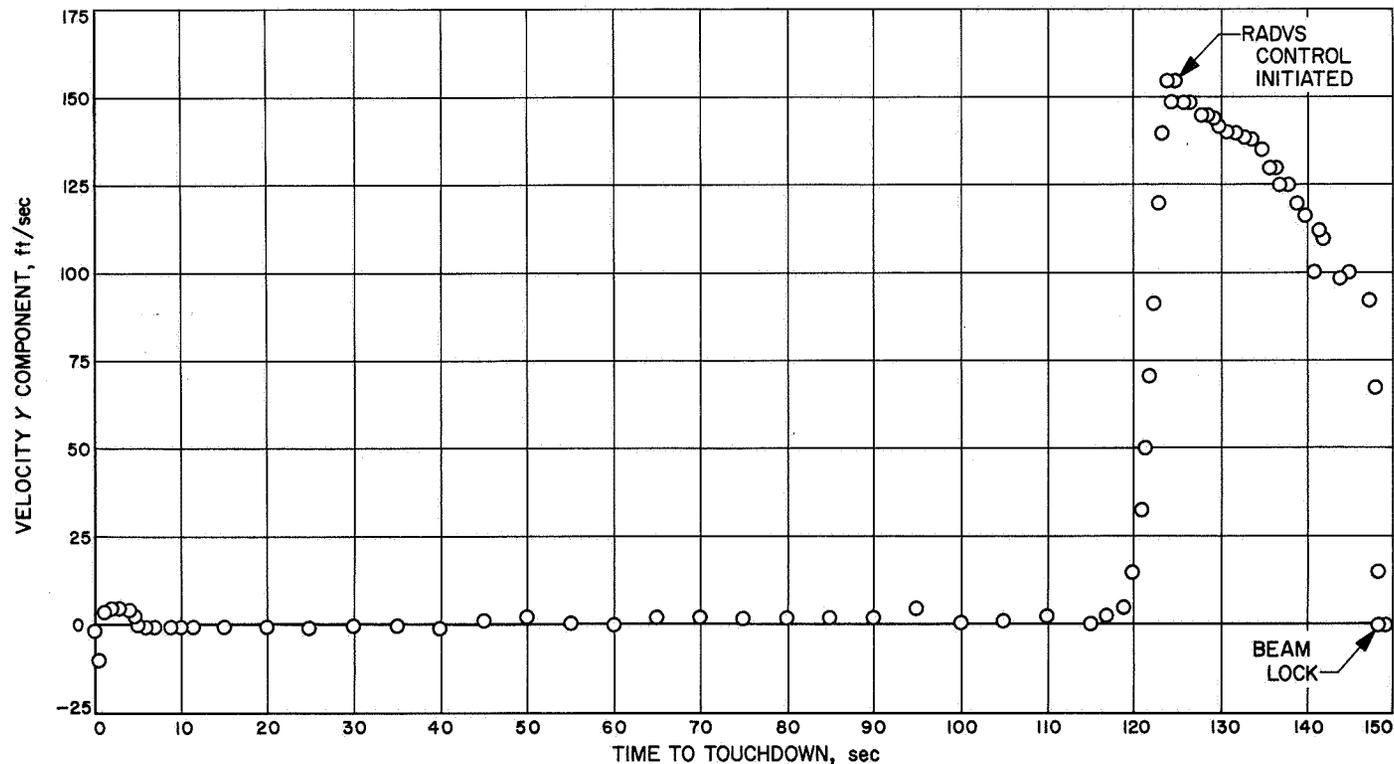


Fig. IV-50. Y-component of velocity during descent
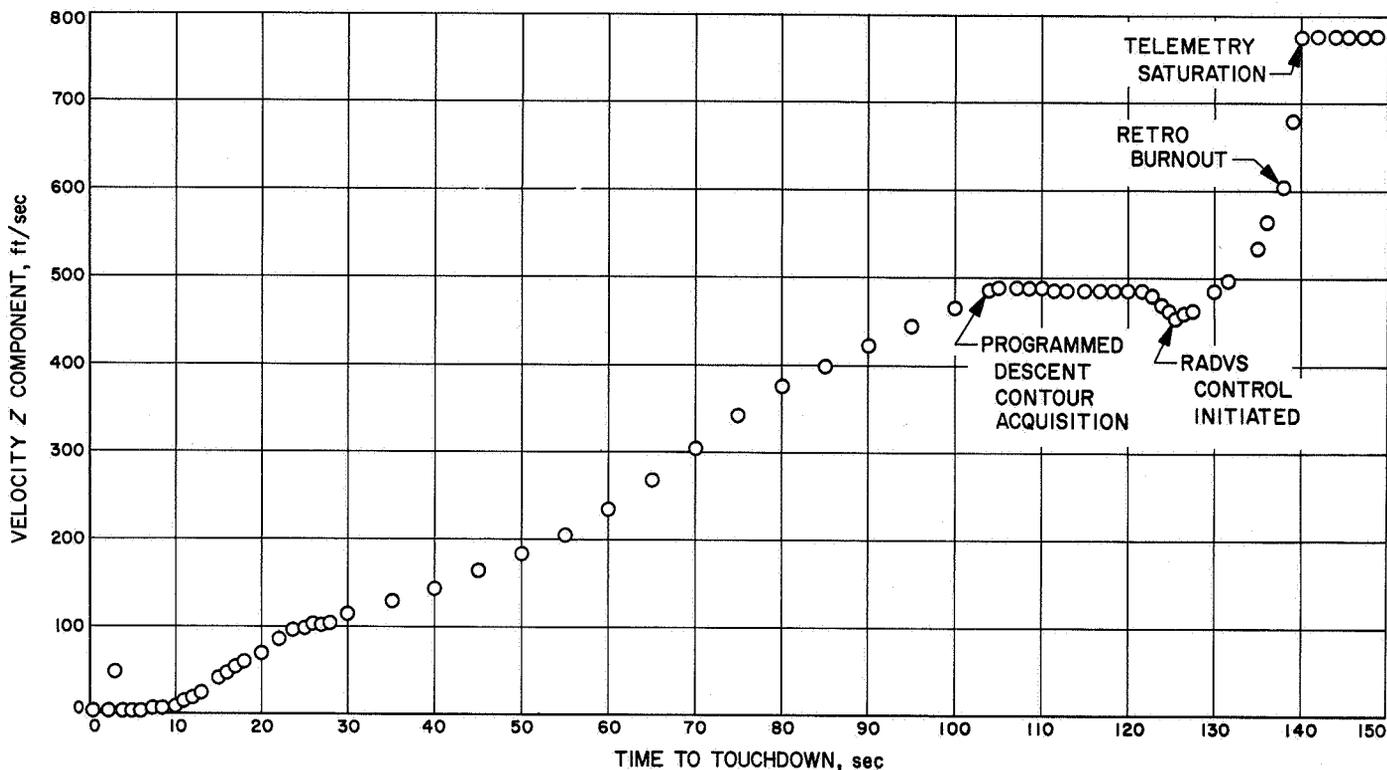
**Fig. IV-51. Z-component of velocity during descent**

during terminal descent. As can be seen, the X-velocity increased to about 85 ft/sec before RADVS control, after which it was removed in about 5 sec. Similarly, the Y-velocity increased to about 100 ft/sec and required about 10 sec to remove. The Z component was controlled to achieve descent segment acquisition in approximately 22 sec (see also Fig. IV-6). Figure IV-52 provides a plot of the Z-component of velocity in an expanded scale at low altitudes. Figure IV-53 is a plot of range vs time during final approach. (Refer to Figs. IV-40 and IV-41 for a higher altitude curve.) The "stair step" appearance of the data shown in Fig. IV-53 reflects the fact that the combined resolution of the telemetry and radar systems is 3 to 4 ft.

About 5 sec before touchdown, at an altitude of about 37 ft, Velocity Beam 3 lost lock and did not relock because the low spacecraft velocity of approximately 5 ft/sec was outside the sweep range. Before loss of lock, Beams 1 and 2 were in saturation and Beam 3 was near saturation, as expected. Loss of lock occurred when Beam 3 showed a drop to 19 db below saturation, even though this signal level was well above tracker threshold. Since the beam diameter at 37 ft range is a little over 3 ft, a surface area of about this size with an adverse slope might have caused the signal to fade. Although the exact

cause of Beam 3 fade cannot be determined, the loss of lock can be explained on the basis of the RADVS cross-coupled sidelobe logic.* For the spacecraft vertical velocity and gain status which existed (Beam 3 in gain state 3, and Beam 2 in gain state 2), if Beam 3 is more than 5 db weaker than Beam 2, break lock will be forced by the logic. Break lock will occur at the 5-db difference, although the sidelobe logic criterion is 25 db difference, because of a 20-db roll-off difference between the two gain states. The altimeter continued to operate satisfactorily down to the lunar surface. However, the altitude information could not be used by flight control below 37 ft because the Z-compartment derived from Beams 1 and 3 is subtracted from the altimeter channel to give a true altitude. Since Beam 3 lost lock, RORA (reliable

---

*To ensure against loss of lock on future missions, the cross-coupled sidelobe logic will be disabled below 1000 ft. The isolation between beam cross coupling will also be increased by utilization of the *Conditional Reliable Operate Doppler Velocity Sensor* (CRODVS) down to 1000 ft altitude which will facilitate landings at increased approach angles. On the *Surveyor III* mission, CRODVS was disabled 1 sec after the three velocity trackers had achieved lock. If CRODVS is inhibited, the spacecraft switches to inertial attitude hold when beam lock is lost. Availability of CRODVS to 1000 ft altitude will allow spacecraft maneuvering to reacquire lock, thus assuring greater probability of maintaining the programmed descent profile.
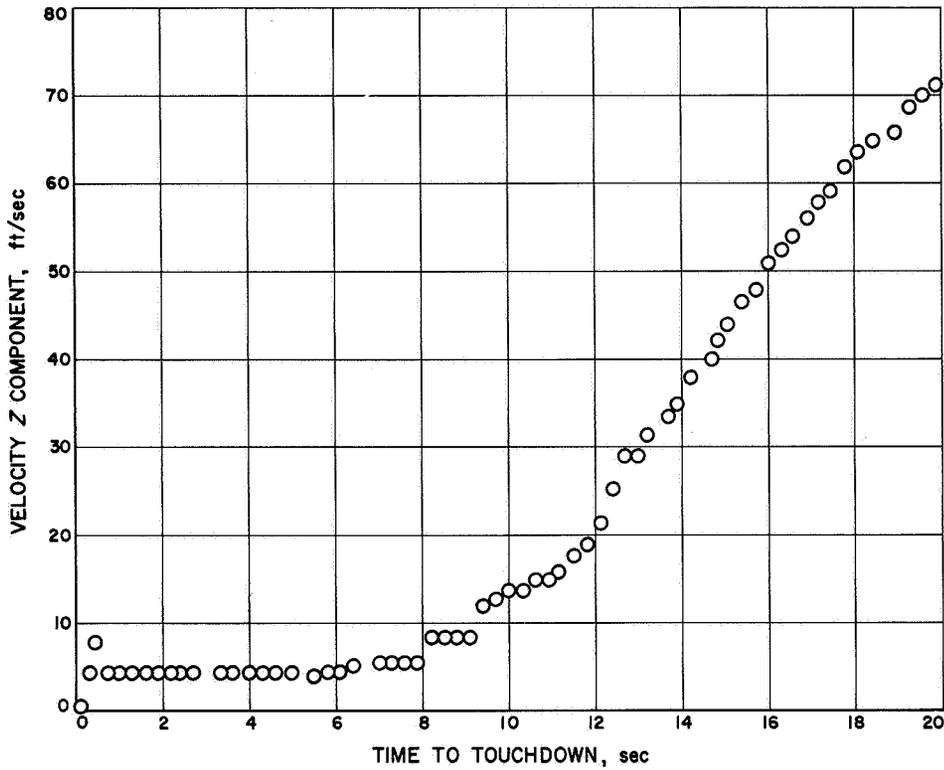
Fig. IV-52. Z-component of velocity during final descent



Fig. IV-53. Range vs time during final descent
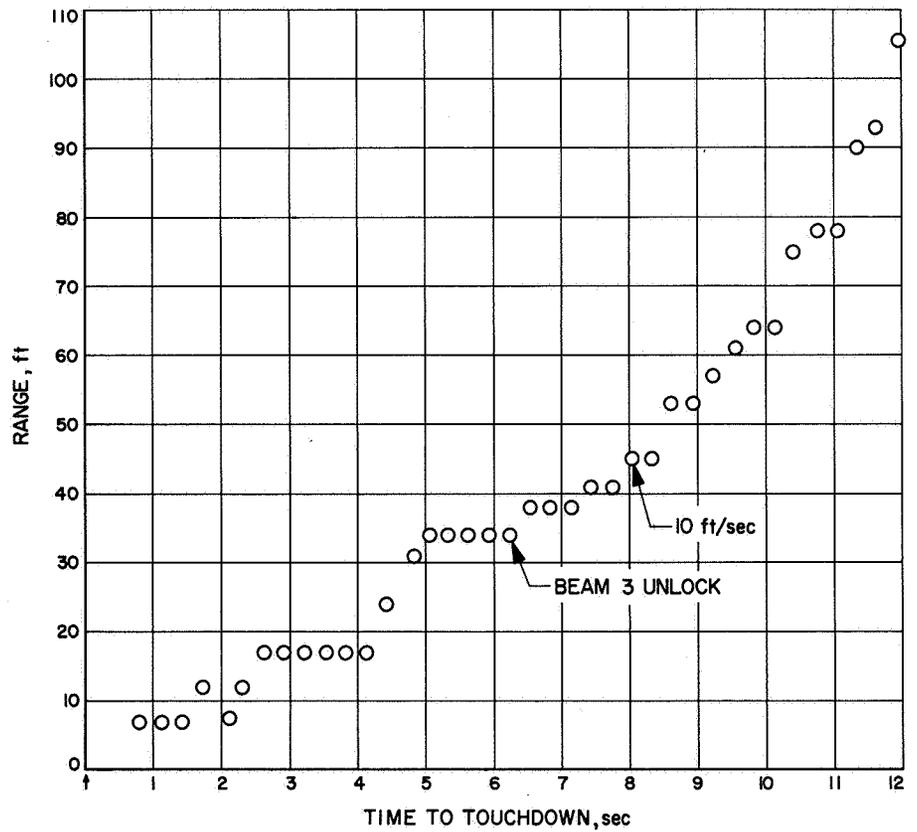
operate radar altimeter) was inhibited, and a 14-ft *mark* was not generated to turn off the vernier engines. Some 45 sec later, however, when the spacecraft was at rest on the lunar surface, the 14-ft *mark* was generated owing to noise.

As was the case on *Surveyor I*, fluctuation of Altitude Beam 4 reflectivity was much more pronounced than the data for the velocity beams. This was particularly true at lower altitudes where the spacecraft attitude was near vertical and was due to the spectral nature of the beam. Beam 4 data is quite difficult to evaluate in terms of the predictions because considerable gain switching occurred. However, at two points, about 90 sec and 20 sec before touchdown, rough comparisons can be made because the gain state was steady and the spacecraft was in a near-vertical attitude. At these points and before steering (25-deg attitude), the returned signals are about 6 to 9 db below predictions.

Coincident with the first and second touchdown, the klystron power supply modulator (KPSM) high voltage turned off as shown in Fig. IV-10, causing the velocity klystron to be inoperative. Off cycles of 18 sec occurred as controlled by a timer that allows for filament warmup before application of anode voltage. Two theories have been advanced to explain this anomaly.

The first theory considers that the ionized vernier exhaust plume may have entered the KPSM through cooling holes at touchdown because the verniers were still burning. The critical pressure may have been reached, causing an arc. Once an arc occurs, a path is usually set up that will allow other arcs to occur. Possibly KPSM arcing also has been suspected as the cause of the telemetry anomaly, which first occurred coincident with the second touchdown. It is conceivable that the KPSM high voltage may have been carried to the signal processing system if arcing also occurred to the KPSM temperature lead. However, this theory does not explain why telemetry degradation did not occur first at the initial touchdown.

The other theory considers that a momentary interruption may have occurred in the 22-Vdc input to the KPSM. A drop to 16.5 V for a 3-msec period could cause high-voltage turnoff. Such a drop in voltage may have occurred because of a bad connection.

The *Surveyor III* KPSM temperature was within the expected range and within 15°F of the temperature on *Surveyor I*. This difference can be attributed to differences in heat transfer properties between the klystrons and their heat sinks.

## H. Telecommunications

The *Surveyor* telecommunications subsystem contains radio, signal processing, and command decoding equipment to provide (1) a method of telemetering information to the earth, (2) the capability of receiving and processing commands to the spacecraft, and (3) angle-tracking one- or two-way doppler for orbit determination.

### 1. Radio Subsystem

The radio subsystem utilized on the *Surveyor* spacecraft is shown schematically in Fig. IV-54. Dual receivers, transmitters, and antennas were originally meant to provide redundancy for added reliability. As presently mechanized, this is not completely true owing to switching limitations. Each receiver is permanently connected to its corresponding antenna and transmitter. The transmitters, which are capable of operation in two different power modes (100-MW low power, and 10-W high power), can each be commanded to transmit through any of the three antennas. The *Surveyor* radio system operates at S-band, 2295-MHz down-link, and 2113-MHz up-link.

*a. Receivers.* Both receivers are identical, crystal-controlled, double-conversion units, which operate continuously as they cannot be commanded off. Each unit is capable of operation in an automatic frequency control (AFC) mode, or an automatic phase control (APC) mode. The receivers provide two necessary spacecraft functions: the detection and processing of commands from the ground stations for spacecraft control (AFC and APC modes), and the phase-coherent spacecraft-to-earth signal required for doppler tracking (APC mode).

*b. Transmitters.* Transmitters A and B are identical units which provide the spacecraft-to-earth link for telemetry and doppler tracking information. The transmitters are commanded on, one at a time, from the ground stations. Each unit contains two crystal-controlled oscillators, wideband for TV and scientific information, narrowband for engineering data. Either unit can be commanded on at will, and, in addition, can operate from the receiver voltage-controlled oscillator (transponder mode) when coherent signals are required for two-way doppler tracking. The transmitters may be commanded to operate through any one of the spacecraft antennas as desired, and both are capable of providing either 100 MW or 10 W of output power.

*c. Transponders.* Two identical transponder interconnections permit each transmitter to be operated, on command, in a transponder mode. In the transponder
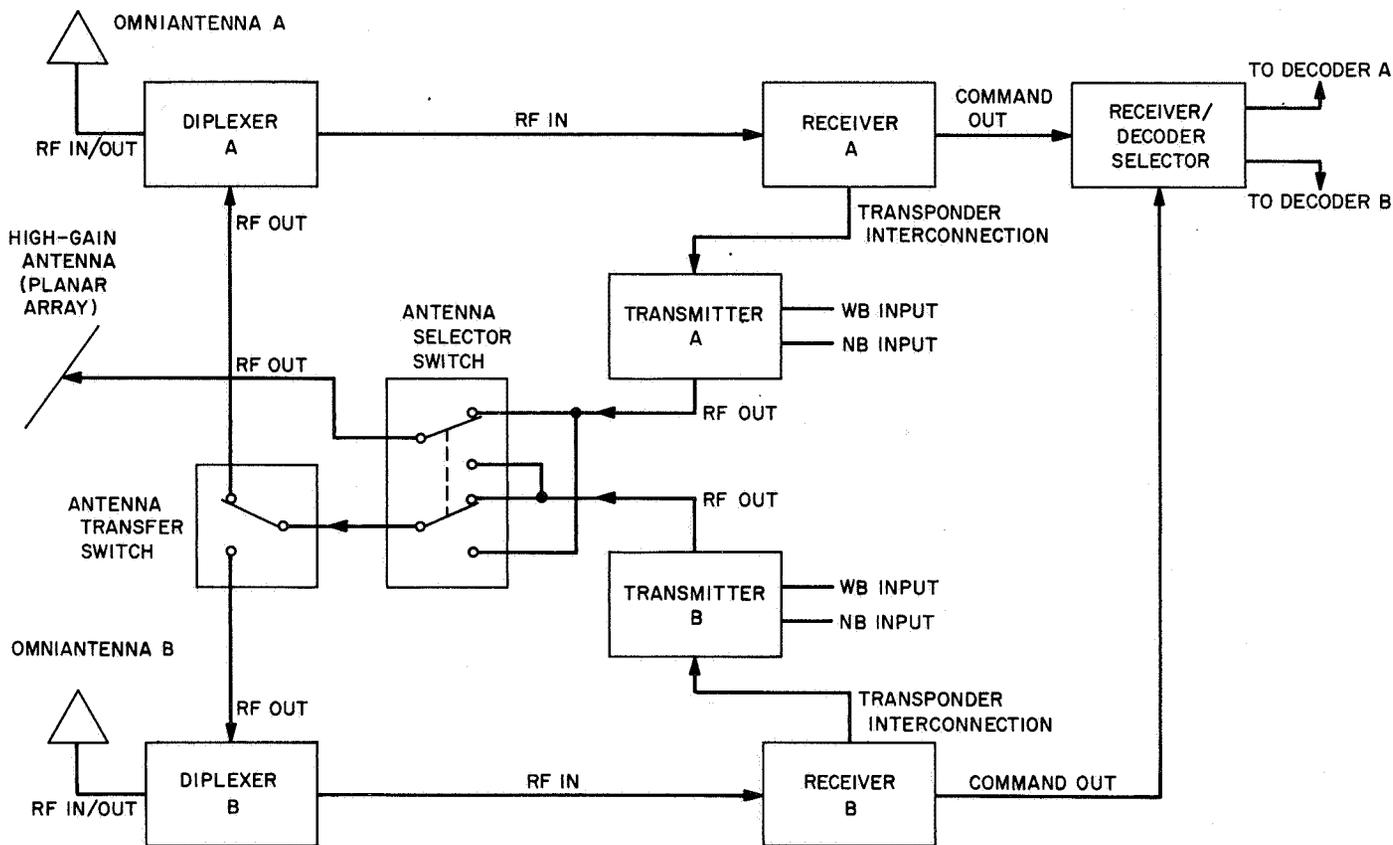
Fig. IV-54. Radio subsystem block diagram

mode, a transmitter is operated with the corresponding receiver voltage-controlled oscillator to provide coherent signals when two-way doppler tracking data is required.

*d. Antennas.* Three antennas are utilized on the *Surveyor* spacecraft. Two antennas are omnidirectional units which provide receive-transmit capability for the spacecraft. The third antenna is a high-gain, 27-db directional planar array used for transmission only of wideband information.

*e. Radio subsystem performance.* The radio system performed well during the *Surveyor III* mission and satisfied the mission requirements. Signal locks appeared to be a little below predictions but within acceptable limits. The transmitter went to high power upon command from the *Centaur* shortly before spacecraft separation and operated in high power for about 30 min before being commanded to low power. The spacecraft was acquired by DSS 42, Canberra, about 50 min after launch with little difficulty.

One discrepancy existed in the DSIF measurement of RF carrier sideband energy which indicates the space-

craft transmitter modulation index. The measurements of both DSS 51 and DSS 42 indicated a spacecraft problem. Different subcarrier oscillators (SCO's) were selected to drive the spacecraft transmitter modulator, with each SCO producing similar results. After changing SCO's, the A/D converter was turned off, and the sideband energy then indicated the proper modulation index. The test results lead to the conclusion that the spacecraft was not in error, and the discrepancy was apparently caused by the DSIF method of measuring sideband carrier power.

No attempt was made to acquire Canopus until about 9 hours after launch. During the Canopus roll, the down-link RF signal strength (Transmitter B/Omniantenna B) varied about 27 db. The Omniantenna B down-link antenna gain pattern obtained from the Canopus roll did not exactly follow the pattern measured on the antenna range, but its general contour was the same, with peaks and nulls deviating from the predicted by as much as 6 db. The maximum deviation of Omniantenna B up-link predicted and measured signal strength was about 6 db, and the deviations occurred at the same time during the roll maneuver. The maximum variation of the signal strength for the up-link was about 21 db for the 360-deg

roll. The Omniantenna B up-link signal exhibited differences between predicted and measured antenna patterns similar to the Omniantenna B down-link signals.

Omniantenna A up-link patterns displayed greater gross deviations in predicted and measured gain characteristics than Omniantenna B patterns. For a region of about 120 deg, the measured antenna gain was down an average amount of about 3 db. The peaks and nulls did not exactly correspond to the predicted throughout the roll maneuver, although the general pattern was similar except for the 120-deg region mentioned earlier. The maximum deviation of the predicted and measured signal was about 7 db. The signal strength varied about 21 db during the 360-deg roll.

The basic configuration of the *Surveyor III* spacecraft was similar to the model used on the JPL antenna range to obtain antenna patterns, except that *Surveyor III* had a soil mechanics/surface sampler (SM/SS) in place of the approach TV camera. The substitution of the SM/SS should have affected the Omniantenna B antenna pattern more than the Omniantenna A pattern because of its physical location. Therefore the presence of the SM/SS does not explain why the Omniantenna A measured pattern differed from the predicted pattern by more than the Omniantenna B pattern.

Results of the Canopus roll as obtained from antenna patterns indicated that the spacecraft was a little more than 20 deg in roll angle position from its estimated orientation prior to Canopus search. The discrepancy is attributed to the fact that the *Centaur* stage is not roll-position-stabilized. The spacecraft orientation was accurately determined by the roll maneuver, however, and Canopus lock was obtained.

Receiver A/Omniantenna A performance is plotted in Fig. IV-55. Receiver A received signal strength is shown to be above predicted levels prior to Canopus lock and typically 4 to 5 db below predicted levels after Canopus lock. At some points after Canopus lock, the signal level, as determined from receiver AGC, was below predicted by as much as 10 db. The large variations in received signal level are believed to be the result of the fact that Omniantenna A was operating in a region where the antenna gain changed 5 or 6 db over a few degrees of roll. Small variation in spacecraft orientation during normal operation and especially during gyro drift checks produced the large signal level changes.

Receiver B/Omniantenna B antenna gain is shown in Fig. IV-56. The gain was below predicted by about 5 db

before Canopus lock. After Canopus lock, the antenna gain was typically 2 or 3 db below predicted but down by as much as 6 db from predicted levels at times. The Canopus roll maneuver indicated that Omniantenna B antenna gain was about 2 db below predicted gain at Canopus lock, which could explain why the measured signal at Receiver B was typically down by about 2 db from predicted values. In general, the largest deviations between predicted and measured signal strength occurred during gyro drift tests. A step in signal strength occurred at the termination of each gyro drift test, when the spacecraft was returned to Canopus lock.

As shown in Fig. IV-57, the measured down-link power followed the predicted signal strength closer than the up-link power did. Typically, it was within 2 db of its predicted value, with the greatest variation occurring during gyro drift tests. Bit rates and bit rate thresholds are also shown in the figure.

The RF frequency during the flight was within its specified limits, and no problems in transmitting commands were experienced. In transferring from narrow-band (NB) engineering data to wide-band (WB) television data it was noted that it was not necessary to retune the ground receiver in order to receive good pictures. This shows the closeness of the NB and WB center frequencies.

During terminal descent the RF signal strength was good, allowing the spacecraft to transmit strain gage information and transmit at the 1100-bit/sec data rate. The signal level was steady to within about 2 db during the terminal descent.

After touchdown, a signal processing problem developed. The modulation capability of the transmitter was questioned, but further investigation proved that the RF portion of the spacecraft was functioning normally.

## 2. Signal Processing Subsystem

The *Surveyor* signal processing subsystem accepts, encodes, and prepares for transmission voltages, currents and resistance changes corresponding to various spacecraft parameters such as events, voltages, temperatures, accelerations, etc.

The signal processor employs both pulse code modulation and amplitude-to-frequency modulation telemetry techniques to encode spacecraft signals for frequency- or phase-modulating the spacecraft transmitters and for
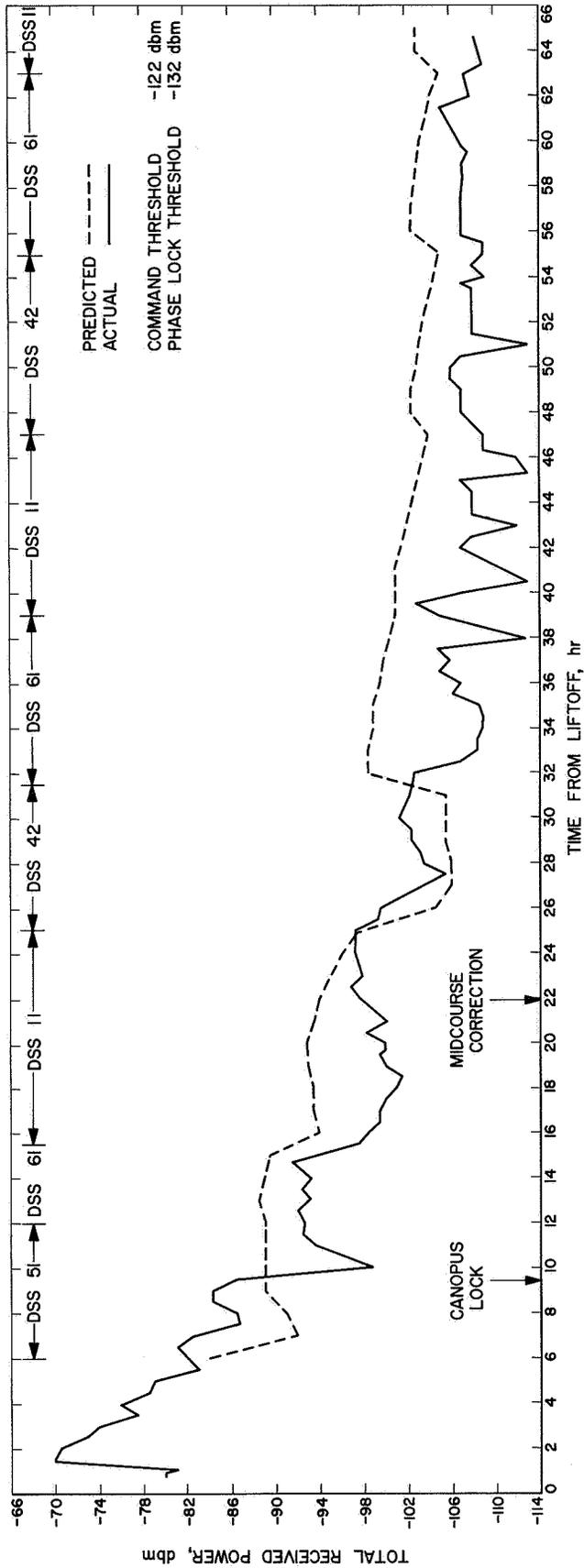
Fig. IV-55. Receiver A/Omniantenna A total received power during transit
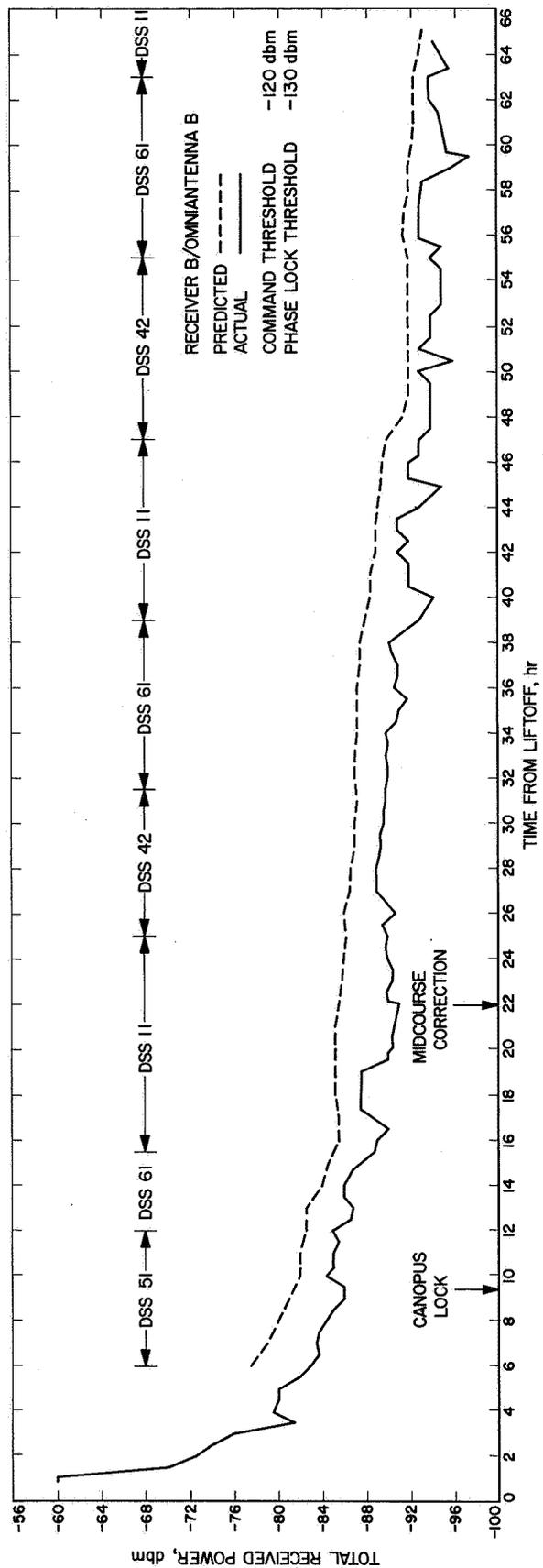


Fig. IV-56. Receiver B/Omniantenna B total received power during transit
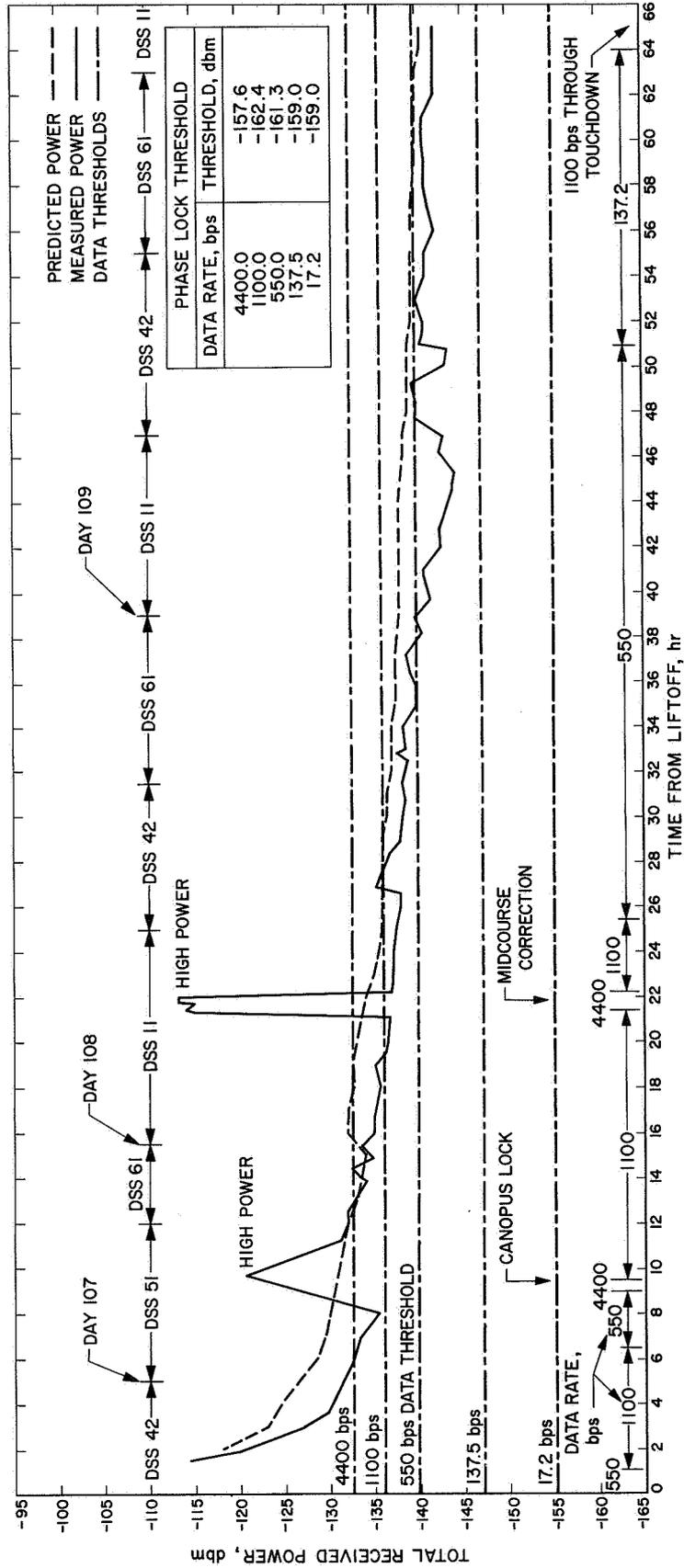
Fig. IV-57. DSIF received power during transit

recovery of these signals by the ground telemetry equipment. A simplified block diagram of the signal processor is shown in Fig. IV-58.

The input signals to the signal processor are derived from various voltage or current pickoff points within the other subsystems as well as from standard telemetry transducing devices such as strain gages, accelerometers, temperature transducers, and pressure transducers. These signals generally are conditioned to standard ranges by the originating subsystem so that a minimum amount of signal conditioning is required by the signal processor.

As illustrated in Fig. IV-58, some of the signal inputs are commutated to the input of the analog-to-digital converter (ADC) while others are applied directly to subcarrier oscillators. The measurements applied directly are accelerometer and strain gage measurements which require continuous monitoring over the short intervals in which they are active.

The commutators apply the majority of telemetry input signals to the ADC, where they are converted to a digital word. Binary measurements such as switch closures or contents of a digital register already exist in digital form and are therefore routed around the ADC. In these cases, the commutator supplies an inhibit signal to the ADC and, by sampling, assembles the digital input information into 10-bit digital words. The commutators are comprised of transistor switches and logic circuits which select the

sequence and number of switch closures. There are six engineering commutator configurations (or modes) used to satisfy the telemetry requirements for the different phases of the mission and one TV commutator configuration located in the TV auxiliary. The content of the telemetry modes is presented in Appendix C.

The ADC generates an 11-bit digital word for each input signal applied to it. Ten bits of the word describe the voltage level of the input signal, and the eleventh bit position is used to introduce a bit for parity checking by the ground telemetry equipment. The ADC also supplies commutator advance signals to the commutators at one of five different rates. These rates enable the signal processor to supply telemetry information at 4400, 1100, 550, 137.5, and 17.2 bit/sec. The bit rates and commutator modes are changed by ground commands.

The subcarrier oscillators are voltage-controlled oscillators used to provide frequency multiplexing of the telemetry information. This technique is used to greatly increase the amount of information transmitted on the spacecraft carrier frequency.

The summing amplifiers sum the outputs of the subcarrier oscillators and apply the composite signal to the spacecraft transmitters. Two types of summing amplifiers are employed because of the transmitter's ability to transmit either a phase-modulated or a frequency-modulated signal.
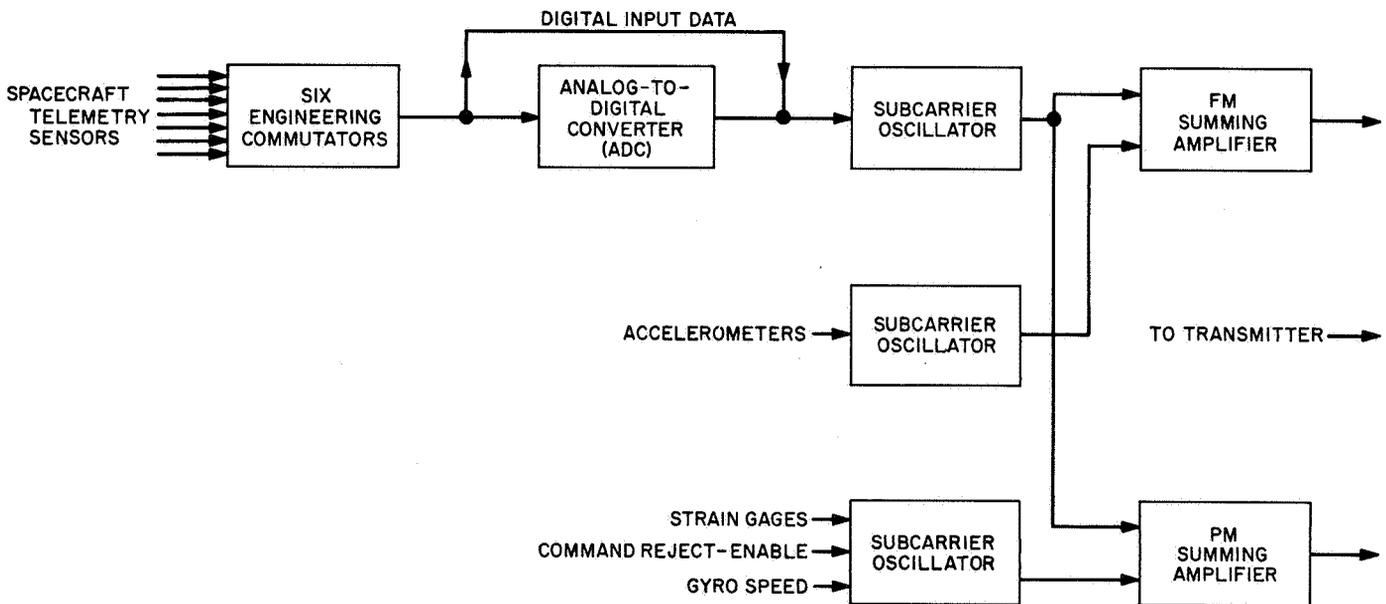


Fig. IV-58. Simplified signal processing functional block diagram

The signal processing subsystem employs a high degree of redundancy to insure against loss of vital spacecraft data. Two ADC's, two independent commutators—the engineering signal processor (ESP) and auxiliary engineering signal processor (AESP)—and a wide selection of bit rates (each with the ADC driving a different subcarrier oscillator) provide a high reliability of the signal processing subsystem in performing its function.

From launch to the first touchdown, 167 commands effecting changes in the signal processor were received and properly executed by the signal processor. Table IV-17 shows representative prelaunch and in-flight values of the telemetered signal processing parameters.

Coincident with the second touchdown, the signal processing subsystem began exhibiting anomalous behavior. Shortly after the anomaly appeared, several attempts were made to discover the trouble source. The other ADC was turned on; another bit rate was selected; RADVS was commanded off several times; flight control power was commanded off; the touchdown and propulsion strain-gage data channels were commanded off; and the AESP was turned off. The ESP was turned on and several bit rates were attempted, including low bit rates and various modes. When these attempts failed to reveal the source of the trouble, it was postulated that part

### Table IV-17. Typical signal processing parameter values

| Parameter | Prelaunch | Flight |
|---|---|---|
| ESP reference volts (Mode 2), V | 4.877 | 4.868 |
| ESP reference return (Mode 4), V | 4.892 | 4.882 |
| ESP reference return, V | 0.000 | 0.000 |
| ESP unbalance current (Mode 2), $\mu$A | −3.39 | −3.39 |
| ESP unbalance current (Mode 4), $\mu$A | −2.22 | −2.03 |
| ESP full-scale current calibration, % error from nominal | 0.46 | 0.55 |
| ESP mid-scale current calibration, % error from nominal | 0.51 | 0.61 |
| ESP zero-scale current calibration, % error from nominal | 0.46 | 0.56 |
| AESP full-scale current calibration, % error from nominal | 0.09 | 0.29 |
| AESP mid-scale current calibration, % error from nominal | 0.36 | 0.33 |
| AESP zero-scale current calibration, % error from nominal | 0.60 | 0.89 |
| AESP unbalance current, $\mu$A | −1.01 | −1.01 |

of the TV master switch had malfunctioned, since the TV data was good. This would have loaded the ESP and the AESP with a maximum of 125 kilohms. It was further theorized that by commanding the SM/SS on, the TV master switch would be inhibited even if it was in a failed condition. This was attempted and proved to be the wrong conclusion.

It was later discovered that all the digital words were reading correctly at all bit rates, and at 17.2 bit/sec some of the analog channels were reading near their expected values. This was sufficient to enable the mission to proceed.

The investigation of the signal processor damage has been limited to attempting to isolate the trouble source by the characteristics of the degraded telemetry. Attempts to determine the time constant affecting the telemetry have been unsuccessful in providing a narrow range. Time constants ranging from 60 to 1000 msec have been computed from various portions of the data.

The theory that the AESP and ESP commutator return and the ADC comparison voltage supply return were at different potentials was explored to some extent. This hypothesis was advanced because of the nonzero reading on the ESP reference return measurement at the higher bit rates. This theory was discarded because two wires provide redundant returns from the ESP and AESP to the ADC reference supply. Furthermore, this failure mode does not account for the many good readings at the 17.2-bit/sec rate.

The failure mode which most fits the characteristics of the data is a shorted commutator switch. This failure mode can be either a single channel failure or multiple channel failures. In the single channel failure, a measurement which is sampled in the AESP and the ESP must have both the ESP switch and the AESP switch partially shorted.

The resistive load on the ADC input has been computed, from data, to be approximately 10 kilohms when the AESP is being used, and approximately 20 kilohms when the ESP is used. The constraints on the inputs to both the ESP and AESP require a normal range of 0.0 to 5.0 V and never exceeding 10 V. An input of 12 V will produce a nondestructive malfunction by causing the sampling switch to turn on without signal processor control. An input of 30 V or higher will produce a nonreversible, component-level, destructive malfunction.

This, in effect, causes that particular sampling switch, and possibly others, to short with an impedance of 0 ohms to 10 kilohms, and with either linear or nonlinear characteristics.

The destructive malfunction is what appears to have happened at the time of the second touchdown. This failure mode was well known prior to the *Surveyor III* mission. The effect is to parallel the source impedance of the shorted channels with any channel the processor is attempting to sample. Since the shorted channels exhibit a source which contains a capacitor, the charging and discharging of the capacitor will affect all samples based on the several previous samples and on the source impedance of the channel being commutated. At the very low bit rate, this capacitor is, in general, given time to discharge or charge to the current sample value, thereby allowing some of the channels to reach a correctable, steady state value before being digitized for transmission. When the capacitive effect has thus been removed by time, the resulting data can be corrected for the resistive loading offset which also exists.

After a thorough review of the data, and the construction of a mathematical model of a portion of the commutator, the following channels are correctable at 17.2 bit/sec:

| | |
|---|---|
| Static phase error | D7, D8 |
| Receiver AGC | D9, DD |
| Receiver AFC | D16, D17 |
| Nonessential bus voltage | EP1 |
| Solar cell array voltage | EP10 |
| Unregulated bus voltage | EP2 |
| Main battery voltage | EP5 |
| Main battery manifold pressure | EP3 |
| Boost regulator preregulated voltage | EP30 |
| Nitrogen gas pressure | FC4 |
| Solar panel position | M3 |
| Polar axis position | M4 |
| Elevation axis position | M6 |
| Roll axis position | M7 |
| Landing gear deflection | V5, 6, 7 |

Correction curves have been provided for all temperature channels and, since the current channels all have a low impedance source, they are not affected by the load and are all reading correctly.

The data channels which cannot be corrected are those in which the immediately preceding word on the commutator causes the sample to be of such a value that the first decision (the most significant bit) is made incorrectly. The remaining bits in that word, then, will be incorrect.

The continuing analysis will be one of further refinement of the mathematical model of a portion of the commutator, or an expansion to a full math model of the ESP, AESP, central signal processor, and input sources. Using the full model, it may be possible to narrow the number of suspect channels to a smaller number, or even find the exact channels failed.

### 3. Command Decoding Subsystem

From liftoff to first touchdown on the moon, the *Surveyor III* mission required a total of 319 earth commands. Nine of these were quantitative commands (QC's) which provided the spacecraft with the quantitative information necessary for attitude and trajectory correction maneuvers; the other 310 were direct commands (DC's) which initiated single actions such as *extend omniantennas, AMR power on, A/D clock rate 1100 bit/ sec*, etc.

These commands were received, detected, and decoded by one of the four receiver/central command decoder (CCD) combinations possible in the *Surveyor* command subsystem. The selection of the combination is accomplished by stopping the command information from modulating the up-link radio carrier for 0.5 sec. Once the selection is made, the link must be kept locked up continuously by either sending serial command words or unaddressable command words (referred to as fill-ins) at the maximum command rate of 2 word/sec.

The command information is formed into a 24-bit Manchester-coded digital train and is transmitted in a PCM/FM/PM modulation scheme to the spacecraft. When picked up by the spacecraft omniantennas, the radio carrier wave is stripped of the command PCM information by two series FM discriminators and a Schmitt digitizer. This digital output is then decoded by the CCD for word sync, bit sync, the 5-bit address and its complement, and the 5-bit command and its complement (this latter only for DC's since the QC's contain 10 bits of information rather than 5 command bits and their complements). The CCD then compares the address with its complement and the command with its complement on a bit-by-bit basis. If the comparisons are satisfactory, the CCD then selects that one of the eight

subsystem decoders (SSD's) having the decoded address bits as its address, applies power to its command matrix, and then selects that one of the 32 matrix inputs having the decoded command bits as its address to issue a 20-msec pulse which initiates the desired single action.

Those DC commands that are irreversible or extremely critical are interlocked with a unique command word. Ten of the DC's and all of the QC's are in this special category. None of these commands can be initiated if the interlock command word is not received immediately prior to the critical command.

The QC's, besides being interlocked, are also treated somewhat differently by the command subsystem. The only differences between the DC and QC are: (1) a unique address is assigned the QC words; (2) the QC word contains 10 bits of quantitative information in place of the 5 command and 5 command complement bits. Therefore, when this unique QC address is recognized, the CCD selects the flight control sensor group (FCSG) SSD and shifts the 10 bits of quantitative information into the FCSG magnitude register. Hence, the QC quantitative bits are loaded as they are decoded.

The command decoding subsystem performed properly throughout flight and through the touchdowns. No substandard behavior was evidenced during lunar operations through spacecraft shutdown shortly after sunset.

## I. Television

The television subsystem is designed to obtain photographs of the lunar surface, lunar sky, and portions of the landed spacecraft. For the *Surveyor III* mission, the subsystem consisted of a survey camera capable of panoramic viewing and a television auxiliary for processing commands and telemetry data.

### 1. Survey Camera

The survey television camera is shown in Fig. IV-59. The camera provides images over a 360-deg panorama and from +40 deg above the plane normal to the camera Z-axis to −60 deg below this same plane. The camera Z-axis is inclined 16 deg from the spacecraft Z-axis. Each picture, or frame, is imaged through an optical system onto a vidicon image sensor whose electron beam scans a photoconductive surface, thus producing an electrical output proportional to the conductivity changes resulting from the varying reception of photons from the subject.

The camera is designed to accommodate scene luminance levels from approximately 0.008 ft-lamberts to 2600 ft-lamberts, employing both electromechanical mode changes and iris control. Camera operation is totally dependent upon reception of the proper commands from earth. Commandable operation allows each frame to be generated by shutter sequencing preceded by appropriate lens settings and mirror azimuth and elevation positioning to obtain adjacent views of the subject. Functionally, the camera provides a resolution capability of approximately 1mm at 4 meters and can focus from 1.23 meters to infinity.

Figure IV-60 depicts a functional block diagram of the survey camera and television auxiliary. Commands for the camera are processed by the telecommunications command decoder, with further processing by the television auxiliary decoder. Identification signals, in analog form, from the camera are commutated by the television auxiliary, with analog-to-digital conversion being performed within the signal processing equipment of the telecommunications subsystem. The ID data in PCM form is mixed in proper time relationship with the video signal in the TV auxiliary and subsequently sent to the telecommunications system for transmission to earth.

The survey camera contains a mirror, filters, lens, shutter, vidicon, and the attendant electronic circuitry.

The mirror assembly is comprised of a 10.5 × 15 cm elliptical mirror supported at its minor axis by trunnions. This mirror is formed by vacuum-depositing a Kanogen surface on a beryllium blank, followed by a deposition of aluminum with an overcoat of silicon monoxide. The mirrored surface is flat over the entire surface to less than ¼ wavelength at $\lambda = 550$ m$\mu$ and exhibits an average specular reflectivity in excess of 86%. The mirror is positioned by means of two drive mechanisms, one for azimuth and the other for elevation.

The mirror assembly contains three filters (red, green, and blue), in addition to a fourth section containing a clear element for nonmonochromatic observations. The filter characteristics are tailored such that the camera responses, including the spectral response of the image sensor, the lens, and the mirror match as nearly as possible the standard CIE tristimulus value curves (Fig. IV-61). Color photographs of any given lunar scene can be reproduced on earth by combining three video photographs, each made with a different monochromatic filter element in the field of view.
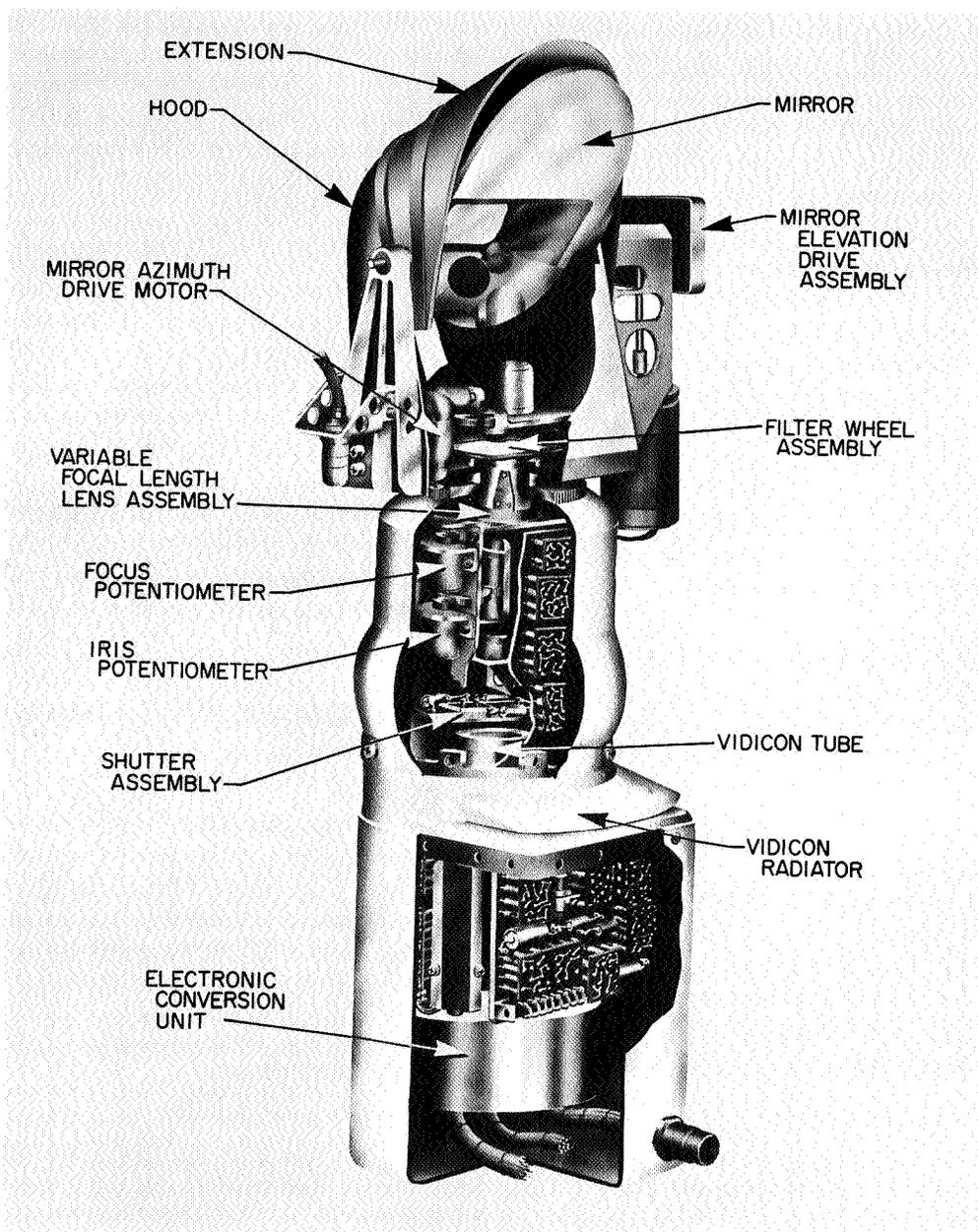
Fig. IV-59. Survey TV camera
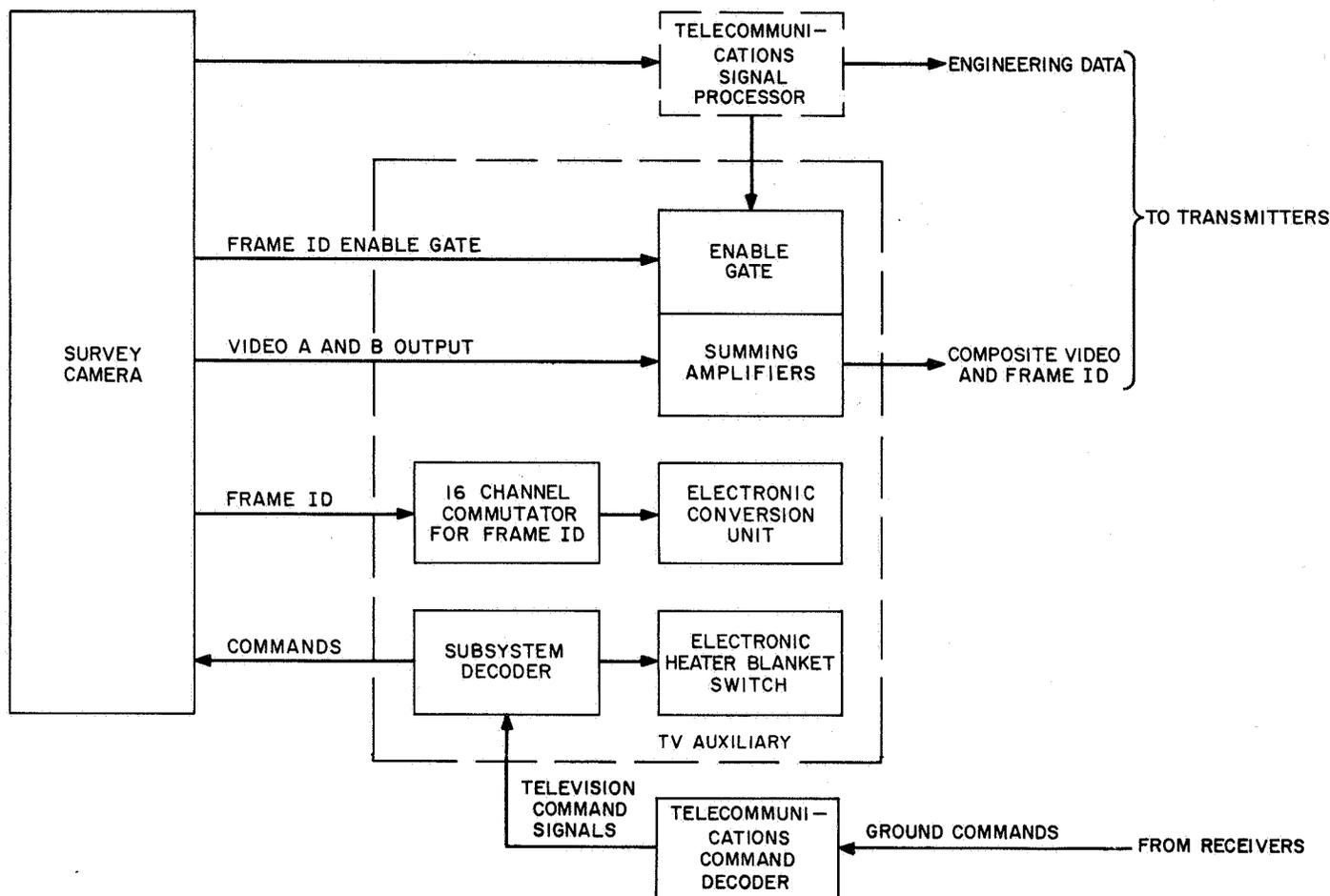
**Fig. IV-60. Simplified survey TV camera functional block diagram**

The optical formation of the image is performed by means of a variable-focal-length lens assembly placed between the vidicon image sensor and the mirror assembly. The lens is capable of providing a focal length of either 100 or 25 mm, which results in an optical field of view of approximately 6.43 or 25.3 deg, respectively. Additionally, the lens assembly may vary its focus by means of a rotating focus cell from 1.23 meters to infinity, while an adjustable iris provides effective aperture changes of from $f/4$ to $f/22$, in increments which result in an aperture area change of 0.5. While the most effective iris control is accomplished by means of command operation, a servo-type automatic iris is available to control the aperture area in proportion to the average scene luminance. As in the mirror assembly, potentiometers are geared to the iris, focal length, and focus elements to allow readout of these functions. A beam splitter, integral to the lens assembly, provides the necessary light sample (10% of incident light) for operation of the automatic iris.

Three modes of exposure control are afforded the camera by means of a mechanical focal plane shutter located between the lens assembly and the vidicon image sensor. In the *normal shutter* mode, upon earth command, the shutter blades are sequentially driven by solenoids across an aperture in the shutter base plate, thereby allowing light energy to reach the image sensor. The time interval between the initiation of each blade determines the exposure interval, nominally 150 msec.

In the second shutter mode (*open shutter* mode) the blades are positioned to leave the aperture open, thereby providing continuous light energy to the image sensor. This mode of operation is useful in the imaging of scenes exhibiting extremely low luminance levels, including star patterns.

A third exposure mode, used for stellar observations and lunar surface observation under earthshine illumination conditions, is referred to as the *integrate* mode.
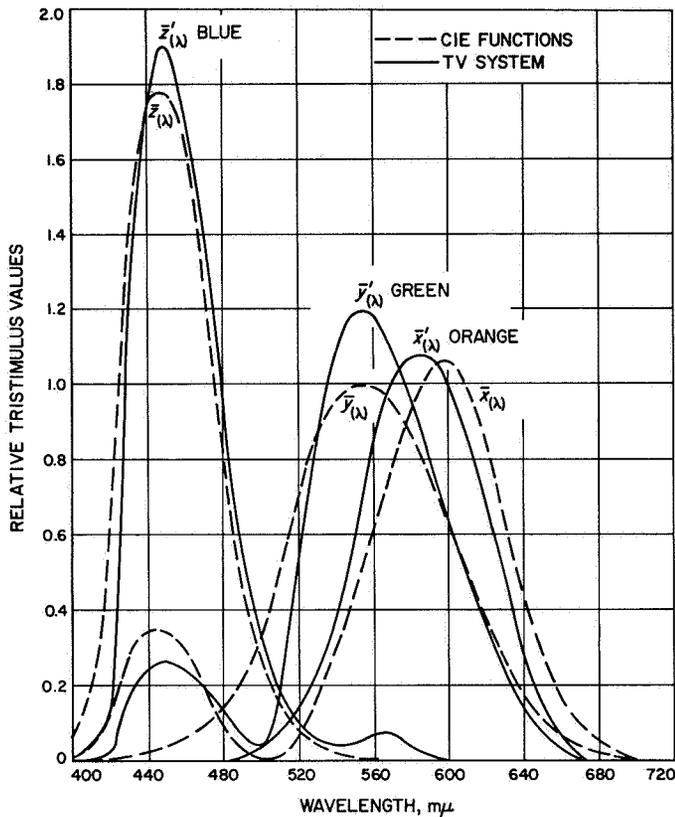
**Fig. IV-61. Relative tristimulus values of the color filter elements**

width of 1.2 kHz. This *200-line* mode is used for transmission over one of the omniantennas.

Integral to the spacecraft and within the viewing capability of the camera are two photometric/colorimetric reference charts (Fig. IV-62). These charts, one on Omniantenna B and the other adjacent to Footpad 3, are located such that the line of sight of the camera when viewing the chart is normal to the plane of the chart. Each chart is identical and contains a series of 13 gray wedges arranged circumferentially around the chart. In addition, three color wedges, whose CIE chromaticity coordinates are known, are located radially from the chart center. A series of radial lines is incorporated to provide a gross estimate of camera resolution. Finally, the chart contains a centerpost which aids in determining the solar angles after lunar landing by means of the shadow information. Prior to launch, each chart is calibrated goniophotometrically to allow an estimation of postlanding camera dynamic range and to aid photometric and colorimetric data reduction.

The survey camera incorporates heaters to maintain proper thermal control and to provide a thermal environment in which the camera components operate. The heater elements are designed to provide a sustaining operating temperature during the lunar night if energized. These consume 36 W of power when activated. A temperature of $-20°F$ must be achieved prior to camera turn-on.

This mode is implemented by turning off the vidicon electron beam, opening the shutter, and then closing it after the desired exposure time. Scene luminances on the order of 0.008 ft-lamberts are reproduced in this mode of operation, thereby permitting photographs under earthshine conditions.

The transducing process of converting light energy from the object space to an equivalent electrical signal in the image plane is accomplished by the vidicon tube. A reference mark is included in each corner of the scanned format, which provides, in the video signal, an electronic level of the scanned image.

In the normal, or *600-line* scan mode, the camera provides one frame every 3.6 sec. Each frame requires nominally 1 sec to be read from the vidicon and utilizes a bandwidth of 220 kHz, requiring transmission over the high-gain (planar array) antenna.

A second scan mode of operation provides one 200-line frame every 61.8 sec. Each 200-line frame requires 20 sec to complete the video transmission and utilizes a band-



**Fig. IV-62. TV photometric/colorimetric reference chart**

The camera used on *Surveyor III* spacecraft was fitted with a newly designed hood extension in order to reduce the possibility of direct sunlight striking the camera lens (through the filter elements). This served to reduce the cases where image glare could be caused by multiple reflections within the lens assembly.

## 2. Performance Characteristics

A premission calibration was performed on the survey camera with the camera mounted on the spacecraft. Each calibration utilized the entire telecommunication system of the spacecraft, thereby including those factors of the modulator, transmitter, etc., which influence the overall image transfer characteristics. The calibration data, in FM form, was recorded on magnetic tape for playback through the ground support equipment (GSE) at Goldstone and Pasadena. Thus the final calibration data recorded on the real-time mission film and tape equipment provides a complete system calibration.

The parameters which were calibrated included light transfer characteristics, color response, sine wave response, erasure characteristics, automatic iris tracking,

geometric linearity, and camera pointing accuracy. Data were taken in both 600- and 200-line scan modes and in normal shutter, open shutter, and integrate exposure modes.

A sampling of the calibration results, at the point of initial recording (i.e., not including the GSE), is shown in Figs. IV-63 through IV-67. The ordinate in these graphs is scaled in frequency units at the input of the TV-GDHS demodulators with sync tip frequency set to the nominal values of 5.25 MHz for 600-line scan mode and 75.0 kHz for 200-line scan mode. The ordinate scale can therefore be viewed as a measure of relative video voltage.

Figures IV-63 through IV-65 show the individual curves that were obtained for various f/stops and color filters for the 200- and 600-line scan modes. The curves depict the sensitivity of the camera system at the central portion of the frame to scenes of constant or static light level. The camera system, however, did not respond the same over the entire frame. This nonuniform response, called "shading," is depicted in Fig. IV-66 for 600-line scan mode.
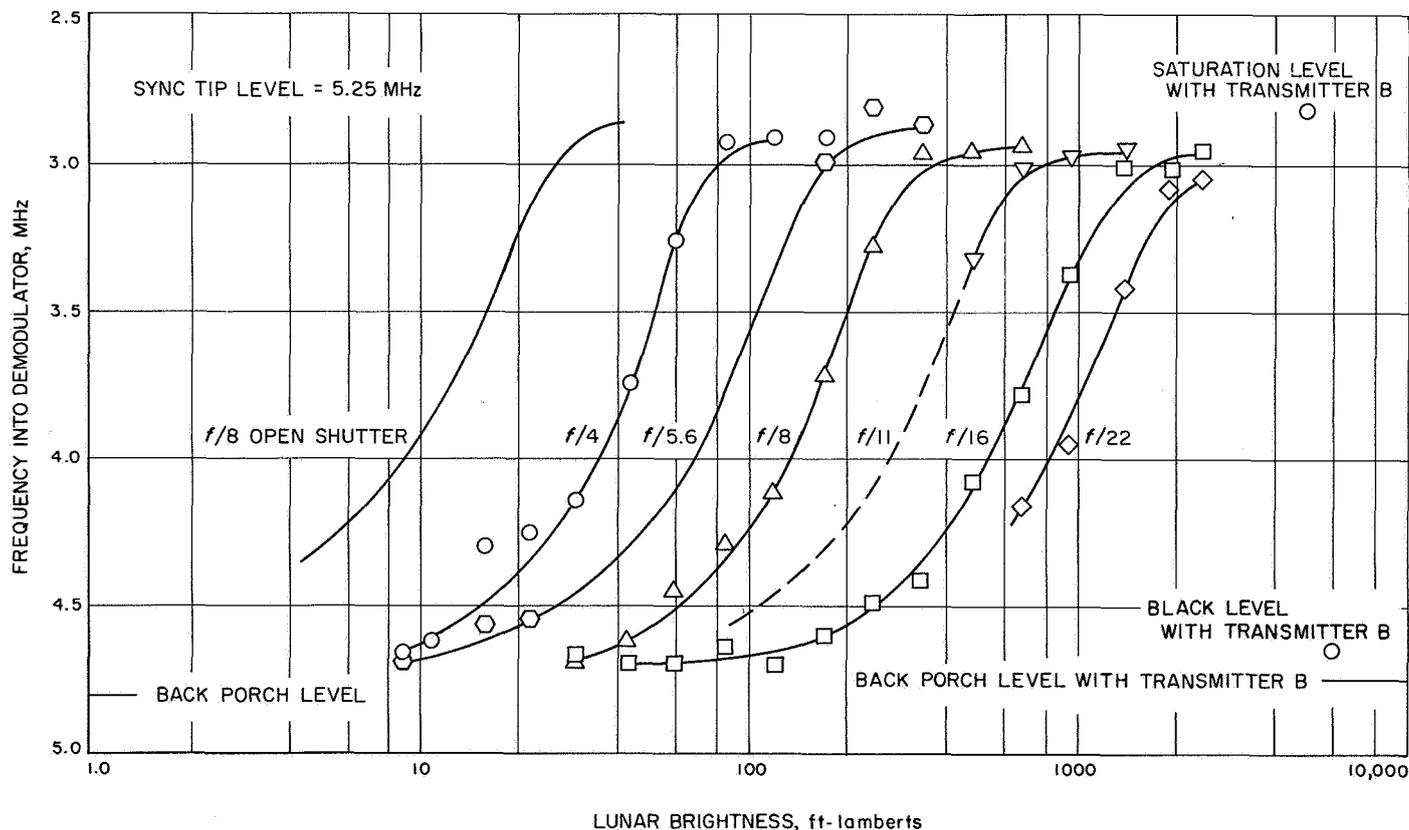


Fig. IV-63. *Surveyor III* camera 600-line transfer characteristic for center of frame with Transmitter A

The data in Fig. IV-64 shows that the light transfer characteristics for the three color filters are almost identical. This results from an improvement in filter design to provide the capability of taking a set of color pictures without the necessity of changing iris position. Reduction of color data is then independent of accuracy or repeatability limitations in iris control.



Fig. IV-64. *Surveyor III* camera 600-line transfer characteristic at f/4 for all filter wheel positions

The response of the spacecraft camera system to sinusoidally varying brightness scenes is shown by Fig. IV-67. Here, the sinusoidal nature of the test scene is given by the abscissa in terms of frequency, and the relative attenuation of the sine wave amplitude by the camera system is given at the ordinate. From these curves it is seen that the spacecraft system has a 40% horizontal response at about 600 TV lines in the 600-line scan mode.

## 3. Mission Performance

During lunar operations, the camera returned over 6300 pictures, in black-and-white and in color. These included spacecraft and lunar surface surveys, pictures of the SM/SS, and views of the earth during solar eclipse.

The failure of the vernier engines to turn off before landing appears to have caused contamination or pitting of the camera optical surfaces. For some camera angles, this resulted in glare in the pictures caused by sunlight scattering due to the mirror surface degradation. The television camera also experienced some problems in stepping which reduced the rate at which pictures were taken. The mirror azimuth drive failed to step 432 times
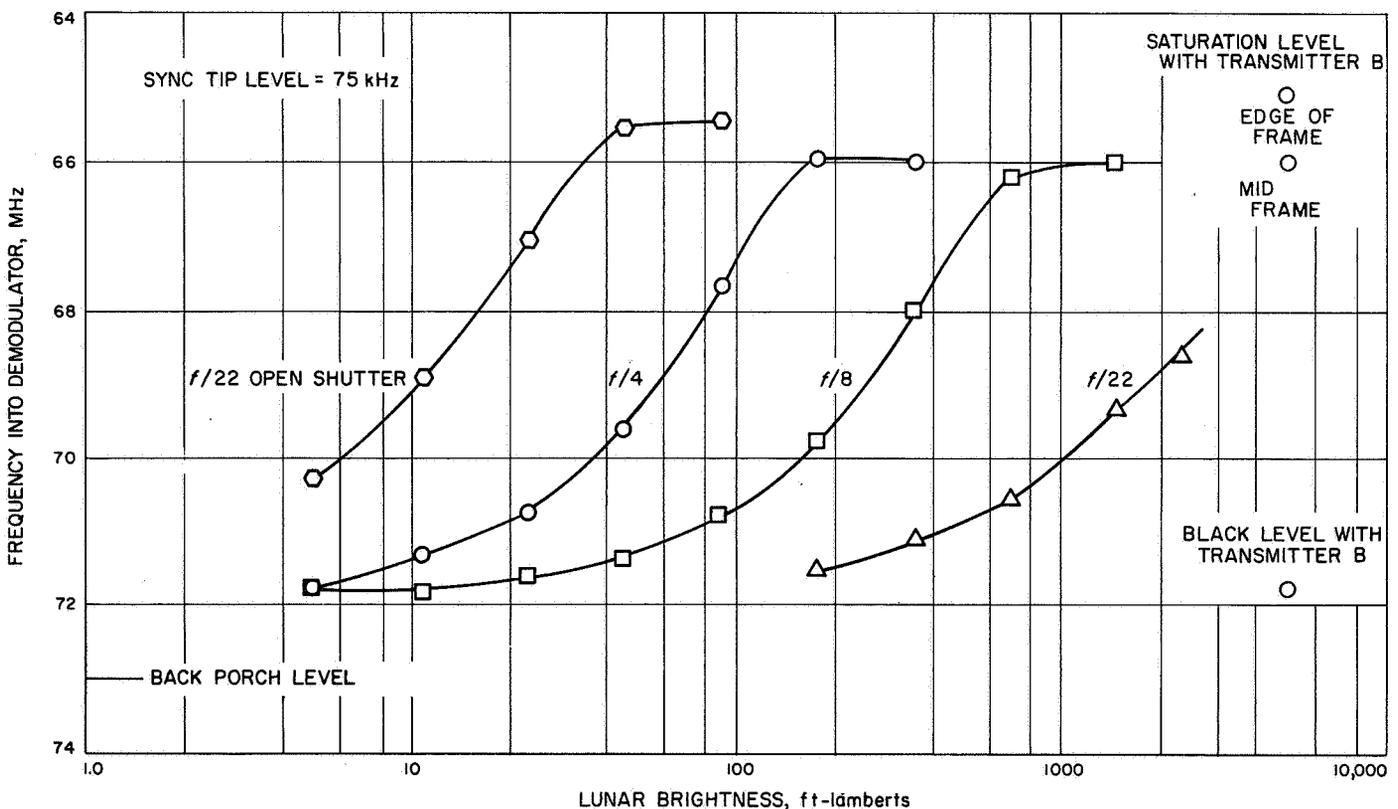


Fig. IV-65. *Surveyor III* camera 200-line light transfer characteristic for center of frame with Transmitter A
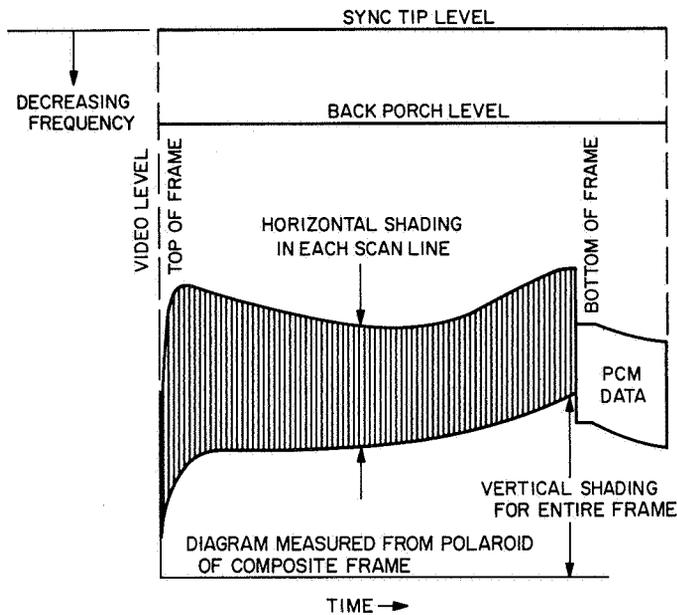
**Fig. IV-66. Surveyor III camera 600-line shading near saturation**
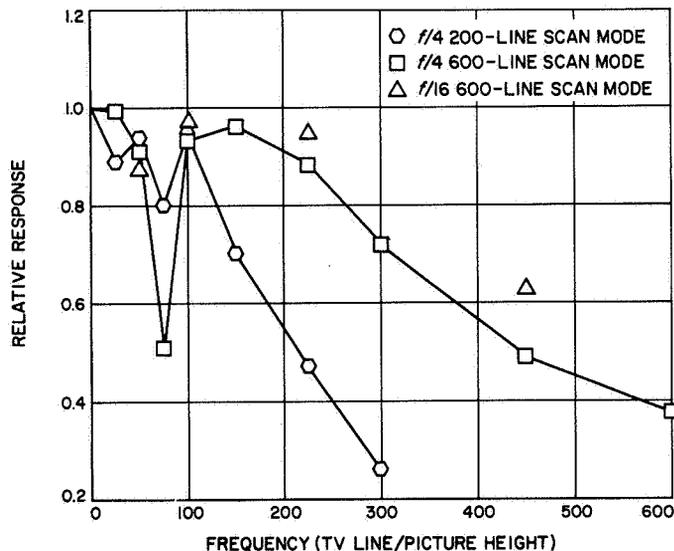


**Fig. IV-67. Camera frequency response characteristic (center of frame, Transmitter A)**

out of a total of 10,045 commands. The elevation drive failed to step 67 times out of a total of 3,594 commands. (The camera also was stepped over 34,000 times in each axis during prelaunch testing.) Analysis of these difficulties, which were most severe when the camera was cold, indicates that the azimuth stepping failures were due to at least three factors: motor wear, binding of the azimuth bearing due to thermal stresses, and increased

friction of the ring gear at one particular azimuth position (possibly due to lunar dust). The elevation stepping failures indicate a motor wearout trend.

On the last earth day of operation, the filter wheel readout data was erroneous, reading a constant value although the filter wheel stepped normally, as verified by the imagery.

## J. Soil Mechanics/Surface Sampler (SM/SS)

The SM/SS is an electromechanical device which is remotely operated by ground command to pick, dig, scrape, trench, and handle lunar surface material. The SM/SS was originally planned for later *Surveyor* missions. However, after the complete success of *Surveyor I*, the decision was made to fly the instrument for the first time on the *Surveyor III* mission. The SM/SS was adapted to the mounting location and interface of the approach television camera and electronics which it replaced. It was necessary also to simplify the instrument to suit the reduced telemetry and commanding capability of the *Surveyor III* spacecraft.

### 1. SM/SS Description

The SM/SS subsystem consists of a mechanism and an electronics auxiliary, with the necessary supporting substructure and interconnecting wire harnesses.

The instrument mechanism is located below the survey television camera, between the auxiliary battery and Leg 2 as shown in Fig. IV-68. The mechanism has an extension/retraction arm which can also be pivoted in azimuth or elevation to permit operations within the surface area indicated in the figure. The arm is locked in the folded position until it is to be deployed after lunar landing, at which time it is unlocked by the firing of a squib. Attached to the end of the arm is a scoop having a sharpened blade and a door. The scoop is capable of holding solid material up to about 1.25 in. (3.2 cm) in diameter and granular material up to about 6 in.³ (100 cm³) in volume. A small footpad is attached to the scoop door to present a flat surface to the lunar surface when the door is closed. Four electric motors are used to manipulate the SM/SS: one each for extension/retraction, azimuth, and elevation motions, and one located at the scoop to open or close the door. An electromechanical clutch can be operated by earth command to disengage the elevation drive train, allowing the scoop to be impelled downward by a pretensioned elevation torque spring to strike the lunar surface.
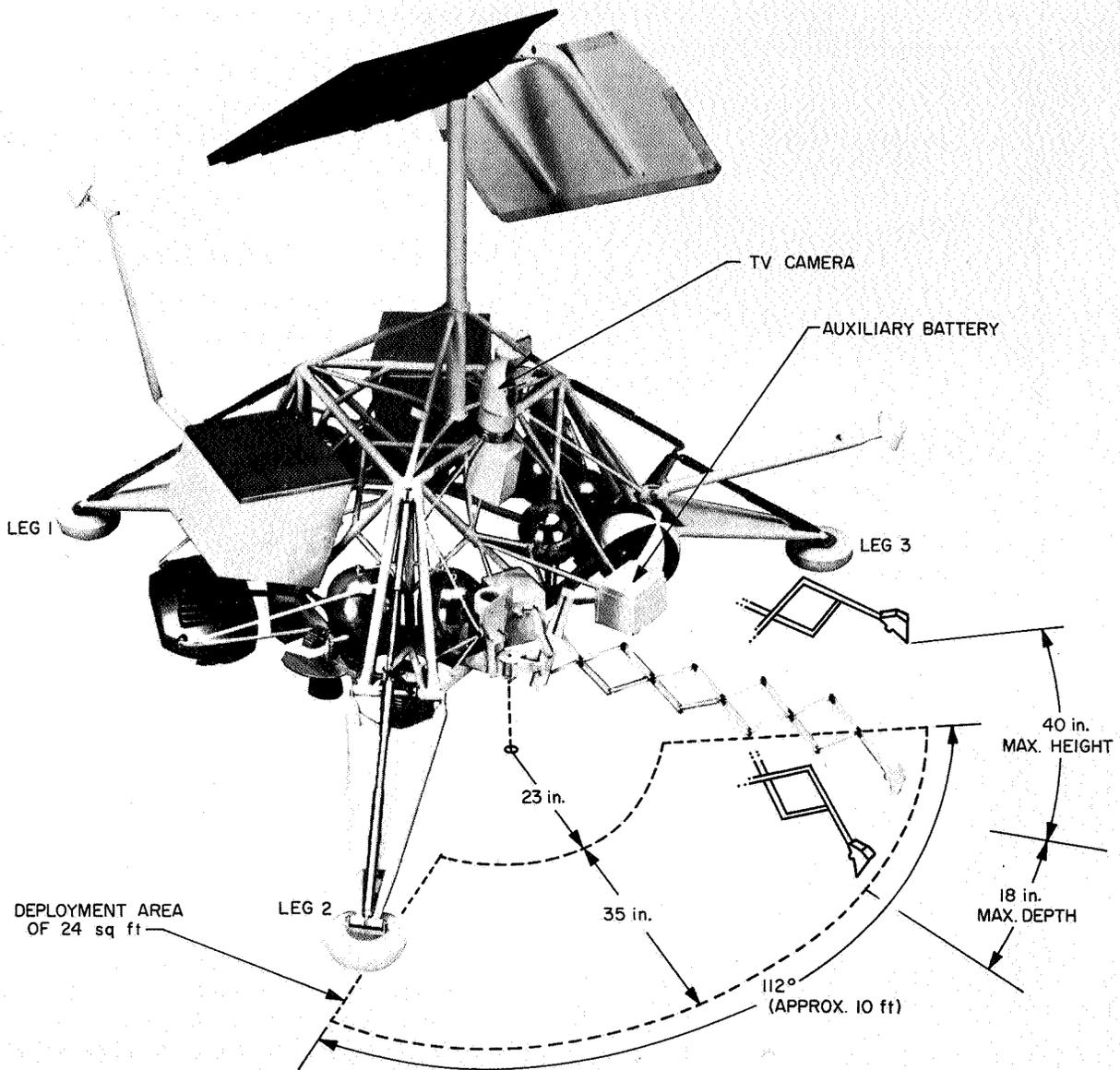
Fig. IV-68. SM/SS deployment envelope

The electronics auxiliary provides command decoding, data buffering, power management, squib firing, and switch control of the mechanism motors and clutch. Either a 2-sec or a 0.1-sec period of operation of any of the motors can be selected by earth command. The angle or distance through which the SM/SS moves by these commands depends on the motor involved, its condition, temperature, voltage, and the working load. To adapt the SM/SS to the *Surveyor III* spacecraft design, the strain-, acceleration-, and position-measuring systems originally planned were removed, and a means was pro-

vided within the auxiliary to measure the current drawn by the motors. It is possible to make rough determinations of lunar surface mechanical properties from motor current data by using the relationship between motor current and operating loads. However, motor current data is commutated, so it is necessary to transmit data at the higher bit rates to obtain current measurements during the short periods of motor operation.

Since SM/SS direct instrumentation is limited to motor current, the primary means of obtaining SM/SS data is

through the coordinated operation of the television camera, wherein television frames are commanded at selected intervals between SM/SS movements. Sequences and priorities of SM/SS tests are therefore dependent upon viewing conditions, spacecraft shadow patterns, and the performance of the television system. The azimuth axes of the SM/SS mechanism and camera are not collinear; therefore, the television viewing angle of the scoop varies with scoop position. When the scoop is positioned near Footpad 2, the camera looks directly down the extension arm, which largely obscures the scoop itself. When positioned near the auxiliary battery, a slight side view of the scoop is afforded.

A static bearing test is performed by exercising the extension and azimuth motions until the scoop is positioned above the desired surface point. Then the scoop is driven downward with the elevation motor until the desired penetration is achieved, or until the motor is stalled. The static test is normally performed with the scoop door closed to provide a flat surface for contact. However, an open scoop static test can also be carried out. As the SM/SS is extended, the angle that the scoop makes with the test surface varies. At contact with a smooth surface, the flat face of the scoop door is normal to the tangential elevation motion, when the arm is fully extended.

For an impact test, the scoop is also positioned first above the desired surface area. Then the elevation drive clutch is released, allowing the scoop to drop to the surface, accelerated by gravity and the elevation torque spring. Impact tests are also performed with the scoop door open or closed, as desired.

A trenching operation is performed by driving the scoop down into the surface with the door open, then drawing it toward the spacecraft by repeated commanding of the retraction motor. Material can be removed from the trench either by retracting the scoop until it is clear of the surface, forming a pile at the foot of the trench, or by closing the scoop and lifting the material out of the trench.

## 2. SM/SS Performance

During the transit phase of *Surveyor III*, the temperature of the electronics auxiliary was cooler than predicted. Although heater power was applied, a temperature of about −33°F occurred, which is about 30° lower than the predicted nominal, but still well above the

survival temperature of −67°F. After touchdown, the heater was off about 2.5 hr, during which time the electronics auxiliary temperature dropped to an estimated −130°F. After thermal power was restored, the auxiliary temperature was maintained within the design operating limits from initial turn-on, late in the Goldstone pass on April 21, until operations were concluded May 2.

Initial operations included firing of the pyrotechnic locking device to release the SM/SS from its stored position and a checkout of the arm drive mechanisms. Normal operation was achieved in all directions except that extension/retraction motion was less than expected for each command. Automatic, taped sequences of spacecraft commands had been prepared to accomplish the planned operations. Corrections for variations in motion magnitude on the moon was easily accomplished by providing additional "manual" commands after a given tape sequence. Table IV-18 presents the estimated size of each of the motion increments which occurred during lunar operations as compared to preflight calibrations.

**Table IV-18. SM/SS motion increments (no load)**

| Direction | Duration, sec | Travel | |
|---|---|---|---|
| | | Preflight[a] | On lunar surface[b] |
| Extend | 2.0 | 3.4 in. (8.6 cm) | 1.75 in. (4.4 cm) |
| Retract | 2.0 | 3.2 in. (8.1 cm) | 1.5 in. (3.8 cm) |
| Right | 0.1 | 1.5 deg | 1.5 deg |
| Left | 0.1 | 1.5 deg | 1.5 deg |
| Up | 2.0 | 6 deg | 6 deg |
| Down | 2.0 | 9 deg | 9 deg |

[a] Nominal values for 22.0 V and 70°F, based on unit and system level tests at three extension distances.

[b] Preliminary estimates based on television observation.

Because of the spacecraft telemetry anomaly, valid SM/SS motor current data could not be obtained, although two attempts were made at the 17.2 bit/sec data rate by initiating 90-sec, 67%-duty-cycle retraction motor sequences. Each time, telemetry indicated parity errors for all samples of motor current transmitted.

The SM/SS auxiliary was turned on for a total of 18 hr, 22 min, during which time 5879 earth-commands were sent to it. All earth-commands were correctly decoded, resulting in the generation of 1898 SM/SS commands, all

TYPE TEST

▽ IMPACT

☐ BEARING

◯ CONTACT

A  BEARING TEST I
B  TRENCH I
C  TRENCH 2
D  CONTACT I
E  BEARING TEST 2
F  BEARING TEST 3
G  TRENCH 3
H  CONTACT 2
I  FOOTPAD CONTACT
J  TRENCH 3 (WIDEN)
K  TRENCH 3 (WIDEN)

L  BEARING TEST 4
M  IMPACT TEST I
N  IMPACT TEST 2
O  IMPACT TEST 3
P  IMPACT TEST 4
Q  IMPACT TEST 5
R  IMPACT TEST 6
S  BEARING TEST 5
T  CONTACT 3
U  BEARING TEST 6

V  BEARING TEST 7
W  IMPACT TEST 7
X  IMPACT TEST 8
Y  IMPACT TEST 9
Z  IMPACT TEST IO
a  CONTACT 4
b  IMPACT TEST II
c  IMPACT TEST I2
d  TRENCH 4
e  IMPACT TEST I3

Fig. IV-69. Location of SM/SS lunar surface tests

of which were correctly responded to. The SM/SS remained in excellent condition when operations were concluded.

During the lunar operations, the SM-SS completed the following test operations (the lunar surface locations of which are shown in Fig. IV-69):

(1) Eight bearing tests were made with the scoop door closed. One of these was conducted on the floor of Trench 3.

(2) Four trenches were made. Of these, the first was made with only a single pass; the second and third were made with multiple passes reaching a maximum depth of about 7 in.; and the fourth was short and about 2 to 3 in. deep.

(3) Fourteen impact tests were carried out from a variety of heights. One of these was performed at the bottom of Trench 4.

(4) Surface material was handled. Material was moved to desired locations, e.g., to the top of Footpad 2, and a small rock was clamped with the scoop door. Surface contacts were also made with the SM/SS to determine surface locations more precisely.

At selected intervals during and after each test using the SM/SS, pictures were obtained with the camera. Additional pictures were obtained of the same disturbances at various sun angles on succeeding days.

The scientific results obtained from operations of the SM/SS are presented in Part II of this report.

# V. Tracking and Data System

The Tracking and Data System (TDS) for the *Surveyor* Project consists of facilities of the Air Force Eastern Test Range (AFETR), Goddard Space Flight Center (GSFC), and the Deep Space Network (DSN). This section summarizes the mission preparation, flight support, and performance evaluation of each facility within the TDS.

The TDS support for the *Surveyor III* mission was considered excellent: some minor problems were experienced during operations but had no effect on required performance. All requirements were met and in most cases exceeded.

## A. Air Force Eastern Test Range

The AFETR performs TDS supporting functions for *Surveyor* missions during the countdown, launch, and near-earth phase of the flight.

The *Surveyor* mission requirements for launch phase tracking and telemetry coverage are classified as follows in accordance with their relative importance to successful mission accomplishment:

Class I requirements consist of the minimum essential needs to ensure accomplishment of first-priority flight test objectives. These are mandatory requirements which, if not met, may result in a decision not to launch.

Class II requirements define the needs to accomplish all stated flight test objectives.

Class III requirements define the ultimate in desired support, and would enable the range user to achieve the flight test objectives earlier in the test program.

The AFETR configuration for the *Surveyor III* mission is listed in Table V-1. The configuration is similar to the *Surveyor II* configuration except for the addition of the Range Instrumentation Ships (RIS) *Timber Hitch* and *Twin Falls*, and two telemetry aircraft, *Audit 1* and *Audit 2*.

Figure V-1 illustrates the disposition of the range instrumentation ships and aircraft and planned coverage for *Surveyor III* launch day. AFETR preparations for *Surveyor III* consisted of routine testing of individual facilities, followed by several Operational Readiness Tests. All requirements were met by AFETR for the *Surveyor III* mission.
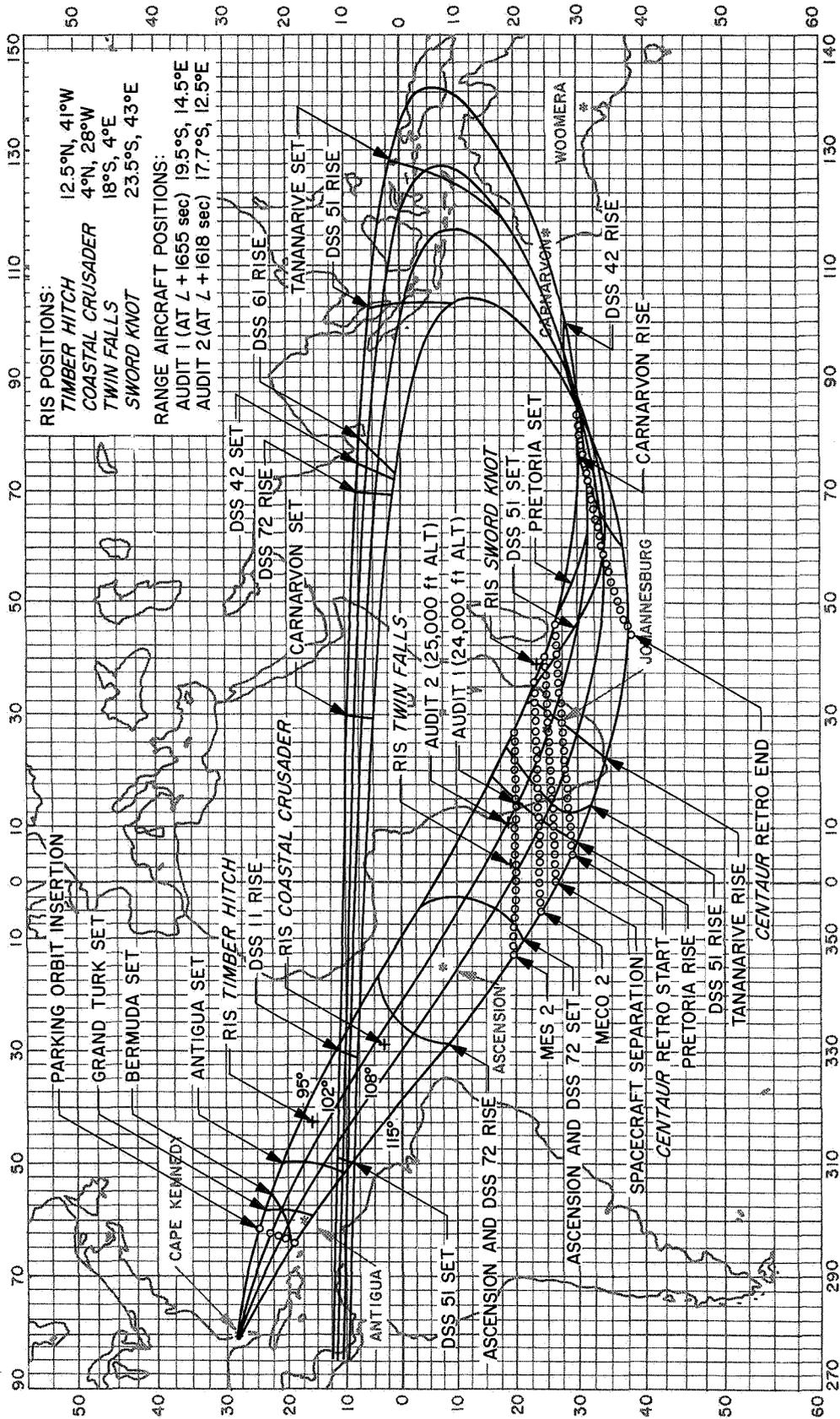
Fig. V-1. Planned launch phase coverage for April 17, 1967

## Table V-1. AFETR configuration

| Station | Radar | VHF telemetry | S-band telemetry |
|---------|-------|---------------|------------------|
| Merritt Island | X | | |
| Cape Kennedy | X | X | X |
| Patrick AFB | X | | |
| Grand Bahama Island | X | X | X |
| Grand Turk | X | | |
| Antigua | X | X | X |
| RIS *Timber Hitch* | | X | |
| RIS *Coastal Crusader* | | X | X |
| Ascension | X | X | X |
| RIS *Twin Falls* | X | X | X |
| Range aircraft *Audit 1* | | X | |
| Range Aircraft *Audit 2* | | X | |
| Pretoria | X | X | X |
| RIS *Sword Knot* | | X | X |

## 1. Tracking (Metric) Data

The AFETR tracks the C-band beacon of the *Centaur* stage to provide metric data. This data is required during intervals of time before and after separation of the spacecraft for use in calculating the *Centaur* orbit, which can be used as a close approximation of the postseparation spacecraft orbit. The *Centaur* orbit calculations also may be used to provide DSIF acquisition information (in-flight predicts).

Estimated and actual radar coverage is shown in Figs. V-2 and V-3. The combined coverage of all stations is represented by the top set of bars in each figure. The Class I requirements were met and exceeded, with AFETR stations downrange to Antigua providing continuous coverage to $L + 803$ sec.

Intermittent tracking conditions were experienced by Grand Bahama owing to a weak C-band beacon signal, apparently caused by a balance-point shift problem.



REQUIRED COVERAGE

ESTIMATED COVERAGE

ACTUAL COVERAGE
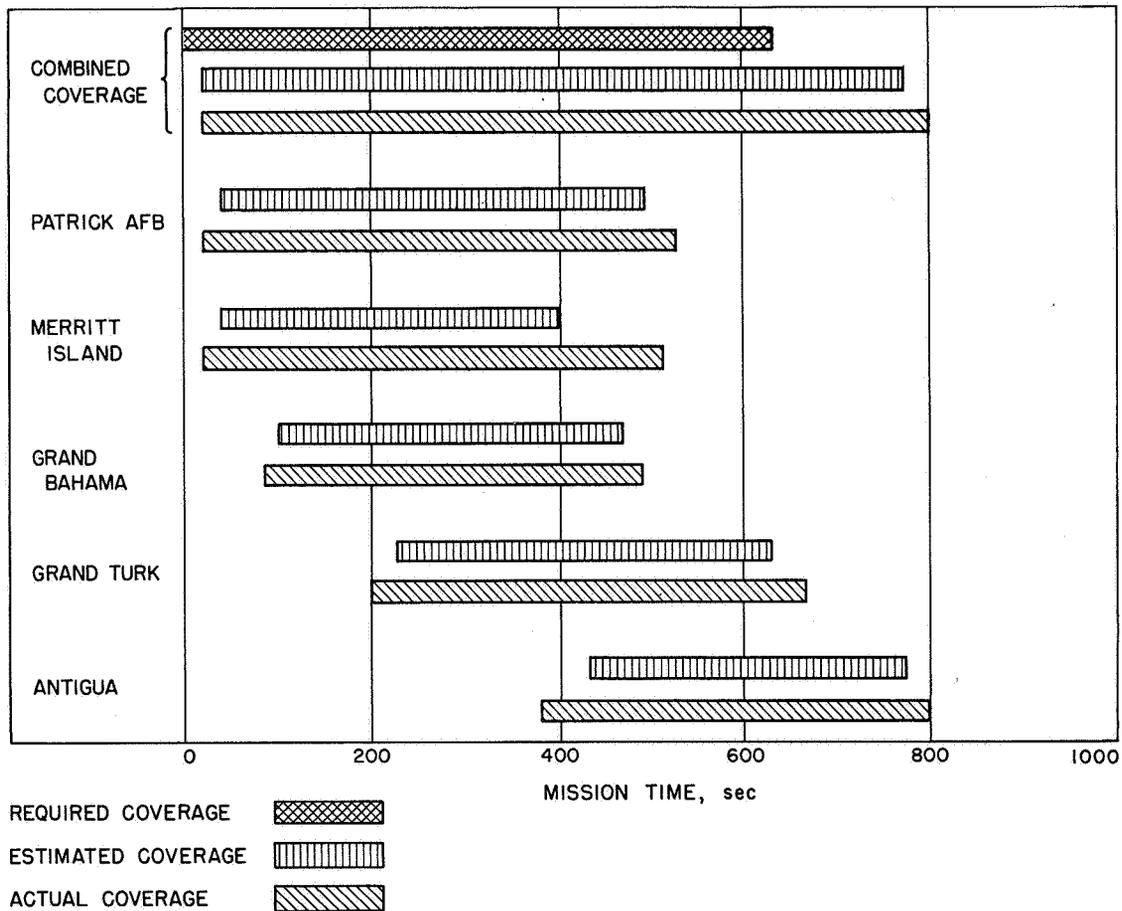
**Fig. V-2. AFETR C-band radar coverage: liftoff through Antigua**
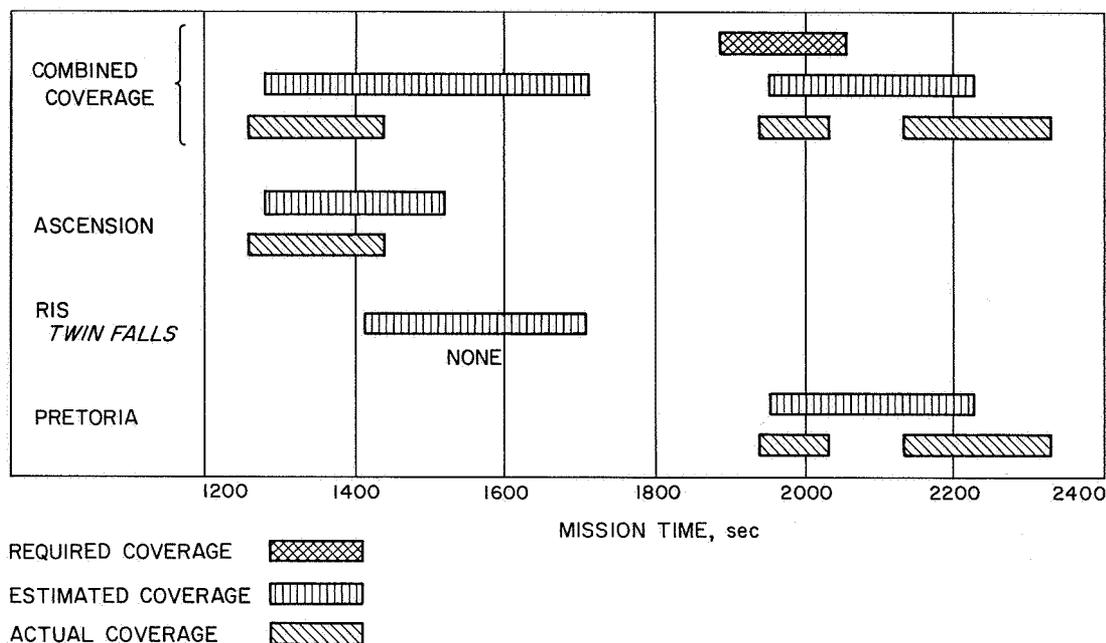
Fig. V-3. AFETR C-band radar coverage: Ascension through Pretoria

Ascension radar experienced a premature deterioration of signal strength toward the end of the pass. The antenna was computer-driven along the trajectory. However, no additional signals were received. The early loss of signal apparently resulted from a roll of the launch vehicle changing the aspect angle, which caused the signal to deteriorate.

Pretoria radar acquired a low-strength signal at $L + 1941$ sec but lost lock 99 sec later. During attempts to reacquire the signal, the antenna drive hydraulic system failed. The station went to a "battle short" mode (bypassing safety shutdown circuits) and reacquired the spacecraft signal shortly thereafter. As was the case with Ascension, Pretoria also acquired in a low-gain portion of the antenna pattern.

The *Twin Falls* did not acquire any radar data, although a thorough precalibration had been made on the radar system before the pass. The *Twin Falls* had received a preflight interrange vector (IRV). However, it did not receive an in-flight IRV. Acquisition attempts included slaving the radar to the ship's S-band system, which was receiving telemetry; these attempts were unsuccessful. Tests were performed immediately after the pass, and all radar systems were verified as functioning normally. Preflight and postflight calibration measurements agreed within very small tolerances. Signal strength records and the ship's position indicated that the *Twin*

*Falls* should have received a good signal. Investigation of this anomaly is being continued by Lewis Research Center, General Dynamics/Convair, and AFETR.

### 2. Atlas/Centaur Telemetry (VHF)

To meet the Class I telemetry requirements, the AFETR must continuously receive and record *Atlas* telemetry (229.9-MHz link) from before liftoff until shortly after *Atlas/Centaur* separation and *Centaur* telemetry (225.7-MHz link) until shortly after spacecraft separation. Thereafter, *Centaur* telemetry is to be recorded as station coverage permits until completion of the *Centaur* retro maneuver. In addition to the land stations, the AFETR provided the Range Instrument Ships *Timber Hitch*, *Sword Knot, Twin Falls* and *Coastal Crusader*. In addition two range telemetry aircraft were provided to help cover the gap between the *Twin Falls* and Pretoria in order to provide coverage during the critical *Centaur* second-burn prestart sequence. The *Twin Falls*/Pretoria gap resulted from a shipboard illness which prevented the ship from reaching its planned support position.

Estimated and actual VHF telemetry coverage is shown in Figs. V-4 and V-5. All Class I, II, and III requirements were met, since continuous and substantially redundant VHF telemetry data was received beginning with the countdown and through *Sword Knot* loss of signal at $L + 2833$ sec. Coverage was greater than predicted.
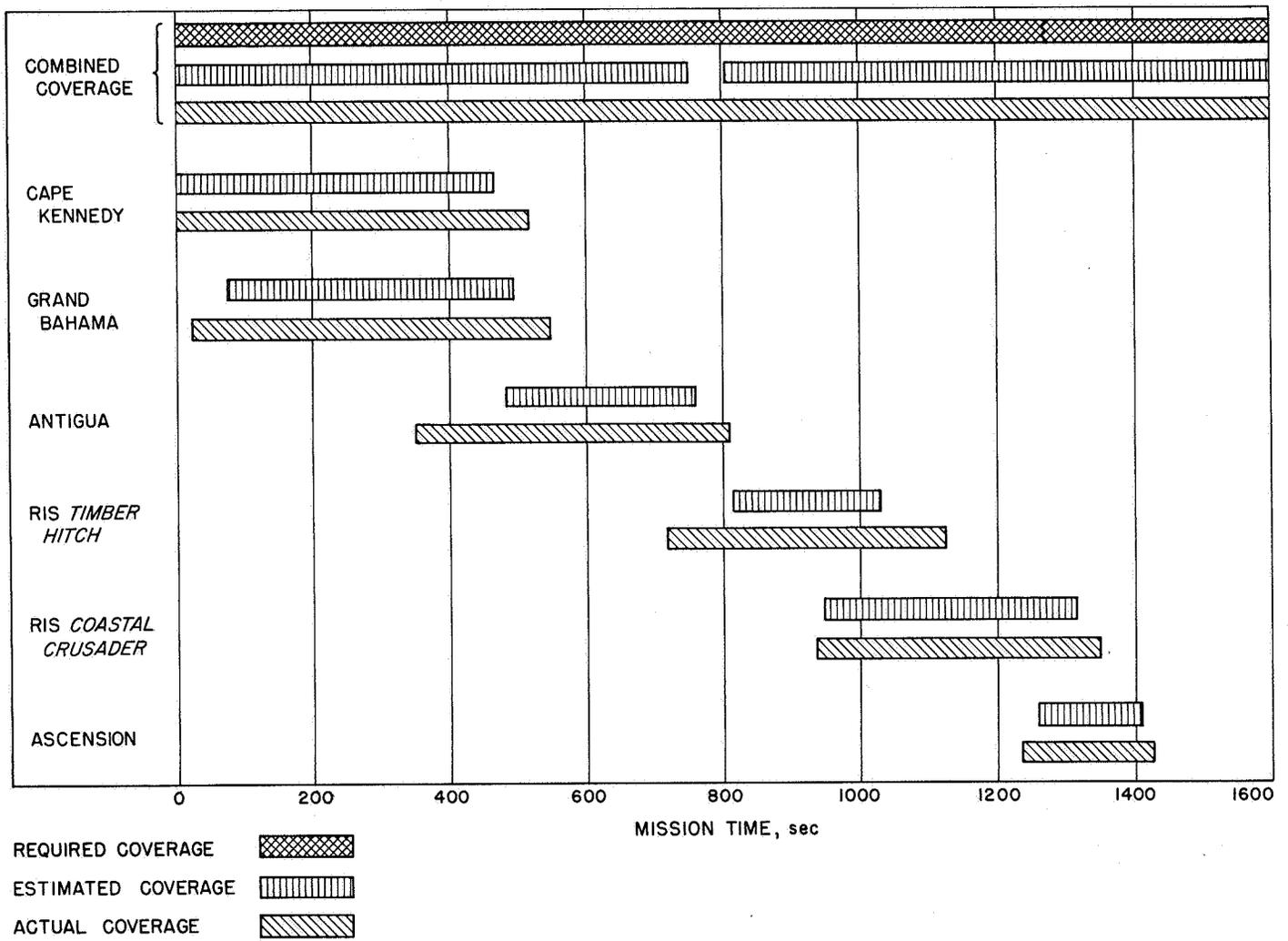
**Fig. V-4. AFETR VHF telemetry coverage: liftoff through Ascension**
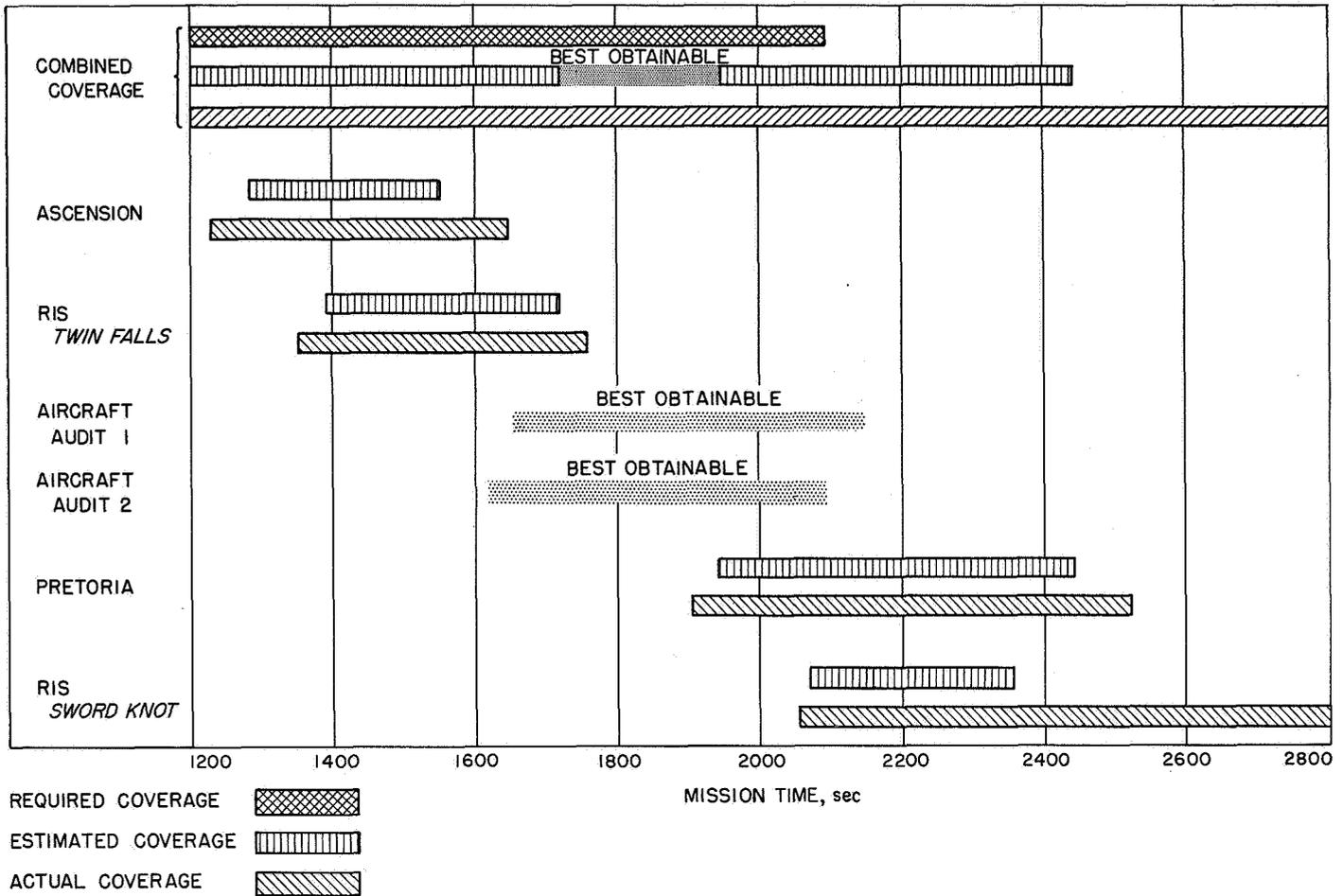
**Fig. V-5. AFETR VHF telemetry coverage: Ascension through RIS *Sword Knot***

The AFETR stations, ships, and aircraft also reported on all but two (*mark* 12 and *mark* 23) of the *mark* events requested for this mission. (See Appendix A, Table A-1, for a list of the mark events.)

### 3. Surveyor Telemetry (S-band)

The AFETR is required to receive, record, and retransmit *Surveyor* S-band (2295-MHz) telemetry in real-time after the spacecraft transmitter high power is turned on until 15 min after DSIF rise. For this mission, since the MSFN station at Carnarvon was configured to transmit S-band telemetry to DSS 42, AFETR was required to provide S-band information until Carnarvon rise.

The AFETR S-band telemetry resources assigned to meet this requirement are shown in Table V-1. All S-band resources committed were on a "best effort" basis since the *Centaur* vehicle is not roll-attitude-stabilized and the aspect angle cannot be predicted.

Estimated and actual S-band telemetry coverages are shown in Figs. V-6 and V-7. All Class I, II, and III requirements were met.

With the exception of a 30-sec gap at $L + 360$ sec, AFETR land stations and ships obtained continuous S-band telemetry coverage from liftoff through Antigua loss of signal at $L + 725$ sec. Although Ascension experienced a dropout between $L + 1492$ and $L + 1522$ sec, the interval was adequately covered by the RIS *Twin Falls*. The RIS *Sword Knot* experienced an expected dropout between $L + 2728$ and $L + 2833$ sec resulting from the acquisition of the spacecraft transponder by DSS 42, which then provided the required coverage.

*Sword Knot* was expected to provide coverage from $L + 2037$ to $L + 3222$ sec. An anticipated loss of receiver lock occurred at about 3159 sec when the ship was required to maneuver from its original position, which is selected for optimum acquisition. During a prolonged
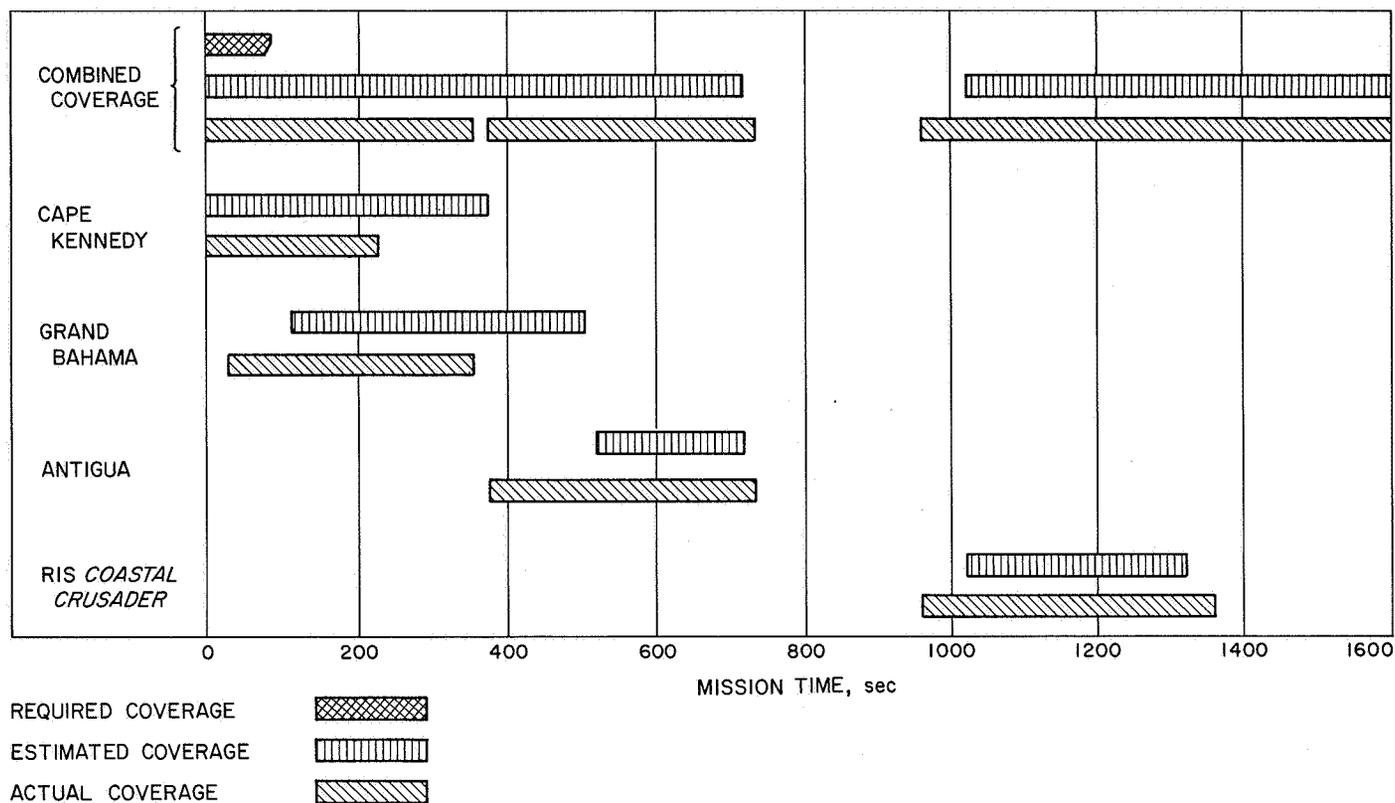
**Fig. V-6. AFETR S-band telemetry coverage: liftoff through RIS *Coastal Crusader***

tracking period, the ship's superstructure may come between the antenna and spacecraft and maneuvers are required to regain an unobstructed view of the spacecraft.

The *Twin Falls* S-band system lost track sooner than expected owing to the spacecraft flight azimuth which, on this mission, passed over the zenith. The *Twin Falls* did not reacquire the spacecraft.

#### 4. *Surveyor* Real-Time Telemetry Data

The AFETR retransmits *Surveyor* data (VHF or S-band) to Building AO, Cape Kennedy, for display and for retransmission to the SFOF. In addition, downrange stations monitor specific channels and report events via voice communication.

For the *Surveyor III* mission, existing hardware and software facilities were utilized to meet the real-time data requirements.

All requirements were met. Spacecraft telemetry data via the VHF telemetry link were transmitted in real-time to the Space Flight Operations Facility (SFOF) from

liftoff to spacecraft high-power on. At high-power on, AFETR switched as planned to real-time transmission of spacecraft telemetry data received on the S-band link. Real-time data flow was very good. In addition, all *mark* events related to spacecraft preseparation and separation events were observed and reported.

#### 5. Real-Time Computer System (RTCS)

For the launch and near-earth phase of the mission, the RTCS provides trajectory computations based on tracking data and vehicle guidance data. The RTCS output includes:

(1) The interrange vector (IRV), the standard orbital parameter message (SOPM), and orbital elements and injection conditions.

(2) Predicts, look angles, and frequencies for acquisition use by downrange stations.

(3) Injection conditions mapped to lunar encounter and I-matrices defining orbit determination accuracies for early trajectory evaluation prior to the highly refined orbits generated by the FPAC group.
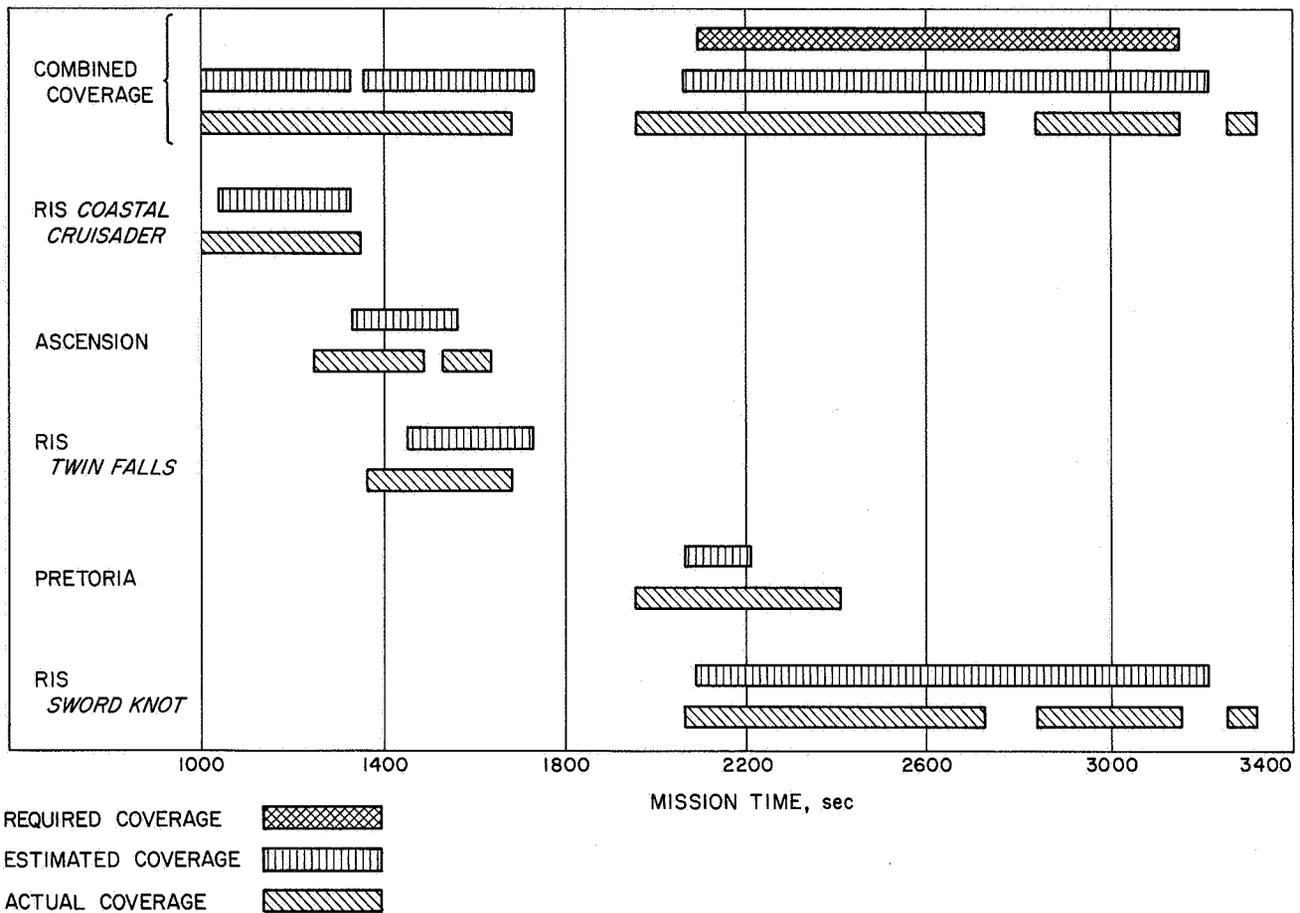
**Fig. V-7. AFETR S-band telemetry coverage: RIS *Coastal Crusader* through RIS *Sword Knot***

The RTCS computed parking and transfer orbit messages as well as predicts. The first lunar orbit computation generated at the RTCS using DSN 'data was transmitted at $L + 85$ min; the second orbit was delivered 20 min later. Both orbits, as well as one generated from Pretoria data, compared favorably with the orbit which was subsequently generated by the SFOF. Support by the RTCS was considered excellent. (Also refer to Sections II-D and VII.)

## B. Goddard Space Flight Center

The Manned Space Flight Network (MSFN), managed by GSFC, supports *Surveyor* missions by performing the following functions:

(1) Tracking of the *Centaur* beacon (C-band).

(2) Receiving and recording *Centaur*-link telemetry from Bermuda acquisition until loss of signal at the stations that have a view of the spacecraft.

(3) Providing real-time confirmation of certain *mark* events.

(4) Receiving and recording S-band telemetry at Carnarvon and transmitting these data to DSS 42, Tidbinbilla, for retransmission to the SFOF in real-time.

(5) Providing real-time reformatting of Carnarvon radar data from the hexidecimal system to the 38-character octal format and retransmitting these data to the RTCS at Cape Kennedy.

(6) Providing NASCOM support to all NASA elements for simulations and launch, and extending this communications support as necessary to interface with the combined worldwide network.

The MSFN supported the *Surveyor III* mission with the tracking facilities and equipment listed in Table V-2. The MSFN also supported the Operational Readiness Test (ORT) prior to launch.

## Table V-2. MSFN configuration

| Location | Acqui-sition aid | VHF telem-etry | C-band radar | SCAMA | Radar high-speed data | Real-time readouts |
|---|---|---|---|---|---|---|
| Bermuda | X | X | X | X | X | X |
| Tananarive | X | X | | X | | X |
| Carnarvon | X | X | X | X | | X[a] |
| GSFC | | | | X | X | |

[a]If telemetry signal is adequate.

### 1. Acquisition Aids

Stations at Bermuda, Tananarive, and Carnarvon are equipped with acquisition aids to track the vehicle and provide RF inputs to the telemetry receivers from Bermuda acquisition to loss of signal at Carnarvon. Performance recorders are used to record AGC and angle errors for postmission analysis. All MSFN acquisition aid systems performed their required functions during the *Surveyor III* mission.

### 2. Telemetry Data

Bermuda, Tananarive, and Carnarvon are also equipped to receive, record, and decommutate telemetry. Mark Event readouts were required from all stations in real-time or as near real-time as possible when the vehicle was in view of a station.

MSFN telemetry support was good. Expected and actual VHF telemetry coverages are shown in Fig. V-8.

There were no equipment failures or discrepancies during the operation.

Bermuda confirmed *mark* events 5 through 9. Range safety commitments on both *Atlas* and *Centaur* links were met without difficulty. Pulse amplitude modulation (PAM) equipment was set up to receive inverted polarity data as specified in the Network Operations Plan (NOP). However, at acquisition of signal the data polarity was noted to be in a normal mode. Analysis of the mission tapes indicated the data on each subcarrier oscillator channel should have been in normal polarity.

Tananarive received a strong signal on the *Centaur* link and achieved good decommutator lock, which permitted *mark* events 22, 24, 25, and 26 to be decommutated, displayed, and confirmed. Owing to differences between the NOP description and the actual signals received, *mark* 23 was not confirmed.

At Carnarvon, heavy interference on the telemetry channels produced decommutation problems. As a result, no readout was obtained for *mark* 25, and only a postpass readout for *mark* 26 was effected. The poor signal quality was due to the extreme range of the vehicle (greater than $3.6 \times 10^6$ yd) and local interference from airport distance measuring equipment (DME) radio signals.

Carnarvon also received and recorded 550-bit/sec unified S-band (USB) telemetry data. Expected and actual S-band telemetry coverages are shown in Fig. V-9. This station could have bridged the gap between near-earth AFETR coverage and DSIF acquisition if such a gap existed. This use of the USB system is different from
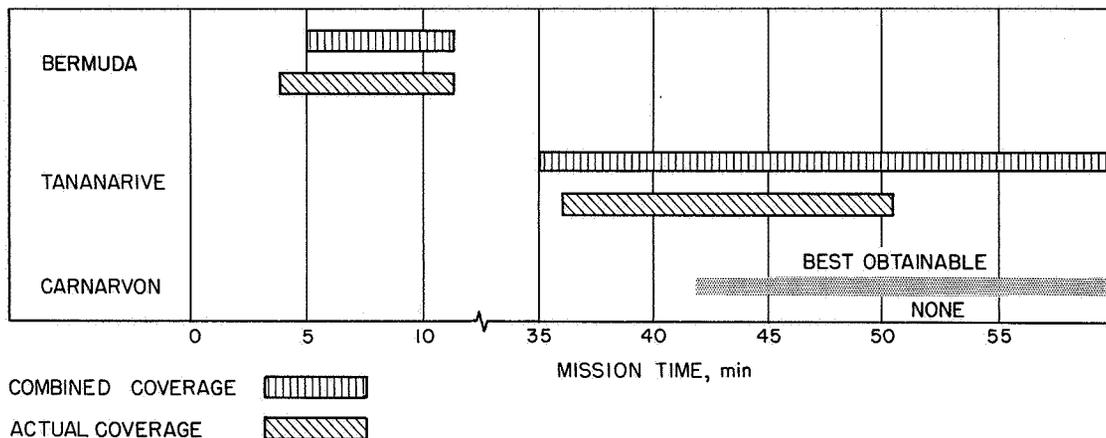


Fig. V-8. MSFN telemetry coverage: VHF

ESTIMATED COVERAGE [|||||||||||]
ACTUAL COVERAGE [\\\\\\\]
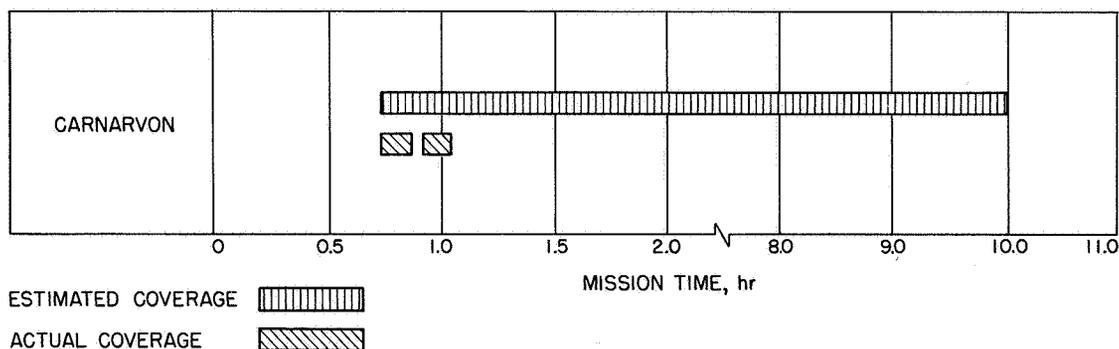
Fig. V-9. MSFN telemetry coverage: S-band

regular Carnarvon telemetry coverage. Coverage for USB telemetry was not committed but was provided on a "best efforts" basis.

### 3. Tracking Data (C-band)

Bermuda and Carnarvon provided C-band beacon radar tracking, magnetic tape recording (at a minimum of 10 points/sec) and real-time data transmission to GSFC and AFETR. Expected and actual C-band radar coverages are shown in Fig. V-10.

The Bermuda FPQ-6 radar provided 432 sec of auto-track, with beacon return signals having a signal-to-noise (S/N) ratio of up to 36 db. The FPS-16 radar provided 246 sec of autotrack, also with strong beacon replies. Owing to the expected obscuration of the FPS-16 antenna by the FPQ-6 antenna, the estimated FPS-16 coverage for the actual launch azimuth was only 232 sec.

Carnarvon FPQ-6 radar provided approximately 4100 sec of autotrack, with beacon return signals having an S/N ratio of 22 db.

### 4. Computer Support, Data Handling, and Ground Communications

The GSFC Data Operations Branch provided computer support during the prelaunch, launch, and orbital phases of the mission. Data was provided by MSFN stations at Bermuda and Carnarvon in accordance with the requirements of the Network Operations Plan.

GSFC provides nominal pointing data to Carnarvon and Tananarive during the prelaunch phase of the mission. During the launch phase, GSFC computers accepted high-speed data from Bermuda and the RTCS, Cape Kennedy. Based on low-speed data from AFETR radars, GSFC computers generated and transmitted acquisition messages to Tananarive and Carnarvon. GSFC generated (off-line) and transmitted unified S-band acquisition messages to Carnarvon based on the actual launch azimuth. Acquisition messages based on the state vector from JPL were also generated and transmitted to MSFN stations as an aid in one-way tracking of the spacecraft. Carnarvon hexadecimal low-speed data was reformatted at GSFC to the standard 38-character radar format and transmitted to the RTCS. Existing NASCOM and DOD Network



ESTIMATED COVERAGE [|||||||||||]
ACTUAL COVERAGE [\\\\\\\]
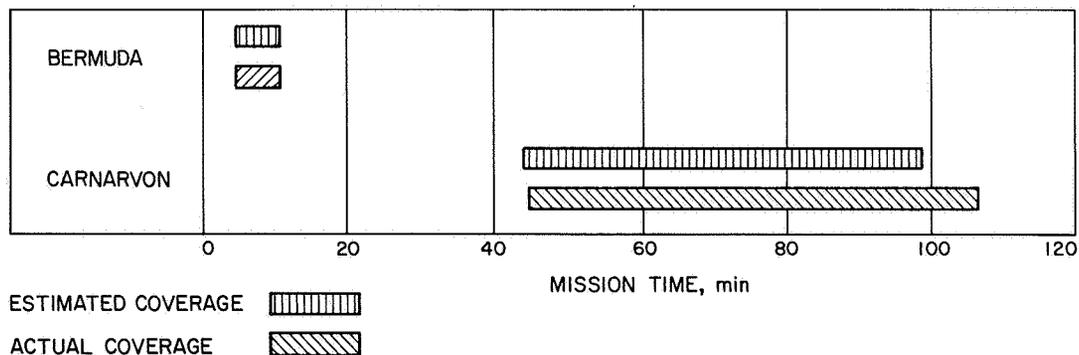
Fig. V-10. MSFN radar coverage: C-band

Facility voice and teletype circuits provided ground communications to all participating stations.

## C. Deep Space Network

The DSN supports *Surveyor* missions with the integrated facilities of the DSIF, the GCS, and the DSN facilities in the SFOF.

### 1. The DSIF

The following Deep Space Stations (DSS) were committed as prime stations for the support of the *Surveyor III* mission:

DSS 11  Pioneer, Goldstone Deep Space Communications Complex (DSCC), Barstow, California

DSS 42  Tidbinbilla, Australia, near Canberra

DSS 61  Robledo, Spain (Fig. V-11)

The DSN was required to track the spacecraft and provide doppler and telemetry data as shown in Table V-3.

For the April 17 launch date, DSS 42 was designated the initial two-way acquisition station. A requirement was also placed on DSS 42 to process real-time telemetry data received by the MSFN station at Carnarvon.
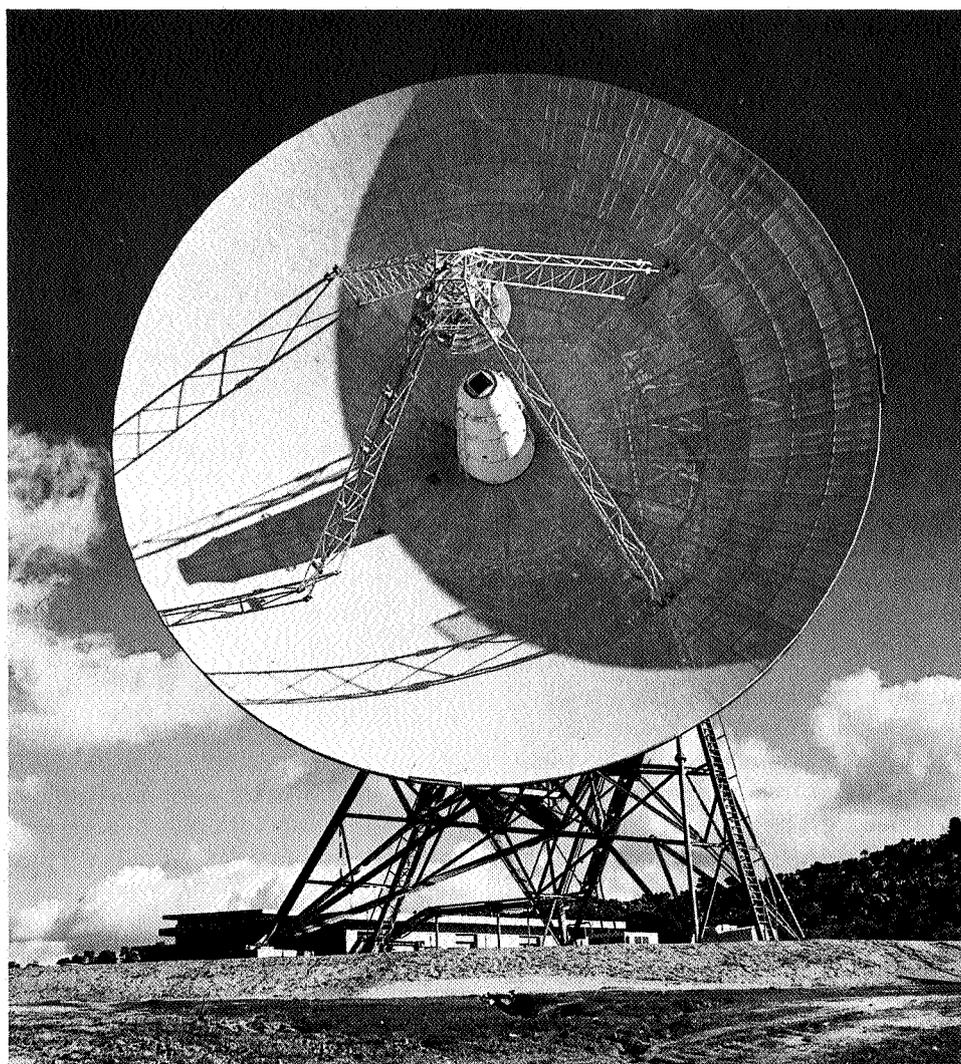


Fig. V-11. DSS 61, Robledo, Spain

**Table V-3. DSN tracking data requirements**

| Coverage and sampling rate | Data required |
|---|---|
| Track spacecraft from separation to first midcourse at 1-min sample rate; (from initial DSIF acquisition to L + 1 hr, the sample rate is 1 sample per 10 sec) | Doppler (two- and three-way), antenna pointing angles, and telemetry |
| Track spacecraft from first midcourse to touchdown at 1-min sample rate | Doppler (two- and three-way), antenna pointing angles, and telemetry |
| Track spacecraft during midcourse maneuver and terminal maneuver executions at 1-sec sample rate, and transmit data at 10-sec sample rate | Doppler (two- and three-way or one-way), antenna pointing angles and telemetry |
| Track spacecraft from touchdown to end of mission at 1-min sample rate during 1 hr following 10-deg elevation rise, during 1 hr centered around maximum elevation, and during 1 hr prior to 10-deg elevation set for DSS 11, DSS 42, and 61 | Doppler (two- and three-way) and telemetry |

In addition to the basic support provided by prime stations, the following support was provided for the *Surveyor III* mission:

(1) DSS 71, Cape Kennedy, provided facilities for spacecraft/DSIF compatibility testing, and also received and recorded telemetry data after liftoff. In addition, DSS 71 used its Command and Data Handling Console (CDC) and Telemetry and Command Processor (TCP) computer to process AFETR range telemetry data for transmission to JPL.

(2) DSS 72, Ascension Island, provided tracking, telemetry, and command functions from launch until 1 hr after DSS 11 acquisition. The DSS 72 two-way doppler tracking capability provided data for pre-midcourse trajectory calculations.

(3) DSS 51, Johannesburg, South Africa, provided telemetry coverage to fill in the gap between DSS 42 set and DSS 61 rise on a best effort basis. In addition, the command and two-way capability of DSS 51 was exercised on a best effort basis.

(4) DSS 12, DSCC, Barstow, California, provided backup command capability during the following critical phases of the mission: midcourse correction, terminal descent, and first pass after touchdown.

Data is handled by the prime DSIF stations as follows:

(1) Tracking data, consisting of antenna pointing angles and doppler (radial velocity) data, is supplied in near-real-time via teletype to the SFOF and post-flight in the form of punched paper tape. Two- and three-way doppler data is supplied full-time during the lunar flight, and also during lunar operations when requested by the *Surveyor* Project Office. The two-way doppler function implies a transmit capability at the prime stations.

(2) Spacecraft telemetry data is received and recorded on magnetic tape. Baseband telemetry data is supplied to the CDC for decommutation and real-time readout. The DSIF also performs precommunication processing of the decommutated data, using an on-site data processing (OSDP) computer. The data is then transmitted to the SFOF in near-real-time over high-speed lines (HSDL).

(3) Video data is received and recorded on magnetic tape. This data is sent to the CDC and, at DSS 11 only, to the spacecraft TV Ground Data Handling System (TV-GDHS, TV-11) for photographic recording. In addition, video data from DSS 11 is sent in real-time to the SFOF for magnetic and photographic recording by the TV-GDHS, TV-1. After lunar landing, DSS 11 performs a special function. Two receivers are used for different functions. One provides a signal to the CDC, the other to the TV-GDHS. (Signals for the latter system are the prime *Surveyor* Project requirement during this phase of a mission.)

(4) Command transmission is another function provided by the DSIF. Approximately 280 commands are sent to the spacecraft during the nominal sequence from launch to touchdown. Confirmation of the commands sent is processed by the OSDP computer and transmitted by teletype to the SFOF.

The S-band tracking system characteristics are given in Table V-4.

The maximum doppler tracking rate depends on the loop noise bandwidth. For phase error of less than 30 deg and strong signal ($-100$ dbm), tracking rates are as follows:

| Loop noise bandwidths, Hz | Maximum tracking rate, Hz/sec |
|---|---|
| 12 | 100 |
| 48 | 920 |
| 152 | 5000 |

**Table V-4. Characteristics for S-band tracking systems**

| Antenna, tracking | | Transmitter | |
|---|---|---|---|
| Type | 85-ft parabolic | Frequency (nominal) | 2113 Hz |
| Mount | Polar (HA-Dec) | Frequency channel | 14b |
| Beamwidth ±3 db | ⌐0.4 deg | Power | 10 kW, max |
| Gain, receiving | 53.0 db, + 1.0, −0.5 | Tuning range | ±100 kHz |
| Gain, transmitting | 51.0 db, + 1.0, −0.5 | Modulator | |
| Feed | Cassegrain | Phase input impedance | $\geq 50\ \Omega$ |
| Polarization | LH[b] or RH circular | Input voltage | $\leq 2.5$ V peak |
| Max. angle tracking rate[a] | 51 deg/min = 0.85 deg/sec | Frequency response (3 db) | DC to 100 kHz |
| Max. angular acceleration | 5.0 deg/sec/sec | Sensitivity at carrier output frequency | 1.0 rad peak/V peak |
| Tracking accuracy ($1\sigma$) | 0.14 deg | Peak deviation | 2.5 rad peak |
| Antenna, acquisition | | Modulation deviation stability | ±5% |
| Type | 2 × 2-ft horn | Frequency, standard | Rubidium |
| Gain, receiving | 21.0 db ±1.0 | Stability, short-term ($1\sigma$) | $1 \times 10^{-11}$ |
| Gain, transmitting | 20.0 db ±2.0 | Stability, long-term ($1\sigma$) | $5 \times 10^{-11}$ |
| Beamwidth ±3 db | ⌐16 deg | Doppler accuracy at $F_{rc}$ ($1\sigma$) | 0.2 Hz = 0.03 m/sec |
| Polarization | RH circular | Data transmission | TTY and HSDL |
| Receiver | S-band | | |
| Typical system temperature With paramp With maser | 270 ±50°K 55 ±10°K | | |
| Loop noise bandwidth threshold ($2B_{L0}$) | 12, 48 or 152 Hz +0, −10% | | |
| Strong signal ($2B_{L0}$) | 120, 255, or 550 Hz +0, −10% | | |
| Frequency (nominal) | 2295 Hz | | |
| Frequency channel | 14a | | |

[a] Both axes.
[b] Goldstone only.

The angle tracking parameters for the DSS 72 30-ft antenna are as follows:

(1) Maximum azimuth tracking rate: 6 deg/sec.

(2) Maximum elevation angle tracking: 3 deg/sec.

(3) Tracking accuracy: 0.01 deg.

(4) The system doppler tracking accuracy and doppler tracking rates are the same as for 85-ft antennas.

*a. DSIF preparation testing.* Operational Readiness Tests (ORT) are conducted for each mission to verify that all prime stations, communication lines, and the SFOF are fully prepared to meet mission responsibility. Selected portions of the Sequence of Events are followed, using both standard and nonstandard procedures.

**Table V-5. Operational readiness tests**

| Test | Stations | Date, 1967 |
|---|---|---|
| C-1.5 | DSS 61 | 1/25, 26 |
| C-3.0 Phase I | DSS 11, 42, 61, 72 and AFETR | 3/20, 21, 30, 31 |
| C-3.0 Phase II | DSS 11 | 3/23, 24 |
| C-5.0 Phase I | DSS 11, 42, 51, 61, 72 and AFETR | 4/3, 4 |
| C-5.0 Phase II | DSS 11 and 61 | 4/12, 13 |

The ORT schedule is presented in Table V-5. DSS 11, 42, 51, 61, 71, and 72 participated in Phase I of the C-5.0 test, which was conducted a week prior to launch. An

evaluation of station and Net Control support during the ORT indicated the readiness of the TDS.

*Surveyor* on-site computer program (SOCP) integration tests are conducted to check out the SOCP and to verify that data can be transmitted from a DSIF station to the SFOF and then processed. Such tests were run on a regular basis with each prime station (DSS 11, 42, and 61). These tests were concluded with a checkout of the final SOCP program in April 1967. Operational tests continued up until 4 days prior to launch to provide additional training for operational personnel.
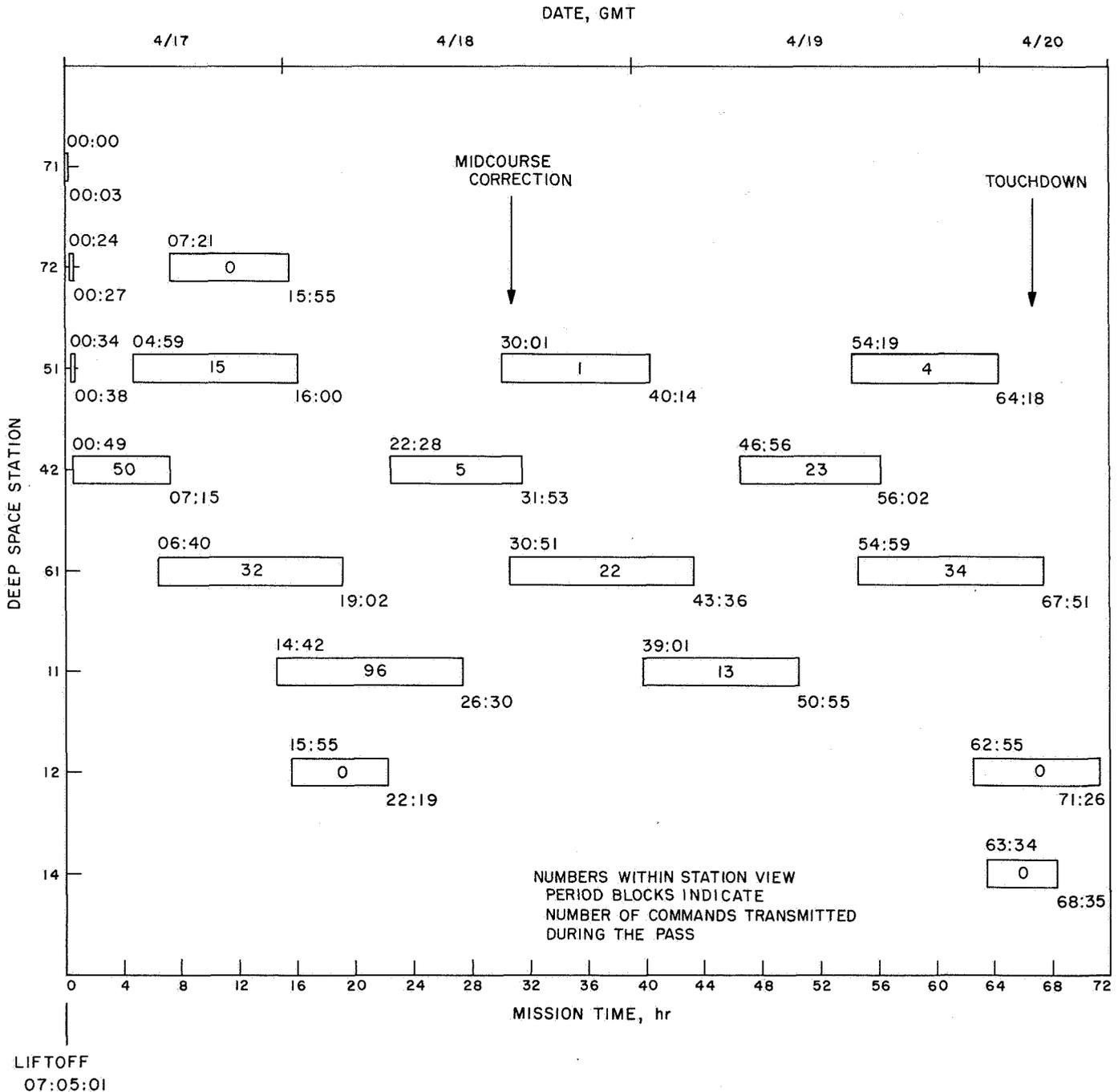


**Fig. V-12. DSIF station tracking periods and command activity: transit phase**
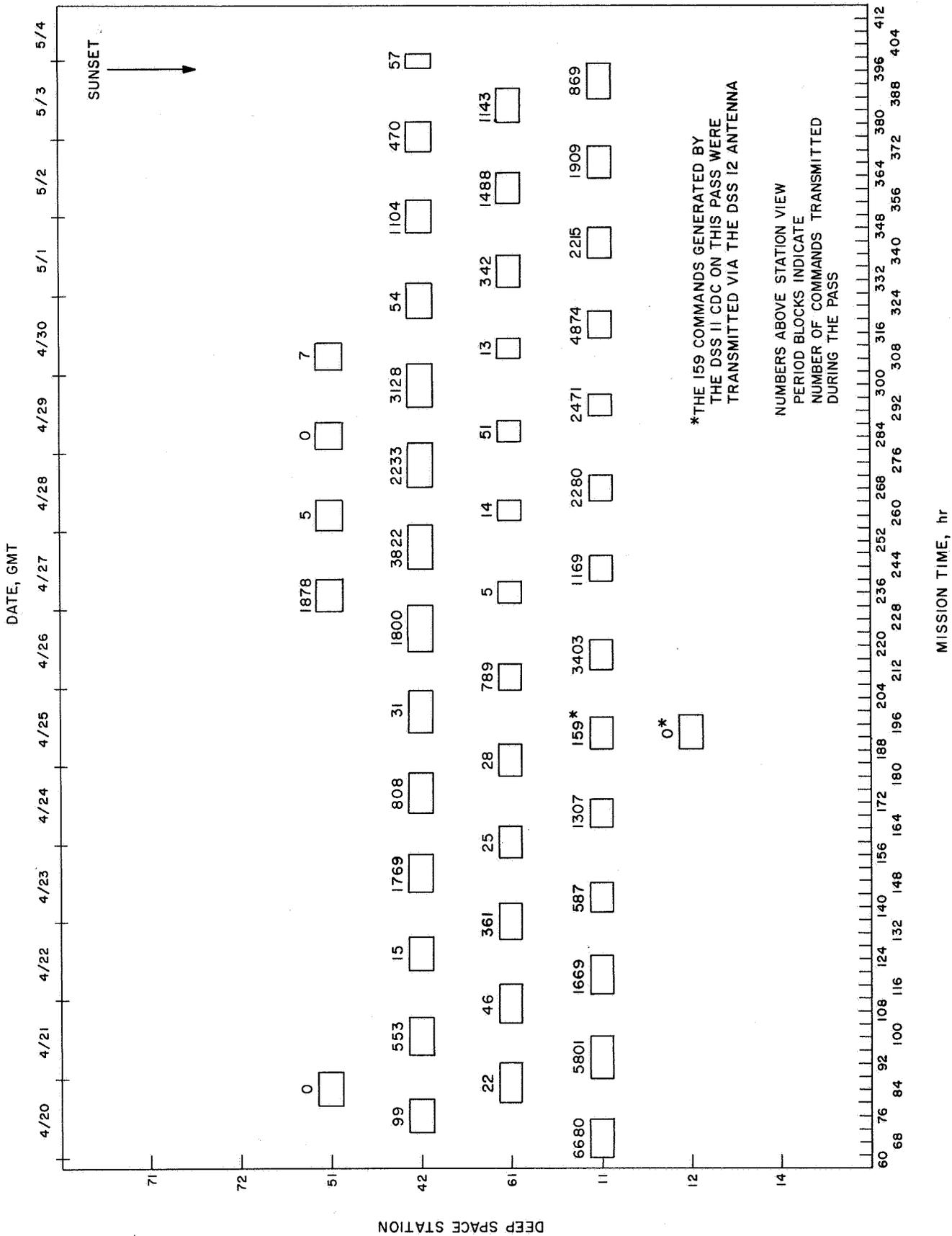
Fig. V-13. DSIF station tracking periods and command activity: posttouchdown

*b. DSIF flight support.* All of the DSIF prime and engineering training stations reported "go" status during the countdown. All measured station parameters were within nominal performance specifications, and communications circuits were up.

Figs. V-12 and V-13 are profiles of the DSIF mission activity from launch until the end of the first lunar day. (Also refer to the station view periods indicated in Fig. VII-3.) This figure contains the periods each station tracked the spacecraft plotted against mission time from liftoff, and the number of commands transmitted by each DSS during each pass. Table V-6 presents the total number of commands sent by each station during the mission.

### Table V-6. Commands transmitted by DSIF stations

|  | DSS 71 | DSS 72 | DSS 51 | DSS 42 | DSS 61 | DSS 11 |
|---|---|---|---|---|---|---|
| Station total | 0 | 0 | 1910 | 16,021 | 4415 | 35,502 |

The DSIF Stations supported *Surveyor III* with a high level of performance. Continuous tracking and telemetry coverage was provided from $L + 00:49$ to the end of the first lunar day.

High-quality angular tracking and two-way doppler data were received throughout the *Surveyor III* mission, the only exception being the first pass of DSS 61. A dropped 8 bit in the least significant digit of the DSS 61 doppler counter caused excessive noise in the DSS 61 data. A transfer to DSS 51 could not be scheduled until approximately 2 hr later because of Canopus acquisition. DSS 61 twice stopped three-way tracking for doppler counter repair, resuming operations 2½ hr later. Approximately 2 hr of two-way doppler data was lost. The effect on the mission was negligible.

The signal levels received at the DSIF stations are shown in Fig. V-14, and correspond very closely to the predicted levels. The predicted levels for the pre-star-acquisition track are not given as the spacecraft was not roll-stabilized during this period. Therefore, the received signal level could vary over a wide range owing to variations in spacecraft antenna patterns. During star acquisition, midcourse correction, and touchdown, the spacecraft was in high-power mode and the received signal was 20 db above the low-power signal level. The periods during which gyro drift test were conducted are shown at the top of the figure. The random gyro drift and sub-

sequent antenna pattern variations produced a spread in the received signal levels of ±3 db.

Consistent with its 30-ft antenna, DSS 72 signal levels were approximately 10 db below signal levels received by the stations with 85-ft antennas.

A number of minor equipment anomalies and procedural problems occurred, but were readily corrected by station personnel without affecting the mission.

The DSS 42 S-band acquisition aid (SAA) exhibited an intermittent fault prior to launch; the SAA servo system developed a bias in the hour angle (HA) channel which could have jeopardized initial acquisition of the spacecraft. Had the fault occurred during acquisition, the angle rates were sufficiently low so that the spacecraft could have been acquired using nonstandard techniques.

The anomalies in several components of the tracking data handling (TDH) system, which resulted in loss of DSS 61 tracking data several times during the mission, also indicate reliability problems with this unit.

The DSN received and recorded a total of 10,029 TV pictures. Of this total, 6324 pictures were sent in response to DSS commands and 3705 were received (noncommanded) simultaneously by other stations during common view periods. Table V-7 shows the support provided by DSIF stations receiving TV pictures.

### Table V-7. TV pictures received by DSIF stations

| DSS | Commanded | Noncommanded |
|---|---|---|
| 42 | 1726 | 1412 |
| 51 | 0 | 70 |
| 61 | 31 | 504 |
| 11 | 4567 | 1719 |
| Total | 6324 | 3705 |

At about 00:04 GMT, May 4, 1967, *Surveyor III* operation was terminated for the lunar night. An attempt to revive the spacecraft for second lunar day activity was initiated at DSS 61 rise, which occurred on May 23 at 20:52 GMT. Engineering and scientific experiments that were to be conducted included telemetry, video, and antenna mapping. The DSN was committed to 24-hr/day coverage for three 24-hour periods, using DSS 61, 11, and 42.

Spacecraft revival was attempted during three passes of DSS 61 and 42, and four passes of DSS 11. These sta-
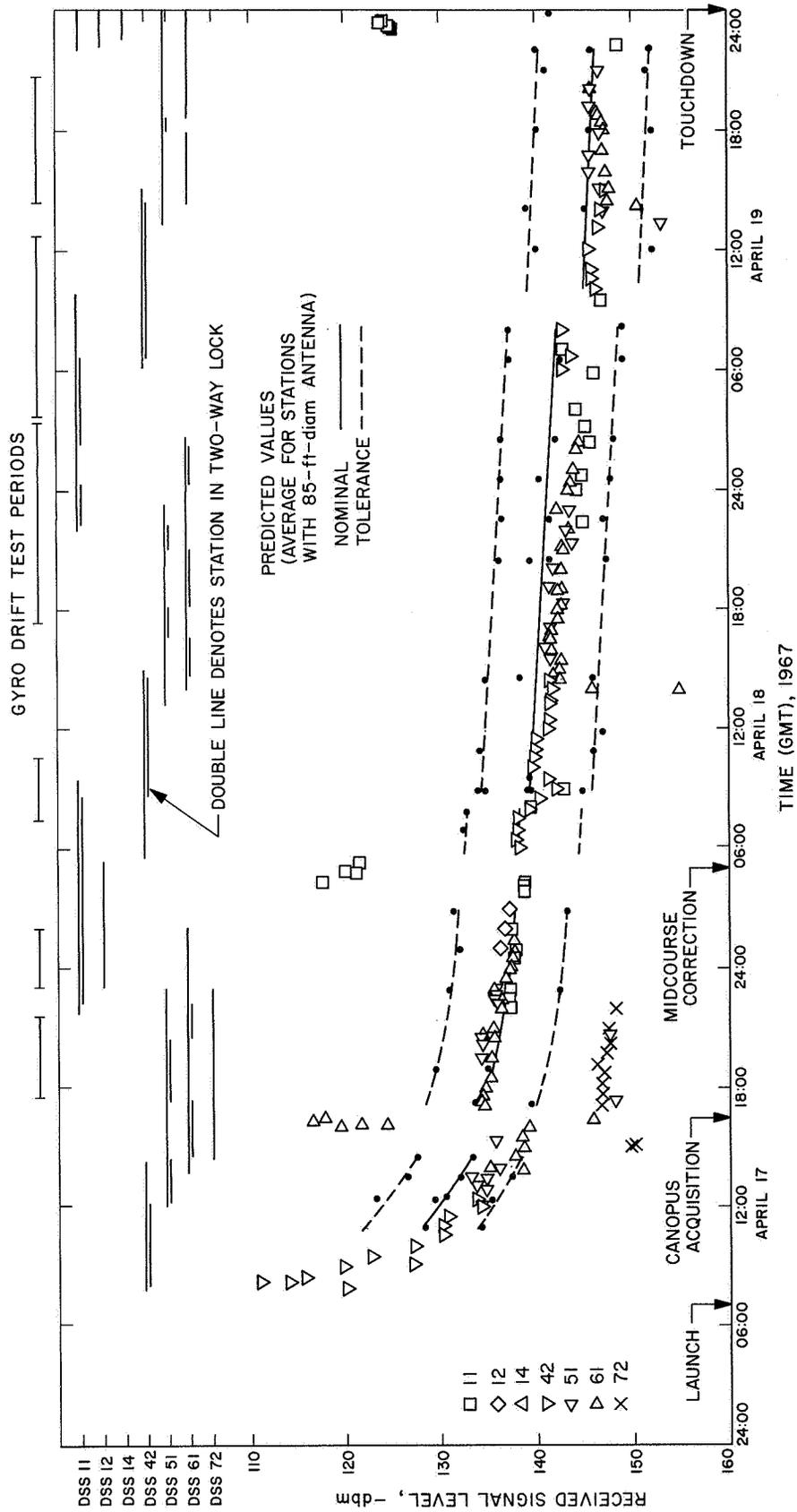
Fig. V-14. DSIF received signal level

Fig. V-15. DSN/GCS communications links

tions performed a spacecraft receiver search over the entire radio frequency tuning range, but no carrier signals were received. All attempts to revive the spacecraft for second lunar day activity were unsuccessful. The final attempt was made by DSS 11 on June 2 after which the *Surveyor III* mission was terminated.

## 2. GCS/NASCOM

For *Surveyor* missions, the GCS transmits tracking, telemetry, and command data from the DSIF to the SFOF, and control and command functions from the SFOF to the DSIF by means of NASCOM facilities. The GCS also transmits simulated tracking data to the DSIF and video data and base-band telemetry from DSS 11, Goldstone DSCC, to the SFOF. The links involved in the system are shown in Fig. V-15.

The GCS/NASCOM demonstrated a high degree of reliability during the Operational Readiness Tests conducted before the mission. The performance of the NASCOM facilities in support of the *Surveyor III* mission was considered excellent, demonstrating a high degree of reliability.

*a. Teletype (TTY) circuits.* Teletype circuits (four available to prime stations) are used for transmitting tracking data, telemetry, commands, and administrative traffic. The teletype circuits were exceptionally reliable, the weakest circuits (DSS 61) showing approximately 98% reliability.

Approximately 3 hr of data was lost on DSS 51 teletype circuits because of propagation problems over high-frequency radio paths. DSS 61 was called up on an emergency basis to cover the remainder of the DSS 51 pass.

During the mission and the final operational readiness test (C-5.0), the DSS 72 tracking data and operational message circuits were routed via satellite and performed excellently. A 3-hr delay in bringing up one circuit from DSS 71 during the first operational readiness test (C-3.0) was due to rewiring at Cape Kennedy, with no make-good circuits available. All circuits to DSS 61 were lost during the C-5.0 test because of a shorted cable at Garden City, Va.

*b. Voice circuits.* The voice circuits are shared between the DSIF and the *Surveyor* Project for administrative, control, and commanding functions. The NASCOM voice circuits provided for the *Surveyor III* mission performed perfectly except for failures which occurred in the circuits

to the Johannesburg station (DSS 51) prior to launch due to propagation conditions. A commercial overseas telephone circuit was established but also was not usable. The NASCOM voice circuit was restored at $L + 25$ min.

The DSS 72 voice circuit was routed via satellite during both the mission and C-5.0 test and performed exceptionally well.

*c. High-speed data line (HSDL).* One HSDL is provided to each prime site for telemetry data transmission to the SFOF in real-time. This part of the communications system performed well during both the mission and testing phase.

Both modem* types (NASCOM and Hallicrafter) were required during the *Surveyor III* mission, since the Johannesburg station (DSS 51) is not equipped with NASCOM modems.

During the C-3.0 ORT, DSS 51 experienced a test pattern acquisition problem which subsequently cleared before a valid cause could be determined. The transmit side of the lines was used during testing to transmit simulation data to the stations and during the mission to backfeed various voice nets as required.

*d. Wideband microwave system.* The wideband microwave link between DSS 11, Goldstone DSCC, and the SFOF consists of one 6-MHz simplex (one-way) channel for video, and one 96-kHz duplex (two-way) data channel. The link performed with 100% reliability during the *Surveyor III* mission.

## 3. DSN in SFOF and DSN Interfaces with AFETR and MSFN, Carnarvon

The DSN supports the *Surveyor* missions by providing mission control facilities and performing special functions within the SFOF. The DSN also provides an interface with the AFETR for real-time transmission of downrange spacecraft telemetry data from Building AO at Cape Kennedy to the SFOF.

*a. Data processing system (DPS).* The SFOF Data Processing System performs the following functions for *Surveyor* missions.

(1) Computation of acquisition predictions for DSIF stations (antenna pointing angles and receiver and transmitter frequencies).

---

*A modem (modulator-demodulator) is a device for converting a digital signal to a signal which is compatible with telephone line transmission (e.g., a frequency-modulated tone).

(2) Orbit determinations.

(3) Midcourse maneuver computations analysis.

(4) On-line telemetry processing.

(5) Command tape generation.

(6) Simulated data generation (telemetry and tracking data for tests).

The DPS general configuration for the *Surveyor III* mission is shown in Fig. V-16 and consists of two PDP-7 computers in the telemetry processing station (TPS), two strings of IBM 7044/7094 computers in the Central Computing Complex (CCC), and a subset of the input/output (I/O) system.

The DPS performed in a nominal manner, with only minor hardware problems which did not detract from mission support. The two PDP-7 computers were used extensively to process high-speed telemetry data for the

*Surveyor III* mission. This processing consisted of de-commutating and transferring the data to the 7044 computer via the 7288 data channels, generating a digital tape for non-real-time processing, and supplying digital-to-analog converters with discrete data parameters to drive analog recorders in both the Spacecraft Analysis Area and the Space Science Analysis Area.

The IBM 7044/7094 computer string dual configuration successfully processed all high-speed data received from the TPS and all teletype data received from the communications center, as well as all input/output requests from the user areas.

The problems experienced in the Central Computing Complex were quite easily remedied and had little or no effect on the mission.

The input/output system provides the capability for entering data control parameters into the 7044/7094 computers and also for displaying computed data in the
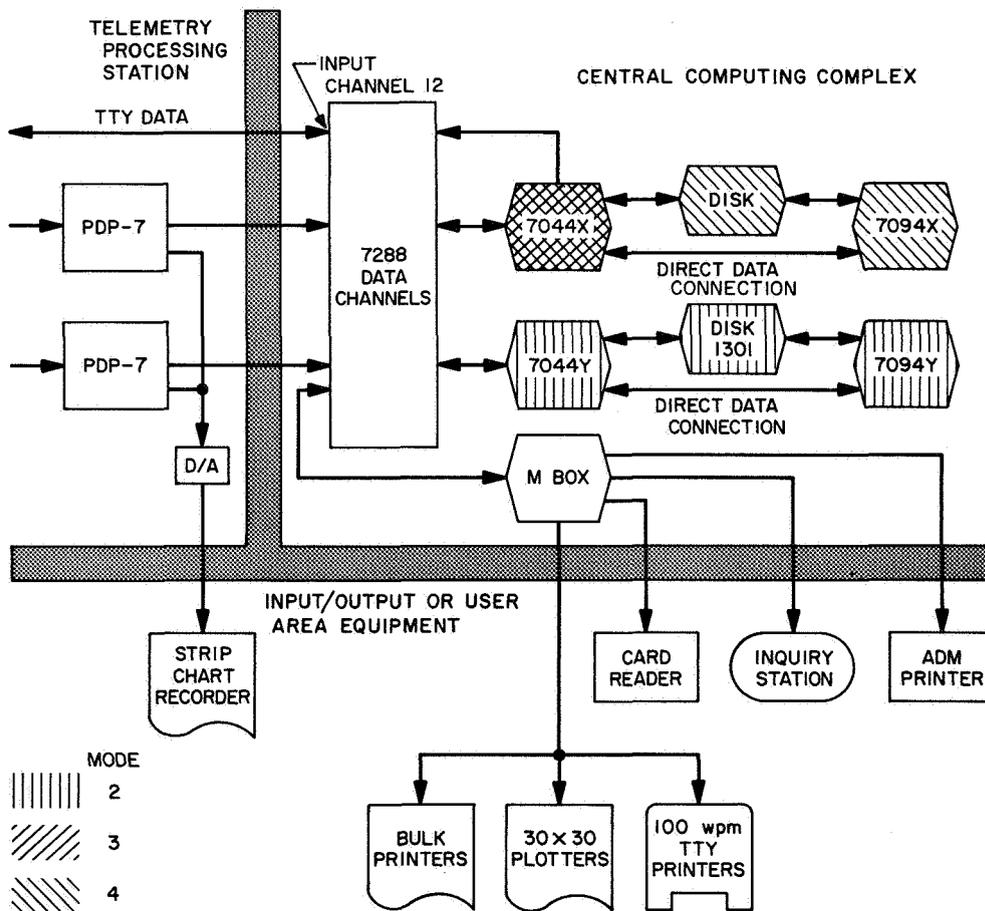


Fig. V-16. General configuration of SFOF data processing system

user areas via the various display devices. The input/ output system performed adequately, with only a few problems reported.

**b. DSN Intracommunications System (DSN/ICS).** The DSN/ICS provides the capability of receiving, switching, and distributing all types of information required for spaceflight operations and data analysis to designated areas or users within the SFOF. The system includes facilities for handling all voice communications, closed circuit television, teletype, high-speed data, and data received over the microwave channels.

The DSN/ICS performed in an exceptional manner, with only minor anomalies. The large number of patches required on the Mission Commentary Net ("Voice of Surveyor") caused minor patching problems. During the touchdown phase, patches were made to Edwards Air Force Base and The Boeing Company, Seattle, in addition to the NASA and DSN requirements. The Surveyor Command Net was patched at all times to the active voice net. However, a delay in patching to the DSS 11 voice net was rectified in real-time.

NASCOM modems were used for sending high-speed data from all stations except DSS 51, and reliability was very high. DSS 51 used the Hallicrafter modem, which performed reliably, with only circuit problems due to propagation.

The Communications/TV Ground Handling System 6-MHz video line was subjected to extensive tests prior to the mission, and no problems were experienced during the mission.

**c. DSN/AFETR interface.** The DSN/AFETR interface provides real-time data transmission capability for both VHF and S-band downrange telemetry. The nominal switchover time is after the spacecraft S-band transmitter is turned to high power. The interface with the Surveyor Project is at the input to the CDC, Building AO, where it is sent to DSS 71 for processing by the CDC and the telemetry and command processor (TCP) computer. The output of the CDC is transmitted to the SFOF via the GCS/NASCOM. On the Surveyor III mission, this configuration was established as the prime link between the SFOF and AFETR to provide an interface similar to the data transmission links with prime DSIF stations. The previously used link between Building AO and SFOF, via Bell modems, was retained as backup.

In-flight spacecraft telemetry was received from the AFETR stations and relayed to the SFOF via DSS 71 until approximately $T + 56$ min. The first use of the configuration was quite successful.

**d. DSN/MSFN, Carnarvon interface.** A new system was implemented for transmission of Surveyor real-time telemetry data from the MSFN station at Carnarvon, Australia, to the SFOF. Carnarvon transmitted the 550 bit/sec spacecraft data to DSS 42 using a Bell modem. At DSS 42, the output was fed to the CDC, where it entered the normal system for processing and transmission back to the SFOF. The purpose of implementing this capability was to provide spacecraft data prior to DSS 42 rise in order to extend TDS coverage.

Data was transmitted via this path from Carnarvon acquisition at 07:48:01 GMT until switchover to DSS 42 data at 07:58:50, a period of just under 11 min.

# VI. Mission Operations System

## A. Functions and Organization

The basic functions of the Mission Operations System (MOS) are the following:

(1) Continual assessment and evaluation of mission status and performance, utilizing the tracking and telemetry data received and processed.

(2) Determination and implementation of appropriate command sequences required to maintain spacecraft control and to carry out desired spacecraft operations during transit and on the lunar surface.

The *Surveyor* command system philosophy introduces a major change in the concept of unmanned spacecraft control: virtually all in-flight and lunar operations of the spacecraft must be initiated from earth. In previous space missions, spacecraft were directed by a minimum of earth-based commands. Most in-flight functions of those spacecraft were automatically controlled by an on-board sequencer which stored preprogrammed instructions. These instructions were initiated by either an on-board timer or by single direct commands from earth. For example, during the *Ranger VIII* 67-hr mission, only

11 commands were sent to the spacecraft; whereas for a standard *Surveyor* mission, approximately 280 commands must be sent to the spacecraft during the transit phase, out of a command vocabulary of 256 different direct commands. For *Surveyor III*, 345 commands were sent during transit and 57,503 commands were sent following touchdown.

Throughout the space flight operations of each *Surveyor* mission, the command link between earth and spacecraft is in continuous use, transmitting either fill-in or real commands every 0.5 sec. The *Surveyor* commands are controlled from the SFOF and are transmitted to the spacecraft by a DSIF station.

The equipment utilized to perform MOS functions falls into two categories: mission-independent and mission-dependent equipment. The former is composed chiefly of the *Surveyor* TDS equipment described in Section V. It is referred to as mission-independent because it is general-purpose equipment which can be utilized by more than one NASA project when used with the appropriate project computer programs. Selected parts of this equipment have been assigned to perform the functions

necessary to the *Surveyor* Project. The mission-dependent equipment (described in Section VI-B, following) consists of special equipment which has been installed at DSN facilities for specific functions peculiar to the project.

The *Surveyor* Project Manager, in his capacity as Mission Director, is in full charge of all mission operations. The Mission Director is aided by the Assistant Mission Director and a staff of mission advisors. During the mission, the MOS organization was as shown in Fig. VI-1.

Mission operations are under the immediate, primary control of the Space Flight Operations Director (SFOD) and supporting *Surveyor* personnel. Other members of

the team are the TDS personnel who perform services for the *Surveyor* Project.

During space flight and lunar surface operations, all commands are issued by the SFOD or his specifically delegated authority. Three groups of specialists provide technical support to the SFOD in the flight path, spacecraft performance, and science areas.

### 1. Flight Path Analysis and Command Group

The Flight Path Analysis and Command (FPAC) group handles those space flight functions that relate to the location of the spacecraft. The FPAC Director maintains control of the activities of the group and makes specific
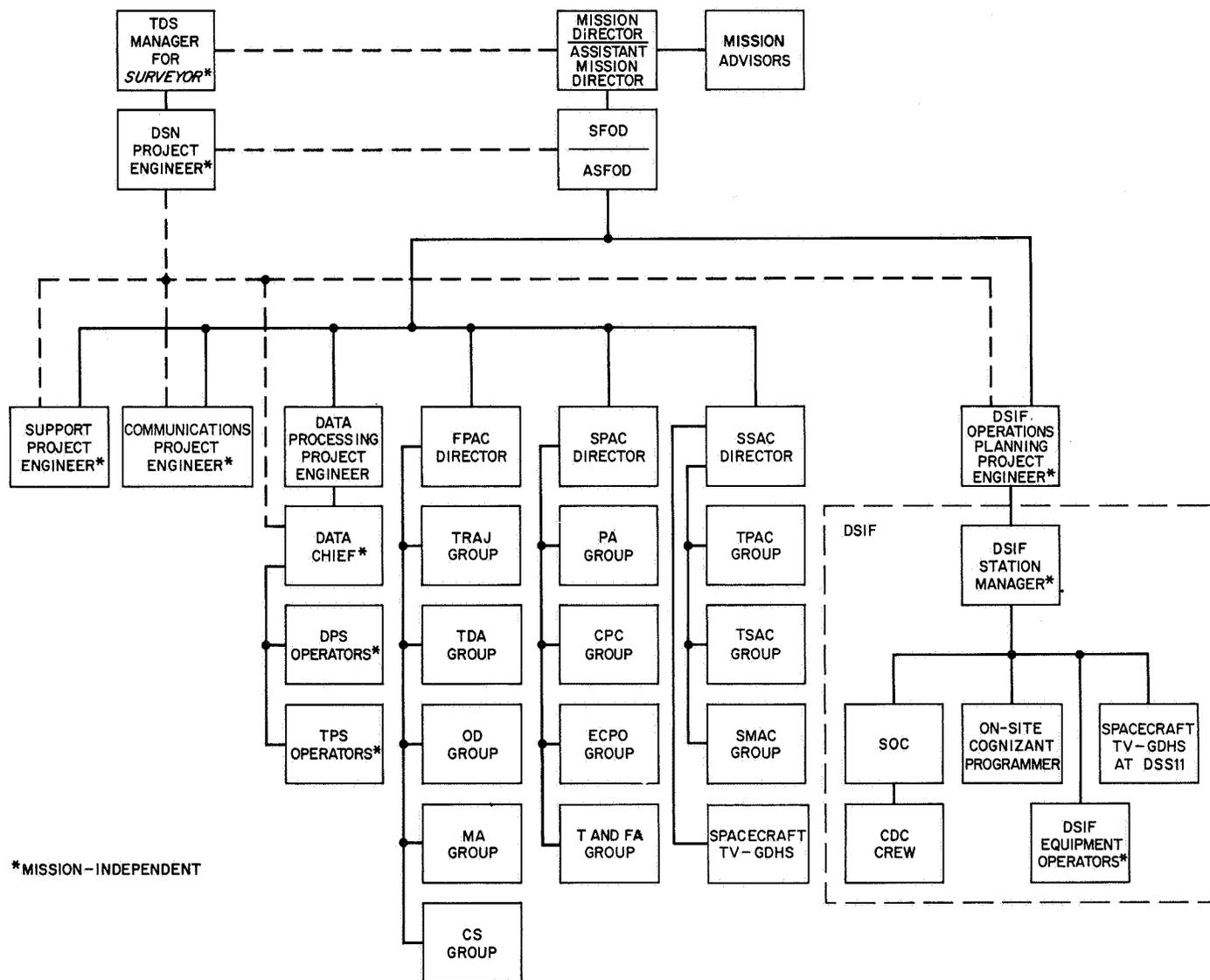


**Fig. VI-1. Organization of MOS during the *Surveyor III* mission**

recommendations for maneuvers to the SFOD in accordance with the flight plan. In making these recommendations, the FPAC Director relies on five subgroups of specialists within the FPAC group.

(1) The Trajectory (TRAJ) group determines the nominal conditions of spacecraft injection and generates lunar encounter conditions based on injection conditions as reported by AFETR and computed from tracking data by the Orbit Determination group. The actual trajectory determinations are made by computer.

(2) The Tracking Data Analysis (TDA) group makes a quantitative and descriptive evaluation of tracking data received from the DSIF stations. The TDA group provides 24-hr/day monitoring of incoming tracking data. To perform these functions the TDA group takes advantage of the Data Processing System (DPS) and of computer programs generated for their use. The TDA group acts as direct liaison between the data users (the Orbit Determination group) and the DSIF and provides predicts to the DSIF.

(3) The Orbit Determination (OD) group, during mission operations, determines the actual orbit of the spacecraft by processing the tracking data received from the DSN tracking stations by way of the TDA group. Also, statistics on various parameters are generated so that maneuver situations can be evaluated. The OD group generates tracking predictions for the DSIF stations and recomputes the orbit of the spacecraft after maneuvers to determine the success of the maneuver.

(4) The Maneuver Analysis (MA) group is the subgroup of FPAC responsible for developing possible midcourse and terminal maneuvers for both standard and nonstandard missions in real-time during the actual flight. In addition, once the decision has been made as to what maneuver should be performed, the MA group generates the proper spacecraft commands to effect these maneuvers. These commands are then relayed to the Spacecraft Performance Analysis and Command group to be included with other spacecraft commands. Once the command message has been generated, the MA group must verify that the calculated commands are correct.

(5) The Computer Support (CS) group acts in a service capacity to the other FPAC subgroups, and is responsible for ensuring that all computer programs

used in space operations are fully checked out before mission operations begin and that optimum use is made of the Data Processing System facilities.

## 2. Spacecraft Performance Analysis and Command Group

The Spacecraft Performance Analysis and Command (SPAC) group, operating under the SPAC Director, is basically responsible for the operation of the spacecraft itself. The SPAC group is divided into four subgroups:

(1) The Performance Analysis (PA) group monitors incoming engineering data telemetered from the spacecraft, determines the status of the spacecraft, and maintains spacecraft status displays throughout the mission. The PA group also determines the results of all commands sent to the spacecraft. In the event of a failure aboard the spacecraft, as indicated by telemetry data, the PA group analyzes the cause and recommends appropriate nonstandard procedures.

(2) The Command Preparation and Control (CPC) group is basically responsible for preparing command sequences to be sent to the spacecraft. In so doing they provide inputs for computer programs used in generating the sequences, verify that the commands for the spacecraft have been correctly received at the DSS, and then ascertain that the commands have been correctly transmitted to the spacecraft. If nonstandard operations become necessary, the group also generates the required command sequences. The CPC group controls the actual transmission of commands at the DSS by the *Surveyor* operations chief.

(3) The Engineering Computer Program Operations (ECPO) group includes the operators for the DPS input/output (I/O) console and related card punch, card reader, page printers, and plotters in the spacecraft performance analysis area (SPAA). The ECPO group handles all computing functions for the rest of the SPAC group, including the maintenance of an up-to-date list of parameters for each program.

(4) The Trend and Failure Analysis (T&FA) group consists of spacecraft design and analysis specialists who provide in-depth, near-real-time spacecraft performance analysis (in contrast to the PA group's real-time analysis). The group also manages the interface for the SCCF computer facility at Hughes Aircraft Company. The SCCF 1219 is used mainly

for premission spacecraft ground testing, but during the mission the T&FA group is provided two dataphone out-links to the SCCF 1219 via the TPS and seven incoming lines terminating at seven teleprinters in the SPAC area. The T&FA group uses the system to process and display engineering data transmitted from the spacecraft. The group also includes draftsmen who perform wall chart plotting and maintain wall displays of spacecraft condition and performance.

### 3. Space Science Analysis and Command Group

The Space Science Analysis and Command (SSAC) group performs those space flight functions related to the operation of the survey TV camera and the SM/SS. SSAC is divided into three operating subgroups:

(1) The Television Performance Analysis and Command (TPAC) group analyzes the performance of the TV equipment and is responsible for generating standard and nonstandard command sequences for the survey TV camera.

(2) The Television Science Analysis and Command (TSAC) group analyzes and interprets the TV pictures for the purpose of ensuring that the mission objectives are being met. The TSAC group is under the direction of the Project Scientist and performs the scientific analysis and evaluation of the TV pictures.

(3) The Soil Mechanics Analysis and Command (SMAC) group prepares and recommends the commands to be sent to the SM/SS. This group is also responsible for operating the SM/SS and analyzing its performance.

The portion of the spacecraft TV Ground Data Handling System (TV-GDHS) in the SFOF provides direct support to the SSAC group in the form of processed electrical video signals and finished photographic prints. The TV-GDHS operates as a service organization within the MOS structure. Documentation, system checkout, and quality control within the system are the responsibility of the TV-GDHS Operations Manager. During operations support the TV-GDHS Operations Manager reports to the SSAC Director.

### 4. Data Processing Personnel

The use of the Data Processing System (DPS) by *Surveyor* is under the direction of the Assistant Space Flight Operations Director (ASFOD) for Computer Programming. His job is to direct the use of the DPS from

the viewpoint of the MOS. He communicates directly with the Data Chief, who is in direct charge of DPS personnel and equipment. Included among these personnel are the I/O console operators throughout the SFOF, as well as the equipment operators in the DPS and Telemetry Processing Station (TPS) areas.

Computer programs are the means of selecting and combining the extensive data processing capabilities of electronic computers. By means of electronic data processing, the vast quantities of mission-produced data are assembled, identified, categorized, processed and displayed in the various areas of the SFOF where the data are used. Their most significant service to the MOS is providing knowledge in real-time of the current state of the spacecraft throughout the entire mission. This service is particularly important to engineers and scientists of the technical support groups since, by use of the computer programs, they can select, organize, compare and process current-status data urgently needed to form their time-critical recommendations to the SFOD. (See Section V-C-3 for a description of the DPS.)

### 5. Other Personnel

The Communications Project Engineer (PE) controls the operational communications personnel and equipment within the SFOF, as well as the DSN/GCS lines to the DSIF stations throughout the world.

The Support PE is responsible for ensuring the availability of all SFOF support functions, including air conditioning and electric power; for monitoring the display of *Surveyor* information on the Mission Status Board and throughout the facility; for directing the handling, distribution, and storage of data being derived from the mission; and for ensuring that only those personnel necessary for mission operations are allowed to enter the operational areas.

The DSIF Operations Planning PE is in overall control of all DSIF stations; his post of duty is in the SFOF in Pasadena. At each station, there is a local DSIF station manager, who is in charge of all aspects of his DSIF station and its operation during a mission. The *Surveyor* personnel located at each station report to the station manager.

### B. Mission-Dependent Equipment

Mission-dependent equipment consists of special hardware provided exclusively for the *Surveyor* Project to

support the Mission Operations System. Most of the equipment in this category is contained in the Command and Data Handling Consoles (CDC) and spacecraft Television Ground Data Handling System (TV-GDHS), which are described below.

## 1. Command and Data Handling Console

*a. CDC equipment.* The Command and Data Handling Console comprises that mission-dependent equipment, located at the participating Deep Space Stations, that is used to:

(1) Generate commands for control of the *Surveyor* spacecraft by modulation of the DSS transmitter.

(2) Process and display telemetered spacecraft data and relay telemetry signals to the on-site data processor (OSDP) for transmission to the SFOF.

(3) Process, display, and record television pictures taken by the spacecraft.

The CDC consists of four major subsystems:

(1) The command subsystem generates FM digital command signals from punched tape or manual inputs for the DSS transmitter, and prints a permanent record of the commands sent. The major units of the command subsystem, which can accommodate 1024 different commands, are the command generator, the command subcarrier oscillator, the punched tape reader, and the command printer. Outgoing commands are logged on magnetic tape by the DSS and are relayed to the SFOF.

(2) The FM demodulator subsystem accepts the FM intermediate-frequency signal of the DSS receiver and derives from it a baseband signal. The baseband signal consists of either video data or a composite of engineering subcarrier signals. Depending upon the type of data constituting the baseband signal, the CDC processes the data in either the TV data subsystem or the telemetry data subsystem.

(3) The TV data subsystem receives video data from the FM demodulator and processes it for real-time display at the CDC and for 35-mm photographic recording. In addition, telemetered frame-identification data is displayed and photorecorded. A long-persistence-screen TV monitor is mounted in the CDC. The operator, when requested, can thus evaluate the picture and, upon the SFOD's direction, initiate corrective commands during lunar television surveys.

(4) The telemetry data subsystem of the CDC separates the various data channels from the baseband signal coming from either the FM demodulator or the DSS receiver phase-detected output and displays the desired data to the operators. Discriminators are provided for each subcarrier channel contained in the baseband signal. In the case of time-multiplexed data, the output of each discriminator is sent to the pulse code modulation (PCM) decommutator and then relayed to both the OSDP computer for subsequent transmission to the SFOF and to meters for evaluation of spacecraft performance. In the case of continuous data transmissions, the output of the discriminator is sent to an oscillograph for recording and evaluation.

The CDC contains built-in test equipment to ensure normal operations of its subsystems. A CDC tester, consisting of a spacecraft transponder with the necessary modulation and demodulation equipment, ensures day-to-day compatibility of the CDC and DSIF stations.

*b. CDC operations.* Table VI-1 lists the CDC mission-dependent equipment provided for support of *Surveyor III* at the DSIF stations. CDC's were located at DSS 11, 42, 51, 61, 71, and 72, and during the mission, CDC operations were conducted at each of these stations.

**Table VI-1. CDC mission-dependent equipment support of *Surveyor III* at DSIF stations**

| | |
|---|---|
| DSS 11, Goldstone | Prime station with command, telemetry, and TV |
| DSS 42, Canberra | Prime station with command, telemetry, and TV |
| DSS 51, Johannesburg | Prime station for telemetry during cislunar phase |
| DSS 61, Madrid | Prime station with command, telemetry, and TV |
| DSS 71, Cape Kennedy | Station used for spacecraft compatibility tests and pre- and post-launch telemetry data processing |
| DSS 72, Ascension | Station used in a standby basis for telemetry and command |
| DSS 12, Goldstone | Station configured for command backup and telemetry reception via the DSS 11 CDC |
| DSS 14, Goldstone | Station used to record terminal descent and landing phase |

**Table VI-2. *Surveyor III* command and TV activity**

| Station | Commands transmitted | TV pictures commanded |
|---------|---------------------|----------------------|
| DSS 11 | 35,502 | 4,567 |
| DSS 42 | 16,021 | 1,726 |
| DSS 51 | 1,910 | 0 |
| DSS 61 | 4,415 | 31 |
| DSS 71 | 0 | 0 |
| DSS 72 | 0 | 0 |

Table VI-2 lists the number of commands transmitted and the number of TV frames initiated by each station during the first lunar day.

(1) DSS 11, Goldstone

The *Pioneer* station at Goldstone participated in 16 passes. This station used a full CDC with command, telemetry, and TV equipment. During SM/SS operation, the CDC was not used to process television pictures; the TV-GDHS processed these pictures since rapid changeover from TV to telemetry was desired.

An interface was established with DSS 12, Echo station, for command backup. If necessary the CDC command subcarrier oscillator could be patched to the intersite microwave link for transmission to the Echo site. This mode was used during Pass 8 (April 25), and 159 commands were transmitted from DSS 12. That station also received the telemetry signal, and it was sent via the microwave link to the CDC at DSS 11, where it was processed in the normal manner.

Two dataphone links were established with Hughes Aircraft Company (HAC), El Segundo, California. One line carried the reconstructed telemetry PCM waveform to HAC from the CDC decommutator. The second line carried the command waveform obtained at the CDC system tester.

During the mission, several commands were transmitted to the spacecraft in error. These were all the result of operator error. None had an effect upon the mission except for two extra mirror stepping commands sent and one extra TV start frame command.

(2) DSS 42, Canberra

The first data processed by this station was approximately 11 min of spacecraft telemetry data

received from the MSFN tracking station at Carnarvon, Australia, via a dataphone line with DSS 42. DSS 42 processed the data and relayed it to the SFOF. Eleven minutes later DSS 42 was in view of the spacecraft and started to process its own data. This station participated in 17 passes during the first lunar day. The CDC configuration was standard, with the full capability available.

(3) DSS 51, Johannesburg

This station participated in 8 passes during the first lunar day. The station was committed to receive and record telemetry and tracking data during the mission on a best effort basis only. Shortly prior to *Surveyor III* launch, the DSS 51 equipment was changed from the L/S-band configuration to the full S-band configuration and full testing had not been completed. The CDC was operating with less than a full complement of spares and test equipment since some items had been sent to DSS 61 for this mission. The CDC was able to process approximately 3 min of data during the initial postinjection phase immediately after *Surveyor/Centaur* separation.

AFETR Station 13 at Pretoria observed the *Surveyor/Centaur* separation event. One CDC operator from DSS 51 was at Pretoria for this event and performed real-time evaluation of the data.

(4) DSS 61, Madrid

This station participated in 15 passes during the first lunar day. Between the *Surveyor II* and the *Surveyor III* missions, the CDC at DSS 61 was moved and the station was modified for Manned Space Flight Network support. Consequently, retesting was required on much of the CDC equipment. During the mission the performance of the equipment was all normal.

(5) DSS 71, Cape Kennedy

This station participated in several prelaunch systems readiness tests with the spacecraft. In addition it participated in the DSIF/*Surveyor* compatibility test on March 5 and March 6, 1967. The countdown and launch support included the processing of telemetry data from the station and from various downrange stations via TEL-2* using the CDC

_____

*AFETR telemetry processing facility at Cape Kennedy.

and the telemetry and command processor (TCP) computer, and transmitting the data to the SFOF via the high-speed data line. This was the first mission wherein the data sent to the SFOF was in the same format as received from the other DSIF stations. By switching in the various down-range data, the CDC decommutator was able to remain locked until 45 min after liftoff, which was after first DSS 51 view of the spacecraft.

**(6) DSS 72, Ascension**

As in both the previous missions, DSS 72 was again activated for a standby role for *Surveyor III*. This station acquired the spacecraft signal in its preinjection configuration (low power and antennas not extended), and processed approximately 6 min of good telemetry data. Nine hours later, during a DSS 61 to DSS 51 station transfer, approximately 2 min of data was received by DSS 72 when the spacecraft was in high power.

## 2. The Spacecraft Television Ground Data Handling System

The spacecraft Television Ground Data Handling System (TV-GDHS) was designed to record, on film, the television images received from *Surveyor* spacecraft. The principal guiding criterion was photometric and photogrammetric accuracy with negligible loss of information. This system was also designed to provide display information for the conduct of mission operations, and the production of user products, such as archival negatives, prints, enlargements, duplicate negatives, and a digital tape of the TV ID information for use in production of the ID catalogs.

The System is in two parts—TV-11 at DSS 11, Goldstone, and TV-1 at the SFOF, Pasadena. At DSS 11 is an on-site data recovery (OSDR) subsystem and an on-site film recorder (OSFR) subsystem. These subsystems are duplicated in the media conversion data recovery (MCDR) subsystem, and the media conversion film recorder (MCFR) subsystem at the SFOF. The portion of the system used in real-time at the SFOF is comprised of the MCDR, the MCFR, the media conversion computer, the video display and driver subsystem (VDDS), the FR-700 and FR-1400 magnetic tape recorders, and the Bimat* processor. Equipment used in near-real-time are the strip contact printer and strip contact print processor. The photographic subsystem used in non-real-time

---

*Trademark of Eastman Kodak Co.

is comprised of several enlargers, a copy camera, the identity copier, two film processors, a film chip file, other photographic equipment, and film storage areas.

*a. TV-GDHS at DSS 11 (TV-11).* Data for the TV-GDHS is injected into the system at the interface between the DSS 11 receiver and the OSDR. In both the 200- and 600-line modes, the OSDR provides to the film recorder subsystem: (1) the baseband video signal, (2) the horizontal sync signal, (3) the vertical frame gate, (4) the resynchronized raw ID telemetry information, and (5) the time code. In 200-line mode, the OSDR also supplies a 500-kHz predetection signal to the DSS 11 FR-800 and FR-1400 magnetic tape recorders and to the SFOF via the microwave communication link. In 600-line mode, the OSDR provides: (1) a 4-MHz predetection signal to the DSS 11 FR-800 and to the SFOF via the microwave communication link, and (2) a baseband video signal to the DSS 11 FR-1400 magnetic tape recorder.

The OSFR records the following on 70-mm film: the video image, the raw ID telemetry in bit form, the "human readable" time and record number, and an internally generated electrical gray-scale. The film is then sent to the SFOF for development.

The TV-11 portion of the TV-GDHS performed its function well throughout the mission with only minor anomalies which had minimal effect on the mission. A few 200-line frames were not recorded on film during the touchdown view period because of a high drift rate in spacecraft frequency. There were a few other occasions when film recordings were lost at TV-11 because of OSFR equipment anomalies (which were corrected in each case). However, as a result of the redundancy designed into the TV-GDHS, this represented the temporary loss of only one source of science data.

*b. TV-GDHS at the SFOF (TV-1).* The signal presented to the microwave terminal at DSS 11 is transmitted to the SFOF, where it is distributed to the MCDR and the VDDS. The MCDR processes the signal in the same manner as the OSDR. In addition, the MCDR passes the raw ID information to the media conversion computer, which converts the data to engineering units. This converted data is used by: (1) the film recorder, where it is recorded as human readable ID, (2) the wall display board in the SSAC area, (3) the disc file where the film chip index file is kept, and (4) the history tape.

The VDDS produces the signals to drive the scan converter and the signals to drive the various display

monitors and the paper camera in the SSAC area. The VDDS also supplies the signals recorded by the FR-700 and the FR-1400 video magnetic tape recorders in the same manner as the FR-800 and FR-1400 recorders at DSS 11. The scan converter converts the slow scan information from the spacecraft to the standard RETMA television signal for use by the SFOF closed circuit television and the public TV broadcasting stations.

The MCFR records on two different films. One of these films is passed directly to the Bimat processor; the other is accumulated in a magazine. This second film is wet-processed off-line. The Bimat processor laminates the exposed film with Bimat-imbibed material, producing a developed negative and a positive transparency. The negative is used to make strip contact prints which are delivered to the users. The negative is then cut into chips and entered into the chip file where they are available for use in making additional contact prints and enlargements.

On the *Surveyor III* mission, a new requirement was satisfied by using the positive transparency from the Bimat processor to make a duplicate negative, which was used in turn by the JPL Photographic Laboratory to produce prints for public information and other needs. The photometric quality of the prints produced by this procedure was not entirely satisfactory owing to the resultant transfer characteristic from exposure to a duplicate negative.

During each lunar view period, from five to seven strip contact prints were made of images received. There were some cases where equipment anomalies delayed deliveries of the strip prints. The production of multiple negatives and print copies of up to 25 mosaics per day was accomplished very satisfactorily. Approximately 200 enlargements were also produced each day of operation. On one occasion, 150 enlargements were made with special characteristics.

Several equipment problems created a serious difficulty in keeping the data records correct and in supplying accurate data and acceptable images to the science users. In each case, appropriate action was taken in real-time to reduce the effects of these problems. However, the data sometimes could be regenerated only by replay of the FR-700 tapes, which caused considerable delay.

## C. Mission Operations Chronology

Inasmuch as mission operations functions were carried out on an essentially continuous basis throughout the *Surveyor III* mission, only the more significant and special, or nonstandard, operations are described in this chronicle. Refer also to the sequence of mission events presented in Table A-1 of Appendix A.

### 1. Countdown and Launch Phase

No significant problems were reported in the early phases of the countdown, which proceeded normally down to the built-in hold at $T$-5 min. The count was not picked up as scheduled after the planned 10-min hold, however, because of an apparent anomaly in the spacecraft roll actuator position signal. The hold was extended an additional 51 min, while special trouble-shooting sequences were performed on *Surveyor III* at Cape Kennedy and SC-5* at Hughes Aircraft Company in El Segundo. Both of these tests and a *Surveyor II* data review showed similar characteristics. It was determined that the spacecraft was performing properly, and the countdown was resumed.

Liftoff $(L+0)$ occurred at 07:05:01.059 GMT on April 17, 1967, with all systems reported in a "go" condition. Launch vehicle performance appeared to be nominal, with no significant anomalies on either the *Atlas* or *Centaur*. Following the parking orbit coast period, *Centaur* second burn occurred and the spacecraft was injected into a lunar transfer trajectory which was well within established limits. The required retro maneuver was successfully performed by the *Centaur*. A description of launch vehicle performance and sequence of events from launch through injection is contained in Section III.

Following separation at 07:39:54 GMT $(L+00:34:53)$, the spacecraft executed the planned automatic sequences as follows. By using its cold-gas jets, which were enabled at separation, the flight control subsystem nulled out the small rotational rates imparted by the separation springs and initiated a roll-yaw sequence to acquire the sun. After a minus roll of 181 deg and a plus yaw of 38 deg, acquisition and lock-on to the sun by the spacecraft sun sensors were completed at 07:48:00 GMT. Concurrently with the sun acquisition sequence, the A/SPP stepping sequence was initiated to deploy the solar panel and roll axes. At 07:45:55 and 07:50:08 GMT, the solar panel and A/SPP roll axes, respectively, were locked in the proper transit positions. All of these operations were confirmed in real-time from the spacecraft telemetry.

---

*Serial designation for the *Surveyor* spacecraft scheduled for the fifth *Surveyor* mission.

Following sun lock-on, the spacecraft coasted with its pitch and yaw axes controlled to track the sun and with its roll axis held inertially fixed.

## 2. DSIF and Canopus Acquisition Phase

DSS 42 (Tidbinbilla) achieved one-way lock (downlink) with the spacecraft at approximately 07:55 GMT, 50 min after liftoff; two-way communication was established at 08:01:50 GMT to complete initial acquisition.

The first ground-controlled sequence ("initial spacecraft operations") was initiated at 08:09 GMT ($L+01:04$) and consisted of commands for (1) turning off spacecraft equipment required only until DSIF acquisition, such as high-power transmitter and accelerometer amplifiers, (2) seating the solar panel and roll axis locking pins securely, (3) increasing the telemetry sampling rate to 1100 bit/sec from 550 bit/sec, and (4) performing the initial interrogation of commutator Modes* 1, 4, 2, 6, and 5, in that order. All spacecraft responses to the commands were normal.

Initial spacecraft operations were completed at 08:23:25 GMT, with *Surveyor III* configured in low power, coast phase commutator on (Mode 5), and transmitting at 1100 bit/sec. During the operations, it was determined from the star intensity telemetry signal that a bright object (believed to be the earth) was in the field of view of the Canopus sensor. Therefore, it was recommended that the roll axis be held in the inertial mode and that the *cruise mode on* command, which at this time would have caused the roll attitude to be slaved to the high-intensity light source, not be sent to the spacecraft. (Cruise mode was commanded on a few hours later at 10:52:48 GMT when the intensity signal had dropped to approximately 0.5 V.) It was also determined that there was no need to turn on Transponder A since the Receiver A AFC telemetry indicated only 2 kHz error.

The spacecraft continued to coast normally, with its pitch–yaw attitude controlled to track the sun and with its roll axis held inertially fixed. Tracking and telemetry data were obtained by use of Transponder B and Transmitter B. (The spacecraft telemetry data rate/mode profile for the complete mission is shown in Fig. IV-9.)

At 11:10 GMT, DSS 42 reported that the sideband energy of the spacecraft signal appeared lower than anticipated. This report was quickly evaluated as an

indication of possible modulation index problems. DSS 51 (Johannesburg), which acquired the spacecraft an hour later, also noted the anomaly and therefore performed a telecommunications troubleshooting sequence to determine whether the spacecraft 7.35-kHz subcarrier oscillator or the measurement procedures of the stations was the problem. The latter proved to be at fault; only part of the sideband power was being measured. The spacecraft telecommunications subsystem was operating normally.

At about $L + 09:04$, DSS 61 (Robledo) commanded a positive spacecraft roll maneuver which initiated the star verification/acquisition sequence. This was done in order to measure the intensity of light received from celestial objects passing in and out of the Canopus sensor's field of view, to identify the light sources on a star map which had been prepared for April 17, and then to acquire the star Canopus. At the recommendation of SPAC, the following spacecraft configuration was used during the sequence: telemetry Mode 5 at 4400 bit/sec,* Omniantenna B with Transmitter B in high-power, and the transponder turned off. The first revolution was used for the verification part of the sequence.

The roll maneuver proceeded smoothly, as the moon, Jupiter, the stars Procyon, Adhara, Canopus (after 205 deg) of roll), the earth, and finally the star Altair were successively detected by the Canopus sensor and identified on the map in the SPAC area. The spacecraft continued to roll, and as Adhara passed the field of view the second time, the star acquisition mode was commanded on. When light from Canopus was sensed, *Surveyor III* ended the maneuver by automatically locking onto the star. (In both the *Surveyor I* and *II* missions, the Canopus intensity was above the upper threshold of lock-on range, necessitating manual acquisition.) Canopus acquisition occurred at 16:27:51 GMT, after the spacecraft had rolled through 565 deg for 18 min, 39 sec. The star map prepared by the SPAC group and used during this sequence, and the spacecraft's predicted position relative to Canopus as computed by the FPAC group, both proved to have been very accurate.

At the end of the star verification/acquisition sequence, the spacecraft was coasting with pitch and yaw axes controlled to track the sun and the roll axis controlled to track Canopus. *Surveyor III* was in a fixed attitude, a precise position from which midcourse maneuvers could be initiated.

---

*See Section IV-A (Table IV-1) and Appendix C for data content of telemetry modes.

*This nonstandard bit rate was selected to obtain a greater sampling rate of Canopus sensor signals than was possible at 1100 bit/sec. After the sequence, the rate was lowered to 1100 bit/sec.

## 3. Premidcourse Coast Phase

About an hour after Canopus lock-on, the first gyro drift check was initiated by commanding the spacecraft to inertial mode. The vehicle continued to coast as before, but with its attitude held inertially so that the sun and star sensors continued to point at the sun and Canopus, respectively. At $L+12:11$, the gyro drift check was terminated, but a second check was begun 7 min later. In fact, although only four gyro drift checks were scheduled during the mission, about three times that number were actually performed during both coast phases. The first check had indicated drift slightly higher than specification. Therefore, other checks were desirable to increase confidence in the measured values so that drift could be compensated for accurately during retro maneuvers.

Final computation of midcourse parameters was conducted following the selection of a final target site and midcourse correction plan from the alternatives which had been studied. (Refer to Section VII for a discussion of the factors considered in selecting the midcourse correction plan and final aiming point.)

The premidcourse engineering interrogation was started at $L + 19:49$. This sequence was executed using low-power transmitter operation and indicated that the spacecraft was operating normally. As part of this sequence, the gyro speed outputs were measured and were found to be exactly nominal at 50 Hz.

## 4. Midcourse Maneuver Phase

The midcourse correction sequence was initiated at $L + 21:07$ on April 18, with an engineering interrogation in commutator Modes 4, 2, and 1. The telemetry readings indicated that the spacecraft was in satisfactory condition for midcourse operations. The interrogation was followed by commands to turn on Transmitter B high-power and increase the telemetry sampling rate from 1100 to 4400 bit/sec. Starting at $L + 21:41$, the required roll ($+56.74$ deg) and pitch ($-39.12$ deg) maneuvers were executed satisfactorily, thereby aligning the spacecraft axes in the desired direction for applying the midcourse thrust. Following engineering interrogation in commutator Modes 2 and 1, the spacecraft was prepared for thrusting, including sending commands to (1) turn on propulsion strain gage power, (2) turn on inertial mode, (3) pressurize the vernier propulsion system, and (4) load the desired thrust time (4.278 sec) in the flight control programmer magnitude register. Midcourse velocity correction was executed

at 05:00:02 GMT ($L + 21:55$) on April 18 in accordance with the planned thrust time. All engines fired simultaneously, burned for 4.277 sec (a velocity change of 4.19 m/sec), then shut down automatically. The spacecraft remained stable throughout the thrusting period.

Following midcourse velocity correction (which corrected the miss distance to within 2.67 km of the aiming point selected during flight), commands were sent to turn off various power sources used during the thrusting phase and to execute attitude maneuvers in reverse order and opposite direction. The sun was reacquired at 05:04:37 GMT after a positive pitch, and Canopus was reacquired at approximately 05:08:11 GMT at the end of a negative roll. Thus, confirmation was obtained that the gyros had retained inertial reference during vernier engine shutdown, eliminating the need for performing a postmidcourse star verification to insure lock-on to Canopus.

The spacecraft was returned to flight control cruise mode, and a high-power engineering interrogation was conducted in Modes 2, 4, and 5, after which the 1100-bit/sec data rate and low-power transmission were established.

## 5. Postmidcourse Coast Phase

The second coast phase was relatively uneventful. As mentioned previously, extra gyro drift checks were performed. Eight engineering interrogations of Modes 2 and 4 plus the final two preterminal descent interrogations were also conducted during this period. The data rate was lowered to 550 bit/sec at $L + 25:45$, then to 137.5 bit/sec at $L + 50:52$, where it remained until the start of terminal descent operations. Postmidcourse analysis of flight control thrust command signals indicated a possible imbalance in the thrust levels of the vernier engines during the thrust period. The most likely cause of this anomaly was traced to uncertainty in Engine 2 calibration data and/or uncertainties in telemetered signals. It was decided to adhere to the normal mission sequence because there were no special checks which could be devised to verify or correct any of the other possible causes of this anomaly without jeopardizing the mission.

As in the *Surveyor I* mission, power-mode cycling checks were made to help predict the percentage of electrical load that would be supplied by each spacecraft battery (main and auxiliary) during terminal descent, when both batteries are placed directly on the power bus. The spacecraft was also commanded to turn on Vernier Oxidizer Tank 2 heater and the survey television electronics and vidicon temperature controls.

## 6. Terminal Maneuver and Descent Phase

In preparation for the terminal maneuver conference, the SFOD held a preliminary internal mission operations conference to generate a list of alternate terminal maneuver plans and an outline of postlanding operations for presentation to the Mission Director.

The terminal maneuver conference was held about five hours before main retro ignition. The plan which was presented ·and approved by the Mission Director contained the following items:

(1) Use of a yaw–pitch–roll maneuver sequence with Omniantenna B to optimize telecommunications performance.

(2) Initiation of the three-maneuver sequence 38 min prior to retro ignition.

(3) Transmission of 1100-bit/sec PCM data plus touchdown strain gage data.

(4) Attempt to obtain strain gage data only if received signal level is at least −127.2 dbm after terminal maneuvers are completed.

(5) Turnoff of the transponder prior to start of the maneuvers.

About five and one half hours before main retro ignition, in preparation for terminal descent, the spacecraft was commanded to switch to the *main battery* mode, in which both batteries are on-line. The last roll gyro drift check was terminated 2 hr 35 min later, and the accumulated error was nulled.

About an hour before retro ignition, Transmitter B high power was turned on and the last engineering interrogation performed. In addition, the telemetry rate was increased to 1100 bit/sec and power was turned on as required for monitoring vernier propulsion and touchdown forces by means of strain gages. The spacecraft transponder was then turned off to put DSS 11 (Goldstone) on one-way lock for the terminal maneuvers.

The terminal maneuvers were begun approximately 38 min prior to the predicted time of retro ignition. During the first maneuver the spacecraft yawed −157.9 deg, turning the solar panel steadily away from the sun. This was followed by a pitch maneuver of −76.7 deg. With the retro thrust axis oriented in the desired direction, the roll maneuver (−63.9 deg) was initiated at 23:34:35 GMT, about 26 min before retro ignition. This established optimum roll positioning of the spacecraft to reduce the

probability of the RADVS locking onto a cross-coupled sidelobe.

In the remaining time before the automatic retro sequence, final preparations were made for terminal descent. The thrust level of the vernier engines was set at 200 lb, and a delay time of 5.075 sec between the AMR *mark* event and ignition of the vernier engines was stored in the spacecraft. The AMR was turned on and then enabled less than 2 min before retro ignition. Except for the standard emergency AMR signal (sent three times) and a command to turn on the presumming amplifier for touchdown strain gage data, the remaining operations were automatically performed by the spacecraft.

The AMR *mark* signal occurred at 00:01:11.72 GMT, April 20. At 00:01:16.7 GMT, with the spacecraft at a 47-mile altitude above the target and traveling 5874 mph, the vernier engines followed by the main retro motor ignited automatically, slowing the spacecraft to 458 ft/sec at the time of retro burnout (00:01:59.4 GMT). The retrorocket case was then ejected. Continuing its descent under RADVS control of the vernier engines, *Surveyor III* touched down on the lunar surface approximately 2 min later at 00:04:16.88 GMT, April 20. The landing point, 2.94 deg south latitude and 23.34 deg west longitude, was within 2.67 km of the aiming point established at the time of midcourse correction and approximately 625 km east of *Surveyor I*. (Refer to Section IV-A for a more complete description of the automatic terminal descent sequence.)

## 7. Lunar Phase

Spacecraft telemetry received at Goldstone during descent had not included confirmation of vernier engine cutoff, which is normally initiated by the RADVS 14-ft *mark* signal. It was immediately suspected that the engines had been firing at touchdown. However, since initial strain gage data indicated a soft-landing and since communication with the apparently upright spacecraft had not been lost, operational emphasis was placed on the more pressing problem of removing the high electrical loads of the flight control subsystem while SPAC and FPAC continued to investigate the touchdown data and SSAC prepared for initial television operations.

Postlanding analog telemetry data became garbled about 24 sec after the initial touchdown, making it difficult to verify that thrust phase power and flight control power were off. Therefore, the first 23 min after touchdown were spent in an effort to isolate the problem by sending commands to accomplish the following: turn off

terminal descent power loads, receive spacecraft data in three different commutator modes to assess spacecraft status, turn off *high current* mode and turn on *main battery* mode, isolating the auxiliary battery, and, finally, reduce the transmission rate in two steps from 1100 to 137.5 bit/sec and switch the transmitter from high to low power. Subsequent telemetry readings seemed to indicate that thrust phase power was off. It was also concluded that all analog data was erroneous at the bit rates sampled, and that all discrete signals were normal.

The presence of bad analog data prevented accurate determination of landing gear positions; however, sufficient information including video data was obtained to determine that leg deflections were not excessive. Therefore, the landing gear were not locked and the helium was not dumped at this time. (Later in the mission, the helium was dumped to assure the safety of the spacecraft; the landing gear were left unlocked.)

In an attempt to get pictures of the battery, SSAC turned the camera power on at 01:00:57 GMT and initiated 200-line television operations which confirmed that the camera was functioning properly, but this gave no information about the battery because of low sun angle and resulting glare in the 11 pictures received. Control of the spacecraft was returned to SPAC 0.5 hr later. After an engineering interrogation in commutator Modes 5 and 4, all loads on the 29-V nonessential bus were turned off. Then, one at a time, they were turned back on in the same sequence as that used to revive the spacecraft at the end of a lunar night. At the end of the sequence the data rate was lowered to 17.2 bit/sec and commutator Mode 4 was commanded on; the electrical current and mechanisms signals appeared normal. It was concluded that no spacecraft power subsystem malfunction existed. The apparent cause of the problem was failure of a master switch in the central signal processor. Therefore, since *Surveyor III* appeared essentially in good condition and operating properly with the exception of erroneous analog transmission, SPAC reconfigured the spacecraft for a second 200-line-mode television sequence and, via Mission Control, again transferred command responsibility to SSAC.

Attention was then concentrated on the touchdown analysis that FPAC, SPAC, and Project Science representatives had been conducting and reporting on throughout the first few hours of lunar operations. The analysis confirmed that *Surveyor III* not only landed with the vernier engines firing, it lifted off after initial contact with the lunar surface, touched down a second time, then

lifted off once more before the engines had been commanded off (34 sec after initial touchdown), and finally came to rest after a third touchdown.

Events during the approach and landing sequence were determined from studies of various data sources. Just before initial touchdown, when the spacecraft was about 35 ft from the lunar surface, telemetry indicated that RADVS Beam 3 tracker lost lock. At the same time, loss of two RADVS signals (*reliable operate doppler velocity sensor* and *reliable operate radar altimeter*) occurred, one of which generates the 14-ft *mark* at the appropriate time to cut off the vernier engines. (As mentioned above, the 14-ft *mark* was not received by Goldstone.) Confirmation of spacecraft rebound was provided by gyro error signals which were received during the 36 sec between first and last touchdown. These signals also indicated that spacecraft attitude was returned to the pretouchdown attitude by the flight control subsystem (in response to the signals) and that attitude remained stable between touchdowns.

One-way doppler received at Goldstone and the complete touchdown strain gage data printed out in the SFOF clearly indicated three separate touchdowns. In addition, the gages measured forces in the shock absorbers during the first two events which were about one half those measured at *Surveyor I* touchdown. Such forces were indicative of a landing with vernier engines thrusting.

In the final analysis, a correlation was established between the landing sequence and the anomalies encountered during initial posttouchdown operations. At initial touchdown, RADVS high voltage went off, then came back on after 18 sec. About 6 sec later, when the spacecraft touched down a second time, RADVS high voltage went off again, the decoders indexed, *high current* mode went off with the power system reverting to *auxiliary battery* mode, and all analog signals became erroneous. Since digital data was not affected by the landing and since the television frames and ID data were normal, the anomalies observed at touchdown were relegated to later investigation by SPAC's Trend and Failure Analysis Group. Mission operations were continued in an effort to conduct tests and experiments as originally planned with rescheduling as necessary.

The second 200-line television sequence was completed at 03:51:59 GMT after 25 additional pictures had been received. Following an engineering interrogation that was standard except that the transponder was not turned on, the spacecraft was reconfigured for the third and final

200-line television sequence, during which 18 pictures were taken. This 42-min sequence was completed at 05:00:58 GMT, after which an engineering interrogation was conducted, and the spacecraft was placed in the low-power mode transmitting on Omniantenna A.

Of the 54 200-line television photographs taken, about 39 were affected by glare. This had been anticipated and was caused by the low sun angle and the landed roll orientation. (The sun as viewed from the touchdown site was just above the lunar horizon when the spacecraft landed.) For this mission, the Project Scientist had requested a roll orientation which would provide favorable lighting for lunar photography, enhance the quality of pictures to be taken in the SM/SS deployment area, and prevent obscuration of the camera's field of view for solar corona sequences at lunar sunset. However, a RADVS sidelobe cross-coupling problem, identified long before the launch of *Surveyor III*, constrained the selection of final roll attitude, and it was not possible to meet the science-preferred orientation.

From a study of the 200-line photographs, it was determined that not all of the glare was caused by sun angle and spacecraft orientation. It was eventually assumed that vernier thrusting near the surface had caused contamination or pitting of the camera mirror, contributing to the haziness of the photographs. Intense analysis of these pictures had been underway since receipt of the first picture at 01:03 GMT, an hour after touchdown, for it was suspected that the spacecraft had come to rest on a slope and possibly in a depression. This was confirmed after integrating and evaluating specific data sources. Operations groups knew in advance the type of information to expect from various lunar surface conditions and landing angles, and the data received from *Surveyor III* was quite different from that which would identify a horizontal landing site with a clear view of the horizon. Six hours after touchdown, Mission Control confirmed that *Surveyor III* had landed on a 10- to 12-deg slope; this report was followed by an announcement that the spacecraft was located in a crater.

The FPAC group had determined landing coordinates, SPAC had confirmed spacecraft orientation, and SSAC had approximated the slope angle of the landing site. Therefore, 6 hr 19 min after touchdown, planar array (the high-gain antenna) and solar panel positioning was begun. Accomplishment of this sequence permits 600-line-mode television data transmission and ensures that sufficient electrical power will be available for continued lunar operations. Sun acquisition by the solar panel involved 3490 stepping commands and was completed at 07:18 GMT. This was followed by gross planar array positioning in order to acquire the earth, and then fine positioning in order for the Goldstone receiver to detect and lock onto the planar array's main lobe signal. The sequence was completed at 08:15 GMT after 857 stepping commands had been sent; the received signal level was −121.9 dbm. The spacecraft was commanded to high power, which increased the signal level to −98.2 dbm, placed in a 4400-bit/sec data rate and, at 08:38 GMT, was ready for television operations.

The first 600-line, high-resolution picture sequence was initiated at 08:40:36 GMT with a 10-min lens inspection followed by a wide-angle panorama. After 323 600-line pictures had been received, television operations were concluded at 10:10 GMT, April 20, about 9 min prior to the end of Goldstone visibility. (The 200-line configuration was not used again during the mission.)

During Tidbinbilla's second and third posttouchdown view periods, solar panel operations were conducted in order to refine the spacecraft's attitude and tilt. Based upon these operations, it was calculated at this early stage of lunar operations that *Surveyor III*, resting on the inside east wall of a crater, was tilted 12.45 deg with Leg 2 positioned about 14 deg south of east and pointing in an uphill direction, Leg 1 pointing southwest, and Leg 3 about 14 deg west of north. The downhill slope was determined to lie halfway between Legs 1 and 3 at an angle 6.43 deg north of west.*

Preliminary confirmation of this attitude determination came from later operations which included photographing Venus during the eclipse (April 24) at the exact camera position predicted and conducting a thermal experiment which involved A/SPP shading calculated from attitude data.

During Goldstone passes, the lunar operations sequences, other than routine engineering interrogations, consisted largely of picture surveys of the spacecraft, the crater in which it landed, and results of experiments conducted with the SM/SS. (Because of *Surveyor's* landing location, the local horizon could not be photographed over the edge of the crater.) On April 24, pictures of the

---

*Spacecraft attitude, tilt, and location within the crater were also calculated by the scientific investigators and working groups. Their methods of determination and the results obtained are given in Part II of this Mission Report.

earth were taken during the eclipse of the sun by the earth. On April 30, the earth was again photographed. Both sequences involved use of the color filters for later reconstruction into color composites. *Surveyor's* tilted position made possible the taking of earth pictures. Many picture surveys were repeated to obtain comparisons at different sun elevation angles or under spacecraft shadow conditions. Surface pictures included numerous studies of the sharp, clear imprint made by Footpad 2 on the spacecraft's third touchdown.

Initial exercising of the SM/SS occurred during Goldstone's April 21 pass, and on the following day the first bearing test was performed. SM/SS operations were commanded only from Goldstone and, with the exception of April 24 and 25, were conducted on each pass until May 2. In response to earth commands, the SM/SS dug, scraped, picked, trenched, and manipulated the lunar surface material. These operations were preceded and followed by television pictures. The SM/SS was also commanded to scoop up some surface material and drop it on a footpad, and the pad was photographed with the color filters. In addition, the SM/SS was photographed in color. During the total 8 hr 22 min of the SM/SS auxiliary's operations, it decoded the 5879 SM/SS commands sent from Goldstone and generated the required 1898 commands necessary for SM/SS operations.

Thermal experiments were conducted at intervals throughout the mission. During the eclipse, thermal data was obtained as the earth's shadow passed over the spacecraft. No TV pictures were taken on April 25, and the spacecraft was cycled between high and low power to provide thermal data and to provide a strong signal level for Goldstone antenna calibration.

During early lunar operations, there were indications of overheating of the TV camera. This was due to calibration errors rather than equipment malfunction. Another problem occurred during picture-taking sequences. When stepping commands were sent, the mirror had a tendency to stick, particularly in azimuth position. This was overcome by sending special commands to step the mirror in elevation and then in azimuth past the problem point. It is possible that a particle of lunar material (disturbed during landing) had become wedged in the mechanism.

Television and SM/SS operations, interrupted periodically by engineering interrogations, were conducted through May 2, Goldstone's next to last pass before lunar sunset. On this date, shadow progression pictures were begun by overseas DSIF stations, and were taken more and more frequently as sunset approached. Finally, at 20:58 GMT on May 3 the last picture (making a total of over 6300) was taken by Goldstone when only a thin line was visible at the eastern rim of the crater. Command was transferred to DSS 42 and, at 00:04 GMT on May 4, 14 days after touchdown, the spacecraft was turned off for the lunar night. Maximum power had been left in the spacecraft battery to enhance the chance of lunar night survival. Between May 23 and June 2, repeated attempts were made to revive the spacecraft for operations during a second lunar day, but *Surveyor III* did not respond. The more important lunar operations sequences, other than routine engineering interrogations, are listed in Table A-2 of Appendix A.

# VII. Flight Path and Events

*Surveyor III* was injected first into a parking orbit and then into a near perfect lunar transfer trajectory. A small midcourse maneuver of 4.19 m/sec was properly executed to compensate for injection errors and to adjust the spacecraft trajectory to a slightly refined aiming point. Soft-landing occurred at 2.94 deg south latitude and 23.34 deg west longitude, only 2.76 km from the midcourse aiming point.

## A. Prelaunch

For *Surveyor III*, the landing site selected prior to launch for targeting of the launch vehicle ascent trajectory was in a mare area of the *Apollo* zone of interest at 3.33 deg south latitude and 23.17 deg west longitude. The following factors influenced the selection of this site: predicted terrain smoothness, desire to land within the *Apollo* zone at a new site, and an off-vertical, unbraked impact angle of about 23.6 deg, which was within the range of spacecraft capability (minimum, 18 deg; maximum, 45 deg) for this mission. An unbraked impact speed was selected so that the Goldstone postarrival visibility would be maximized while still satisfying the prearrival visibility constraint for all launch days in the launch period.

## B. Launch Phase

The *Surveyor III* spacecraft was launched from AFETR launch site 36B at Cape Kennedy, Florida, April 17, 1967. The launch was delayed until 51 min after opening of the window because of anomalous spacecraft telemetry indications of a vernier engine roll actuator problem (see Sections II and IV). Liftoff occurred at 07:05:01.059 GMT. At 2 sec after liftoff, the *Atlas/Centaur* launch vehicle began a 13-sec programmed roll that oriented the vehicle from a pad-aligned azimuth of 115 deg to a launch azimuth of 100.81 deg. At 15 sec, a programmed pitch maneuver was initiated which was completed at *Atlas* booster engine cutoff (BECO). The *Centaur* first burn injected the vehicle into a parking orbit having a 92-nm apogee, 86-nm perigee, and 87.7-min period. The spacecraft was in the earth's shadow during the first 16.5 min of flight, but left the shadow during parking orbit coast and remained in sunlight during the remainder of flight. After a 22.1-min coast, the *Centaur* burned a second time to inject the *Surveyor III* spacecraft into the desired lunar transfer trajectory. All event times for the launch phase were close to nominal except for the duration of *Centaur* burn periods, which were longer than expected due to 2 to 3% low main engine thrust. The launch phase sequence is discussed in greater detail

in Section III. Nominal and actual event times for all phases of the mission are summarized in Table A-1 of Appendix A.

## C. Cruise Phase

Separation of *Surveyor III* from the *Centaur* occurred at 07:39:54.4 GMT on April 17, 1967, at an approximate geocentric latitude of −24 deg and longitude of 30 deg. Automatic sun acquisition began about 53 sec after separation and was completed after a maneuver of −181 deg roll and +38 deg yaw.

Initial DSIF two-way acquisition by the Tidbinbilla station (DSS 42) was close to optimum. DSS 42 reported good one-way data at 07:55:42, only seconds after predicted rise over the station's horizon mask. Good two-way data was reported at 08:01:50. After DSS 42 acquisition, the DSIF stations continued to provide good two-way doppler data for the remainder of flight, with a few exceptions including noisy data from DSS 61 on its first pass. The station tracking periods are presented in Fig. V-12.

A plot of the actual *Centaur* and *Surveyor III* trajectories, projected on the earth's equatorial plane, is provided in Fig. VII-1. The earth track traced by *Surveyor III* appears in Fig. VII-2. Specific events such as sun and Canopus acquisition and rise and set times for DSIF stations are also noted.
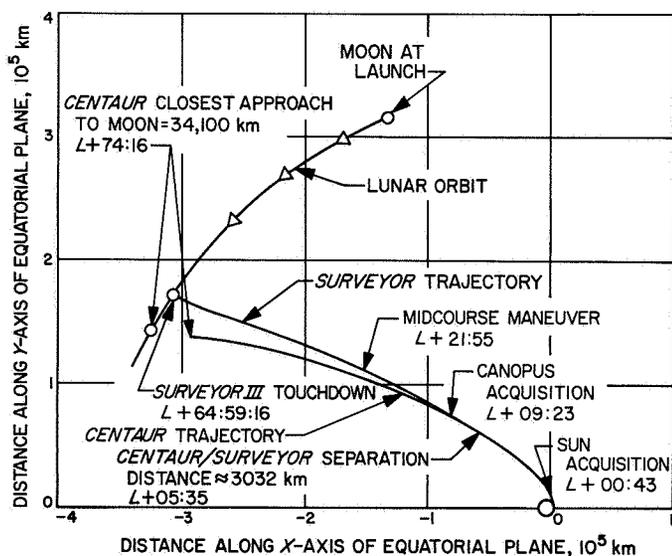


**Fig. VII-1. *Surveyor* and *Centaur* trajectories in earth's equatorial plane**

Prior to Canopus acquisition, the spacecraft was rolled to generate a star map. Then Canopus was acquired automatically at $L + 09:23$ with a net spacecraft roll of +205 deg. In the normal cruise mode the spacecraft -Z axis is aligned to the sun and the -X axis to the projection of Canopus in the spacecraft X-Y plane.

The uncorrected, unbraked impact point and the original aiming point are shown in Fig. VII-3. Based upon the current best estimate, the uncorrected, unbraked impact point is located just to the east of the crater Letronne at 10.07 deg south latitude and 36.99 deg west longitude. The original aiming point was 3.33 deg south latitude and 23.17 deg west longitude, which is southeast of the crater Lansberg. The two points are approximately 466 km (290 miles) apart on the surface of the moon. Also shown in Fig. VII-3 are the final landing sites of *Surveyors I* and *III*.

Figure VII-4 is an enlarged section of the area containing the uncorrected impact point. A few selected premidcourse orbit computations mapped to the moon are shown. The numerical data for these selected premidcourse computations are presented in Table VII-1. Included in the computations shown are the orbit determinations from the Real Time Computer System (RTCS), Cape Kennedy, which were obtained at $L + 01:25$ and $L + 02:05$ based upon DSS 42 data only. The first RTCS computation used Pretoria data and, when mapped forward to the moon, gave the initial indication that lunar encounter would be achieved without a midcourse correction (coordinates for this computation are outside area shown in Fig. VII-4. Refer to Table VII-1). The first orbit computed at JPL (PROR) at $L + 01:54$ confirmed that the correction required to achieve the prelaunch aiming point was well within the midcourse correction capability. These results were verified by the second (ICEV) and third (PREL) orbit computations completed at $L + 02:50$ and $L + 03:48$, respectively. During the third orbit computational period, a comparison between orbits with (PREL-YA) and without (PREL-XA) angular data showed a magnitude difference of 132 km in the B-plane. Eight data consistency (DACO) orbital solutions were made which indicated that the two-way doppler data from the three DSIF stations, DSS 42, 51, and 61, were consistent, although the DSS 61 data was excessively noisy owing to a counter problem which was corrected before the second pass. The last premidcourse (LAPM) orbit was used to determine the required midcourse correction. The current best estimate of the spacecraft uncorrected orbit (PRCL) was computed based upon all

Fig. VII-2. Surveyor III earth track
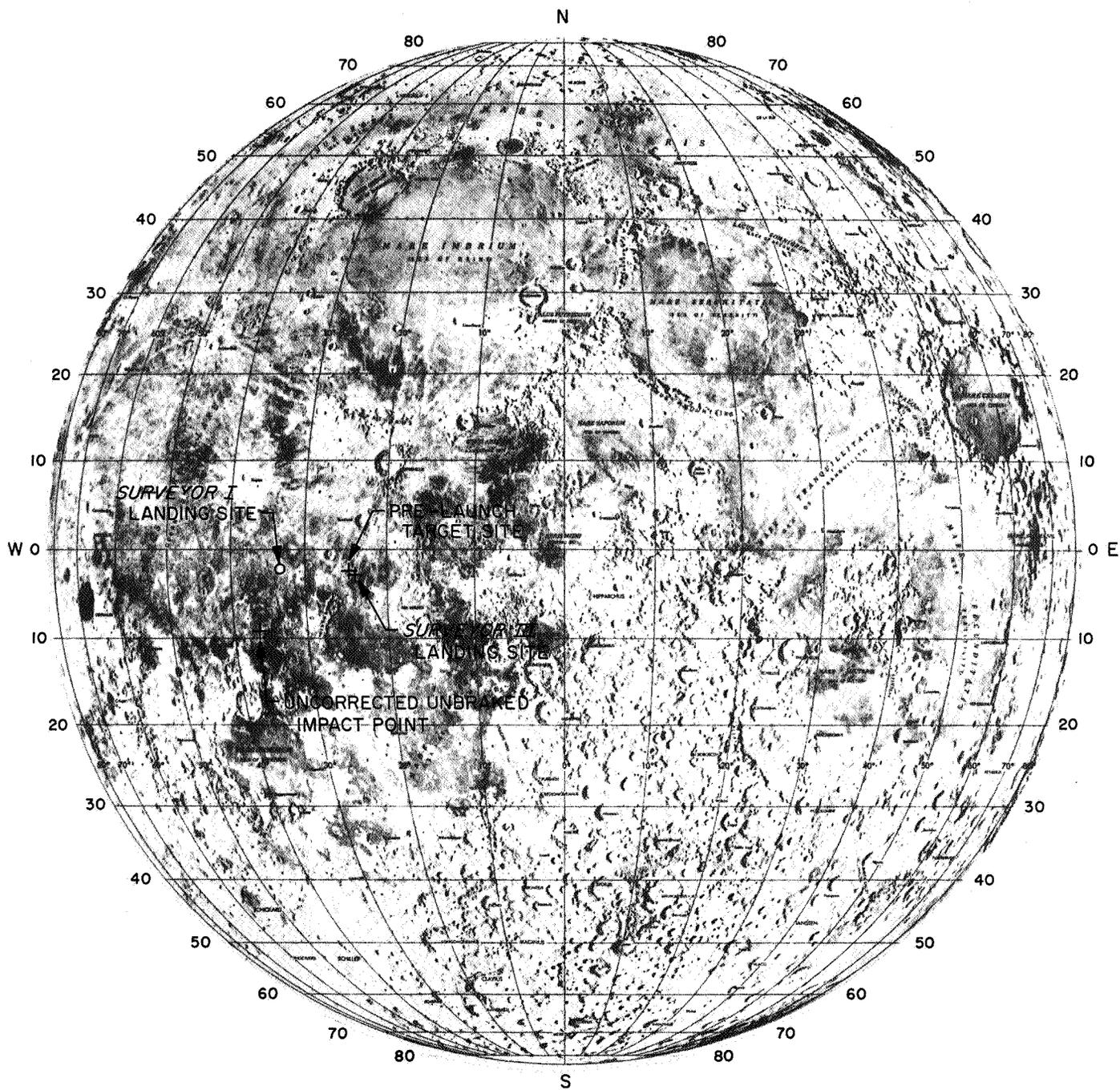
**Fig. VII-3.** *Surveyor III* target and uncorrected impact points
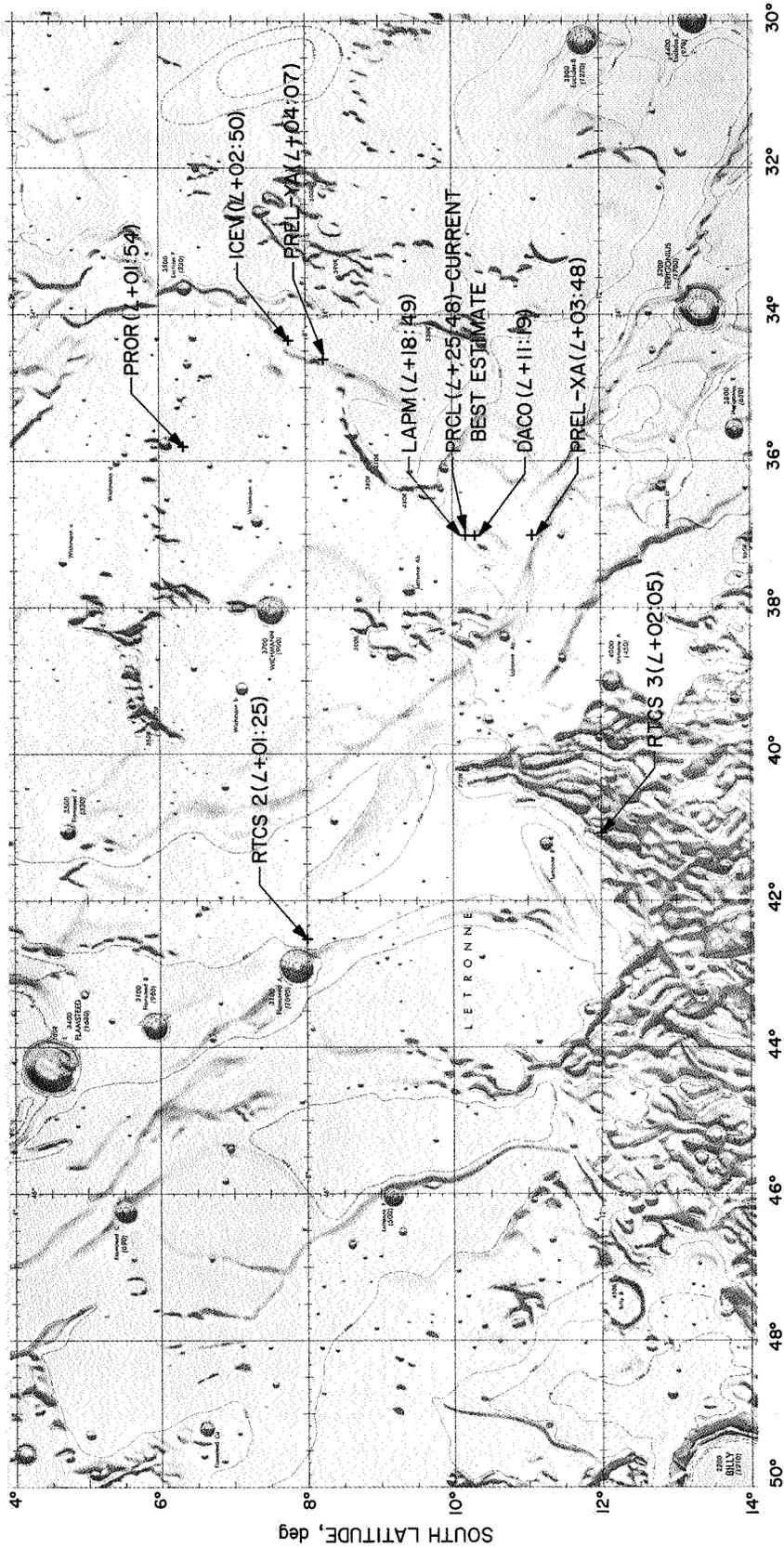
Fig. VII-4. Computed Surveyor III premidcourse unbraked impact locations

WEST LONGITUDE, deg

SOUTH LATITUDE, deg

| Orbit | Time computation completed (from liftoff) | Target statistics | | | | | | |
|---|---|---|---|---|---|---|---|---|
| | | B, km | B•TT, km | B•RT, km | TL, hr | SMAA, (1σ) km | SMIA, (1σ) km | Theta, deg |
| RTCS 1 | 00:53 | 2714.35 | 2519.91 | −1008.81 | 64.87 | | | |
| RTCS 2 | 01:25 | 602.148 | 561.863 | −216.547 | 64.124 | | | |
| PROR YA | 01:54 | 922.123 | 878.773 | −279.411 | 64.425 | 564.03 | 107.01 | 60.638 |
| RCTS 3 | 02:05 | 617.446 | 617.156 | −18.909 | 63.946 | | | |
| ICEV YA | 02:50 | 962.949 | 942.159 | −199.016 | 64.424 | 82.216 | 54.19 | 78.017 |
| PREL XA | 03:48 | 817.395 | 815.762 | −51.641 | 64.442 | 1668.94 | 98.850 | 90.346 |
| PREL YA | 04:07 | 948.797 | 930.556 | −185.153 | 64.425 | 65.835 | 31.176 | 102.07 |
| DACO YA | 11:19 | 826.531 | 816.582 | −90.046 | 64.44 | 186.6 | 3.752 | 88.73 |
| LAPM YC[a] | 18:49 | 821.443 | 815.595 | −97.845 | 64.440 | 6.633 | 1.771 | 71.395 |
| PRCL YL[b] | 25.48 | 821.533 | 815.644 | −98.192 | 64.440 | 10.18 | 1.779 | 70.77 |

[a] Orbit used for midcourse computations.
[b] Current best estimate.
SMAA   semi-major axis of dispersion ellipse.
SMIA   semi-minor axis of dispersion ellipse.
Theta   orientation angle of dispersion ellipse measured counterclockwise from TT axis in B-plane.

usable premidcourse two-way doppler data from DSS 42, 51, and 11. No DSS 61 data was used because of the possibility of a bias being hidden in the noisy data and the belief that the good DSS 61 data would not have contributed significantly to the solution.

## D. Midcourse Maneuver Phase

The original aim point was selected assuming the 99% landing dispersions to be a 30-km-radius circle on the lunar surface. (On previous *Surveyor* missions, a 50-km circle had been assumed. The reduction in assumed dispersion circle size reflects improved confidence in the landing accuracy.) However, primarily because of the small midcourse correction required and high quality of the tracking data, the 99% (3σ) dispersion computed in-flight from the assumed execution and tracking errors was an ellipse having a semimajor axis of 15.1 km and a semiminor axis of 10.6 km as shown in Fig. VII-5. Because of this smaller dispersion and based upon high-resolution *Lunar Orbiter III* photographs, the aim point was biased in a northward direction approximately 0.42 deg in accordance with the recommendations of the Project Scientist to maximize the probability of soft-landing. The initial and final aim points are also shown in Fig. VII-5 together with the actual soft-landing site. The latitude and longi-

tude for these locations as well as for the uncorrected impact point are given below:

| | South latitude, deg | West longitude, deg |
|---|---|---|
| Original aim point | 3.33 | 23.17 |
| Uncorrected impact point | 10.07 | 36.99 |
| Final aim point | 2.92 | 23.25 |
| Actual landing site | | |
| Based on tracking data | 3.00 | 23.43 |
| Based on *Lunar Orbiter III* photographic evaluation | 2.94 | 23.34 |

The maximum midcourse correction capability is shown in Fig. VII-6 for three values of unbraked impact speed $V_{imp}$. Also shown are the expected 3σ *Centaur* injection guidance dispersions, the effective lunar radius, and the maximum maneuver which could have been executed in the normal mode (i.e., thrusting terminated automatically by the spacecraft timer). The midcourse capability contours are in the conventional R-S-T coordinate system.*

―――――――――

*Kizner, W. A., *A Method of Describing Miss Distances for Lunar and Interplanetary Trajectories*, External Publication 674, Jet Propulsion Laboratory, Pasadena, August 1, 1959.

Table VII-1. *Surveyor III* premidcourse orbit determinations

| Target statistics | | | Unbraked impact conditions | | | Data used |
|---|---|---|---|---|---|---|
| $\sigma_T$ impact, (1$\sigma$) sec | PHIP 99 deg | SVFIX R, (1$\sigma$) km/sec | Lat, deg | Long, deg | GMT | |
| | | | 12.782 | 2.806 | | Pretoria radar |
| | | | −7.965 | 317.536 | | DSS 42 angular and two-way doppler |
| 48.0449 | 7.654 | 0.000696 | −6.277 | 324.184 | 23:57:35.184 | DSS 42 angular and two-way doppler |
| | | | −11.968 | 318.867 | | DSS 42 angular and two-way doppler |
| 10.2877 | 1.3636 | 0.000608 | −7.832 | 325.613 | 23:57:36.961 | DSS 42 angular and two-way doppler |
| 252.453 | 24.702 | 0.0008834 | −11.0217 | 323.072 | 23:58:23.988 | DSS 42 two-way doppler |
| 8.23346 | 0.99335 | 0.000608 | −8.1333 | 325.379 | 23:57:39.781 | DSS 42 angular and two-way doppler |
| 27.68 | 2.790 | 0.0006116 | −10.236 | 323.04 | 23:58:17.935 | DSS 42 and 61 two-way doppler |
| 1.767 | 0.1142 | 0.0006079 | −10.078 | 323.014 | 23:58:16.856 | DSS 42, 51, 61 and 11 two-way doppler |
| 2.74 | 0.176 | 0.000607 | −10.071 | 323.015 | 23:58:16.592 | DSS 42, 51, and 11 two-way doppler |

$\sigma_T$ impact   uncertainty in predicted unbraked impact time.
PHIP 99   99% velocity vector pointing error.
SVFIX R   uncertainty in magnitude of velocity vector at unbraked impact.
TL   flight time from injection.

A midcourse correction of 4.19 m/sec (equivalent to a burn time of 4.278 sec) was selected and executed upon ground command at approximately 05:00 GMT on April 18, 1967. This velocity increment was required in the critical plane to correct for "miss only." The velocity component normal to the critical plane is referred to as the noncritical component since it does not affect the miss to the first order. Figure VII-7 presents the variations in flight time, main retro burnout velocity, vernier propellant margin, and landing site dispersions with the noncritical velocity component $\dot{U}_3$. The propellant margin and burnout velocity were acceptable over a wide spectrum. To achieve a flight time which would result in arrival 80 min after Goldstone rise, thereby maximizing postarrival visibility, the noncritical component magnitude would have had to be 18.7 m/sec. A noncritical component of 0.0 m/sec was selected based upon weighted considerations of flight time, main retro burnout velocity, vernier propellant margin and landing accuracy. The chosen value of $\dot{U}_3$ minimized landing site dispersions. The resultant 99% circular miss dispersion shown in Fig. VII-7 is based upon the tracking errors expected from the intermediate premidcourse calculations. The actual tracking errors determined at time of midcourse were considerably less than the expected error. If the maneuver strategy had been to correct "miss-plus-flight-

time," the required noncritical component would have been +5.57 m/sec, giving a total correction of 6.99 m/sec.

Since the aiming point was changed during the flight, the above required correction does not properly evaluate the performance of the *Centaur* guidance system. Using the results of the last premidcourse orbit and correcting to the original aim point gives a miss-only requirement of 4.00 m/sec and a miss-plus-flight-time requirement of 6.63 m/sec for a midcourse conducted 20 hr after injection.

The predicted results of the selected midcourse correction and other alternatives considered are given in Table VII-2. The possibility of not performing a midcourse correction was eliminated because the uncorrected impact site was outside the *Apollo* region, which is defined as ±5 deg latitude and ±45 deg longitude. Execution of the midcourse correction during the second Goldstone pass (approximately 46 hr after injection) would have doubled the magnitude of the velocity correction while reducing the expected landing site dispersions by one-fourth, owing to greater tracking accuracy. However, the very small net gain in successful soft-landing probability did not outweigh personnel staffing considerations, the possibility of not being able to make the

correction during the second Goldstone pass because of hardware failure, and the fact that more time would be available after an early maneuver to correct possible mid-course execution problems if they had occurred. The possibility of performing a correction along the spacecraft–sun direction was eliminated because neither the desired site nor the *Apollo* region could be reached. Table VII-2 contains midcourse and terminal data for a sunline correction to a landing site 230 km southwest of the final aiming point.
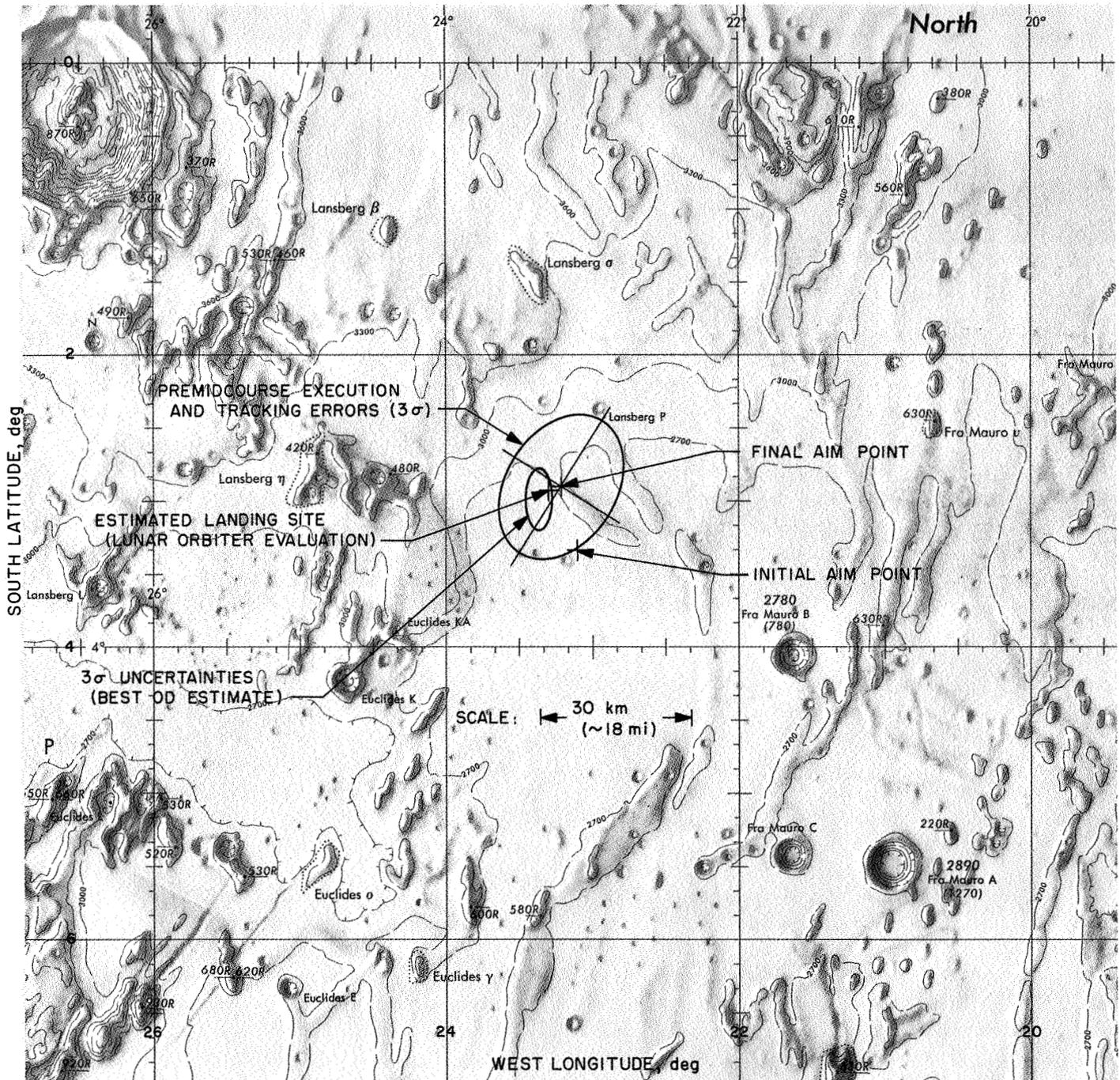


**Fig. VII-5.** *Surveyor III* landing location
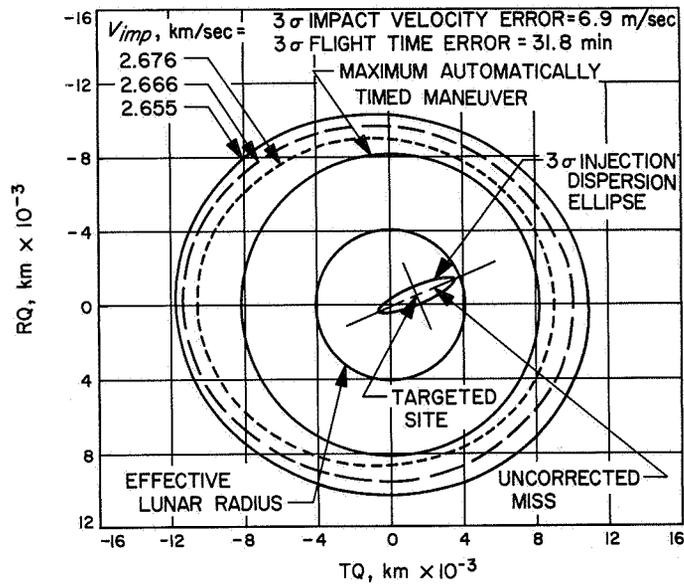
Fig. VII-6. Midcourse correction capability contours (for a 20-hr-after-injection correction)
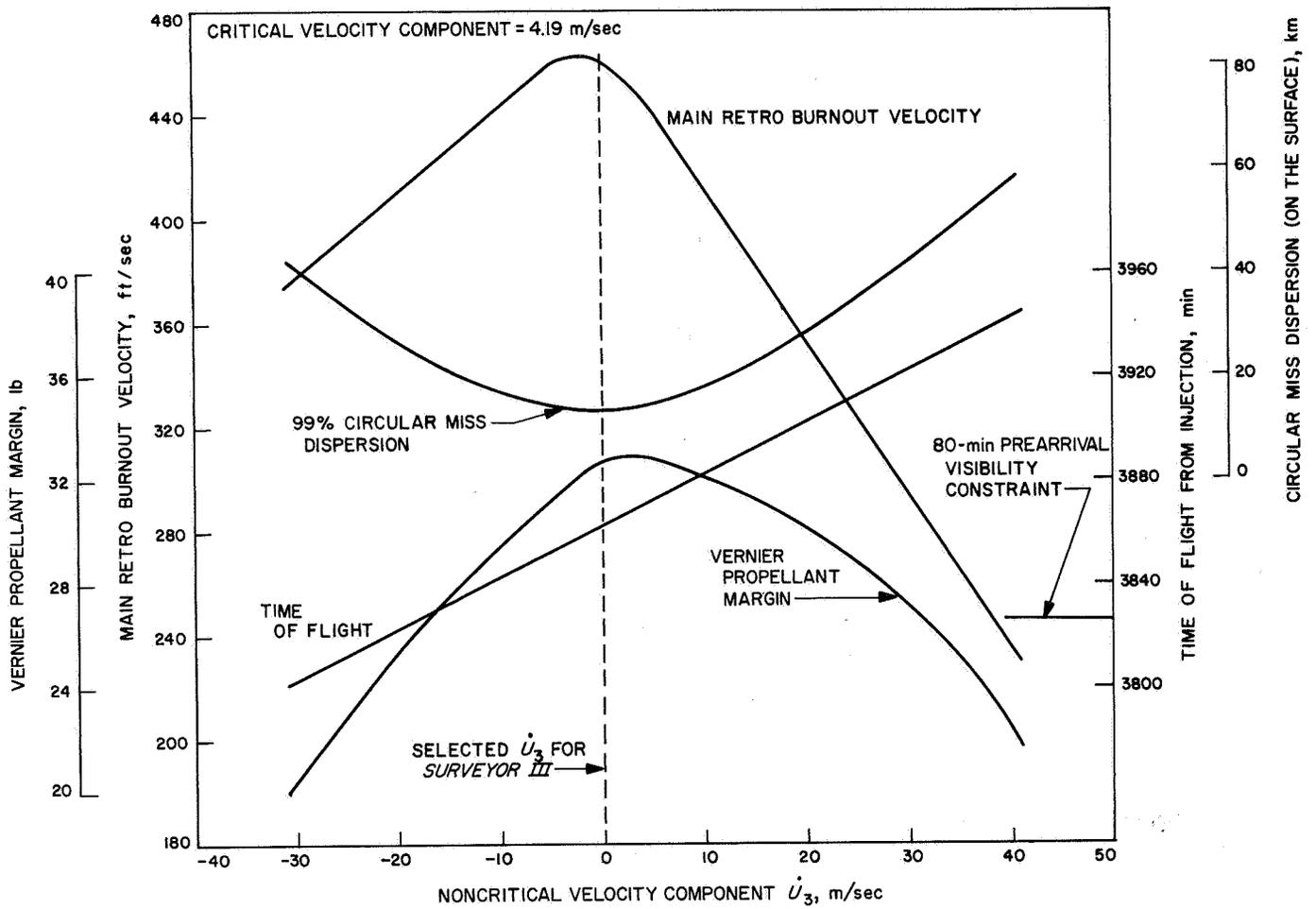


Fig. VII-7. Effect of noncritical velocity component on terminal descent parameters
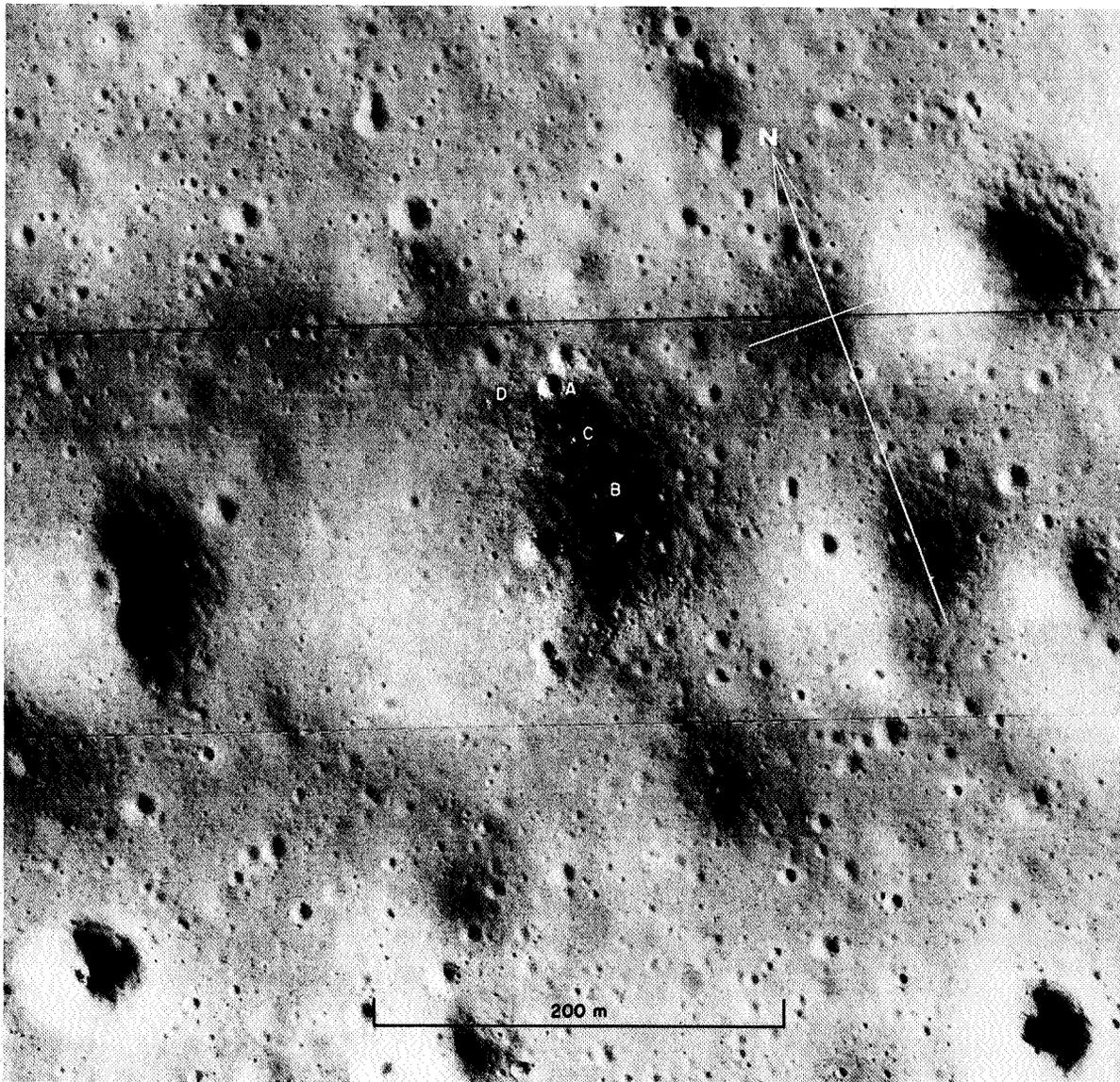
Fig. VII-8. *Surveyor III* landing site located on *Lunar Orbiter III* frames (*Surveyor III* indicated to scale by white triangle)

## Table VII-2. Midcourse maneuver alternatives

| | Selected midcourse 21.4 hr[a] midcourse | No midcourse | 46 hr[a] midcourse | Sunline |
|---|---|---|---|---|
| **Midcourse parameters** | | | | |
| Velocity magnitude, m/sec | 4.19 | | 9.69 | 2.83 |
| Critical plane, m/sec | 4.19 | | 9.69 | |
| Noncritical direction, m/sec | 0.0 | | 0.0 | |
| Propellant weight, lb | 3.58 | | 8.28 | 2.42 |
| First rotation, roll, deg | 56.74 | | 61.23 | 0.0 |
| Second rotation, pitch, deg | −39.13 | | −35.34 | 0.0 |
| Omnidirectional antenna | B | | B | B |
| Engine burn time, sec | 4.278 | | 9.885 | 2.89 |
| Midcourse mechanization plus tracking, 3σ: | | | | |
| SMAA, km | 15.1 | | 12.7 | |
| SMIA, km | 10.6 | | 8.3 | |
| THETA, deg | −64.4 | | −62.9 | |
| **Terminal parameters** | | | | |
| Aim point: latitude, deg | 2.92S | 10.08S | 2.92S | 9.8S |
|          longitude, deg | 336.75E | 323.02E | 336.75E | 333.0E |
| Incidence angle, deg | 23.6 | 12.5 | 23.8 | 20.0 |
| Impact speed, m/sec | 2671.5 | 2671.3 | 2671.2 | 2671.0 |
| Burnout velocity, ft/sec | 461.4 | 498.0 | 436.6 | 465.0 |
| Burnout altitude, ft | 34,733.8 | | 33,167.4 | |
| Propellant margin, lb | 33.69 | 35.0 | 32.12 | 34.0 |
| Descent propellant, lb | 134.07 | 136.0 | 130.9 | 134.5 |
| Descent time, sec | 183.5 | | 181.8 | |
| First rotation, yaw, deg | −157.90 | | −157.90 | |
| Second rotation, pitch, deg | −76.78 | | −76.78 | |
| Third rotation, roll, deg | −63.92 | | −63.92 | |
| Ignition delay, sec | 5.07 | | | |

[a]Time from spacecraft separation.

Table VII-3. Premidcourse and postmidcourse injection and terminal conditions

**Premidcourse injection conditions, April 17, 1967, 07:38:39.838 GMT**

| Coordinate[a] system | | | | | | |
|---|---|---|---|---|---|
| Inertial Cartesian | X = 5839.9674 km | Y = -1729.9083 km | Z = -2413.6500 km | DX = 1.8347366 km/sec | DY = 10.101912 km/sec | DZ = -3.8398219 km/sec |
| Inertial spherical | RAD = 6551.6035 km | RA = 343.49972 deg | DEC = -21.617345 deg | VI = 10.961711 km/sec | PTI = 2.0008262 deg | AZI = 111.29573 deg |
| Earth-fixed spherical | RAD = 6551.6035 km | LAT = -21.617345 deg | LON = 24.084089 deg | VE = 10.549386 km/sec | PTE = 2.0790634 deg | AZE = 112.17243 deg |
| Orbital elements | C3 = -1.5214047 km²/sec² | ECC = 0.97502433 | INC = 29.981599 deg | TA = 4.0529269 deg | LAN = 120.11582 deg | APF = 223.44238 deg |

**Premidcourse encounter conditions, April 19, 1967, 23:58:16.529 GMT**

| Coordinate system | | | | | |
|---|---|---|---|---|---|
| Selenocentric | RAD = 1737.4997 km | LAT = -10.071655 deg | LON = 323.01355 deg | VP = 2.6703809 km/sec | PTP = -77.605566 deg | AZP = 79.621153 deg |
| Miss parameter earth equator | BTQ = 804.06463 km | BRQ = -168.21555 km | B = 821.47209 km | | | |
| Miss parameter moon equator | BTT = 815.58632 km | BRT = -98.162497 km | B = 821.47241 km | | | |

**Postmidcourse injection conditions, April 18, 1967, 05:00:05.000 GMT**

| Coordinate system | | | | | |
|---|---|---|---|---|---|
| Inertial Cartesian | X = -152114.15 km | Y = 111776.63 km | Z = 43748.412 km | DX = -1.3821824 km/sec | DY = 0.60989540 km/sec | DZ = 0.51919356 km/sec |
| Inertial spherical | RAD = 193769.58 km | RA = 143.69078 deg | DEC = 13.048480 deg | VI = 1.5974863 km/sec | PTI = 76.614582 deg | AZI = 62.147263 deg |
| Earth-fixed spherical | RAD = 193769.58 km | LAT = 13.048480 deg | LON = 223.04319 deg | VE = 13.528751 km/sec | PTE = 6.5963098 deg | AZE = 270.73663 deg |
| Orbital elements | C3 = -1.5622155 km²/sec² | ECC = 0.97442763 | INC = 30.534675 deg | TA = 163.33814 deg | LAN = 120.55533 deg | APF = 223.04603 deg |

**Postmidcourse encounter conditions, April 20, 1967, 00:01:47.441 GMT**

| Coordinate system | | | | | |
|---|---|---|---|---|---|
| Selenocentric | RAD = 1736.0997 km | LAT = -2.9651627 deg | LON = 336.77828 deg | VP = 2.6697918 km/sec | PTP = -66.518379 deg | AZP = 70.673893 deg |
| Miss parameter earth equator | BTQ = 1430.5217 km | BRQ = -512.61836 km | B = 1519.5953 km | | | |
| Miss parameter moon equator | BTT = 1468.8581 km | BRT = -389.39488 km | B = 1519.5962 km | | | |

[a] Holdridge, D. B. Space Trajectories Program for the IBM 7090 Computer, Technical Report 32-223, Jet Propulsion Laboratory, Pasadena, March 2, 1962.

An analysis was made of eight pairs of premidcourse attitude rotations, any pair of which would have correctly oriented the spacecraft for the midcourse velocity correction. A combination of +56.74 deg roll and −39.13 deg pitch was chosen because it maximized probability of mission success by providing continuous high antenna gain, no antenna switching requirements, and maximum sun-lock time. Table VII-3 presents the premidcourse and postmidcourse injection and encounter conditions.

## E. Terminal Phase

A terminal attitude maneuver, consisting of −157.90 deg yaw, −76.78 deg pitch, and −63.92 deg roll, was initiated 38 min prior to retro ignition with a nominal 2-min allowance between rotations. This maneuver combination, using Omniantenna B, was selected to optimize telecommunication performance during the terminal maneuver and terminal descent phases. The roll attitude of the spacecraft was constrained by a problem with sidelobe crosscoupling of the radar altimeter and doppler velocity sensor (RADVS). The maneuver magnitudes included compensation for flight sensor group deflection and gyro drift rates.

The terminal descent sequence is described in detail in Section IV-A. Table A-1 of Appendix A gives terminal phase event times. Initial touchdown occurred at 00:04:16.88 GMT on April 20, 1967, at a mission time of L + 64:09:15.82.

## F. Landing Site

The landing site of *Surveyor III* was computed to be 3.00 deg south latitude and 23.43 deg west longitude, based upon final postflight orbit determination. Early television pictures from *Surveyor III* indicated the spacecraft had landed within a crater having a diameter of about 200 m. The *Lunar Orbiter III* high-resolution photographs of the general landing area were scanned, resulting in the discovery of a likely looking crater. Close examination of this crater, which is shown in Fig. IV-8, has revealed sufficient landmarks recognizable in the *Surveyor III* photos to give a high degree of confidence in the site identification.

The *Surveyor III* picture shown in Fig. VII-9 is a view of the lunar surface to the north of the crater illustrating typical features (craters and boulders) which are also visible in the *Lunar Orbiter* photo (Fig. VII-9). Using simple triangulation methods, the *Surveyor III* spacecraft has been placed to scale in Fig. VII-8 at the exact location where it finally came to rest. This position is 2.94 deg south latitude and 23.34 deg west longitude. As shown in Fig. VII-5, the actual landing site, as determined from the *Lunar Orbiter* photos, is only 2.76 km (1.71 mi) from the final aim point and only 3.1 km from the final postflight orbit determination. Postlanding doppler tracking data was obtained and is currently being analyzed to obtain an even more accurate orbit determination. (Refer to Part II of this report for a detailed description of the landing site.)
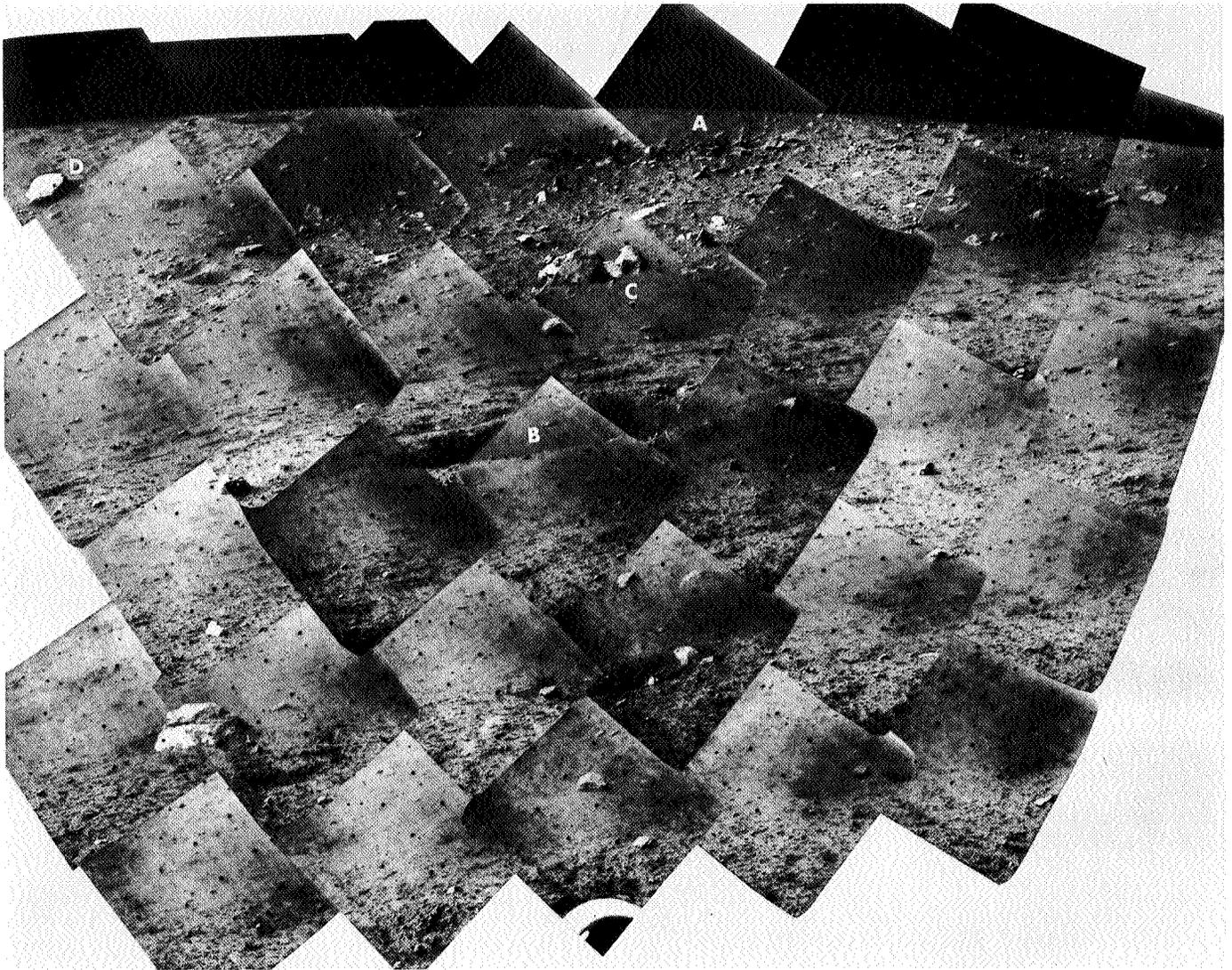
Fig. VII-9. Mosaic of *Surveyor III* frames taken looking north; lettered objects also seen in Fig. VII-8 (Catalog No. 9051, April 30, 1967, 14:38:57 through 15:07:45 GMT)

# Appendix A
# Surveyor III Flight Events

## Table A-1. Mission flight events

| Event | Mark No. | Mission time (predicted) | Mission time (actual) | GMT (actual) |
|---|---|---|---|---|
| **Liftoff to DSIF acquisition** | | | | |
| | | | April 17, 1967 | |
| Liftoff (2-in. rise) | | L + 00:00:00.00 | L + 00:00:00.00 | 07:05:01.059 |
| Initiate roll program | | L + 00:00:02 | L + 00:00:02 | 07:05:03 |
| Terminate roll, initiate pitch program | | L + 00:00:15 | L + 00:00:15 | 07:05:16 |
| Mach 1 | | | L + 00:00:58 | 07:05:59 |
| Maximum aerodynamic loading | | | L + 00:01:14 | 07:06:15 |
| *Atlas* booster engine cutoff (BECO) | 1 | L + 00:02:22.77 | L + 00:02:22.3 | 07:07:23.4 |
| Jettison booster package | 2 | L + 00:02:25.44 | L + 00:02:25.4 | 07:07:26.5 |
| Admit guidance steering | | L + 00:02:30.34 | L + 00:02:30.4 | 07:07:31.4 |
| Jettison *Centaur* insulation panels | 3 | L + 00:02:56.34 | L + 00:02:56.1 | 07:07:57.2 |
| Jettison nose fairing | 4 | L + 00:03:23.34 | L + 00:03:23.0 | 07:08:24.0 |
| Start *Centaur* boost pumps | | L + 00:03:24.34 | L + 00:03:24.0 | 07:08:25.0 |
| *Atlas* sustainer engine cutoff (SECO) | 5 | L + 00:03:58.64 | L + 00:03:57.7 | 07:08:58.8 |
| *Atlas/Centaur* separation | 6 | L + 00:03:59.63 | L + 00:03:59.6 | 07:09:00.7 |
| Prestart *Centaur* main engines (chilldown) | | L + 00:04:01.23 | L + 00:04:01.2 | 07:09:02.3 |
| *Centaur* main engines start (MES 1) | 7 | L + 00:04:09.23 | L + 00:04:09.2 | 07:09:10.3 |
| *Centaur* main engines cutoff (MECO 1) | 8 | L + 00:09:36.47 | L + 00:09:49.7 | 07:14:50.8 |
| 100-lb thrust on | 9 | L + 00:09:36.47 | L + 00:09:49.7 | 07:14:50.8 |
| Vehicle destruct system safed by ground command | | | L + 00:09:57 | 07:14:58 |
| 100-lb thrust off | 10 | L + 00:10:52.47 | L + 00:11:05.2 | 07:16:06.2 |
| 6-lb thrust on | 11 | L + 00:10:52.47 | L + 00:11:05.2 | 07:16:06.2 |
| 100-lb thrust on | 12 | L + 00:31:17.33 | L + 00:31:17.3 | 07:36:18.4 |
| Start *Centaur* boost pumps | | L + 00:31:29.33 | L + 00:31:29.0 | 07:36:30.1 |
| Prestart *Centaur* main engines (chilldown) | | L + 00:31:40.33 | L + 00:31:40.3 | 07:36:41.4 |
| *Centaur* C1 main engine start (MES 2) | 13 | L + 00:31:57.33 | L + 00:31:57.3 | 07:36:58.4 |
| *Centaur* C2 main engine start (MES 2) | 14 | L + 00:31:57.33 | L + 00:31:57.3 | 07:36:58.4 |
| *Centaur* main engines cutoff (MECO 2) | 15 | L + 00:33:43.97 | L + 00:33:48.6 | 07:38:49.7 |
| Extend *Surveyor* landing legs command | 16 | L + 00:34:11.33 | L + 00:34:12 | 07:39:13 |
| Extend *Surveyor* omniantennas command | 17 | L + 00:34:21.83 | L + 00:34:22 | 07:39:23 |
| *Surveyor* transmitter high power on command | 18 | L + 00:34:42.33 | L + 00:34:42 | 07:39:43 |
| *Surveyor/Centaur* electrical disconnect | 19 | L + 00:34:47.83 | L + 00:34:48 | 07:39:49 |
| *Surveyor/Centaur* separation | 20 | L + 00:34:53.33 | L + 00:34:53.3 | 07:39:54.4 |
| Start *Surveyor* solar panel stepping | | | L + 00:34:54.0 | 07:39.55.1 |
| Start *Centaur* 180-deg turn | 21 | L + 00:34:58.33 | L + 00:34:58.3 | 07:39:59.4 |
| Start *Centaur* lateral thrust | 22 | L + 00:35:38.33 | L + 00:35:38.4 | 07:40:39.4 |
| Start *Surveyor* sun acquisition roll | | | L + 00:35:46.4 | 07:40:47.4 |
| Cut off *Centaur* lateral thrust | 23 | L + 00:35:58.33 | L + 00:35:58.4 | 07:40:59.4 |
| Start *Centaur* tank blowdown (retro) | 24 | L + 00:38:53.33 | L + 00:38:54 | 07:43:55 |
| Solar panel locked for transit, start A/SPP roll axis stepping | | | L + 00:40:54.0 | 07:45:55.0 |
| Complete *Surveyor* roll, begin sun acquisition yaw turn | | | L + 00:41:42.8 | 07:46:43.8 |
| *Surveyor* primary sun sensor lock-on | | | L + 00:42:59.6 | 07:48:00.6 |
| Cut off *Centaur* blowdown, 100-lb thrust on | 25 | L + 00:43:03.33 | L + 00:43:03 | 07:48:04 |
| Cut off *Centaur* electrical power, 100-lb thrust off | 26 | L + 00:44:43.33 | L + 00:44:43.5 | 07:49:44 |
| A/SPP roll axis locked for transit | | | L + 00:45:06.7 | 07:50:07.7 |
| Initial DSIF acquisition (two-way lock) completed | | | L + 00:56:49 | 08:01:50 |

**Table A-1 (contd)**

| Event | Mission time (actual) | GMT (actual) |
|---|---|---|
| **DSIF acquisition to star acquisition** | | |
| Initial spacecraft operations | | |
| 1. Command Transmitter B from high to low power | L + 01:04:47 | 08:09:48 |
| 2. Command off basic bus accelerometer amplifiers and solar panel deployment logic | L + 01:06:04 | 08:11:05 |
| 3. Command off propulsion strain gage power and auxiliary accelerometer amplifiers | L + 01:06:05 | 08:11:06 |
| 4. Command off touchdown strain gage power | L + 01:06:06 | 08:11:07 |
| 5. Command rock solar panel back and forth to seat locking pin | L + 01:07:11 | 08:12:12 |
| 6. Command rock roll axis back and forth to seat locking pin | L + 01:08:06 | 08:13:07 |
| 7. Command on telemetry mode 1 for interrogation at 550-bit/sec data rate | L + 01:09:12 | 08:14:13 |
| 8. Command on telemetry modes 4, 2, 6, and 5 for interrogation at 1100-bit/sec data rate | L + 01:11:40 to L + 01:18:24 | 08:16:41 to 08:23:25 |
| Command on flight control cruise mode | L + 03:47:47 | 10:52:48 |
| Command on 4400-, 1100-, and 550-bit/sec data rates to check out sideband energy of spacecraft signal received at DSS 42 and 51 | L + 06:02:03 to L + 06:27:34 | 13:07:04 to 13:32:35 |
| Command on telemetry modes 4, 2, 1, and 5 for interrogation at 550-bit/sec data rate | L + 08:37:56 to L + 08:49:26 | 15:42:57 to 15:54:27 |
| Star verification/acquisition | | |
| 1. Command on Transmitter B in high power | L + 08:57:23 | 16:02:24 |
| 2. Command on 4400-bit/sec data rate | L + 08:59:04 | 16:04:05 |
| 3. Command off transponder power | L + 09:00:51 | 16:05:52 |
| 4. Command on cruise mode, then manual delay mode | L + 09:01:53 | 16:06:54 |
| 5. Command execution of positive roll (light sources successively detected by Canopus sensor: moon; Jupiter; stars Procyon, Adhara, Canopus; earth; star Altair) | L + 09:04:11 | 16:09:12 |
| 6. Command on star acquisition mode (after Adhara passed field of view during second revolution) | L + 09:22:34 | 16:27:35 |
| 7. Automatic Canopus acquisition and lock-on | L + 09:22:50 | 16:27:51 |
| 8. Command on cruise mode | L + 09:25:26 | 16:30:27 |
| 9. Command on Transponder B power | L + 09:26:24 | 16:31:25 |
| 10. Command on 1100-bit/sec data rate | L + 09:32:39 | 16:37:40 |
| 11. Command Transmitter B from high to low power | L + 09:34:27 | 16:39:28 |
| **Premidcourse coast phase** | | |
| Command on inertial mode (start first gyro drift check, all axes) | L + 10:24:16 | 17:29:17 |
| Command on cruise mode (end first gyro drift check) | L + 12:11:31 | 19:16:32 |
| Command on inertial mode (start second gyro drift check, all axes) | L + 12:18:34 | 19:23:25 |
| Command on telemetry modes 4, 2, and 5 for interrogation at 1100-bit/sec data rate | L + 14:14:54 to L + 14:21:09 | 21:19:55 to 21:26:10 |
| Command on cruise mode (end second gyro drift check) | L + 14:36:53 | 21:41:54 |
| Command on sun acquisition mode (start third gyro drift check, roll axis only) | L + 16:06:19 | 23:11:20 |
| Command on telemetry modes 4 and 2 for interrogation at 1100-bit/sec data rate | L + 16:48:35 and L + 16:53:13 | 23:53:36 and 23:58:14 |
| | April 18, 1967 | |
| Command on telemetry mode 5 for interrogation at 1100-bit/sec data rate | L + 16:55:42 | 00:00:43 |
| Command on cruise mode (end third gyro drift check) | L + 19:06:20 | 02:11:21 |
| Command on telemetry modes 4, 2, 1, and 5 for premidcourse interrogation at 1100 bit/sec | L + 19:49:40 to L + 19:54:47 | 02:54:41 to 02:59:48 |
| Command on gyro speed signal processor and check angular rate of gyro spin in roll, pitch, and yaw axes; return to 1100-bit/sec data rate | L + 19:56:49 to L + 19:59:48 | 03:01:50 to 03:04:49 |

| Event | Mission time (actual) | GMT (actual) |
|---|---|---|
| **Midcourse maneuver** | | |
| Command on telemetry modes 4, 2, and 1 for interrogation at 1100-bit/sec data rate | L + 21:07:59 to L + 21:12:54 | 04:13:00 to 04:17:55 |
| Command Transmitter B from low to high power | L + 21:15:47 | 04:20:48 |
| Command on 4400-bit/sec data rate | L + 21:16:30 | 04:21:31 |
| Premidcourse attitude maneuvers | | |
| 1. Command on cruise mode | L + 21:24:58 | 04:29:59 |
| 2. Command roll maneuver direction and magnitude: positive roll for 113.4875 sec (+56.7438 deg) | L + 21:25:00 | 04:30:01 |
| 3. Command roll execution | L + 21:41:48.7 | 04:46:49.8 |
| 4. Roll maneuver completed (113.494 sec; +56.747 deg) | L + 21:43:42.2 | 04:48:43.3 |
| 5. Command on sun acquisition mode | L + 21:44:26 | 04:49:27 |
| 6. Command pitch maneuver magnitude: pitch for 78.2501 sec (−39.1251 deg) | L + 21:44:27 | 04:49:28 |
| 7. Command pitch execution | L + 21:45:07.1 | 04:50:08.2 |
| 8. Pitch maneuver completed (78.25 sec; −39.125 deg) | L + 21:46:25.3 | 04:51:26.4 |
| Command on telemetry modes 2 and 1 for interrogation at 4400-bit/sec data rate | L + 21:47:35 and L + 21:48:59 | 04:52:36 and 04:54:00 |
| Command on propulsion strain gage power and inertial mode | L + 21:49:28 | 04:54:29 |
| Command off thermal control power to the SM/SS, AMR, vernier lines, fuel tank 2, and oxidizer tanks 2 and 3 | L + 21:50:17 to L + 21:50:19 | 04:55:18 to 04:55:20 |
| Command unlock vernier engine 1 roll actuator and pressurize vernier system (helium) | L + 21:50:20 | 04:55:21 |
| Command on flight control thrust phase power | L + 21:52:02 | 04:57:03 |
| Midcourse correction | | |
| 1. Command magnitude of vernier engines burn time: 4.2777 sec (a velocity correction of 4.19 m/sec) | L + 21:52:23 | 04:57:24 |
| 2. Command midcourse velocity correction | L + 21:55:01.1 | 05:00:02.2 |
| 3. Midcourse velocity correction completed | L + 21:55:05.37 | 05:00:06.47 |
| 4. Command standard emergency terminate midcourse velocity correction (twice) | L + 21:55:08.0 | 05:00:09.1 |
| Command off flight control thrust phase power, propulsion strain gage power, auxiliary accelerometer amplifiers, and touchdown strain gage power | L + 21:55:29 to L + 21:55:49 | 05:00:30 to 05:00:50 |
| Command on telemetry mode 5, vernier lines temperature control, AMR temperature control, and SM/SS heater power | L + 21:56:14 to L + 21:56:53 | 05:01:15 to 05:01:54 |
| Postmidcourse attitude maneuvers | | |
| 1. Command reverse pitch maneuver direction and magnitude | L + 21:57:32 | 05:02:23 |
| 2. Command pitch execution | L + 21:58:17.6 | 05:03:18.7 |
| 3. Pitch maneuver completed (78.25 sec; +39.125 deg) and sun reacquired | L + 21:59:35.8 | 05:04:36.9 |
| 4. Command on sun acquisition mode | L + 22:00:10 | 05:05:11 |
| 5. Command reverse roll maneuver magnitude | L + 22:00:45 | 05:05:46 |
| 6. Command roll execution | L + 22:01:16.6 | 05:06:17.7 |
| 7. Roll maneuver completed (113.494 sec; −56.747 deg) and Canopus reacquired | L + 22:03:10.1 | 05:08:11.2 |
| 8. Command on cruise mode | L + 22:04:03 | 05:09:04 |
| Command on telemetry modes 2, 4, and 5 for interrogation at 4400-bit/sec data rate | L + 22:05:51 to L + 22:10:08 | 05:10:52 to 05:15:09 |
| Command on 1100-bit/sec data rate | L + 22:10:42 | 05:15:43 |
| Command Transmitter B from high to low power | L + 22:11:07 | 05:16:08 |

## Table A-1 (contd)

| Event | Mission time (actual) | GMT (actual) |
|-------|----------------------|--------------|
| **Postmidcourse coast phase** | | |
| Command on telemetry modes 4, 2, and 5 for interrogation at 1100-bit/sec data rate | L + 23:58:12 to L + 24:06:48 | 07:03:13 to 07:11:49 |
| Command on inertial mode (start fourth gyro drift check, all axes) | L + 24:30:57 | 07:35:58 |
| Command on 550-bit/sec data rate | L + 25:45:07 | 08:50:08 |
| Command on cruise mode (end fourth gyro drift check) | L + 26:38:44 | 09:43:45 |
| Command on telemetry modes 6, 4, 2, and 5 for interrogation at 550-bit/sec data rate | L + 32:03:21 to L + 32:16:11 | 15:08:22 to 15:21:12 |
| Command on inertial mode (start fifth gyro drift check, all axes) | L + 34:26:24 | 17:31:25 |
| Command on sun acquisition mode (continue gyro drift check, roll axis only) | L + 36:26:49 | 19:31:50 |
| Command on inertial mode (continue gyro drift check, all axes) | L + 36:32:25 | 19:37:26 |
| Command on telemetry modes 4, 2, and 5 for interrogation at 550-bit/sec data rate | L + 36:57:55 to L + 37:07:13 | 20:02:56 to 20:12:14 |
| Command on cruise mode (end fifth gyro drift check) | L + 37:17:33 | 20:22:34 |
| Command on inertial mode (start sixth gyro drift check, all axes) | L + 37:22:19 | 20:27:20 |
| Command on cruise mode (end sixth gyro drift check) | L + 39:45:03 | 22:50:04 |
| Command on sun acquisition mode (start seventh gyro drift check, roll axis only) | L + 39:48:59 | 22:54:00 |
| | **April 19, 1967** | |
| Command on telemetry modes 4, 2, and 5 for interrogation at 550-bit/sec data rate | L + 41:47:32 to L + 42:02:18 | 00:52:33 to 01:07:19 |
| Command on cruise mode (end seventh gyro drift check) | L + 42:10:42 | 01:15:43 |
| Command on inertial mode (start eighth gyro drift check, all axes) | L + 42:18:34 | 01:23:35 |
| Command on cruise mode (end eighth gyro drift check) | L + 44:31:30 | 03:36:31 |
| Command on sun acquisition mode (start ninth gyro drift check, roll axis only) | L + 44:52:25 | 03:57:26 |
| Command on telemetry modes 4, 2, and 5 for interrogation at 550 bit/sec data rate | L + 46:20:02 to L + 46:34:19 | 05:25:03 to 05:39:20 |
| Perform initial power mode cycling: command on auxiliary battery mode (for 10 min in low current), command on high current, and after 2 min restore main battery mode | L + 46:56:17 to L + 47:08:42 | 06:01:18 to 06:13:43 |
| Command on cruise mode (end ninth gyro drift check) | L + 47:40:12 | 06:45:13 |
| Command on inertial mode (start 10th gyro drift check, all axes) | L + 47:43:51 | 06:48:52 |
| Command on vernier oxidizer tank temperature control | L + 47:58:54 | 07:03:55 |
| Command on cruise mode (end tenth gyro drift check) | L + 50:04:20 | 09:09:21 |
| Command on 137.5-bit/sec data rate | L + 50:52:35 | 09:57:36 |
| Command on telemetry modes 4, 2, 6, and 5 for interrogation at 137.5-bit/sec data rate | L + 50:57:55 to L + 51:14:43 | 10:02:56 to 10:19:44 |
| Command on sun acquisition mode (start eleventh gyro drift check, roll axis only) | L + 51:16:21 | 10:21:22 |
| Perform second power mode cycling: command on auxiliary battery mode (for 8 min in high current); command off high current and restore main battery mode, and after 5 min return to high current | L + 51:54:58 to L + 52:08:32 | 10:59:59 to 11:13:33 |
| Command on cruise mode (end eleventh gyro drift check) | L + 53:36:22 | 12:41:23 |
| Command on telemetry modes 4, 2, and 5 for interrogation at 137.5-bit/sec data rate | L + 53:43:04 to L + 53:48:24 | 12:48:05 to 12:53:25 |
| Command on inertial mode (start twelfth gyro drift check, all axes) | L + 55:23:06 | 14:28:07 |
| Command off transponder power to perform special voltage controlled crystal oscillator (VCXO) check, then command Transponder B power back on | L + 56:54:50 to L + 57:00:24 | 15:59:51 to 16:05:25 |

**Table A-1 (contd)**

| Event | Mission time (actual) | GMT (actual) |
|---|---|---|
| **Postmidcourse coast phase (contd)** | | |
| Command on cruise mode (end twelfth gyro drift check) | L + 57:50:51 | 16:55:52 |
| Command on sun acquisition mode (start thirteenth gyro drift check, roll axis only) | L + 58:00:58 | 17:05:59 |
| Command on telemetry modes 4, 2, and 5 for interrogation at 137.5-bit/sec data rate | L + 58:12:11 to L + 58:19:19 | 17:17:12 to 17:24:20 |
| Perform third power mode cycling: command on auxiliary battery mode (for 5 min in high current); command off high current and restore main battery mode, and after 6 min return to high current | L + 59:09:19 to L + 59:21:23 | 18:14:20 to 18:26:24 |
| Command on survey camera electronics temperature control | L + 59:46:46 | 18:51:47 |
| Command on telemetry modes 6, 4, 2, and 5 for interrogation at 137.5-bit/sec data rate | L + 60:38:08 to L + 60:49:35 | 19:43:09 to 19:54:36 |
| Command on inertial mode (continue gyro drift check, all axes) | L + 61:45:49 | 20:50:50 |
| Command on cruise mode (end 13th gyro drift check) | L + 61:51:11 | 20:56:12 |
| Command on telemetry modes 4, 2, 1, and 5 for preterminal interrogation at 137.5-bit/sec data rate | L + 62:19:47 to L + 62:25:04 | 21:24:48 to 21:30:05 |
| Command on gyro speed signal processor and check angular rate of gyro spin in roll, pitch, and yaw axes; return to 137.5-bit/sec data rate | L + 62:27:16 to L + 62:31:50 | 21:32:17 to 21:36:51 |
| Command off transponder power to perform VCXO check, then command Transponder B power back on | L + 62:35:22 to L + 62:36:39 | 21:40:23 to 21:41:40 |
| **Terminal descent** | | |
| Command on telemetry modes 6 and 4 for interrogation at 137.5-bit/sec data rate | L + 63:56:54 and L + 64:00:59 | 23:01:55 and 23:06:00 |
| Command on survey camera vidicon temperature control | L + 64:02:39 | 23:07:40 |
| Command Transmitter B from low to high power | L + 64:04:39 | 23:09:40 |
| Command on 1100-bit/sec data rate | L + 64:05:39 | 23:10:40 |
| Command off summing amplifiers and command on phase summing amplifier B | L + 64:06:29 | 23:11:30 |
| Command on telemetry modes 2 and 5 for interrogation at 1100-bit/sec data rate | L + 64:07:08 and L + 64:08:16 | 23:12:09 and 23:13:17 |
| Command on propulsion and touchdown strain gage power and touchdown strain gage data channels | L + 64:12:00 to L + 64:12:45 | 23:17:01 to 23:17:46 |
| Command off transponder power (one-way lock) | L + 64:14:20 | 23:19:21 |
| Terminal maneuvers | | |
| 1. Command on cruise mode | L + 64:16:25 | 23:21:26 |
| 2. Command yaw maneuver magnitude: yaw for 315.8 sec (−157.9 deg) | L + 64:16:26 | 23:21:27 |
| 3. Command yaw execution | L + 64:18:28.6 | 23:23:29.7 |
| 4. Yaw maneuver completed | L + 64:23:44.4 | 23:28:45.5 |
| 5. Command pitch maneuver magnitude: pitch for 153.6 sec (−76.8 deg) | L + 64:24:15 | 23:29:16 |
| 6. Command pitch execution | L + 64:25:16.1 | 23:30:17.2 |
| 7. Pitch maneuver completed and retro thrust direction properly aligned | L + 64:27:49.7 | 23:32:50.8 |
| 8. Command roll maneuver magnitude: roll for 127.8 sec (−63.9 deg) | L + 64:28:22 | 23:33:23 |
| 9. Command roll execution | L + 64:29:34.1 | 23:34:35.2 |
| 10. Roll maneuver completed | L + 64:31:41.9 | 23:36:43.0 |
| Command reset nominal thrust bias to increase vernier thrust to 200 lb | L + 64:33:34 | 23:38:35 |
| Command magnitude of retro sequence delay (5.075 sec between AMR *mark* and vernier engines ignition) | L + 64:34:38 | 23:39:39 |

| Event | Mission time (actual) | GMT (actual) |
|---|---|---|
| **Terminal descent (contd)** | | |
| Command on telemetry mode 6 (thrust phase commutator) | L + 64:41:25 | 23:46:26 |
| Command on retro sequence mode | L + 64:50:12 | 23:55:13 |
| Command off thermal control power to vernier lines, Vernier Fuel Tank 2, and Vernier Oxidizer Tanks | L + 64:50:43 | 23:55:44 |
| 2 and 3; to the surface sampler, survey camera vidicon, and survey camera electronics; | to | to |
| and to the AMR | L + 64:50:47 | 23:55:48 |
| Command on AMR power | L + 64:51:31 | 23:56:32 |
| Command on thrust phase power | L + 64:52:31 | 23:57:32 |
| Command enable AMR | L + 64:54:31.8 | 23:59:32.9 |

| Event | Mission time (predicted) | Mission time (actual) | GMT (actual) |
|---|---|---|---|
| | | April 20, 1967 | |
| Terminal descent[a] | | | |
| 1. AMR mark at 60-mile altitude and start of delay quantity countdown | L + 64:56:10.4 | L + 64:56:10.5 | 00:01:11.6 |
| 2. Command standard emergency AMR signal (three times) | | L + 64:56:10.8 | 00:01:11.9 |
| 3. Vernier engines ignition | L + 64:56:15.5 | L + 64:56:15.6 | 00:01:16.7 |
| 4. Main retro motor ignition | L + 64:56:16.4 | L + 64:56:16.6 | 00:01:17.7 |
| 5. AMR ejection | | L + 64:56:16.7 | 00:01:17.8 |
| 6. RADVS power on | | L + 64:56:17.2 | 00:01:18.3 |
| 7. Main retro motor burnout (3.5g level sensed by inertial switch) and vernier thrust level increase | L + 64:56:57.9 | L + 64:56:58.3 | 00:01:59.4 |
| 8. RADVS altimeter beam tracker out of lock for 2 sec | | L + 64:57:05.9 | 00:02:07 |
| 9. Retro case ejection | L + 64:57:09.9 | L + 64:57:10.3 | 00:02:11.4 |
| 10. RADVS altimeter beam tracker out of lock for 2 sec | | L + 64:57:11.1 | 00:02:12.2 |
| 11. Start RADVS-controlled descent (vernier phase); retro sequence mode off | L + 64:57:12.1 | L + 64:57:12.3 | 00:02:13.4 |
| 12. Descent segment intercept and vernier thrust level increase | L + 64:57:42.1 | L + 64:57:31.4 | 00:02:32.5 |
| 13. Command on PM presumming amplifier (to get touchdown strain gage data) | | L + 64:57:31.6 | 00:02:32.7 |
| 14. 1000-ft mark | L + 64:58:54.1 | L + 64:58:50.7 | 00:03:51.8 |
| 15. 10 ft/sec mark | L + 64:59:11.8 | L + 64:59:08.3 | 00:04:09.4 |
| 16. RADVS velocity Beam 3 tracker out of lock (reliable operate radar altimeter and reliable operate doppler velocity sensor off) | | L + 64:59:11.4 | 00:04:12.5 |
| 17. 14-ft mark (not received until after third touchdown) | L + 64:59:17.3 | — | — |
| 18. First touchdown event (with vernier engines thrusting) | L + 64:59:19.0 | L + 64:59:15.8 | 00:04:16.9 |
| 19. Second touchdown event (with vernier engines thrusting) | | L + 64:59:40.0 | 00:04.41.1 |
| 20. Command off thrust phase power (two times); | | L + 64:59:50.3 | 00:04:51.4 |
| and | | L + 64:59:51.3 | 00:04:52.4 |
| vernier engine cutoff | | L + 64:59:51.6 | 00:04:52.7 |
| 21. Third and final touchdown event | | L + 64:59:52.1 | 00:04:53.2 |

[a]Events are automatic unless a command is indicated, and time of occurrence of terminal descent events has been corrected for radio transmission delay to indicate time of occurrence at spacecraft.

## Table A-2. Lunar operations sequences[a]

| FIRST LUNAR DAY | | | |
|---|---|---|---|

**FIRST LUNAR DAY**

**April 20, 1967**

Posttouchdown nonstandard sequence for turning off power to systems used during terminal descent, lowering data rates, isolating auxiliary battery, and conducting engineering interrogations

First series of 200-line pictures. Selected areas from standard sequence, Pad 3 to Pad 2 survey

Nonstandard sequence for turning off all loads on the 29-V non-essential bus, then turning them back on, one at a time

Second 200-line series. Selected areas from 360-deg W/A panorama

Third and final 200-line series. Selected areas from 360-deg W/A panorama

Initial postlanding solar panel and planar array positioning

First 600-line pictures (lens inspection)

360-deg W/A panorama, selected areas

360-deg N/A panorama, Segment 4

Pad 3 N/A survey

DSS 42 signal-processing trouble-shooting sequences and planar array positioning

**April 21, 1967**

Special area W/A and N/A surveillance: Pad 2 surface and

---

Pad 2/surface interface; auxiliary battery; Crush Block 3 area and special sequence; Compartment B (positive stop); Pad 3/surface interface, Pad 3 top, and special picture of Pad 3 top; Compartment B (negative stop); Crush Block 1 area; Compartment A

Auxiliary mirror W/A and N/A survey

Pad 2 survey

360-deg W/A panorama

Camera introspective test to check for dust and large particles

360-deg N/A panorama, Segment 5

360-deg N/A panorama, Segment 4

Special horizon survey from N/A Segment 5

Special mirror azimuth-stepping test (to the right)

360-deg N/A panorama, Segment 1

Pad 2 filter N/A interrogation

SM/SS area N/A survey using red filter

SM/SS area N/A survey (partial)

Initial SM/SS deployment and functional engineering test with supporting television operations

DSS 42 sun and earth search with the A/SPP

DSS 42 and DSS 61 signal-processing trouble-shooting sequences

---

**April 22, 1967**

360-deg W/A panorama (partial)

SM/SS area N/A survey (partial)

SM/SS operations with television support: one bearing and two trenching tests

DSS 42 sun and earth searches with the A/SPP

DSS 61 RF communications test and telecommunications signal processing test

**April 23, 1967**

SM/SS trench N/A survey

Mirror azimuth-stepping checks

SM/SS operations with television support; two dragging tests in Trench 2 with surveys of trench area and SM/SS in the trench, and a scan up of SM/SS area

DSS 42 sun and earth searches with the A/SPP

**April 24, 1967**

SM/SS trench N/A and W/A color survey

Pad 2 color survey during eclipse

First pictures of earth taken from the moon. Photographs taken during eclipse and included color surveys

Pictures of Venus and stars taken during eclipse

Thermal experiments before, during, and after eclipse

**April 25, 1967**

No TV or SM/SS operations

Thermal experiments

---

RF communications test

DSS 11 antenna calibration using spacecraft

DSS 42 antenna alignment using spacecraft

DSS 61 spacecraft helium dump

**April 26, 1967**

Pad 2 W/A survey

Color chart N/A sequence

Pad 2 imprint N/A color survey

N/A survey, Sectors 9, 10, 11, 12 (with periodic W/A frames)

SM/SS operations with television support: picked up probable rock, deposited soil on Pad 2, and color survey of soil on Pad 2

DSS 42 thermal experiment using planar array for shading

DSS 61 and DSS 51 planar array and solar panel positioning

**April 27, 1967**

Pad 2 color chart surveys

Pad 2 imprint color survey

SM/SS trench color survey

SM/SS operations with television support: two bearing tests and third trenching

Auxiliary mirror survey

Crush Block 1 area survey

N/A survey, Segments 1, 2, 3

DSS 42 television surveys; planar array gain/temperature sensitivity experiment; combined spacecraft, DSIF telemetry performance test; and repositioning of A/SPP

---

[a]Other than routine engineering interrogations. All picture sequences are 600-line unless otherwise noted; wide angle and narrow angle are abbreviated W/A and N/A, respectively.

## Table A-2 (contd)

| | | | |
|---|---|---|---|
| **April 28, 1967**<br><br>Compartment A N/A survey<br>Compartment B N/A survey (negative side)<br>Auxiliary mirror N/A survey<br>360-deg W/A panorama (partial)<br>SM/SS operations with television support: placed probable rock on Pad 2, further operation in Trench 3, and one bearing test<br>Pad 2 color chart survey (green filter only)<br>Pad 2 imprint survey (green filter only)<br>N/A survey, Segments 1, 2, 3<br>Star survey for Sirius and Canopus<br>DSS 42 commanding portion of television surveys<br><br>**April 29, 1967**<br><br>SM/SS operations with television support: six impact tests and an operational interrogation<br>Star survey of Sirius<br>Pad 2 color chart survey<br>Pad 2 imprint survey<br>N/A survey, Segments 1, 2, 3<br>Pad 2/surface survey<br>Compartment A, structure survey<br>Compartment A, top survey<br>Compartment B, top survey<br>Focus ranging, −3- and −39 deg azimuth | DSS 42 commanding portion of television surveys<br>DSS 42 A/SPP positioning<br><br>**April 30, 1967**<br><br>360-deg W/A panorama (partial).<br>Compartment B survey<br>Earth picture, including color survey<br>N/A survey, Segment 2<br>N/A survey, Segment 3 (partial)<br>360-deg W/A panorama (partial, positive azimuth)<br>N/A surveys, Sectors 13 through 17<br>SM/SS operations with television support: three bearing tests and four impact tests<br>DSS 42 solar panel positioning<br><br>**May 1, 1967**<br><br>Omniantenna B photo chart survey<br>Photometric glare survey<br>360-deg W/A panorama (partial)<br>Compartment B N/A survey<br>Crush Block 3 and Vernier Engine 3 survey<br>Focus ranging +18-deg azimuth<br>SM/SS operations with television support: picked up small clod, | color survey of clod and scoop, and operations in Trench 2<br>DSS 42 RF communications test and antenna alignment test using spacecraft<br>DSS 42 camera positioning for shadow progression sequences<br>DSS 61 DSIF axial ratio test to determine spacecraft radio signal polarization<br><br>**May 2, 1967**<br><br>DSS 61 shadow progression sequences, combined spacecraft/DSIF telemetry performance test, and signal processing system checkout<br>Shadow progression and stepping test<br>Final SM/SS operations with television support: new trench (4), functional testing, and SM/SS positioned for lunar night<br>Zero phase television operations (camera pointed in same direction as sun incidence)<br>N/A and W/A survey, Segment 3 (partial)<br>Color survey<br>Focus ranging −39-deg azimuth, −13-deg elevation | DSS 42 shadow progression sequences<br><br>**May 3, 1967**<br><br>DSS 61 shadow progression sequences<br>Shadow progression W/A and N/A sequences<br>Focus ranging −39-deg azimuth, −13-deg elevation<br>Shadow progression<br>Color survey −39-deg azimuth, −13-deg elevation<br>Shadow progression<br>Focus ranging<br>Color survey<br>Shadow progression<br>Color survey, zero phase N/A<br>Shadow progression<br>Camera stepped to −28-deg elevation and secured for lunar night<br>DSS 42 spacecraft temperature monitoring<br><br>**May 4, 1967**<br><br>DSS 42 spacecraft shutdown at 00:04 GMT<br><br>**SECOND LUNAR DAY**<br>**May 23 to June 2, 1967**<br><br>Spacecraft did not respond to commands |

# Appendix B
## Surveyor III Spacecraft Configuration

## POSTLANDING CONFIGURATION



ANTENNA AND SOLAR PANEL POSITIONER

PLANAR ARRAY ANT

SECONDARY SOLAR SENSOR

SOLAR PANEL

LANDING GEAR RELEASE MECHANISM (3 PLACES)

TV CAMERA (SURVEY)

SM/SS

+Y

−Z

LEG 1

LEG 2

CRUSHABLE BLOCK (3 PLACES)

ALTIMETER/VELOCITY SENSING ANTENNA

ROLL ATTITUDE JET NOZZLE ASSEMBLY ——————

+Y    **MIDCOURSE**

LEG I

OMNIANTENNA A ——————

NNA

KLYSTRON POWER
SUPPLY AND MODULATOR ——————

OXIDIZER TANK ——————

ALTIMETER/VELOCITY SENSING ANTENNA ——————

COMPARTMENT A ——————

FUEL TANK ——————

VERNIER THRUST
CHAMBER 2 (FIXED) ——————    +X ←—·—·

SOLAR REFLECTOR
(THERMAL CONTROL) ——————

LEG 2 ——————

OXIDIZER
TANK

TV PHOTOMETRIC CHART ——————

SM/SS ——————

TV CAMERA (SURVEY) ——————

SM/SS ELECTRONICS ——————    AUXILIARY BATTERY ——————

ATTITUDE CONTROL
PRESSURIZATION TANK (N₂) ——————

FUEL SYSTEM PRESSURIZATION TANK (He) ——————

V

STA 166.45 ——————————— ·· ——

NOTE:
ANTENNA AND SOLAR PANEL
POSITIONER HAS BEEN OMITTED
FROM THIS VIEW FOR CLARITY

SPACECRAFT
MAXIMUM
STATIC ENVELOPE —

SPACECRAFT Z STATIONS

—— VERNIER THRUST CHAMBER I (GIMBALLED)

—— FUEL TANK

—— VELOCITY SENSING ANTENNA

—— COMPARTMENT B

—— FLIGHT CONTROL SENSOR GROUP

—— CANOPUS SENSOR

—— AUTOMATIC SUN
ACQUISITION SENSOR

——▶ —X

—— SIGNAL DATA
CONVERTER

—— OXIDIZER TANK

—— FUEL TANK

STA 74.98 ——————— · —

ORIGIN OF
SPACECRAFT
COORDINATE
AXES (STA 46.855) ——

—Y ◀—— STA 47.48
STA 46.855

ACCELEROMETER
AMPLIFIER

STRAIN GAGE
AMPLIFIER

ORIGIN OF
SPACECRAFT
COORDINATE
AXES

LEG 3

PITCH AND YAW
ATTITUDE JET
NOZZLE ASSEMBLY
(2 PLACES)

TV PHOTOMETRIC CHART

OMNIANTENNA B

RNIER THRUST CHAMBER 3 (FIXED)

STA 34.45 ——————— ·· —

MAIN RETRO
ROCKET
MOTOR ——

CENTAUR
HYDROGEI
TANK ——

STA 0 ————— · —— · —

STOWED CONFIGURATION

−Z

STA 6.00

32.774-
in. dia

CENTAUR STATIONS

FOOTPAD I

SPACECRAFT/CENTAUR
SEPARATION PLANE
(SPACECRAFT STA 46.63)

STA 125.82

STA 138.00

ALTITUDE MARKING
RADAR ANTENNA

SPACECRAFT
FORWARD ADAPTER

STA 156.45

ADAPTER FIELD JOINT

THERMAL
DIAPHRAGM

MOUNTING FLANGE
ATTACH STATION

104.704-in. dia

STA 172.45

+Z

SPACECRAFT AFT ADAPTER

174-2

## Appendix C
## Surveyor III Spacecraft
## Data Content of Telemetry Modes

| CHANNEL | NAME | MODE 1 WORDS | MODE 2 WORDS | MODE 3 WORDS | MODE 4 WORDS | MODE C (5) WORDS | MODE T (6) WORDS |
|---|---|---|---|---|---|---|---|
| D-1 | OMNI A TRANSMITTER POWER | | | | | 87 | |
| D-3 | OMNI B TRANSMITTER POWER | | | | | 117 | |
| D-7 | STATIC PHASE ERROR A | | | | | 27 | |
| D-8 | STATIC PHASE ERROR B | | | | | 27 | |
| D-9 | RECEIVER A AGC | | | | | 33 | |
| D-10 | RECEIVER B AGC | | | | | 6 | |
| D-13 | TRANSMITTER A TEMPERATURE | | | | | 30 | 30 |
| D-14 | TRANSMITTER B TEMPERATURE | | | | | 37 | |
| D-16 | RECEIVER A AFC | | | | | 41 | |
| D-17 | RECEIVER B AFC | | | | | | |

**ELECTRICAL POWER**

| CHANNEL | NAME | MODE 1 WORDS | MODE 2 WORDS | MODE 3 WORDS | MODE 4 WORDS | MODE C (5) WORDS | MODE T (6) WORDS |
|---|---|---|---|---|---|---|---|
| EP-1 | 29V NON-ESSENTIAL VOLTAGE | 66 | | | 1 | 11 | |
| EP-2 | UNREGULATED BUS VOLTAGE | | 81 | | 27 | 69 | 69 |
| EP-3 | MAIN BATT MANIFOLD PRESS. | | | | 81 | 63 | 9 |
| EP-4 | UNREGULATED OUTPUT CURRENT | 22 | 22 | | 51 | 9 | 79 |
| EP-5 | MAIN BATTERY VOLTAGE | | 61 | | 22 | 79 | |
| EP-6 | BATTERY CHARGE CURRENT | 32 | 32 | | 61 | 15 | 19 |
| EP-7 | BOOST REG DIFFERENCE CURRENT | | 69 | | 32 | 19 | 40 |
| EP-8 | MAIN BATTERY TEMPERATURE | | | | 69 | 40 | 29 |
| EP-9 | SOLAR CELL ARRAY CURRENT | 72 | 72 | | 72 | 29 | |
| EP-10 | SOLAR CELL ARRAY VOLTAGE | | | | 47 | 29 | |
| EP-11 | SOLAR CELL ARRAY CURRENT | 59 | 59 | | 59 | 67 | |
| EP-12 | SOLAR CELL ARRAY TEMPERATURE | | | | 8 | 25 | 20 |
| EP-13 | BOOST REGULATOR TEMPERATURE | | | | 10 | 36 | 39 |
| EP-14 | REGULATED OUTPUT CURRENT | 42 | 42 | | 42 | 20 | |
| EP-16 | OPT CHARGE REG OUTPUT CURR., | 79 | 79 | | 79 | 39 | 49 |
| EP-17 | RADAR AND SQUIB CURRENT | | 89 | | 89 | 35 | |
| EP-18 | FULL-SCALE CURR. CALIB. (ESP) | 92 | 92 | | 92 | 49 | |
| EP-19 | MID-SCALE CURR. CALIB. (ESP) | 39 | 39 | | 39 | | |
| EP-20 | ZERO SCALE CURR. CALIB. (ESP) | 19 | 19 | | 19 | | |
| EP-21 | COMPARTMENT A HEATER CURRENT | | | | 9 | 45 | |
| EP-22 | COMPARTMENT B HEATER CURRENT | | | | 29 | 81 | 81 |
| EP-23 | AUXILIARY BATTERY VOLTAGE | | | | 57 | 55 | |
| EP-24 | SOLAR CELL STRING 4 CURRENT | | | | 44 | 65 | |
| EP-25 | SOLAR CELL STRING 6 CURRENT | | | | | 75 | |
| EP-26 | AUXILIARY BATTERY TEMP. (AESP) | | 78 | | | 85 | |
| EP-27 | FULL-SCALE CURR. CALIB. (AESP) | 64 | | | 21 | 95 | |
| EP-28 | MID-SCALE CURR. CALIB. (AESP) | | 21 | | 78 | 93 | |
| EP-29 | ZERO SCALE CURR. CALIB. (AESP) | | | | | 46 | |
| EP-30 | BOOST REG., PREREG., VOLTAGE | | | | | | |
| EP-34 | BATTERY CHARGE REG. TEMP. | | | | | | |

**FLIGHT CONTROL**

| CHANNEL | NAME | MODE 1 WORDS | MODE 2 WORDS | MODE 3 WORDS | MODE 4 WORDS | MODE C (5) WORDS | MODE T (6) WORDS |
|---|---|---|---|---|---|---|---|
| FC-4 | NITROGEN GAS PRESSURE | 1,21,41,61,81 3,23,43,63,83 | 30 | | | 7 | |
| FC-5 | PRIM. SUN SENSOR PITCH ERROR | 10,60 | 27 | | | 77 | |
| FC-6 | PRIM. SUN SENSOR YAW ERROR | 20,70 | 35 | | | 101 | |
| FC-7 | SECONDARY SUN SENSOR CELL A | 28,78 | 47 | | | 105 | |
| FC-8 | SECONDARY SUN SENSOR CELL B | 38,88 | 55 | | | 107 | |
| FC-9 | SECONDARY SUN SENSOR CELL C | 7,27,47,67,87 9,29,49,69,89 | | | | 109 | 6,36,66,96 |
| FC-12 | SECONDARY SUN SENSOR CELL D | 11,31,51,71,91 13,33,53,73,93 17,37,57,77,97 | 11 13,73 17,77 | 11 13 17 9,18,19,29,39 | | 115 | 1,31,61,91 3,33,63,93 8,38,68,98 15,45,75,105 |
| FC-14 | CANOPUS ERROR | | 9,18 2,8 | 9,12,21,31,41 2,8,22,32,42 | | 1 | 16,46,76,106 |
| FC-15 | STAR INTENSITY SIGNAL | 8,58 | 2,8 | 24 | | 3 | 47,77,107 |
| FC-16 | ACCELERATION ERROR | | 7,57 49,74 | 24 | | | 18,48,78,108 |
| FC-17 | PITCH GYRO ERROR | | 51,63 | 38 | | | 24,54,84,114 |
| FC-25 | YAW GYRO ERROR | | 43,52 3,53 | 34 | | | 25,55,85,115 |
| FC-26 | THRUST CMD TO VERNIER ENG 1 | 48,98 | 48,91 | 3,23,33,43 | 94 | 18 | 26,56,86,116 |
| FC-27 | THRUST CMD TO VERNIER ENG 2 | | | 7,27,37,47,48 | | 68 | 27,57,87,117 |
| FC-35 | THRUST CMD TO VERNIER ENG 3 | 24 | 60 | | | 48 | |
| FC-39 | RETRO ACCELEROMETER | | | | | 82 | |
| FC-40 | RADAR ALTIMETER RANGE SIGNAL | 44 | | 14 | 18 | 5 | 5,35,65,95 |
| FC-41 | DOPPLER VELOCITY Vx | | 14 | | | 59 | 59 |
| FC-43 | DOPPLER VELOCITY Vy | 14,34,54,74,74 | 75 | | | 89 | 89 |
| FC-44 | DOPPLER VELOCITY Vz | | 87 | | | | |
| FC-45 | ROLL ACTUATOR SIGNAL | | 29 | | | 110 | 110 |
| FC-46 | FLIGHT CONTROL E/U TEMP 1 | | 29 | | | 98 | |
| FC-48 | FLIGHT CONTROL E/U TEMP 2 | | 80 | | | 102 | |
| FC-49 | ROLL GYRO TEMPERATURE | | | | | 104 | |
| FC-50 | CANOPUS SENSOR TEMPERATURE | | | | | | |
| FC-51 | NITROGEN GAS TANK TEMP. | | 23 | | | | 99 |
| FC-53 | ROLL PRECESSION COMMAND | | | | | | |
| FC-54 | PITCH PRECESSION COMMAND | | | | | | |
| FC-55 | YAW PRECESSION COMMAND | | | | | | |
| FC-71 | SEC. SUN SENSOR CENTER CELL | | | | | | |
| FC-73 | ATTITUDE GAS JET 2 TEMP | | | | | | |
| FC-75 | ROLL ACTUATOR TEMPERATURE | | | | | | |
| FC-77 | FLT. CONT'L REFERENCE RETURN | | | | | | |

**MECHANISMS**

| CHANNEL | NAME | MODE 1 WORDS | MODE 2 WORDS | MODE 3 WORDS | MODE 4 WORDS | MODE C (5) WORDS | MODE T (6) WORDS |
|---|---|---|---|---|---|---|---|
| M-3 | SOLAR PANEL POSITION | | 98 | | 71 | 57 | |
| M-4 | POLAR AXIS POSITION | | | | 98 | 61 | |
| M-6 | ELEVATION AXIS POSITION | | | | 77 | | |
| M-7 | ROLL AXIS POSITION | | | | 87 | 91 | |
| M-8 | SOLAR ARRAY TEMPERATURE | | | | 14 | 38 | |
| M-10 | SOLAR PANEL MOTOR TEMP. | | | | 58 | 44 | |
| M-12 | ELEV. AXIS STEP. MOTOR TEMP | | | | 64 | | |

**PROPULSION**

| CHANNEL | NAME | MODE 1 WORDS | MODE 2 WORDS | MODE 3 WORDS | MODE 4 WORDS | MODE C (5) WORDS | MODE T (6) WORDS |
|---|---|---|---|---|---|---|---|
| P-1 | HELIUM PRESSURE | 84 | 25 | | | 21 | 21 |
| P-2 | OXIDIZER PRESSURE 3 | 86 | 41 | | | 51 | 51 |
| P-3 | UPPER RETRO CASE TEMPERATURE | | 48 | | | | |
| P-4 | VERNIER LINES 2 TEMPERATURE | 2 | | | | 80 | 80 |
| P-5 | VERNIER FUEL TANK 2 TEMP. | | | | | | |
| P-6 | VERNIER OXIDIZER TANK 3 TEMP. | | 66 | | | 56 | 70 |
| P-7 | VERNIER ENGINE 1 TEMPERATURE | 26 | 86 | | | 70 | 90 |
| P-8 | VERNIER LINES 1 TEMPERATURE | 52 | 24 | | | 90 | 100 |
| P-9 | VERNIER ENGINE 3 TEMPERATURE | 82 | | | | 50 | 50 |
| P-10 | VERNIER ENGINE 2 TEMPERATURE | 80 | 34 | | | 80 | 60 |
| P-11 | VERNIER ENGINE 3 TEMPERATURE | 46 | 48 | | | 28 | |
| P-12 | LOWER RETRO CASE TEMPERATURE | | 88 | | | 4 | |
| P-13 | VERNIER FUEL TANK 3 TEMP. | | 56 | | | 54 | |
| P-14 | VERNIER FUEL TANK 1 TEMP. | | 76 | | | 92 | |
| P-15 | VERNIER OXIDIZER TANK 1 TEMP. | | 82 | | | 2 | |
| P-16 | VERNIER OXIDIZER TANK 2 TEMP. | | 84 | | | 86 | |
| P-17 | HELIUM TANK TEMP. | 15,35,55,75,95 | 15 | | 20 | | 7,37,67,97 |
| P-18 | VERNIER ENGINE 1 STRAIN GAGE | 16,36,56,76,96 | 37 | | | | 11,41,71,101 |
| P-19 | VERNIER ENGINE 2 STRAIN GAGE | 90 | 90 | | | | 28,88 |
| P-20 | VERNIER ENGINE 3 STRAIN GAGE | | | | | 42 | |
| P-22 | RETRO NOZZLE TEMPERATURE | | | | | | |

**RADAR**

| CHANNEL | NAME | MODE 1 WORDS | MODE 2 WORDS | MODE 3 WORDS | MODE 4 WORDS | MODE C (5) WORDS | MODE T (6) WORDS |
|---|---|---|---|---|---|---|---|
| R-2 | RADVS-R AMPLITUDE | | 26 | 26 | | | 4,64 |
| R-3 | RADVS-D1 AMPLITUDE | | 28 | 28 | | | 44,104 |
| R-4 | RADVS-D2 AMPLITUDE | | 36 | 36 | | | 14,74 |
| R-5 | RADVS-D3 AMPLITUDE | | 36 | 46 | | | 34,94 |
| R-6 | AMR ANTENNA TEMPERATURE NO. 1 | | 54 | | | 26 | |
| R-7 | AMR ELECTRONICS TEMPERATURE | | 64 | | | 10 | 10 |
| R-8 | RADVS KLY. UNIT TEMP. | | 38 | | | 22 | |
| R-9 | RADVS DATA CONVERT TEMP. | | 62 | | | 76 | |
| R-10 | DOPPLER RADAR SENSOR TEMP. | | 94 | | | | |
| R-12 | AMR PWR OUTPUT (MAG CURRENT) | | 96 | | | 24 | 43 |
| R-13 | ALTIMETER MARKING RADAR AGC | | 33 | | | 84 | 109 |
| R-14 | ALTITUDE MARKING RADAR SENSOR TEMP. | | | | | | |
| R-27 | AMR ANTENNA TEMPERATURE NO. 2 | | | | | | |
| R-29 | AMR LATE GATE SIGNAL | | 71 | | | | 58 |

**SIGNAL PROCESSING**

| CHANNEL | NAME | MODE 1 WORDS | MODE 2 WORDS | MODE 3 WORDS | MODE 4 WORDS | MODE C (5) WORDS | MODE T (6) WORDS |
|---|---|---|---|---|---|---|---|
| S-1 | REFERENCE VOLTAGE | | 67 | | 67 | | |
| S-2 | REFERENCE RETURN | | 97 | | 97 | | |
| S-5 | COMMUTATOR UNBAL. CURR. (ESP) | | 31 | | 31 | | |
| S-7 | COMMUTATOR UNBAL. CURR. (AESP) | | | | | 47 | |

**TELEVISION**

| CHANNEL | NAME | MODE 1 WORDS | MODE 2 WORDS | MODE 3 WORDS | MODE 4 WORDS | MODE C (5) WORDS | MODE T (6) WORDS |
|---|---|---|---|---|---|---|---|
| TV-16 | SURV. CAM. ELECTRONICS TEMP. | | | | 16 | 116 | |
| TV-17 | SURV. CAM. MIRROR ASSY. TEMP. | | | | | | |

**SURFACE SAMPLER EXPERIMENT**

| CHANNEL | NAME | MODE 1 WORDS | MODE 2 WORDS | MODE 3 WORDS | MODE 4 WORDS | MODE C (5) WORDS | MODE T (6) WORDS |
|---|---|---|---|---|---|---|---|
| SS-10 | MOTOR CURRENT | | 10 | | | 97 | |
| SS-17 | AUX. ELECTRONICS TEMPERATURE | | 70 | | | 16 | |

**STRUCTURES (VEHICLE)**

| CHANNEL | NAME | MODE 1 WORDS | MODE 2 WORDS | MODE 3 WORDS | MODE 4 WORDS | MODE C (5) WORDS | MODE T (6) WORDS |
|---|---|---|---|---|---|---|---|
| V-5 | LANDING GEAR 1 DEFLECTION | | 93 | | | | |
| V-6 | LANDING GEAR 2 DEFLECTION | | 95 | | | 66 | |
| V-7 | LANDING GEAR 3 DEFLECTION | | 83 | | 24 | 78 | |
| V-15 | COMP. A TEMP. THERMAL TRAY TOP | | | | 28 | | |
| V-16 | COMP. A TEMP. LOWER SUPPORT | | | | 30 | 64 | |
| V-18 | COMP. A TEMP. INSUL RETAINER | | | | 34 | | |
| V-19 | COMP. A TEMP. CANISTER | | | | 36 | 32 | |
| V-20 | COMP. A TEMP. SW. 5 IN CONT. RING | | | | 44 | 58 | |
| V-21 | COMP. A TEMP. SW. 5 IN FACE RAD. | | | | 46 | 74 | |
| V-22 | COMP. B TEMP. TRAY TOP CENTER | | | | 48 | | |
| V-23 | COMP. B TEMP. LOWER SUPPORT | | | | 52 | 34 | |
| V-24 | COMP. B TEMP. CANISTER | | | | 38 | 94 | |
| V-25 | COMP. B TEMP. SW 5 IN FACE RAD. | | 58 | | 54 | | |
| V-27 | COMP. B TEMP. SW 4 IN CONT. RING | | | | 62 | 12 | |
| V-28 | UPPER SPACEFRAME TEMP., NO. 1 | | | | 66 | 14 | |
| V-29 | SPACEFRAME TEMP. UNDER COMP. A | | | | 68 | 62 | |
| V-30 | WIRE HARN., TEMP., THERM TUNNEL | | | | | | |
| V-31 | SHOCK ABSORB 1 TEMP/ERATURE | | | | | 52 | |
| V-32 | LEG 2 UPPER WEB TEMP. | | | | 76 | 8 | |
| V-33 | SHOCK ABSORB 2 TEMPERATURE | | | | 82 | | |
| V-34 | SHOCK ABSORB 3 TEMPERATURE | | | | 74 | | |
| V-35 | ASP TEMPERATURE | | | | 76 | | |
| V-37 | UPPER SPACEFRAME TEMP., NO. 2 | | | | 84 | 72 | 72 |
| V-38 | SPACEFRAME TEMP. UNDER COMP. 3 | | | | 86 | | |
| V-39 | RETRO ATTACH POINT 1 TEMP. | | | | 88 | | |
| V-44 | RETRO ATTACH POINT 3 TEMP. | | | | | 88 | |
| V-45 | CRUSHABLE BLOCK TEMP. | | | | | 108 | |
| V-46 | COMP. B TEMP. SW 1 IN FACE RAD. | | | | | 112 | |
| V-48 | COMP. B TEMP. SW 2 IN FACE RAD. | | | | | 114 | |
| SPARE | (VOLTAGE) | | | | 37, 41, 91 | 106 | |
| SPARE | (HIGH-ACCURACY TEMP.) | | | | 60, 70, 80, 90 | | |

## COMMUTATED DIGITAL WORDS

| DIGITAL WORD | COMMUTATOR WORDS | | | | MODE C (5) | MODE T (6) |
|---|---|---|---|---|---|---|
| | MODE 1 | MODE 2 | MODE 3 | MODE 4 | | |
| 1 | 40 | 40 | --- | 40 | 23 | 23 |
| 2 | 50 | 50 | --- | 50 | 53 | 53 |
| 3 | 5, 25, 45, 65, 85 | 65 | --- | --- | 13, 43, 73, 103 | 13 |
| 4 | --- | 5, 45, 85 | 5, 10, 15, 20, 25, 30, 35, 40, 45 | --- | --- | 2, 12, 22, 32, 42, 52, 62, 72, 82, 92, 102, 112 |
| 5 | --- | 6 | 6 | 6 | --- | --- |
| 6 | 6 | --- | --- | 50 | --- | --- |
| 7 | --- | --- | --- | --- | --- | --- |
| 8 | --- | 16 | 16 | --- | --- | --- |
| 9 | 4 | 4 | 4 | --- | --- | --- |
| 10 | --- | --- | --- | --- | 83 | 83 |
| 11 | --- | --- | --- | --- | 111 | 111 |
| 12 | --- | --- | --- | --- | 113 | 113 |
| 13 | --- | --- | --- | --- | --- | 103 |

## TV COMMUTATOR

| CHANNEL | NAME | MODE 7 WORDS |
|---|---|---|
| TV-1 | CAMERA NUMBER | 2 |
| TV-2 | MIRROR AZIMUTH | 3, 11 |
| TV-3 | MIRROR ELEVATION | 7 |
| TV-4 | LENS FOCAL LENGTH SETTING | 12 |
| TV-5 | LENS FOCAL SETTING | 5 |
| TV-6 | LENS IRIS SETTING | 13 |
| TV-7 | LENS IRIS SERVO ON | 15 |
| TV-8 | FILTER WHEEL POSITION | 10 |
| TV-9 | VIDICON FACEPLATE TEMP. | 8 |
| TV-10 | CAMERA ELECTRONICS TEMP. | 4 |
| TV-11 | SHUTTER MODE (OPEN OR NORMAL) | 9 |
| TV-12 | CALIBRATE VOLTAGE | 6, 14 |
| TV-13 | MULTIPLE STEP FOCUS ON | 16 |

## SUBCARRIER SUMMARY

| CHANNEL | NAME | SCO FREQ. (KC) | CARRIER MOD MODE ** |
|---|---|---|---|
| D-11, 15 | COMMAND REJECT/ENABLE | 2.3 | PM |
| FC-1 | ROLL GYRO SPEED | | |
| FC-2 | PITCH GYRO SPEED | 5.4 | PM |
| FC-3 | YAW GYRO SPEED | | |
| V-8 | VEH. ACCEL. 1, COL'M. BASE LEG 1 | 52.5 | FM |
| V-9 | VEH. ACCEL. 2, COL'M. BASE LEG 2 | 70 | |
| V-10 | VEH. ACCEL. 3, COL'M. BASE LEG 3 | 90 | |
| V-11 | VEH. ACCEL. 4, FCG | 110 | |
| V-12 | LEG 1 SHOCK ABSORBER STRAIN GAGE | 1.7 | |
| V-13 | LEG 2 SHOCK ABSORBER STRAIN GAGE | 1.3 | PM |
| V-14 | LEG 3 SHOCK ABSORBER STRAIN GAGE | .96 | |
| V-40 | VEH. ACCELEROMETER 5, ASPP | | |
| V-41 | VEH. ACCELEROMETER 6, DVS ANTENNA | 130 | |
| V-42 | VEH. ACCELEROMETER 7, COMPART. A | | |
| V-43 | VEH. ACCELEROMETER 8, COMPART. B | 150 | FM |

## COMMUTATED PCM DATA

| BIT RATE (BPS) | SCO CENTER FREQ. (KC) | CARRIER MODULATION |
|---|---|---|
| 4400 | 33 | FM OR PM |
| 1100 | 7.35 | FM OR PM |
| 550 | 3.9 | FM OR PM |
| 550 (LOW MOD INDEX) | 3.9 | PM |
| 137.5 | .96 | PM |
| 17.2 | .56 | FM |
| V-14 COMPOSITE VIDEO | CARRIER | |

## COMMUTATED BINARY SIGNALS

### RADIO AND COMMAND DECODING (DATA LINK)

| CHANNEL | NAME | DIGITAL WORD (BIT) |
|---|---|---|
| D-2 | TRANSMITTER A FILAMENT ON | 6, 10(5) |
| D-4 | TRANSMITTER B FILAMENT ON | 6, 10(6) |
| D-5 | TRANSPONDER A PHASE LOCKED | 6, 10(3) |
| D-6 | TRANSPONDER B PHASE LOCKED | 6, 10(4) |
| D-11 | MESSAGE REJECT | 5, 6, 10, 12(2) |
| D-12 | CENTRAL DECODER A ON | 6, 10(8) |
| D-15 | MESSAGE ENABLE | 5, 6, 10, 12(1) |
| D-18 | CENTRAL DECODER B ON | 6, 10(7) |

### ELECTRICAL POWER

| CHANNEL | NAME | DIGITAL WORD (BIT) |
|---|---|---|
| EP-31 | AUXILIARY BATTERY MODE ON | 7, 11(5) |
| EP-32 | HIGH CURRENT MODE OFF | 7, 11(6) |
| EP-33 | EMA RADVS PYRO SWITCHES | 7, 11(8) |

### FLIGHT CONTROL

| CHANNEL | NAME | DIGITAL WORD (BIT) |
|---|---|---|
| FC-13 | CANOPUS LOCK-ON | 1(6) |
| FC-18 | MAGNITUDE REGISTER READOUT | 2 |
| FC-19 | PROGRAMMER ROLL SIGNAL | 3(1) |
| FC-21 | PROGRAMMER PITCH SIGNAL | 3(2) |
| FC-23 | PROGRAMMER YAW SIGNAL | 3(5) |
| FC-28 | VERNIER IGNITION SIGNAL | 3(0), 4(3) |
| FC-29 | RETRO IGNITION SIGNAL | 4(4) |
| FC-30 | RETRO BURNOUT SIGNAL | 4(5) |
| FC-31 | RETRO EJECT SIGNAL | 4(6) |
| FC-33 | RELIABLE OPERATION-RADAR ALT | 9(9) |
| FC-34 | RELIABLE OPERATION-DOPP. RADAR | 9(10) |
| FC-36 | TEN FOOT PER SECOND MARK | 4(9) |
| FC-37 | ONE THOUSAND FOOT MARK | 4(8) |
| FC-38 | THIRTEEN FOOT MARK | 4(10) |
| FC-42 | START RADVS CONTR'LD DESCENT | 4(7) |
| FC-52 | NOMINAL ENGINE THRUST BIAS | 9(8) |
| FC-56 | MANUAL DELAY MODE ON | 3(2) |
| FC-57 | GAS JET AMPL. INHIBITED | 1(8) |
| FC-58 | VERNIER IGNITION SIGNAL | 9(1) |
| FC-59 | RATE MODE ON | 9(2) |
| FC-60 | SUN MODE ON | 9(3) |
| FC-61 | STAR MODE ON | 9(4) |
| FC-63 | CRUISE MODE ON | 4(1) |
| FC-64 | RETRO SEQ. MODE ON | 9(5) |
| FC-65 | INERTIAL SWITCH SIGNAL | 4(2) |
| FC-66 | ALTITUDE MARKING RADAR SIG. | 3(9) |
| FC-67 | M/C VELOCITY CORRECTION SIG. | 3(7) |
| FC-69 | THRUST PHASE POWER ON | 3(4) |
| FC-73 | PROG. POS., ANGLE MANEUVER SIG. | 3(7) |
| FC-74 | PRIM SUN SENSOR CNTR., CELL L-O | 9(7) |
| FC-75 | MAN. L-O (SUN OR STAR) | 1(9) |
| FC-76 | PITCH GYRO HTR. CONTROL OFF | 1(10) |
| FC-77 | ROLL GYRO HTR. CONTROL OFF | 1(10) |
| FC-78 | ACQUISITION SUN SENSOR ILLUM. | 1(7) |
| FC-79 | YAW GYRO HEATER CONTROLLER OFF | 3(8) |

### MECHANISMS

| CHANNEL | NAME | DIGITAL WORD (BIT) |
|---|---|---|
| M-1 | OMNI ANTENNA A EXTENDED | 7, 11(9) |
| M-2 | OMNI ANTENNA B EXTENDED | 7, 11(10) |
| M-9 | VEHICLE ELECTRICAL DISCONNECT | 1(4) |
| M-11 | ROLL AXIS LOCK-IN TRANS. POS. | 7, 11(3) |
| M-13 | ROLL AXIS LOCK-IN TRANS. POS. | 7, 11(4) |
| M-14 | SOLAR PANEL LAUNCH LOCK UNLOCKED | 7, 11(2) |
| M-15 | SOLAR PANEL DEPLOY. LOGIC ON | 7, 11(7) |

### RADAR

| CHANNEL | NAME | DIGITAL WORD (BIT) |
|---|---|---|
| R-1 | ALTITUDE MARKING RADAR ON | 5, 12(7) |
| R-11 | AMR ENABLED | 5, 12(8) |
| R-15 | RADVS-D1 TRACKER LOCK | 8, 13(10) |
| R-16 | RADVS-D2 TRACKER LOCK | 5, 12(3) |
| R-17 | RADVS-D3 TRACKER LOCK | 5, 12(6) |
| R-18 | RADVS-R TRACKER LOCK | 5, 12(9) |
| R-19 | RADVS-D1 GAIN 1 (65 TO 40 db) | 8, 13, (3) |
| R-20 | RADVS-D1 GAIN 2 (90 TO 65 db) | 8, 13(4) |
| R-21 | RADVS-D2 GAIN 1 (65 TO 40 db) | 8, 13, (3) |
| R-22 | RADVS-D2 GAIN 2 (90 TO 65 db) | 8, 13(5) |
| R-23 | RADVS-D3 GAIN 1 (65 TO 40 db) | 8, 13(6) |
| R-24 | RADVS-D3 GAIN 2 (90 TO 65 db) | 8, 13(7) |
| R-25 | RADVS-R GAIN 1 (60 TO 40 db) | 8, 13(8) |
| R-26 | RADVS-R GAIN 2 (80 TO 60 db) | 8, 13(9) |
| R-28 | RADVS ON SIGNAL | 3(6) |

### SIGNAL PROCESSING

| CHANNEL | NAME | DIGITAL WORD (BIT) |
|---|---|---|
| S-3 | COMUT. SEL. F/F R500 (ESP MODE 2-3) | 5, 6(10) |
| S-4 | COMUT. SEL. F/F R501 (ESP MODE 3-4) | 5, 6(9) |
| S-6 | COMUT. SEL. F/F R500 (AESP MODE C) | 10(10) |

### SURFACE SAMPLER EXPERIMENT

| CHANNEL | NAME | DIGITAL WORD (BIT) |
|---|---|---|
| SS-1 | DECODER POWER ON | 7, 11(1) |
| SS-2 | COMMAND ENTERED | 5, 12, (4) 10 (9) |

### STRUCTURES (VEHICLE)

| CHANNEL | NAME | DIGITAL WORD (BIT) |
|---|---|---|
| V-1 | LANDING GEAR 1 EXTENDED | (1) |
| V-2 | LANDING GEAR 2 EXTENDED | (2) |
| V-3 | LANDING GEAR 3 EXTENDED | 1(3) |
| V-4 | RETRO NOT EJECTED | 5, 12(5) |
| SPARE | (AESP) | 12 (9, 10) |
| SPARE | (F/C) | 9 (6) |

** BRACKETED SCO'S TURNED ON BY A SINGLE COMMAND

## Appendix D
## Surveyor III Spacecraft Temperature Histories
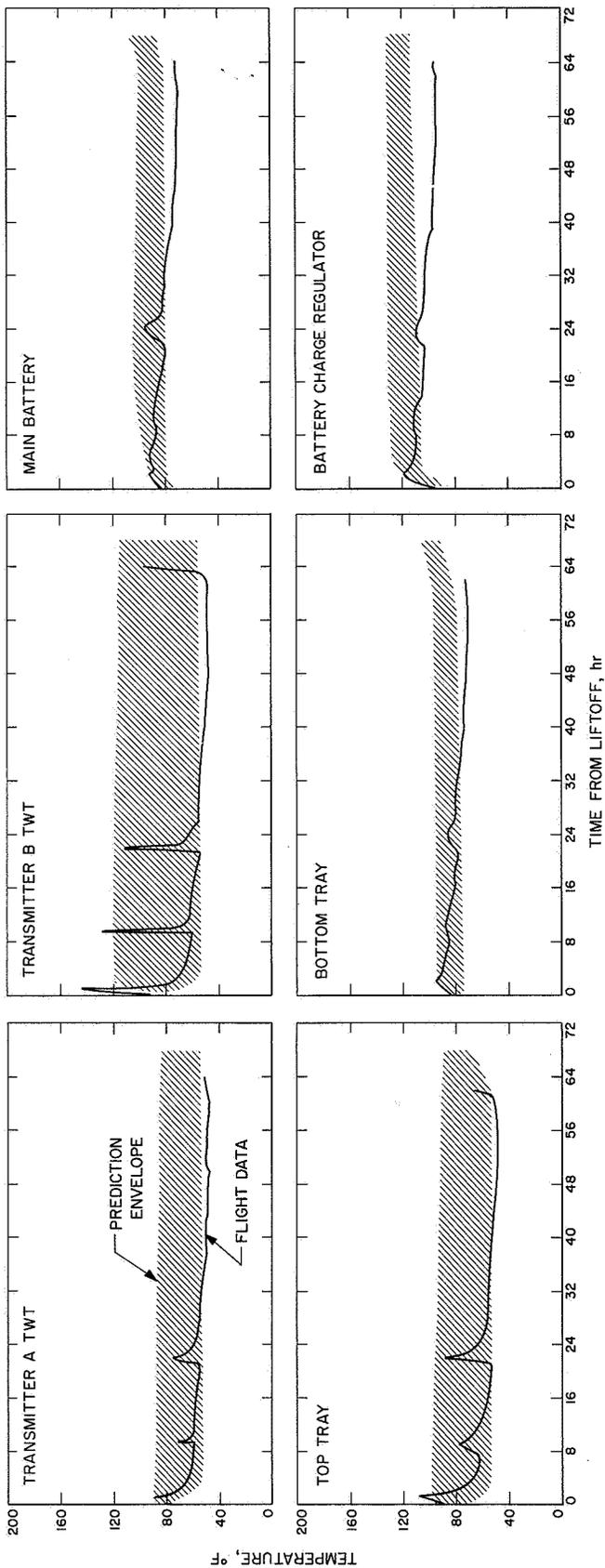
Fig. D-1. Compartment A transit temperatures
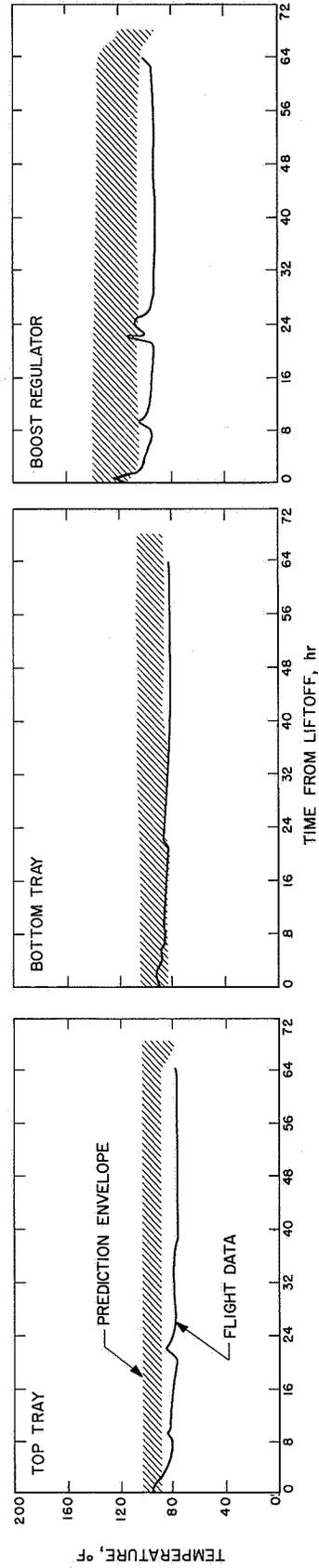
Fig. D-2. Compartment B transit temperatures
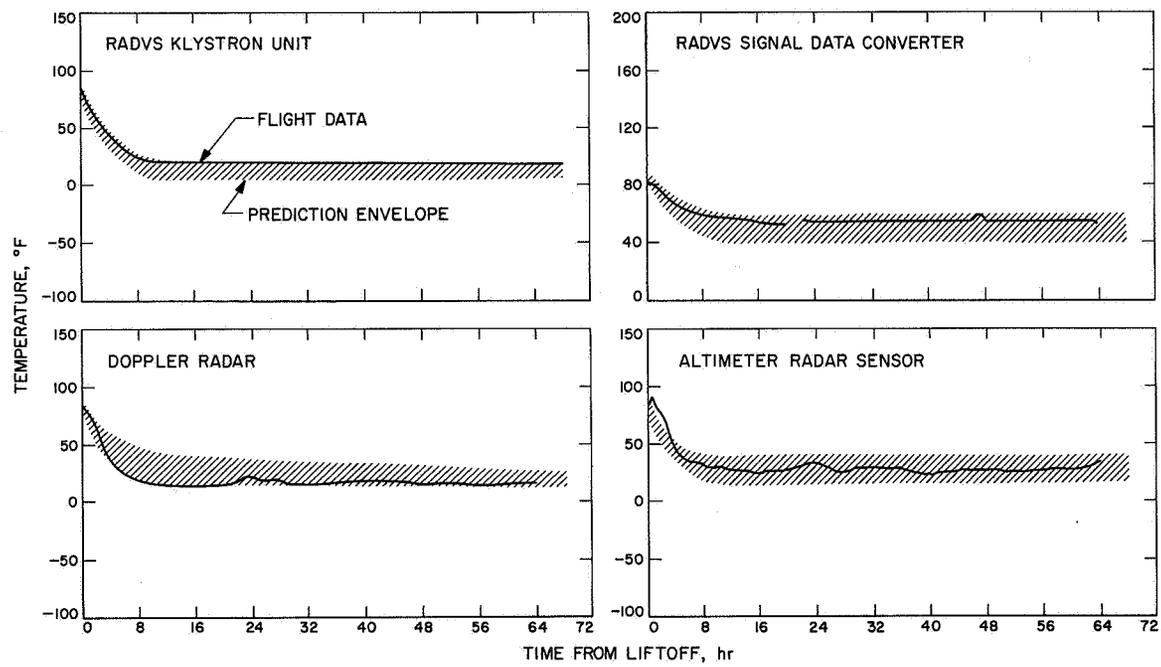
**Fig. D-3. RADVS transit temperatures**
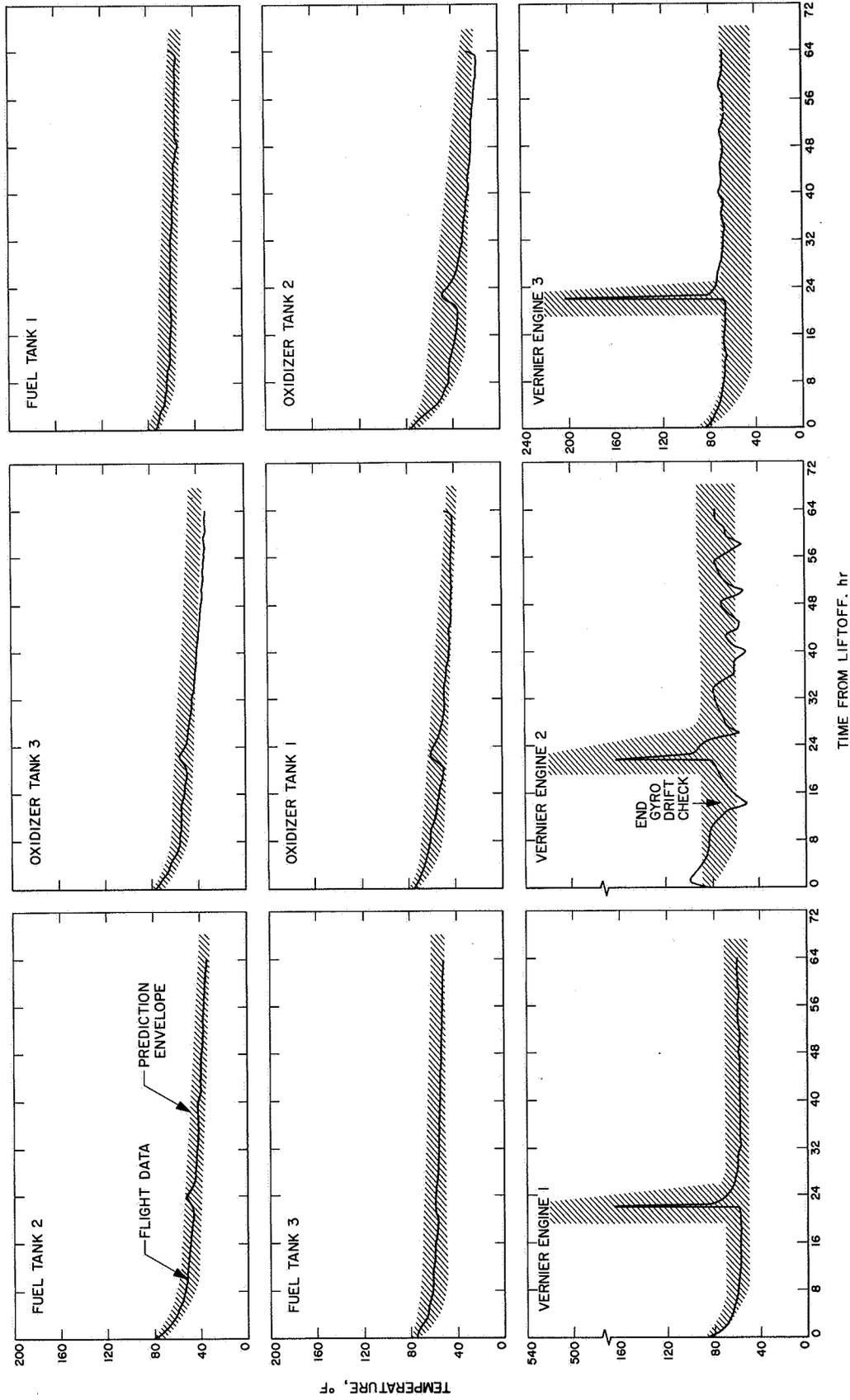
Fig. D-4. Vernier propulsion transit temperatures
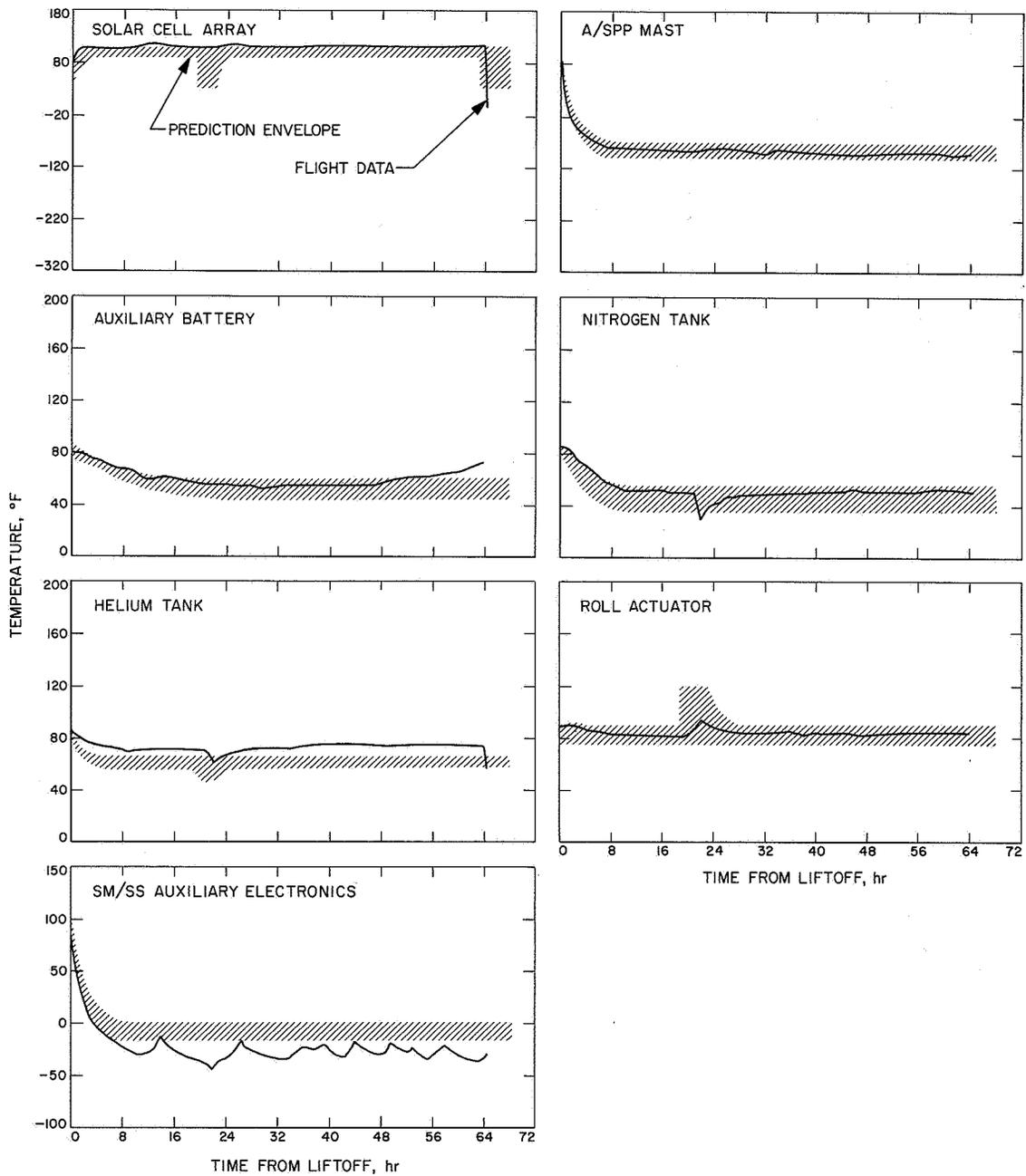
**Fig. D-5. Miscellaneous transit temperatures**
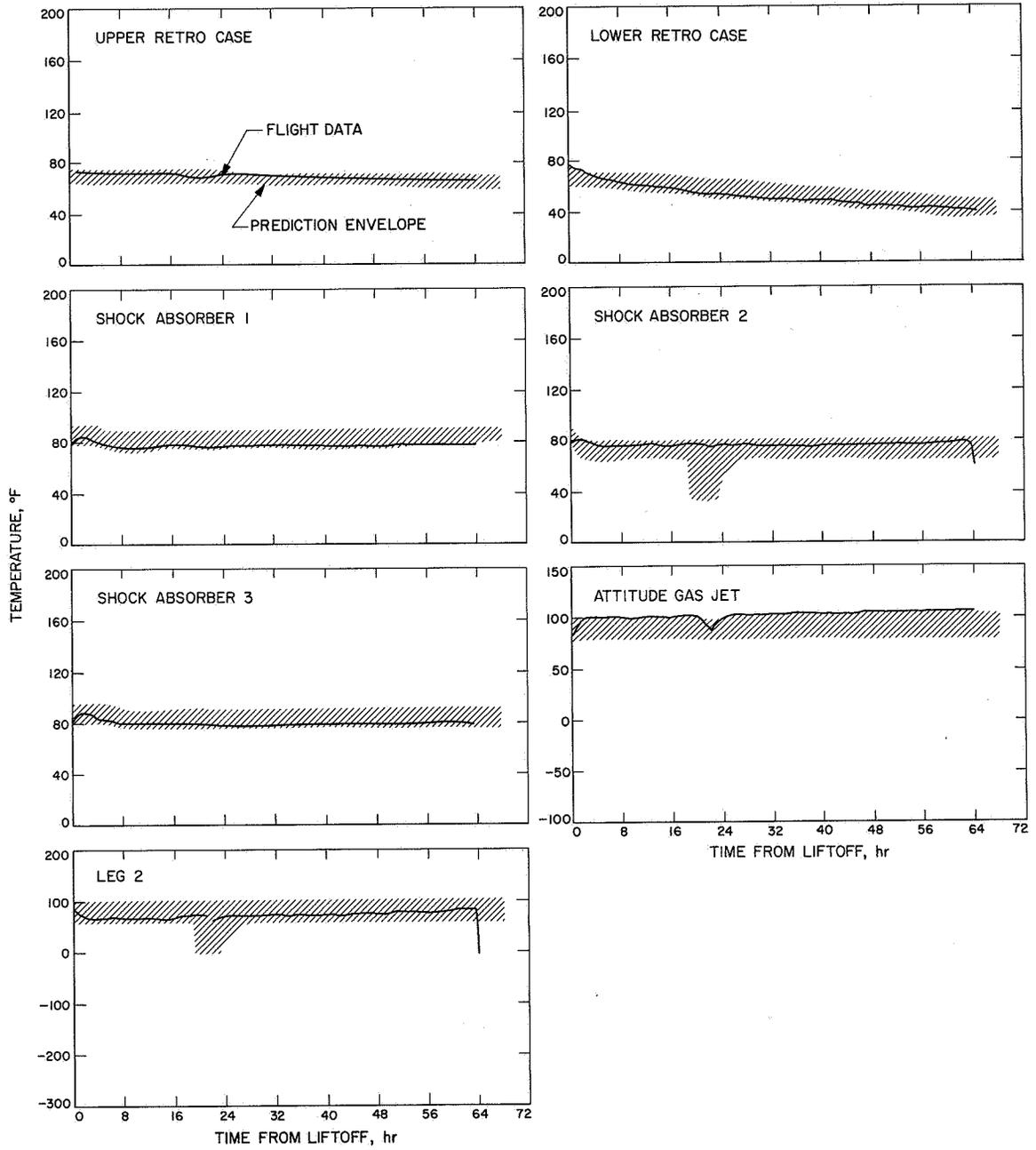
Fig. D-5 (contd)
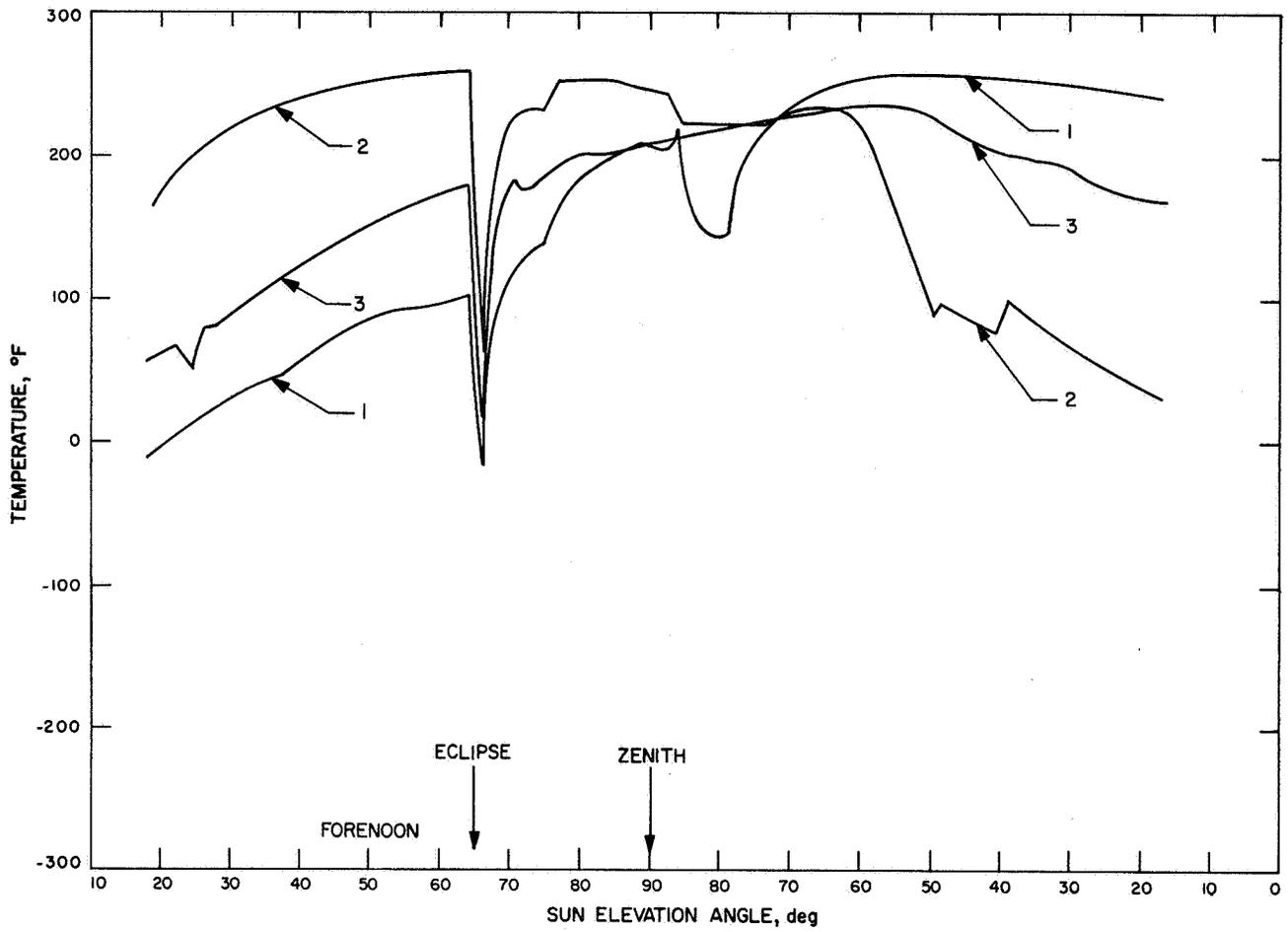
**Fig. D-6. Vernier propulsion postlanding temperatures**
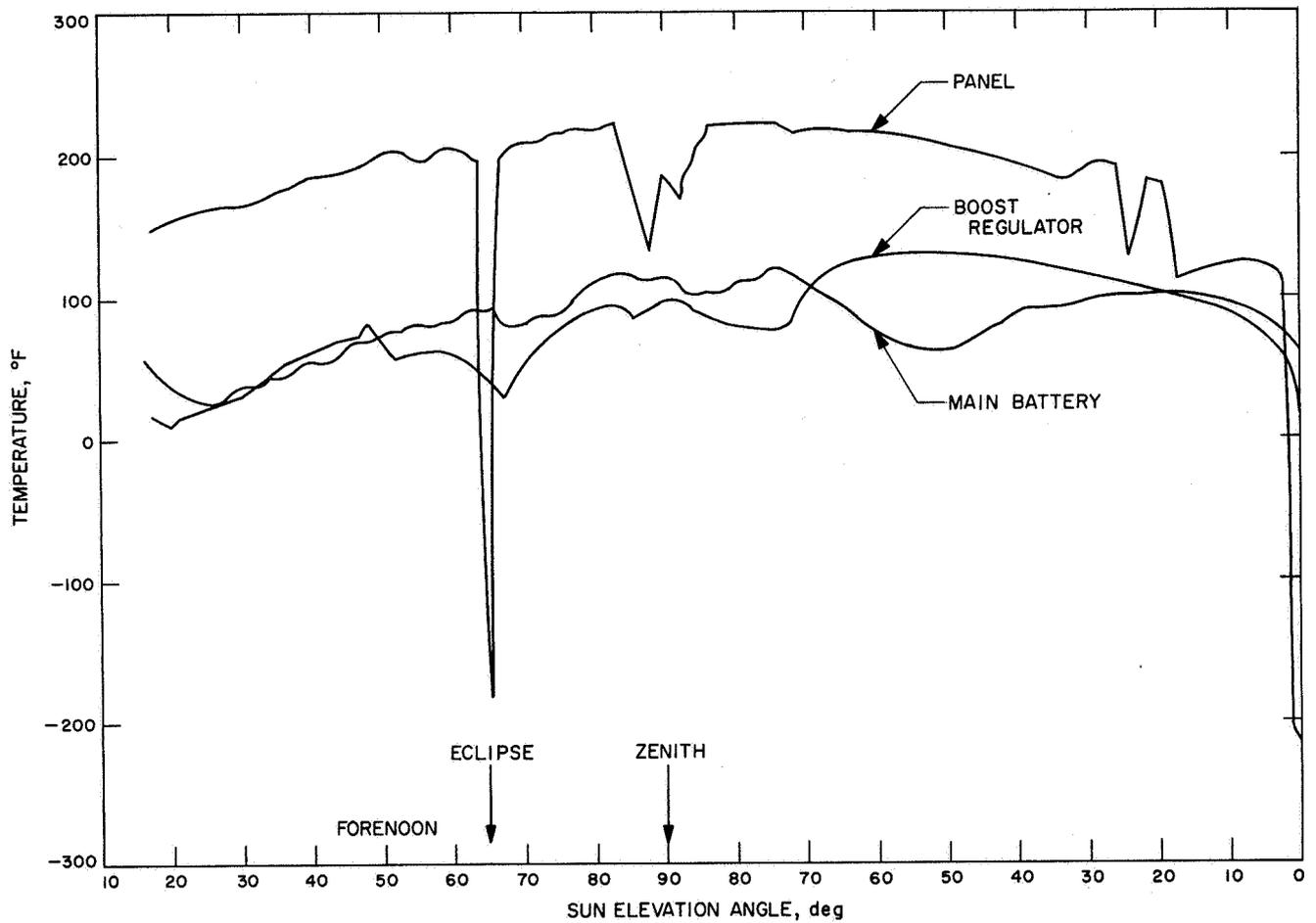
**Fig. D-7. Electrical power system postlanding temperatures**
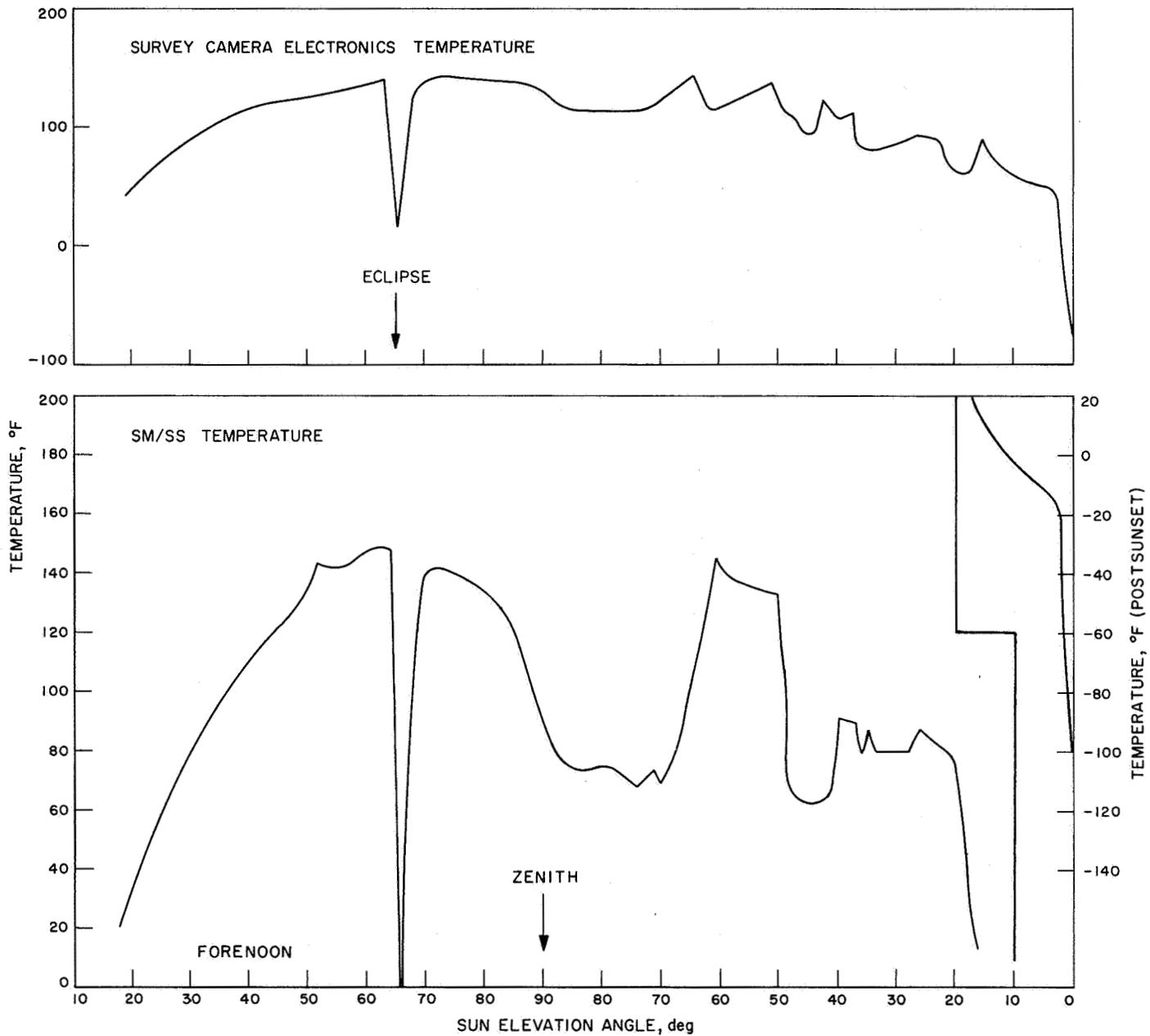
**Fig. D-8. Instrument postlanding temperatures**

# Glossary

| | |
|---|---|
| ABC | auxiliary battery control |
| AC | *Atlas/Centaur* |
| A/D | analog-to-digital |
| ADC | analog-to-digital converter |
| AESP | auxiliary engine signal processor |
| AFC | automatic frequency control |
| AFETR | Air Force Eastern Test Range |
| AGE | aerospace ground equipment |
| APC | automatic phase control |
| A/SPP | antenna and solar panel positioner |
| BCD | binary coded digital |
| BECO | booster engine cutoff |
| BR | boost regulator |
| CCC | Central Computing Complex |
| CDC | command and data (handling) console |
| CDS | computer data system |
| CP | Command Preparation (Group) |
| CRT | Composite Readiness Test |
| CSP | central signal processor |
| CSTS | Combined Systems Test Stand |
| DC | direct command |
| DOD | Department of Defense |
| DPS | Data Processing System |
| DSCC | Deep Space Communications Complex |
| DSIF | Deep Space Instrumentation Facility |
| DSS | Deep Space Station |
| DVS | doppler velocity sensor |
| ECPO | Engineering Computer Program Operations (Group) |
| EMA | engineering mechanism auxiliary |
| ESF | Explosive Safe Facility |
| ESP | engineering signal processor |
| FC | flight control |
| FCSG | Flight Control Sensor Group |
| FPAC | Flight Path Analysis and Command |
| FRB | Failure Review Board |
| FRT | fine resolution tracking |
| GCS | Ground Communication System |

| | |
|---|---|
| GSE | ground support equipment |
| GSFC | Goddard Space Flight Center |
| HSDL | high-speed data line |
| ICS | Intracommunications System |
| IF | intermediate frequency |
| I/O | input/output |
| IRV | interrange vector |
| J-FACT | Joint Flight Acceptance Composite Test |
| KPSM | klystron power supply modulator |
| KSC | Kennedy Space Center |
| LOS | loss of signal |
| MAG | Maneuver Analysis Group |
| MCDR | media conversion data recovery (subsystem) |
| MCFR | media conversion film recorder (subsystem) |
| MECO | main engine cutoff |
| MEIG | main engine ignition |
| MSFN | Manned Space Flight Network |
| NASCOM | NASA World-Wide Communication Network |
| OCR | optimum charge regulator |
| ODG | Orbit Determination Group |
| ORT | Operational Readiness Test |
| OSDP | on-site data processing |
| OSDR | on-site data recovery (subsystem) |
| OSFR | on-site film recorder (subsystem) |
| OTC | overload trip circuit |
| OVCS | operational voice communication system |
| PA | Performance Analysis (Group) |
| PCM | pulse code modulation |
| PU | propellant utilization |
| PVT | Performance Verification Tests |
| QC | quantitative command |
| RETMA | Radio Electronics Television Manufacturing Association |
| RFI | radio frequency interference |
| RIS | range instrumentation ship |
| RODVS | reliable operate doppler velocity sensor |
| RORA | reliable operate radar altimeter |

# Glossary (contd)

RTCS    real-time computer system

SDC    signal data converter

SECO    sustainer engine cutoff

SFOD    Space Flight Operations Director

SFOF    Space Flight Operations Facility

SOCP    *Surveyor* on-site computer program

SOPM    standard orbital parameter message

SOV    solenoid-operated valves

SRT    System Readiness Test

SCAT    Spacecraft Analysis Team

SPAC    Spacecraft Performance Analysis and Command (Group)

SSAC    Space Science Analysis and Command

SSD    subsystem decoder

SSE    Standard Sequence of Events

STEA    system test equipment assembly

STV    solar-thermal-vacuum

TCP    telemetry and command processor

TDA    Tracking Data Analysis (Group)

TDS    Tracking and Data System

T&DA    tracking and data acquisition

TelPAC    Television Performance Analysis and Command (Group)

TPS    Telemetry Processing Station

TSAC    Television Science Analysis and Command (Group)

TTY    teletype

TV-GDHS    TV Ground Data Handling System

VCXO    voltage controlled crystal oscillator

VECO    vernier engine cutoff

VPS    vernier propulsion system

# Bibliography

## Project and Mission

*Surveyor A-G Project Development Plan,* Project Document 13, Vol. 1, Jet Propulsion Laboratory, Pasadena, January 3, 1966.

Clarke, V. C., Jr., *Surveyor Project Objectives and Flight Objectives for Missions A through D,* Project Document 34, Jet Propulsion Laboratory, Pasadena, March 15, 1965.

Macomber, H. L., *Surveyor C Mission Plan,* Project Document 110, Jet Propulsion Laboratory, Pasadena, March 31, 1967.

"Space Exploration Programs and Space Sciences," *Space Programs Summary 37-45,* Vol. VI, Jet Propulsion Laboratory, Pasadena, May 31, 1967.

*Surveyor I Mission Report. Part I. Mission Description and Performance,* Technical Report 32-1023, Jet Propulsion Laboratory, Pasadena, August 31, 1966.

*Surveyor II Mission Report. Mission Description and Performance,* Technical Report 32-1086, Jet Propulsion Laboratory, Pasadena, April 1, 1967.

## Launch Operations

Macomber, H. L., *Surveyor Launch Constraints Document,* Project Document 43, Rev. 1, Jet Propulsion Laboratory, Pasadena, March 6, 1967.

Macomber, H. L., and O'Neil, W. J., *Surveyor Launch Constraints Mission C— April 1967 Launch Opportunity,* Project Document 43, Rev. 1, Addendum No. 3, Jet Propulsion Laboratory, Pasadena, March 24, 1967.

*Centaur Unified Test Plan, AC-12/SC-3 Launch Operations and Flight Plan (Surveyor Mission C),* Section 8.12, Report AY62-0047, Rev. B, General Dynamics/Convair, San Diego, April 17, 1967.

*Test Procedure Centaur/Surveyor Launch Countdown Operations, AC-12/SC-3 Launch (CTP-INT-1001D),* Report AA65-0500-008-04D, General Dynamics/Convair, San Diego, March 9, 1967.

*Atlas/Centaur-12 Surveyor C, Operations Summary,* TR-531, Centaur Operations Branch, KSC/ULO, Cape Kennedy, April 11, 1967.

*Atlas/Centaur-12 Surveyor C, Flash Light Report,* Report TR-536, Centaur Operations Branch, KSC/ULO, Cape Kennedy, April 20, 1967.

Barnum, P. W., *JPL ETR Field Station Launch Operations Plan, Surveyor Mission B,* Engineering Planning Document 423, Jet Propulsion Laboratory, Pasadena, July 27, 1966 (also utilized for *Surveyor* Mission C).

## Launch Vehicle System

Galleher, V. R., and Shaffer, J., Jr., *Surveyor Spacecraft/Launch Vehicle Interface Requirements,* Project Document 1, Rev. 2, Jet Propulsion Laboratory, Pasadena, December 14, 1965.

*Atlas Space Launch Vehicle Systems Summary,* Report GDC-BGJ67-001, General Dynamics/Convair, San Diego, February, 1967.

# Bibliography (contd)

*Centaur Systems Summary,* Report GDC-BGJ67-003, General Dynamics/Convair, San Diego, April 1967.

*Centaur Technical Handbook,* Convair Division, Report GD/C-BPM64-001-1, Rev. B, General Dynamics/Convair, San Diego, January 24, 1966.

*Centaur Monthly Configuration, Performance and Weight Status Report,* Report GDC63-0495-47, General Dynamics/Convair, San Diego, April 21, 1967.

*Preliminary AC-12 Atlas-Centaur Flight Evaluation* (by staff of Lewis Research Center, Cleveland, Ohio), NASA Technical Memorandum X-52300, NASA, Washington, D.C., 1967.

*Atlas/Centaur AC-12 Flight Evaluation Report,* GDC-BNZ67-033, General Dynamics/Convair, San Diego, in publication.

## Spacecraft System

*Surveyor Spacecraft A-21 Functional Description,* Document 239524 (HAC Pub. 70-93401), 3 Vols., Hughes Aircraft Co., El Segundo, Calif., November 1, 1964 (with revision sheets).

*Surveyor Spacecraft A-21 Model Description,* Document 224847B, Hughes Aircraft Co., El Segundo, Calif., March 1, 1965 (with revision sheets).

*Surveyor Spacecraft Monthly Performance Assessment Report,* SSD68252-6, Hughes Aircraft Co., El Segundo, Calif., April 21, 1967.

*Surveyor Spacecraft System—Bimonthly Progress Summary,* mid-April through mid-June 1967, Number SS-134, SSD 68218-5, Hughes Aircraft Co., El Segundo, Calif., June 24, 1967.

*Surveyor Spacecraft System-SC-3 Flight Performance Report* (Preliminary), SSD-78079, Hughes Aircraft Co., El Segundo, Calif., May 1967.

*Surveyor III Flight Performance Final Report,* SSD 68189-3R, Hughes Aircraft Co., El Segundo, Calif., July 1967.

Goble, M. E., *Surveyor Lunar Operations Plan—Mission C,* Engineering Planning Document 486, Jet Propulsion Laboratory, Pasadena, March 31, 1967.

Goble, M. E., *Surveyor Lunar Operations Plan—Mission C (Second Lunar Day Activity),* Project Document 620-1, Jet Propulsion Laboratory, Pasadena, May 17, 1967.

*Surveyor Mission C Space Flight Operations Report,* Report SSD 74071, Hughes Aircraft Company, El Segundo, Calif., May 1967.

## Flight Path

*Surveyor Spacecraft/Launch Vehicle Guidance and Trajectory Interface Schedule,* Project Document 14, Rev. 3, Jet Propulsion Laboratory, Pasadena, November 30, 1966 (and revision sheet of December 7, 1966).

"Design Specification *Surveyor/Centaur* Target Criteria *Surveyor Mission C,*" Specification SAO-50650-DSN-B, Jet Propulsion Laboratory, Pasadena, January 10, 1967.

# Bibliography (contd)

*Surveyor Station View Periods and Trajectory Coordinates—Launch Dates* April, May, June, 1967, SSD 68242R, Hughes Aircraft Co., El Segundo, Calif., November 1966.

Cheng, R. K., Meredith, C. M., and Conrad, D. A., *Design Considerations for Surveyor Guidance*, IDC 2253.2/473, Hughes Aircraft Co., El Segundo, Calif., October 15, 1965.

Fisher, J. N., and Gillett, R. W., *Surveyor Trajectory Characteristics*, SSD 68219R, Hughes Aircraft Co., El Segundo, Calif., November 1966.

O'Connell, H. P., *Pre-Injection Trajectory Characteristics*, Report AC-12, GDC-BKM66-040, and Supplement, General Dynamics/Convair, San Diego, February 1967.

Dunn, H. S., *Surveyor Mission C Post Injection Standard Trajectories*, SSD 68169-2R and SSD 68256R (Appendix A to SSD 68169-2R), Hughes Aircraft Co., El Segundo, Calif., February 1967.

Gans, J. F., *Surveyor Mission C Final Preflight Maneuver Analysis Report*, SSD 68230 and SSD 78009 (Appendix A of SSD 68230), Hughes Aircraft Co., El Segundo, Calif., February 1967.

Davids, L., Meredith, C., and Ribarich, J., *Midcourse and Terminal Guidance Operations Programs*, SSD 4051R, Hughes Aircraft Co., El Segundo, Calif., April 1964.

Seiley, R. E., Nelsen, H. D., and Winkler, M. K., *AC-12 Final Guidance Equations and Performance Analysis*, GDC-BKM66-054, General Dynamics/Convair, San Diego, December 29, 1966.

*Firing Tables—AC-12, April Opportunity*, GD/C-BKM67-002, General Dynamics/Convair, San Diego, March 17, 1967.

*Surveyor III Flight Path Analysis and Command Operational Report*, SSD 74075, Hughes Aircraft Co., El Segundo, Calif., May 10, 1967.

## Tracking and Data Acquisition

*Program Requirements No. 3400, Surveyor Revision 11*, Air Force Eastern Test Range, Patrick Air Force Base, Fla., November 4, 1966.

*Operations Requirement 3400, Surveyor Launch, Revision 8*, Air Force Eastern Test Range, Patrick Air Force Base, Fla., April 10, 1967.

*Operations Directive 3400, Surveyor Launch*, Air Force Eastern Test Range, Patrick Air Force Base, Fla., March 13, 1967.

*Project Surveyor-Support Instrumentation Requirements Document, Rev. |2|*, prepared by JPL for NASA, January 1967.

*Surveyor Project/Deep Space Network Interface Agreement*, Engineering Planning Document 260, Rev. 2, Jet Propulsion Laboratory, Pasadena, November 22, 1965.

*DSIF Tracking Instruction Manual (TIM), Surveyor Mission B* (4 volumes), Engineering Planning Document 391, Jet Propulsion Laboratory, Pasadena, August 1966 (with revision sheets for Mission C).

# Bibliography (contd)

## Mission Operations System

*Surveyor Mission Operations System,* Technical Memorandum 33-264, Jet Propulsion Laboratory, Pasadena, April 4, 1966.

*Space Flight Operations Plan—Surveyor Mission C,* Engineering Planning Document 180-S/MC, Jet Propulsion Laboratory, Pasadena, November 5, 1966 (and revision sheets through March 28, 1967).